Molecular mechanisms of nucleosome positioning and DNA methylation in chromatin

Dissertation zur Erlangung des Doktorgrades

der Naturwissenschaften (Dr. rer. nat.) der Naturwissenschaftlichen

Fakultät III - Biologie und vorklinische Medizin der Universität Regensburg

durchgeführt am Lehrstuhl für Biochemie III

der Universität Regensburg

vorgelegt von:

ANNA SCHRADER

SENSERSTR. 8

81371 MÜNCHEN

Abgabedatum: 29. Juli 2009

Die vorliegende Arbeit wurde unter der Betreuung von Prof. Dr. Gernot Längst in der Zeit von Februar 2006 bis Juli 2009 am Institut für Biochemie III der Universität Regensburg erstellt.

Prüfungskomitee:

Vorsitzender: Prof. Dr. Reinhard Wirth

1. Gutachter: Prof. Dr. Gernot Längst

2. Gutachter: Prof. Dr. Alexander Brehm

3. Gutachter (Prüfer): Prof. Dr. Ralf Wagner

Ersatzprüfer: Prof. Dr. Michael Thomm

Table of Contents

Index of Figures

Index of Tables

Abbreviations

α	Anti
aa	Amino acid
A	Adenine
ACF	ATP-utilizing chromatin assembly and remodeling factor
ADP	Adenosindiphosphate
Amp	Ampicillin
APS	Ammonium persulfate
ATP	Adenosintriphosphate
BAF	Brg1-associated factors
BAP	Brahma-associated proteins
bp	Basepair
BRM	Brahma
Brg1	Brahma-related gene 1
BSA	Bovine serum albumin
°C	degree Celsius
C	Cytosine
CENP-A	Centromere protein A
CHD	Chromodomain-helicase-DNA-binding
CHRAC	Chromatin accessibility complex
C-terminal	Carboxy-terminal
Ci	Curie
CpG	cytosine-phospatidyl-guanosine
Cpm	counts per minute
CV	Column volume
Da	Dalton
dATP	Desoxyadenosintriphosphate
dCTP	Desoxycytosintriphosphate
dGTP	Desoxyguanidintriphosphate
DEAE	Diethylaminoethyl
DMR	Differentially methylated region
DMSO	Dimethylsulfoxide
DNA	Desoxyribonucleic acid
Dnmt	DNA methyltransferase

dNTP	Desoxyribonucleotidetriphosphate
DREX	*Drosophila* embryonic extract
DTT	Dithiothreitol
dTTP	Desoxythymidintriphosphate
EDTA	Ethylendiamintetraacetate
EGTA	Ethylenglycol-bis(2-aminoethyl)-N,N,N',N'-tetraacetic acid
EM	Electron microscopy
EMSA	Electrophoretic mobility shift assay
EtBr	Ethidiumbromide
EX	Extraction buffer
FCS	Fetal calf serum
Fig	Figure
fw	Forward
G	Guanine
g	gram
GST	glutathione-S-transferase
H	histone
H2Av	H2A variant
HAT	Histone acetyltransferase
HDAC	Histone deacetylase
HEPES	(N-(2-Hydroxyethyl)piperazine-H'-(2-ethanesulfonic acid)
HDM	Histone demethylase
His	Hexahistidine
HMG	High mobility group
HMT	Histone methyltransferase
HP1	Heterochromatin protein 1
HRP	Horseradish peroxidase
Ig	Immunoglobulin
Ino80	Inositol requiring
IPTG	1-isopropyl-β-D-1-thiogalacto-pyranoside
IP	Immunoprecipitation
Isw1/Isw2	Imitation switch (Sacharomyces cerevisiae)
ISWI	Imitation switch (*Drosophila*, Xenopus)
Itc1	ISW2 ('ISW two') complex subunit
K	Lysine

kb	Kilobase
kDA	Kilo dalton
LB	Luria-Bertani
m	mouse
M	molar
MBD3	Methyl-CpG-binding protein 3
met	methylated
MNase	Micrococcal nuclease
MWCO	Molecular weight cut-off
MW	Molecular weight
NAP-1	Nucleosome assembly protein 1
NASP	Nuclear autoantigenic sperm protein
NCP	Nucleosome core particle
NFR	Nucleosome free region
Ni-NTA	nickel-nitroacetic acid
NoRC	Nucleolar remodeling complex
NPS	Nucleosome positioning sequence
NURD	Nucleosome remodeling and deacetylation
NURF	Nucleosome remodeling factor
OD	Optical density
PAA	Poly acryl amide
PAGE	Polyacrylamide gel electrophoresis
PBAF	Polybromo-associated BAF
PBAP	Polybromo-associated BAP
PBS	Phosphate buffered saline
PCNA	Proliferating cell nuclear antigen
PCR	Polymerase chain reaction
PHD	Plant homeo domain
PMSF	Phenylmethanesulfonyl fluoride
PNK	Polynucleotide kinase
PTM	Posttranslational modification
PVDF	Polyvinylidene Fluoride
Rad54	Radiation sensitive
rDNA	ribosomal DNA
RNA	Ribonucleic acid

RNAi	RNA interference
rpm	Revoltations per minute
RSC	Remodels the structure of chromatin
RSF	Remodeling and spacing factor
RT	Room temperature
Rv	Reverse
s	second
SAM	S-adenosyl-methionine
SDS	Sodiumdodecylsulfate
SLIDE	SANT-like ISWI domain
S/MAR	Scaffold/matrix attachement region
Snf2	Sucrose non-fermenting protein 2 homolog
Snf2H	Sucrose non-fermenting protein 2 homolog
Snf2L	Sucrose non-fermenting protein 2-like
Sth1	Snf two homologous 1
SUMO	Small ubiquitin-related modifier
SWI/SNF	Switch/sucrose non-fermenting
Swr1	Swi2/Snf2-related 1
T	Thymine
Tip5	TTF-I interacting protein 5
Temed	N,N,N',N'-Tetramethylethylenediamine
Tris	Tris(hydroxymethyl)aminomethane
TS-domain	targeting sequence domain
TSA	Trichostatin A
UV	Ultraviolet
v/v	Volume per volume
WICH	WSTF-ISWI chromatin remodeling complex
WSTF	Williams syndrome transcription factor
WT	Wild-type
w/v	Weight per volume
Xenopus	Xenopus laevis

A. Summary

In the eukaryotic cell nucleus DNA needs to be highly condensed. The initial level of DNA compaction is mediated by the wrapping of DNA around histone octamers to form nucleosomes. For efficient DNA metabolism, including DNA replication, transcription, repair and recombination, access to the required sequences must be granted. Hence, nucleosomes need to be highly dynamic. This is mediated by ATP-dependent chromatin remodeling complexes. It is still unclear to what extent these enzymes are influenced by local DNA sequences when shifting a nucleosome to different positions.

During my PhD thesis I studied ATP-dependent chromatin remodeling factors focusing on the molecular mechanisms of action in dependence on the underlying DNA sequence. I showed that each individual remodeling enzyme possesses distinct nucleosome translocation properties. The direction (outcome) of nucleosome translocation is determined by its underlying DNA sequence and is influenced by other remodeling complex subunits. I demonstrated that nucleosome positioning by two specific motor proteins is determined by the reduced affinity of the remodeling enzyme to the end product of the reaction.

In the following, I characterized the kinetic properties of the DNA methyltransferase Dnmt1 in the context of chromatin. DNA methylation is an important epigenetic modification required for a variety of DNA associated processes. Dnmt1 is responsible for the maintenance of methylation patterns. In a second wave of DNA methylation following DNA replication, Dnmt1 needs to access nucleosomal DNA. Using an *in vitro* approach, I demonstrated that Dnmt1 requires a minimal length of DNA overhangs to bind to mononucleosomes. Furthermore, *in vitro* mapping of Dnmt1 interactions with its nucleosomal substrate suggests that Dnmt1 needs to contact flanking DNA as well as nucleosomal DNA for efficient binding. Finally, I could show that Dnmt1 methylation activity is inhibited within the nucleosomal core region. Interestingly, addition of recombinant ATP-dependent chromatin remodeling factors abolish the inhibitory effect of the nucleosome, most likely by rendering the nucleosomal DNA accessible to Dnmt1.

Taken together, these results suggest a major role for chromatin remodeling enzymes in nucleosome positioning which in turn might be crucial for epigenetic DNA modifications such as DNA methylation.

Zusammenfassung

Im eukaryotischen Zellkern liegt die DNA in stark kondensierter Form vor. Die erste Ebene der Chromatin-Kompaktierung wird durch die Windung der DNA um ein Histonoktamer erreicht, wobei ein sogenanntes Nukleosom gebildet wird. Zur Gewährleistung eines effizienten DNA Metabolismus, wie DNA Replikation, -Transkription, -Reparatur und -Rekombination müssen die entsprechenden Sequenzen zugänglich sein. Aus diesem Grund müssen Nukleosomen hoch-dynamisch sein, was von ATP-abhängigen "Chromatin Remodeling"-Komplexen sichergestellt wird. Jedoch bleibt es bisher unklar, in welchem Ausmaß diese Enzyme von der lokalen DNA Sequenz beeinflußt werden, wenn sie ein Nukleosom zu verschiedenen Positionen dirigieren.

In meiner Doktorarbeit habe ich mich mit ATP-abhängigen Chromatin Remodeling Faktoren beschäftigt, wobei der Fokus auf deren molekularen Wirkungsmechanismen in Abhängigkeit von der lokalen DNA Sequenz lag. Ich konnte zeigen, dass jedes individuelle Chromatin Remodeling Enzym spezifische Eigenschaften zur Nukleosomen-Positionierung besitzt. Der Endpunkt der Nukleosomen-Translokation wird hierbei durch die lokale DNA Sequenz und zusätzliche Proteinuntereinheiten des Remodeling Komplexes bestimmt. Weiterhin konnte ich für zwei spezifische Motorproteine nachweisen, dass die Nukleosomen-Positionierung durch eine verminderte Bindungsaffinität der Enzyme zum Endprodukt bestimmt wird.

Im weiteren Verlauf meiner Arbeit charakterisierte ich die kinetischen Eigenschaften der DNA Methyltransferase 1 (Dnmt1) am nucleosomalen DNA-Substrat. DNA Methylierung ist eine epigenetische Modifikation, die für verschiedene DNA-basierte Prozesse essentiel ist. Dnmt1 ist für die Aufrechterhaltung des Methylierungsmusters im Anschluß an die DNA Replikation verantwortlich. Dabei benötigt Dnmt1 Zugang zu nucleosomaler DNA. Anhand eines *in vitro* Ansatzes konnte ich zeigen, dass Dnmt1 eine an das Nukleosom angrenzende minimale Länge von DNA-Überhängen ("Linkern") benötigt, um an Mono-Nukleosomen binden zu können. Weiterhin zeigten Dnmt1 *in vitro* "Mapping"-Experimente Interaktionen mit dem nukleosomalen Substrat; ein Hinweis, dass Dnmt1 für eine effiziente Bindung sowohl den Kontakt zu flankierenden DNA-Sequenzen als auch zu nukleosomaler DNA benötigt. Ferner konnte ich nachweisen, dass die katalytische Aktivität von Dnmt1 in der Nukleosomenkern-Region stark vermindert ist. Die Zugabe von Remodeling Komplexen zum nukleosomalen Reaktionsansatz stimulierte die enzymatische Dnmt1 Gesamt-Aktivität auf das an freien DNA-Substraten gemessene Ausgangsniveau. Zusammenfassend zeigen diese Resultate die spezifische und präzise Positionierung von Nukleosomen durch Chromatin Remodeling Enzyme und den damit verbundenen wichtigen Einfluss auf epigenetische Modifikationen wie die DNA Methylierung.

B. Introduction

I. THE CHROMATIN STRUCTURE

1. In General

The evolution of multi-cellular organisms demands for functional specialization of individual cells and therefore differential gene expression. The linear length of approximately two meters DNA as well as the complexity of eukaryotic genomes confront the cell with several topological challenges. Genomic DNA has to be tightly condensed to fit into the sub-cellular compartment of the nucleus but simultaneously the genetic information has to be readily accessible. Eukaryotic cells fulfill these requirements by organizing genomes into a structure called chromatin, a compact but highly dynamic nucleoprotein complex. The term "chromatin" (greek: color) was first introduced by Walter Flemming in 1982 (Flemming, 1982). In his work, Flemming defined "chromatin" as the "stainable substance of the nucleus". Its accessibility is important for DNA binding factors. Chromatin represents the functional state of eukaryotic genomes and thereby serves as natural substrate for all kinds of DNA-dependent processes. Such are the control of gene expression, as well as DNA replication, recombination and repair (Felsenfeld and Groudine, 2003; Khorasanizadeh, 2004).

The dynamic of chromatin is regulated by a variety of related mechanisms: ATP-dependent nucleosome remodeling (Becker and Hörz, 2002; Tsukiyama, 2002; Varga-Weisz and Becker, 2006), post-translational modifications of histones, (Fischle, 2008; Fischle *et al.*, 2003a; Fischle *et al.*, 2003b; Vaquero *et al.*, 2003) the exchange of canonical histones through histone variants and in certain eukaryotes DNA methylation (Bernstein and Hake, 2006). These modulations influence chromatin structure by regulating the accessibility of nucleosomal DNA, and thereby regulating DNA-dependent cellular processes.

1.1. The nucleosome - basic packaging unit of chromatin

The nucleosome core particle (NCP) represents the basic structural unit of chromatin (Oudet *et al.*, 1975), harboring a molecular weight of 210 kDa (Kornberg, 1974) (see Fig. 1). In 1997, a detailed structure of a nucleosome core particle at high resolution was provided by X-ray crystallography (Luger *et al.*, 1997; Richmond and

Davey, 2003). The terminology "nucleosome core particle" is now used to refer to a nucleosome consisting of 147 bp +/- 2 or 3 bp of DNA, that are wrapped in 1.67 left-handed superhelical turns around a disc-like histone protein core (Luger *et al.*, 1997). In the presence of DNA or at high salt concentrations, two copies each of the four core histone proteins H2A, H2B, H3 and H4 assemble to form the octamer from which the unstructured histone tails protrude (Luger and Richmond, 1998; Lusser and Kadonaga, 2004). The core histones are small basic proteins (11-16 kDa) that are among the best-conserved eukaryotic proteins. They are bipartite proteins, composed of a carboxy-terminal globular domain and a less structured N-terminal domain. The globular domain consists of a characteristic ternary structure called "histone fold" motif formed by three α-helices connected by two loops. The intermolecular interaction of histone folds occurs in a "handshake"-like manner resulting in H2A/H2B and H3/H4 dimers (Davey *et al.*, 2002; Luger *et al.*, 1997). The highly basic N-terminal domains ("tails") that extend from the surface of the nucleosome serve as targets for post-translational modifications and are important for higher order chromatin structure (Fischle *et al.*, 2003a; Vaquero *et al.*, 2003). These structural components organize the nucleosomal DNA and mediate both intranucleosomal and internucleosomal interactions (Luger, 2006; Richmond and Davey, 2003).
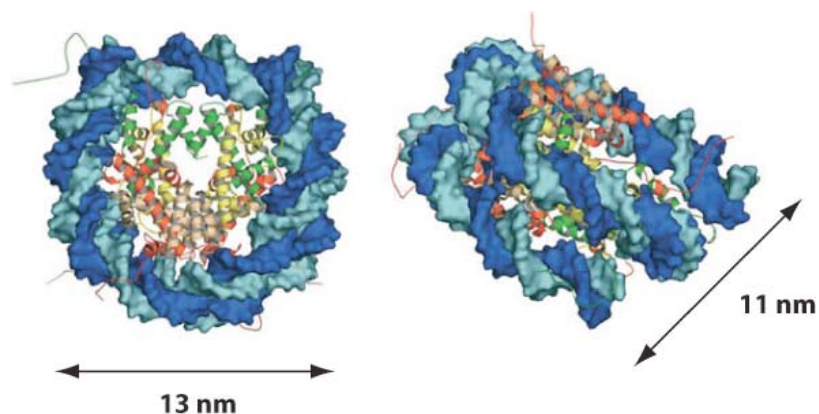
Figure 1: The nucleosome core particle
Structure of the "nucleosome core particle". 147 bp DNA (blue) are wrapped around the histone octamer that is composed of two copies each of histone H2A (red), H2B (pink), H3 (green) and H4 (yellow) to form a "nucleosome core particle" (adapted from (Khorasanizadeh, 2004)).

1.2. Chromatin higher order structures

In eukaryotic genomes the packaging of DNA into chromatin can be divided into several hierarchal levels. Nucleosomes are usually connected by short stretches (10-80 bp) of linker DNA, depending on the species and tissue, which enters and exits the

nucleosome at sites close to each other, referred to as the entry/exit site. *In vivo*, the majority of nucleosomes are bound by a fifth histone, the linker histone H1. It binds additional 20 bp on DNA at the entry/exit site of the nucleosome (Wolffe, 1997; Wolffe and Kurumizaka, 1998).

At low salt concentrations, extended nucleosomal arrays form the "beads-on-a-string"-like structure called 10 nm fiber where the nucleosomes represent the beads and the DNA the string (Olins and Olins, 1974) (van Holde, 1996), (Fig. 2A and B). This nucleosomal repeat ("array"), that allows a 6 to 7-fold compaction is considered the primary level of chromatin structure, but cannot account for the organization observed in the cell's nucleus.
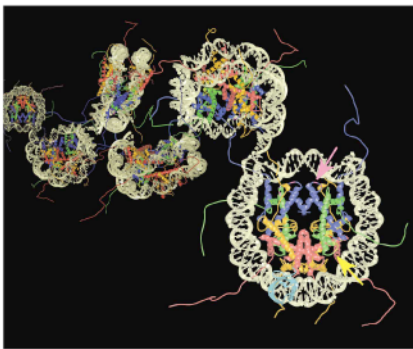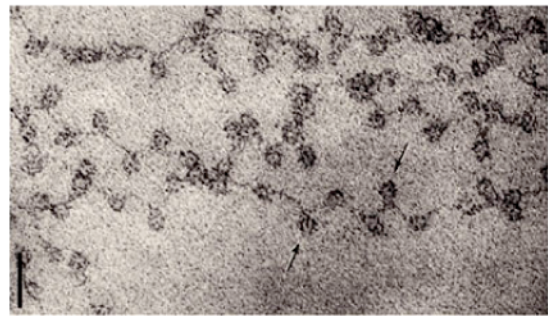
Figure 2: "Beads-on-a-string"
A) Structural model of nucleosomal DNA forming the 10 nm fiber (adapted from (Luger, 2002)). B) Electron micrograph showing the 10 nm fiber "beads-on-a-string" (adapted from (Olins and Olins, 2003)).

The 30 nm fiber, the second level of chromatin compaction, is formed at physiological salt concentrations. The formation of these folded nucleosomal arrays is facilitated by the presence of linker histones (Clark and Kimura, 1990), in a way that binding induces the formation of the 30 nm fiber, as demonstrated in numerous *in vitro* studies (Allan *et al.*, 1980a; Allan *et al.*, 1980b; Felsenfeld and McGhee, 1986; Graziano *et al.*, 1996; Ramakrishnan, 1997; Thomas and Butler, 1980). For complete fiber compaction a basic patch on the H4 tail, residues 16-20, is essential, most likely because of its interaction with an acidic patch of the H2A/H2B dimer of the neighboring nucleosomes (Davey *et al.*, 2002; Dorigo *et al.*, 2003; Luger *et al.*, 1997).

The exact structure of the 30 nm fiber is still under debate. Two competing, but not necessarily exclusive models have been proposed: the "solenoid model" and the "zig-zag" or "crossed-linker model".
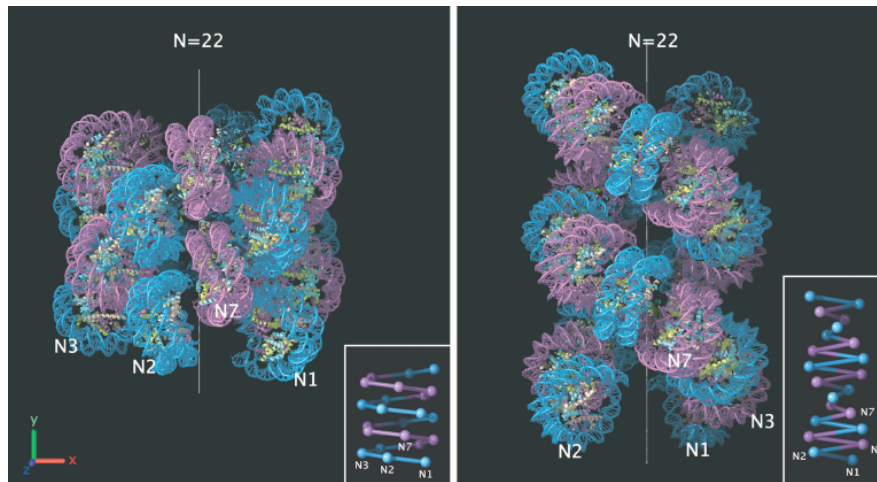
Figure 3: Schematic representation of two different topologies for the 30 nm fiber
Structural predictions of the 30 nm fiber. Two different topological models: "Solenoid helix" (Left): The interdigitated one-start helix. According to this model, neighboring nucleosomes follow each other along the same helical path, "Zig-Zag helix" (Right): A two-start helix with neighboring nucleosomes crossing between two helical stacks adapted from (Robinson and Rhodes, 2006).

According to the first model, successive nucleosomes follow each other along the same helical path, thereby forming a one-start helical structure (6 to 8 nucleosomes/turn). Under these conditions linker DNA has to be bent to allow fiber formation (Finch and Klug, 1976; Robinson and Rhodes, 2006; Routh *et al.*, 2008), (Thoma *et al.*, 1979; Widom and Klug, 1985). The second model proposes, that consecutive nucleosomes are connected by straight linkers and nucleosomes alternate between two helical stacks in a zig-zag arrangement, resulting in a two-start helix (Bednar *et al.*, 1998; Dorigo *et al.*, 2004; Khorasanizadeh, 2004). These alternate packaging would result in a more compact 30 nm fiber (Woodcock and Dimitrov, 2001).

A low-resolution crystal structure of a tetranucleosome strongly supports the "zig-zag model", because it showed nucleosomes alternating between two stacks of two nucleosomes (Schalch *et al.*, 2005). A recent study provided good arguments for a third, interdigited structure (Robinson *et al.*, 2006; Robinson and Rhodes, 2006). It is important to point out, that the obtained data did not demonstrate that the 30 nm fiber really exists *in vivo*. All studies performed until now, were done by using *in vitro* systems or on purified fibers. The structure could not be observed up to now in sections of whole nuclei (Tremethick, 2007). Alternative structures of the 30 nm fiber could exist *in vivo*,

depending on the linker DNA length and the presence of linker histones (Robinson and Rhodes, 2006).

Packaging into the 30 nm fiber compacts DNA by a factor of 30 to 40. Further chromatin compaction beyond the 30 nm fibers (tertiary structures) is poorly understood (Felsenfeld and Groudine, 2003), (Fig. 4A and B). Different biophysical studies give evidence, that chromatin fibers could be further organized into large domains by attaching to an underlying supporting structure. This structure called "nuclear scaffold" or "nuclear matrix" consists of RNA and proteins (Fisher and Merkenschlager, 2002; Hancock, 2000). Scaffold or matrix attachment regions (S/MARs) are found every 5-200 kb in eukaryotic genomes and are believed to organize chromatin into distinct domains by dynamic binding to the nuclear matrix. However, the existence of a rigid nuclear scaffold is still controversial (Bode *et al.*, 2003).

A
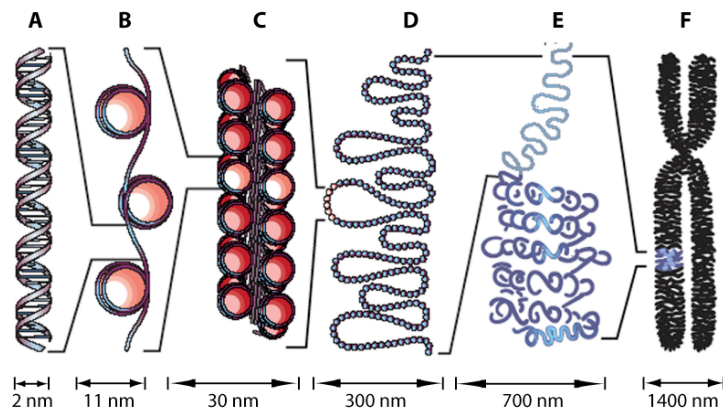
B
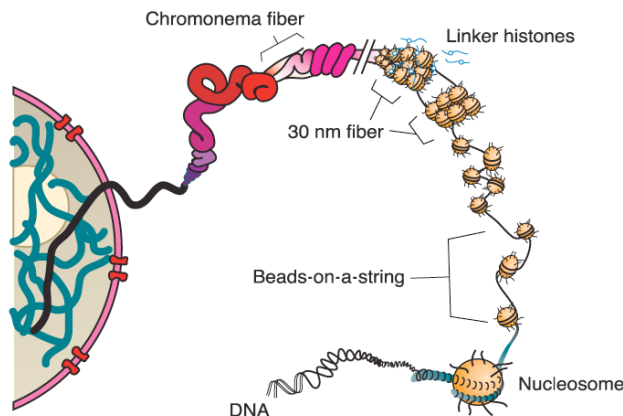
Figure 4: Miscellaneous view of chromatin fiber condensation
A) Different levels of chromatin compaction. The DNA double helix structure (A) is wrapped in 1.67 superhelical turns around the histone octamer to form the "nucleosomal array" (B). This "beads-on-a-string"-like structure is

further folded into the 30 nm fiber (C) and higher order chromatin structures (D and E), finally forming the highest condensed structure of mitotic chromosomes (adapted from (Felsenfeld and Groudine, 2003)). B) Alternative model illustrating chromatin organization in the nucleus. The different steps involved in the folding of nucleosomal arrays into maximally folded chromatin fibers are shown (adapted from (Horn and Peterson, 2002)).

1.3. Compartmentation of chromatin within the nucleus

Chromatin is evenly dispersed throughout the nucleus of eukaryotic cells with the exception of cell division when chromatin is highly condensed to form individual chromosomes. Despite this distribution, chromatin appears to be organized in more and less condensed regions (Pederson, 2004). Distinct compartments within the cell nucleus suggest influencing the functional activities of chromatin (Baxter *et al.*, 2002; Cremer *et al.*, 2001; Cremer and Cremer, 2001). A gene locus might become transcriptional active if it is arranged within an open, accessible chromatin domain. Contrary, transcriptional silencing could more easily occur if a locus is relocated to a compact chromatin environment (Chubb and Bickmore, 2003).

Emil Heitz cointed the terms "euchromatin" and "heterochromatin" (Heitz, 1928; Passarge, 1979; Zacharias, 1995). He hypothesized that "euchromatin is genetically active and gene-rich, whereas heterochromatin is genetically passive and harbors less genes", Figure 5. These simplistic principles remain rather close to the current categorization of "euchromatin" and "heterochromatin": Heterochromatic domains, generally gene poor, are less accessible for DNA binding factors due to their highly condensed regions that are mostly transcriptional inactive (Fisher and Merkenschlager, 2002; Grewal and Elgin, 2002; Grewal and Moazed, 2003). Euchromatin is defined by a less condensed state, harboring a more nuclease sensitive configuration and more transcriptional active regions.
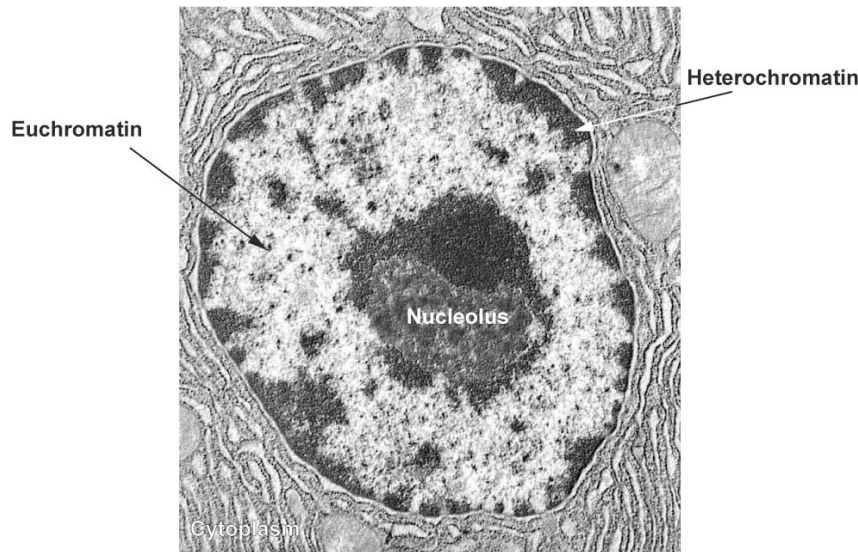
Figure 5: Functional compartments of the vertebrate cell nucleus
"Euchromatin" and "Heterochromatin" formation in the cell nucleus. A nucleolus is surrounded by electron-dense heterochromatin, which is also localized at the nuclear periphery. Contrary, the electron-permeable euchromatin can be found in the more central domains (after Kenneth M. Bart, Hamilton College, New York).

Furthermore, both chromatin configurations differ in their replication timing: Euchromatin is replicated earlier in S-phase, whereas heterochromatin becomes replicated in mid to late S-phase. For heterochromatin there exists a further sub-categorization into constitutive and facultative forms (Brown, 1966). Constitutive heterochromatin is generally poor in genes and occurs mainly in repetitive sequences, e.g. satellite centromeric and pericentromeric repeats as well as telomeric regions. Apart from being replicated in late S-phase, these regions are modified by H3K9me3 and H4K20me3. The histone methyltransferase Suv39h1 as well as HP1, which binds specifically to H3K9me3, are localized therein (Bannister *et al.*, 2001; Maison *et al.*, 2002). Further, centromeric regions of constitutive chromatin are characterized by the presence of the specific histone variant CENP-A, substituting histone H3 (Bernstein and Hake, 2006).

In contrast, facultative heterochromatin is formed by DNA regions that are transcriptionally silenced by regulatory mechanisms like extracellular stimuli, cell cycle and developmental stage. Prominent examples for silencing of facultative heterochromatin regions are "X-inactivation" in female mammals, "Mating type locus silencing" in yeast, "Position effect variegation" in *Drosophila*. "Position effect variegation" is the term used to describe silencing of a gene if it is localized within heterochromatin. In spite of this it becomes transcriptional active if the same gene is located away from chromatin (Wilson *et al.*, 1990). Little is known about the stochastic

on/off gene expression, but it is suggested, that occasional "spreading" of the condensed heterochromatin into euchromatic regions alters the chromatin structure, resulting in gene inactivation (Reuter and Spierer, 1992; Schotta *et al.*, 2003).

The described heterochromatic domains are further associated with a variety of factors, histone modifications and specific histone variants. Additionally, interplay between chromatin remodeling, histone modification, DNA methylation and also the RNAi machinery seems to be important for the formation and maintenance of the heterochromatic state of chromatin (Vermaak *et al.*, 2003).

2. Nucleosome assembly

The coordinated packaging of DNA into a nucleosome is called "nucleosome assembly". To precisely direct this staged process, the deposition of the basic histone proteins onto the negatively charged DNA, suitable machinery is needed. These are specialized factors, like histone chaperones ("histone-transfer vesicles") and ATP-dependent machines that exactly deposition histones, e.g. ACF and CHRAC (Fyodorov and Kadonaga, 2002; Haushalter and Kadonaga, 2003; Kadam and Emerson, 2002). Two main assembly pathways have been described: As mentioned above, the majority of histones are expressed during S-phase and then deposited during DNA replication, a process mediated by histone chaperone CAF-1 (<u>c</u>hromatin <u>a</u>ssembly <u>f</u>actor <u>1</u>, (Smith and Stillman, 1989) with which ASF1 (anti-silencing function 1) (Mello *et al.*, 2002; Tyler, 2001) or RCAF (<u>r</u>eplication-<u>c</u>oupling <u>a</u>ssembly <u>f</u>actor) synergizes (Vaquero *et al.*, 2003). The replication-independent deposition of histone variants is mediated by different complexes. Histone H3.3 has been found to be deposited by the HIR/HIRA (<u>hi</u>stone <u>r</u>egulation) complex (Ray-Gallet *et al.*, 2002; Tagami *et al.*, 2004), whereas the deposition of H2A.Z is mediated by the SWR1 complex (Korber and Hörz, 2004; Mizuguchi *et al.*, 2004). Apart from histone deposition, histone chaperones are important for histone transport and storage, e.g. NAP1 (nucleosome assembly protein-1; (Mosammaparast *et al.*, 2002) and Nucleoplasmin (Akey and Luger, 2003; Wolffe, 1998). Chromatin assembly itself is a two-step process: At first a histone $(H3-H4)_2$ tetramer is deposited on the DNA, thereby forming a tetrasome (Smith and Stillman, 1989; Worcel *et al.*, 1978). Subsequently, two H2A-H2B dimers (Jackson, 1990; Wolffe and Kurumizaka, 1998) are placed on each side of the tetrasome. A model according to

which H3 and H4 can be deposited as dimers rather than tetramers has also been proposed (Tagami *et al.*, 2004).

II. MODIFICATIONS IN CHROMATIN

The many levels of chromatin condensation provide the cell with a way of organizing its genome into the nucleus but also play an important role in regulating the accessibility of DNA sequence. Chromatin mostly exists in a highly ordered state and the unfolding of the highly condensed chromatin fiber to the 10 nm nucleosomal filament seems to be transient and/or spatially restricted (Widom, 1998). Hence, to allow the DNA-mediated processes, chromatin needs to be highly dynamic. There are two main states of changing the chromatin configuration: transiently, e.g. temporary alterations of transcription, or permanently. The latter, which implies the propagation of the chromatin state to daughter cells, is commonly referred to as "epigenetic memory" (Allis *et al.*, 2007). Several principles, frequently acting in concert with each other are used for the alteration of chromatin structure. Firstly, histone tails can suffer covalent posttranslational modifications (see section B.I.1.1.). An additional principle is the substitution of canonical histones by histone variants (see section B.I.1.2). Furthermore, enzymes that utilize the energy of ATP hydrolysis to alter canonical histone-DNA interactions alter the chromatin structure as well (see section B.I.2; reviewed in (Becker and Hörz, 2002; Henikoff *et al.*, 2004). Finally, DNA methylation at the ^{5}C of its base components is known as the most stable epigenetic mark. This modification will be described in detail in section B.II.4.

1. Histone modifications

1.1. Posttranslational modifications of histones

A multitude of posttranslational modification (PTMs) of the core histones are mostly attached at, but not limited to, amino acids at the flexible N-terminal domains (Kouzarides, 2007). Among these PMTs are methylation of lysines (mono-, di-, and trimethylation) and arginines (mono-, asymmetrical and symmetrical dimethylation), acetylation of lysines, ubiquitinylation of lysines, phosphorylation of serines and threonines, SUMOylation and ADPribosylation (Bonisch *et al.*, 2008; Cosgrove *et al.*, 2004; Fischle *et al.*, 2003b; Vaquero *et al.*, 2003).

Figure 6 shows a summary of the known histone modifications. Histone modifications like histone methylation and histone acetylation have already been identified more than 40 years ago (Allfrey *et al.*, 1964; Murray, 1964). They serve as markers for the chromatin environment, being involved in the regulation of chromatin structure as well as in the control of gene activity (Iizuka and Smith, 2003; Khorasanizadeh, 2004).
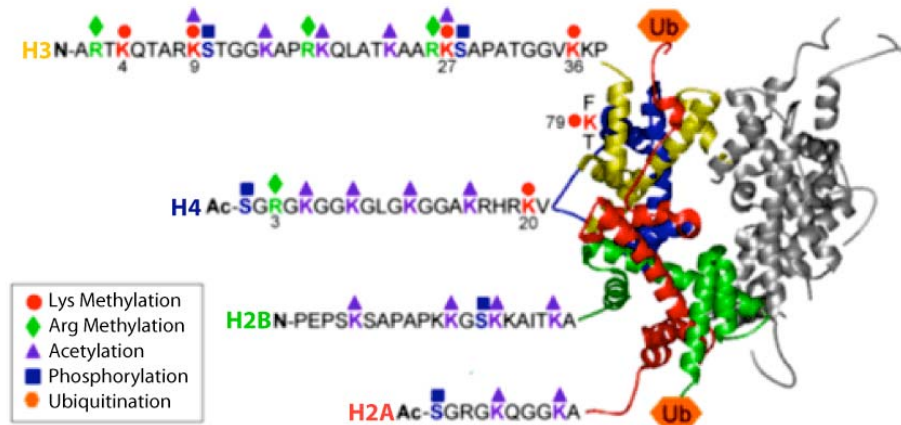
Figure 6: Posttranslational modifications of histones
Illustration of the histone octamer of the NCP. Specific amino acid sites of posttranslational modifications (acetylation, phosporylation, ubiquitinylation and methylation) that are known to occur on histones are indicated by colored symbols: H4 (blue); H3 (yellow) H2A (red), H2B (green) (After Briggs http://www.ag.purdue.edu/biochem/Pages/sdbriggs.aspx).

Specific enzymes establish and erase histone modifications, for instance histone acetyltransferases (HATs), histone deacetylases (HDACs), histone methyltransferases (HMTs) and histone demethylases (HDMs) (reviewed in Jenuwein, 2001; Bonisch, 2008). Until recently, with the discovery of enzymes that demethylate histone tails, methyl marks, established by histone methyltransferases were considered to be stable and irreversible. Histone arginine deiminases (e.g. PAD4), arginine demethylases (e.g. JMJD6) and lysine-specific demethylases (e.g. LSD1) are examples for these families (Shi *et al.*, 2004), (Chang *et al.*, 2007; Klose *et al.*, 2006a; Klose *et al.*, 2006b; Wang *et al.*, 2004).

The covalent histone modifications change the structural properties of histones or modify the interactions of the histone tails. This could affect histone-DNA interactions within the same or neighboring nucleosome. The acetylation of histone H4 on lysine 16 (H4K16Ac) is a prominent example for preventing complete chromatin compaction (Robinson *et al.*, 2008; Shogren-Knaak *et al.*, 2006). However, this could also happen indirectly through the recruitment of specific "readers" (effector molecules), Figure 7.

Several modifications serve as targets for protein recognition modules, e.g. the chromodomain that recognizes methylated lysine (Jacobs and Khorasanizadeh, 2002) or the bromodomain that interacts with acetylated lysine (Jacobson *et al.*, 2000).
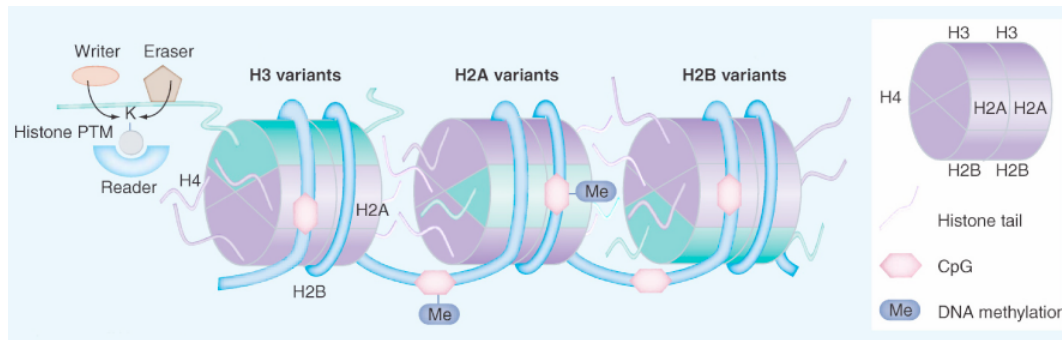
Figure 7: Schematic illustration of the components that constitute chromatin
The DNA strand harbors CpG dinucleotides that can be methylated (blue). Variants of the core histones (H2A, H2B, H3) are depicted in green. Posttranslational modifications (PTM) of histones are set by a "writer", deleted by an "eraser" and can be recognized by "readers" that bind to specific epitopes (adapted from (Bonisch *et al.*, 2008)).

The "histone code" hypothesis suggests that a specific combinatorial set of histone modification marks either in "*cis*" (on same tail) or in "*trans*" (on proximal tails) can trigger the recruitment of particular transacting factors (effector proteins). A modification by itself would at times have consequences on itself, but mostly it would depend on the context of other modifications. This would subsequently result in the mediating of specific functions (Jenuwein and Allis, 2001; Turner, 2002). This implies that the modification of histone tails largely broadens the information of the genetic code.

1.2. Histone variants

Apart from histone modifications, nucleosomes can also contain variants of the core histones, H2A, H2B, H3 and H1, so called replacement histones. For histone H4, no variants have been reported so far. Depending on the complexity of the organism, the number of histone variants increases (Hake and Allis, 2006). The difference between individual histone variants is determined by their amino acid composition, mainly in the N-terminus and their induction of specialized functions to the nucleosomes. Generally, several histone variants are enriched in specific chromosomal locations and/or can modulate the nucleosome structure (Henikoff *et al.*, 2004). Until now, the best-characterized histone variants are the H2A variants. In *Drosophila melanogaster* the H2Av variant is required for heterochromatin formation; in mammals

H2A.X is involved in DNA double-strand break repair and the H2A.Z variant is essential for survival (Redon *et al.*, 2002; Swaminathan *et al.*, 2005). MacroH2A, a histone H2A variant harboring a C-terminal extension of 25 kDa, is enriched in the nucleosomes of inactive X-chromosomes (Costanzi and Pehrson, 1998). Further, nucleosomes containing H2A variants such as H2A.X and H2A.Z form specialized chromatin structures, thereby affecting DNA repair, gene silencing and chromatin remodeling (Ausio, 2006; Dhillon and Kamakaka, 2002; Santisteban *et al.*, 2000).

The histone H3 variant H3.3 accumulates on highly transcribed regions like active rDNA arrays and therefore correlates with transcriptional activity (Ahmad and Henikoff, 2002). In contrast to canonical histones, that are expressed during S-phase and deposited during DNA replication, histone variants are synthesized throughout the cell cycle and deposited independent of DNA replication. Another H3 variant, the centromeric-specific CENP-A (<u>cen</u>tromeric <u>p</u>rotein <u>A</u>), seem to be smaller and less stable than canonical ones (Dalal *et al.*, 2007a; Dalal *et al.*, 2007b; Palmer *et al.*, 1991).

2. Chromatin dynamics

In order to fine-tune the gene expression level between a fully active and a fully repressive state in dependence of the temporal cellular context, eukaryotes have developed highly progressive systems. A fluid state of chromatin is necessary to enable DNA-dependent processes. This dynamic balance between genome packaging and genome access is enabled by the tight interplay between histone modifying enzymes with "ATP-dependent nucleosome remodeling factors". Members of this enzyme family utilize the energy of ATP-hydrolysis to alter DNA-histone interactions within the nucleosome (Becker and Hörz, 2002). This mobilizes histone octamers and exactly positions them on regulatory elements, thereby inhibiting or arranging regulatory factors access to their specific sites. All identified ATP-dependent chromatin remodeling factors form multiprotein complexes, consisting of a related motor protein that belongs to the Snf2 family of ATPases (Bao and Shen, 2007; Eberharter and Becker, 2004; Eisen *et al.*, 1995) and additional subunits. The Snf2 family belongs to the DEAD/H superfamily of DNA-stimulated ATPases (Eisen *et al.*, 1995; Peterson and Logie, 2000), which can be further divided into multiple subfamilies. Recently a catalogue of over 1300 Snf2 family members was assembled based on a phylogenetic approach. The categorization into 24 distinct subfamilies was done by sequence alignment of the helicase-related

regions (Figure 8). This study further revealed that all eukaryotes contain members of multiple subfamilies (11 subfamilies were ubiquitous represented in eukaryotic genomes), whereas they are less common and not ubiquitous in bacteria and archaea. Almost all Snf2 family proteins were identified as ATP-dependent ATPases. Several members have been linked to diseases and some are even essential for survival. Snf2 family proteins participate in many biochemical processes in the nucleus, most frequently chromatin packaging (Flaus *et al.*, 2006).
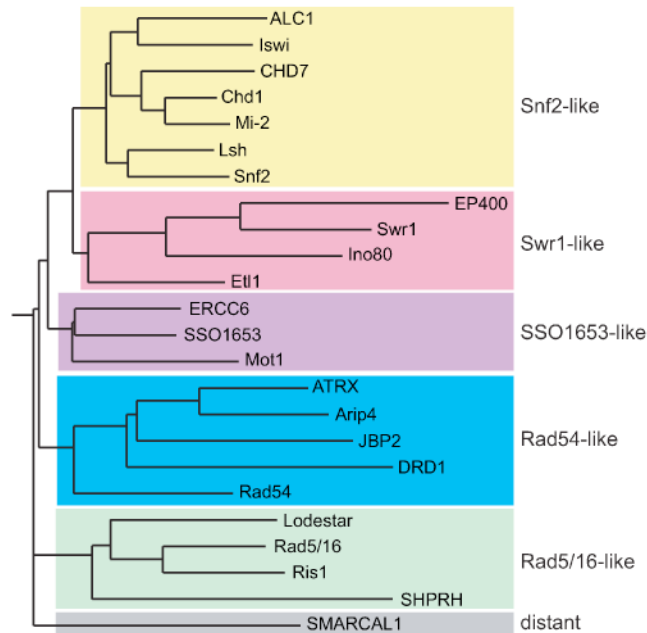
Figure 8: SNF2 family of ATPases
Illustration of the relationship between subfamilies. This was based on a HMM (Hidden Markov model) profile for full-length alignments of helicase regions. Grouping into subfamilies is indicated by coloring (after (Flaus *et al.*, 2006)).

According to the sequence alignment of the helicase-like regions, the subfamilies fall into 5 distinct groups, which are closely related (see Figure 8): Snf2-like, Swr1-like, SSO1653-like, Rad54-like and Rad5/16-like (Flaus *et al.*, 2006).

The effects of the remodeling reaction are determined by the ATPase and the associated regulatory subunit. A number of different reactions are catalyzed by remodeling factors. They have been described to introduce conformational changes to the nucleosome, to reposition nucleosomes along the DNA ("sliding"), to assist nucleosome assembly, to exchange H2A/H2B dimers and to evict entire nucleosomes (Becker and Hörz, 2002; Li *et al.*, 2007; Lusser and Kadonaga, 2003) (Fig. 9A and 9B). *In vivo,* chromatin remodeling factors are involved in processes such as chromatin

assembly, transcription and DNA repair. Inaccurate nucleosome remodeling leads to transcriptional deregulation and diseases, e.g. cancer (Kadam and Emerson, 2002; Kadam and Emerson, 2003; Wang *et al.*, 2007a; Wang *et al.*, 2007b). The fact that chromatin remodeling factors are highly conserved from yeast to human, highlights their necessity for chromatin regulation (Eberharter and Becker, 2004).

In the following section I will give a detailed description on specific chromatin remodeling factors that are important for the present work: The SNF2 subfamily, the Chd1 family and the ISWI family that belong to the Snf2-like group, whereas the Ino80 class is a member of the Swr1-like group (Figure 10). Further information on the different members of the subfamilies and the specific categorization can be found in Flaus *et al.* (Flaus *et al.*, 2006) or http://www.snf2.net.

A
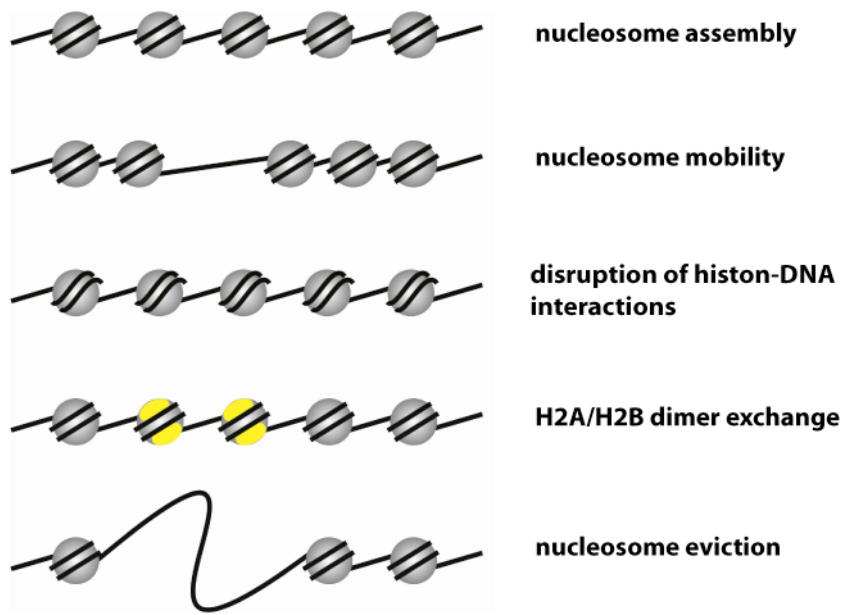
B
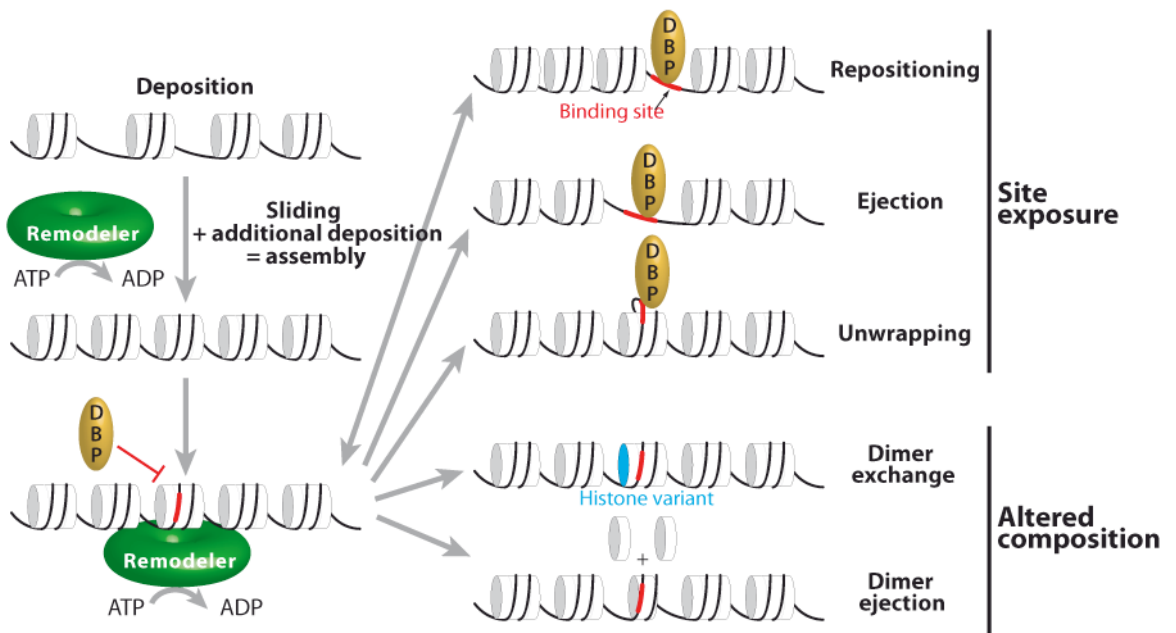
Figure 9: Reactions catalyzed by ATP-dependent chromatin remodeling factors

A) Graphic illustration of enzymatic properties attributed to ATP-dependent chromatin remodeling factors (kindly provided by Verena Maier). B) Schematic representation of divers reactions catalyzed by chromatin remodeling factors. Remodelers (green) assist in chromatin assembly by moving already deposited histone octamers (A). The remodeling activity on a nucleosome array results in various products that can be classified in two categories: (B) a DNA-binding protein (DBP) (red) becomes accessible by "nucleosomal sliding" (repositioning), or "nucleosomal eviction" (ejection), or local unwrapping, and (D) altered histone composition, in which the nucleosome content is modified by dimer replacement [exchange of H2A-H2B dimer with a histone variant (blue)] or through dimer ejection (adapted to (Clapier and Cairns, 2009)).
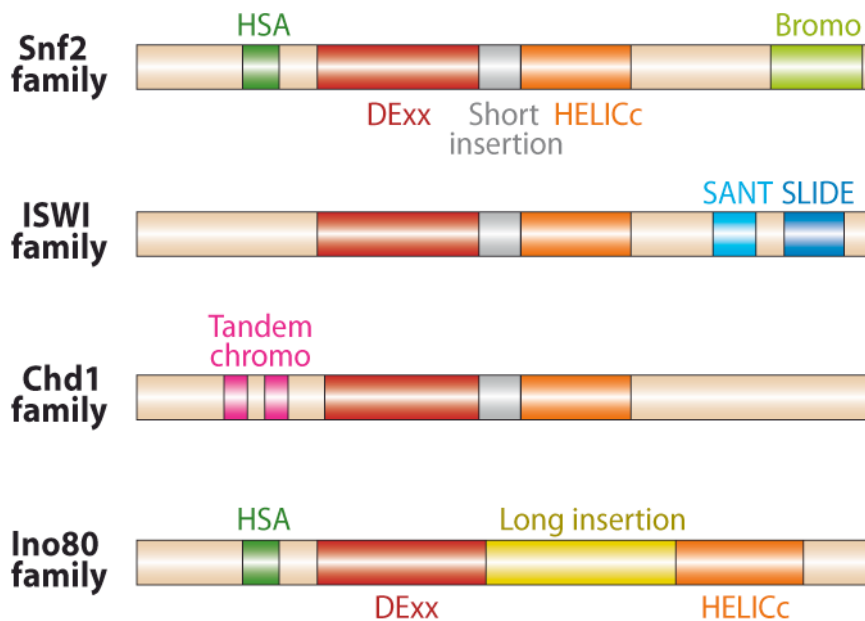
Figure 10: SNF2 family of ATPases

B) DEAD/H superfamily of Snf2-like ATPases. Subdivision of remodeling families according to their ATPase domain. All remodeler families share an SNF2-family ATPase subunit characterized by a split ATPase domain: 1. DExx (red) and HELICc (orange). Each family differs in the unique domains residing within, or adjacent to, the ATPase domain. Remodelers of the Snf2 (SWI/SNF), ISWI, and Chd1 families each have a specific short insertion (grey) within the ATPase domain, whereas remodelers of Ino80 family harbor a long insertion (yellow). Further definition is achieved by the presence of distinct combinations of flanking domains: 1. Bromodomain (light green) and 2. HSA (helicase-SANT) domain (dark green) for Snf2 family; 1. SANT-SLIDE module (blue) for ISWI family; 1. tandem chromodomains (pink) for the Chd family; and 1. HAS domain (green) for the Ino80 family (adapted from (Clapier and Cairns, 2009)).

2.1. Important chromatin remodeling subfamilies for this study

2.1.1. THE SNF2 FAMILY

The first ATP-dependent remodeling complex, SWI/SNF, was identified through a genetic screen in yeast for mutations interfering with mating type <u>switch</u>ing (SWI) and <u>s</u>ucrose <u>n</u>on-<u>f</u>ermentation (SNF). It was suggested that the SWI and SNF genes could be components of the same multi-subunit complex. Through this screening, the 11 subunits of the SWI/SNF complex including its ATPase SWI or SNF2 were purified and identified (Peterson and Herskowitz, 1992; Smith *et al.*, 2003; Sudarsanam and Winston, 2000). SWI/SNF type ATPases harbour a bromodomain, which might target them to acetylated chromatin (Marmorstein and Berger, 2001). A connection with chromatin was established while observing that the purified yeast SWI/SNF complex binds both DNA and nucleosomes with high affinity and alters the chromatin structure in an ATP-dependent manner (Vignali *et al.*, 2000). SWI/SNF catalyses the movement of nucleosomes ("nucleosome sliding") of DNA in *cis* (Whitehouse *et al.*, 1999). *In vivo*, SWI/SNF is required both for transcriptional activation and repression of selected genes (Holstege *et al.*, 1997) (Sudarsanam and Winston, 2000). It often cooperates with histone acetyltransferase complexes to activate transcription. The interaction with specific transcription factors targets it to specific genes.

The RSC complex (<u>R</u>emodels the <u>S</u>tructure of <u>C</u>hromatin) contains several subunits that are closely related to yeast SWI/SNF subunits (e.g. STH1/NSP1) with interchangeable ATPase domains (Laurent *et al.*, 1993), (Martens and Winston, 2003). RSC functionally differs from SWI/SNF complexes and is essential for growth (Cairns *et al.*, 1996). Studies suggest that RSC is involved in chromosome segregation (Hsu *et al.*, 2003) and can facilitate the loading of cohesins onto chromosomes (Huang *et al.*, 2004). Genome-wide studies revealed that RSC regulates many genes, including genes for RNA polymerase III promoters, small nucleolar RNAs and RNA polymerase II promoters (Ng *et al.*, 2002).

Two homologues of the SWI/SNF complexes were discovered in *Drosophila*, BAP and PBAP, both containing the ATPase Brahma. They differ in the associated subunits and are part of large multi-subunit complexes (Mohrmann and Verrijzer, 2005). Mammalian cells also posses two Snf2-like ATPases, mammalian BRM (<u>Bra</u>h<u>m</u>a) and Brg1 (<u>B</u>rahma <u>r</u>elated <u>g</u>ene product<u>1</u>) (Tsukiyama, 2002). They contain one of these proteins

as the central ATPase together with several tissue-specific subunits or additional subcomplexes (Carlson and Laurent, 1994; Martens and Winston, 2003; Wang, 2003). As in yeast, these complexes function in activation and repression of transcription (Martens and Winston, 2003; Sudarsanam and Winston, 2000). According to their subunit composition, different *in vitro* and *in vivo* properties have been described. Human BRM and Brg1 differ in their ability to remodel mononucleosomal core particles (Sif *et al.*, 2001). Brg1 and BRM as well as the core subunit SNF5 were demonstrated to have tumor-suppressive functions in both mice and humans (Wang *et al.*, 2007a).

2.1.2. THE CHD1 FAMILY

The first CHD (chromodomain, helicase, DNA binding) protein was purified from *Xenopus laevis*. The CHD subfamily is defined by two tandem repeats of chromodomains (Chromatin organization modifier) on the N-terminus in addition to an SNF2-related ATPase domain (Paro and Hogness, 1991; Tsukiyama and Wu, 1997). Chromodomains can bind to methylated histone tails, but functional analyses revealed a variety of possible interaction partners, not only histones, but also DNA and RNA (Brehm *et al.*, 2004).

Well-studied remodeling factors belonging to this family include the NURD ("NUcleosome Remodeling and Deacetylation") complex and the ATPase Chd1. NURD has been identified and isolated from various organisms such as *Drosophila*, *Xenopus* and human. CHD family members Mi-2α and Mi-2β (CHD3 and CHD4 respectively) have been recognized as components of the NURD. Apart from nucleosome remodeling and histone deacetylase enzymes (HDAC1/HDAC2), NURD is associated with further subunits, e.g. the methyl DNA binding proteins MeCP2 and MBD3 (methyl-binding domain 3), which target the complex to methylated DNA and couples ATP-dependent remodeling to histone deacetylation, resulting in gene silencing (Tyler *et al.*, 1999), (Bouazoune *et al.*, 2002; Bowen *et al.*, 2004; Brehm *et al.*, 2000; Flaus *et al.*, 2006). The *Drosophila* genome encodes a second putative protein besides dMi-2 that belongs to the Chd3/Chd4 subfamily: dCHD3. It shares both chromodomains, one of the conserved PHD fingers and the ATPase with dMi-2. Regions important for protein-protein interactions are missing or incomplete (Bouazoune and Brehm, 2005). A recent study has shown that dCHD3 is expressed as a nuclear protein during development and in adult females. It colocalizes with RNA polymerase II on polytene chromosomes and

exist as a monomer. Further it was biochemically characterized and shown that dCHD3 is stimulated by nucleosomes (Murawska *et al.*, 2008). Recently, a novel dMi-2 complex was purified from *Drosophila*. This two-subunit complex, *d*Mec (*Drosophila* MEP-1-containing complex) harbors the dMEP-1 protein and was shown to constitute the major dMi-2-containing complex. Recombinant dMec showed a nucleosome stimulated ATPase activity (Kunert *et al.*, 2009).

Chd1 is found as a monomer in yeast, *Drosophila* and mammals. Certain CHD remodelers (Chd1, CHD2) slide or eject nucleosomes thereby promoting transcription. The CHD family has been studied in detail (Delmas *et al.*, 1993; Tsukiyama, 2002). The ATPase Chd1 harbors DNA binding activity and plays a distinct role in the transcription process (Kelley *et al.*, 1999; Tran *et al.*, 2000). *Drosophila* Chd1 assists the formation of regularly spaced nucleosomal arrays *in vitro* and is required for the deposition of histone variant H3.3 *in vivo* (Konev *et al.*, 2007; Lusser *et al.*, 2005).

2.1.3. THE INO80 FAMILY

In contrast to the ATPase domains of other subfamilies, those of the Ino80 (INOsitol requiring 80) are bipartited by the insertion of a large spacer region (split ATPase domain) between the DExx and HELICc domain. In addition, the insertion serves as a binding platform for the helicase-related Rvb1/2 proteins (RuvB), separating DNA strands, and one actin-related ARP protein (Jin *et al.*, 2005; Shen *et al.*, 2000). Yeast Ino80.com consists of 15 subunits and is involved in DNA repair, recombination and transcription (Morrison *et al.*, 2004; Shen *et al.*, 2000; van Attikum *et al.*, 2004), (Papamichos-Chronakis *et al.*, 2006; Tsukuda *et al.*, 2005). Mutants of the Ino80 ATPase showed defects in transcription and increased sensitivity to DNA damaging agents (Shen *et al.*, 2000). Further Ino80 can alter chromatin structure *in vitro* (Ebbert *et al.*, 1999). Orthologues exist in *Drosophila* as well as in mammals.

2.1.4. THE ISWI FAMILY

The ISWI (Imitation SWItch) family of ATPases can be regarded as the subfamily most closely related to the SWI/SNF ATPases (Gangaraju and Bartholomew, 2007a; Gangaraju and Bartholomew, 2007b). Two domains characterize the ISWI ATPase, a SANT domain (switching-defective protein 3, adaptor 2, nuclear receptor co-repressor, transcription factor TF-IIIB), which is required for histone binding, and a SLIDE (SANT-

like ISWI domain) that is responsible for both DNA binding and complete ATPase activity (Clapier *et al.*, 2001; Fazzio *et al.*, 2005; Grune *et al.*, 2003; Hamiche *et al.*, 1999).

In general, all ISWI complexes share the property to catalyze nucleosome translocations. The first identified ISWI complexes NURF, CHRAC and ACF were purified from *Drosophila*. Biochemical studies suggest the ability of ISWI proteins to reposition rather than disrupt nucleosomes and to optimize nucleosomal spacing (Eberharter *et al.*, 2001; Ito *et al.*, 1997a; Ito *et al.*, 1997b; Tsukiyama and Wu, 1995; Varga-Weisz *et al.*, 1997).

The components of NURF are ISWI, the large regulatory subunit NURF301, the pyrophosphatase NURF38 and the WD40 protein NURF55 (Tsukiyama *et al.*, 1994; Tsukiyama and Wu, 1995). The spacing activity (an activity that "crack" chromatin to increase the DNA accessibility) was also obtained with CHRAC (CHromatin Accessibility Complex (Tsukiyama and Wu, 1995) and ACF (ATP-utilizing Chromatin assembly and remodeling Factor) (Ito *et al.*, 1997a). CHRAC and ACF contain ISWI and ACF1, but CHRAC additionally harbors two small histone fold subunits, CHRAC14 and CHRAC16.

Since the discovery of ISWI, several ISWI related proteins have been identified in numerous organisms: ISW1 and ISW2 in yeast (Mellor and Morillon, 2004); xISWI in *Xenopus*, Snf2H and Snf2L in mammals and furthermore, the existence of conserved complexes was confirmed as well. Among them were homologous complexes of NURF, ACF, CHRAC and RSF in mammals and additional ones like NoRC (Nucleolar remodeling complex) and WICH (WSTF-ISWI chromatin remodeling complex) (Guschin *et al.*, 2000; Poot *et al.*, 2000b; Strohner *et al.*, 2001; Tsukiyama *et al.*, 1999), (Bochar *et al.*, 2000; LeRoy *et al.*, 2000). They all have in common that they contain one of the two mammalian ATPases Snf2H or Snf2L. These complexes are involved in a variety of functions including activation and repression of the initiation and elongation of transcription, replication and chromatin assembly (Flaus *et al.*, 2006).

2.2. Mechanism of and influences on nucleosome mobility

All nucleosome remodeling complexes share the property to catalyze some kind of chromatin remodeling reaction, e.g. they convey accessibility to nucleosomal DNA (Becker and Hörz, 2002; Längst and Becker, 2001b). In the face of more than a decade

of functional studies on ISWI remodeling complexes, the mechanisms of nucleosomal translocation are not completely revealed. Nevertheless, these studies have shed light on the biochemical properties of these remodeling machines and provided insight into the mechanisms of how ATP-dependent nucleosome deposition occurs (Becker and Hörz, 2002; Flaus and Owen-Hughes, 2003b; Längst and Becker, 2001a; Längst and Becker, 2001b; Lusser and Kadonaga, 2003). All these analyses, mainly done on SWI/SNF and ISWI-containing complexes, revealed basic differences between the individual groups of remodeling factors (Kagalwala *et al.*, 2004) (Whitehouse *et al.*, 2003; Zofall *et al.*, 2004). The favored current model for the mechanism of nucleosome remodeling can be seen as a variation of the earlier proposed "loop recapture" model (Cairns, 2007; Gangaraju and Bartholomew, 2007b; Längst and Becker, 2004).
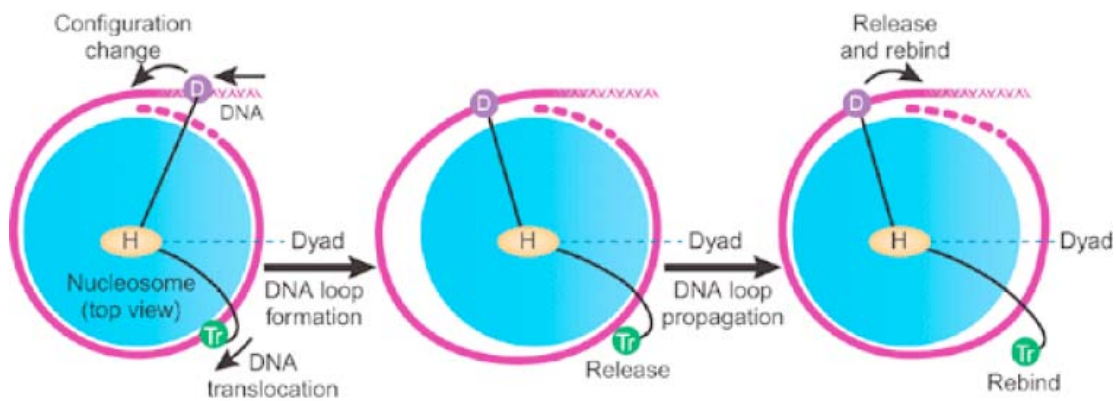
Figure 11: DNA movement during the nucleosome remodeling reaction
Nucleosome sliding catalyzed by ISWI. A DNA loop on the nucleosome surface is formed by the combined action of DNA translocase domain (Tr) binding to nucleosomal DNA at superhelical location 2 and DNA-binding domain (D) binding to the linker DNA, near the nucleosome entry/exit site. Both domains (Tr and D) are connected by a hinge region (H). Nucleosome repositioning is achieved by a conformational change in Tr, that allows DNA release and loop propagation. The DNA-binding domain then rebinds a new DNA stretch and the complex returns to its original starting conformation (adapted from (Cairns, 2007)).

ISWI ATPases have been mapped to contact two sites of the nucleosome: The DNA-binding domain binds to the linker DNA close to the nucleosome entry/exit site and the translocation domain binds a region two helical turns away from the dyad (superhelical location 2-SHL2) (Kagalwala *et al.*, 2004). According to the currently adapted model, DNA is pumped into the nucleosome by a concerted interplay of the DNA-binding domain and the translocase domain of the ATPase. This transformational change results in disruption of histone-DNA contacts and the formation of a small DNA loop. Directional propagation of the loop around the histone octamer due to SHL2 detaching

and loop propagation finally changes the translational position of the nucleosome ~10 bp away from the initial one.

Using *in vitro* assays, ATP-dependent nucleosome remodeling was analyzed by relocation experiments with mononucleosomes performed on a short DNA fragment. It was shown, that ISWI–containing complexes induce ATP-dependent "sliding" of histone octamers without displacing them from DNA (Hamiche *et al.*, 1999; Längst *et al.*, 1999). Although the motor protein alone is capable of nucleosome sliding, the directionality of the nucleosome movement is determined by the unique properties of the additional subunits. The association with regulatory subunits represents an effective way to alter the biochemical properties and modulate the activity qualitatively: for example, both the ACF and the CHRAC complex harbor ACF1 as subunit, which affects the characteristic ISWI functions. The association with ACF1 leads to an up to ten fold increase in the efficiency of mononucleosome sliding, while the DNA-and nucleosome-stimulated ATPase activity remains the same (Eberharter *et al.*, 2001). Additional subunits can also alter the outcome of the remodeling reaction. ISWI alone catalyzes the repositioning of mononucleosomes from the center of a short DNA fragment to its end, whereas ACF and CHRAC mobilize the nucleosomes in the opposite direction. However, the *in vivo* implications of these studies are still topic of research. It is noteworthy that functional differences are also observed between distinct ISWI-containing complexes. For instance, ACF and CHRAC catalyze the formation of regulary spaced nucleosomal arrays (Ito *et al.*, 1997a; Varga-Weisz *et al.*, 1997), whereas NURF does the contrary by disrupting the regularity of chromatin arrays (Tsukiyama and Wu, 1995).

Posttranslational modifications of histones are a second way to take influence on ISWI mobility. Though the ATPase activity is partly stimulated by DNA, nucleosomes are needed for complete activation. This additional stimulation is mediated by a short stretch of the H4 tail, including residue 16-20 (Clapier *et al.*, 2002). In addition to taking influence on the enzymatic properties of ATPases, regulatory subunits can also alter the recruitment to its reaction sites. ACF1 and NURF301 (largest subunit of NURF) harbor two PHD fingers followed by a bromodomain, which target the complexes to specifically modified histone tails (Baker *et al.*, 2008; Zeng and Zhou, 2002), (Wysocka *et al.*, 2006). Further on, ISWI complexes are recruited to their sites of action by interactions with other chromatin binding proteins, e.g. WSTF (subunit of WICH) which interacts with PCNA, thereby recruiting the complex to sites of active replication (Poot *et al.*, 2004).

Also for NURF it was observed that it could act in cooperation with transcription factors to finally induce transcription *in vitro* (Mizuguchi *et al.*, 1997).

Covalent modifications of remodeling complexes can be considered as third way of regulation. For instance, the histone H3 specific acetyltransferase Gcn5 is capable of acetylating *Drosophila* ISWI *in vivo* and *in vitro*. This happens at a site with sequence similarity to the H3 tail (Ferreira *et al.*, 2007b).

3. Positioning of nucleosomes on DNA

Nucleosome positioning has a major role in the regulation of transcription. *In vivo* positioned nucleosomes are a common feature on promoter regions, thereby controlling transcription factor binding. The genome-wide uniform and conserved nucleosomal organization of gene promoters addresses the question by which mechanisms nucleosomes are positioned. Is positioning encoded in the DNA or is it a consequence of the regulatory activity of chromatin remodelers, transcription factors and the transcription machinery? The sequence-directed arrangement of nucleosomes is suggested to be a default (repressive) state that is the consequence of the nucleosome assembly at low energy binding sites. Different studies provide evidence that ATP-remodeling complexes modulate this default chromatin state by the translocation of nucleosomes to remodeling-specific sites, thereby establishing a regulatory level of chromatin organization. In the following section I will summarize the recent results on nucleosome positioning:

3.1. Sequence-dependent nucleosome positioning

More than 30 years ago researchers studied the question whether nucleosomes occur in a specific relation to nucleotide sequences in DNA. Already in 1978 it was observed that the cellular nucleosomal array of single copy genes of rat liver was randomly positioned relative to the underlying DNA sequence (Prunell and Kornberg, 1978). It was shown that precise nucleosome positioning is unlikely to occur in bulk chromatin because nucleosome spacing varied among different cell types of the same organism (Kornberg and Stryer, 1988).

However, in a variety of organisms there was evidently at least a small degree of sequence-specificity (Bloom and Carbon, 1982; Bryan *et al.*, 1981; Fedor *et al.*, 1988; Palen and Cech, 1984; Samal *et al.*, 1981; Wittig *et al.*, 1979; Wu, 1980). Some of these

studies were based on *in vitro* nucleosome assembly methods from purified histones and DNA (Chao *et al.*, 1979; Drew and Travers, 1985; Ramsay *et al.*, 1984; Simpson and Stafford, 1983). The periodicity of nucleosome arrays as revealed by so-called "nucleosomal ladders" following nuclease digestion argues for a specific arrangement. Specific regulatory regions of eukaryotic genes, such as transcription factor binding sites, are organized into specifically positioned nucleosomes. The copy number of the yeast autonomously replicating sequence (ARS) that is normally located in a linker region near the edge of a nucleosome decreased if this sequence is moved into the nucleosomal core (Simpson, 1990).

The histone octamer has no specific binding motif. However, the energy required to bend a specific genomic sequence has influence on the binding affinity of the histone octamer (Thastrom *et al.*, 1999). DNA sequences differ in their ability to bend sharply; therefore it seems likely that the ability of the histone octamer to package different DNA sequences is at least partially dependent on the specific DNA sequence (Anderson and Widom, 2001; Sekinger *et al.*, 2005). Numerous studies have shed light onto the influence of the DNA sequence on the strength of histone-DNA interactions as well as on the bending flexibility of the DNA helix around the histone octamer (Fitzgerald and Anderson, 1998; Ioshikhes *et al.*, 2006; Satchwell *et al.*, 1986; Segal *et al.*, 2006). Specific DNA sequence patterns were shown to be associated with positioned nucleosomes (Fig. 12). Dinucleotides of AA/TT/TA spaced at 10 bp intervals bind the histone octamer with higher affinity due to its intrinsic bendability (Anselmi *et al.*, 1999; Thastrom *et al.*, 1999; Trifonov, 1980; Trifonov and Sussman, 1980). On the contrary, poly-dA/dT sequences differ in their structure from the canonical double helix (Nelson *et al.*, 1987), thereby being resistant to the distortions necessary for wrapping around nucleosomes (Anselmi *et al.*, 1999; Iyer and Struhl, 1995; Kunkel and Martinson, 1981; Segal and Widom, 2009b; Sekinger *et al.*, 2005).
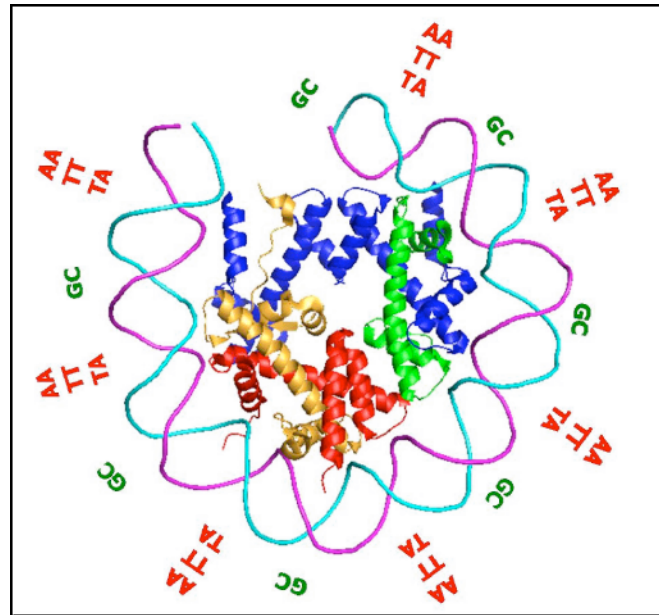
Figure 12: Sequence-dependent nucleosome positioning
Key dinucleotides responsible for nucleosome positioning according to the alignments in Segal et al. A three-dimensional structure of one-half of the symmetric nucleosome is shown. The sequence motif facilitating sharp bending includes 10 bp periodic AA/TT/TA dinucleotides that oscillate in phase with each other and out of phase with 10 bp periodic GC dinucleotides (adapted from(Segal *et al.*, 2006)).

Interestingly, it was also shown that CpG methylation could reposition a nucleosome. For the chicken ß-globin gene it was demonstrated that occupancy of one of the strongest nucleosome positions was abolished by the presence of CpG methylation (Davey *et al.*, 1997; Yenidunya *et al.*, 1994). This methylation-sensitive nucleosome position could be regarded as a switch between two alternating overlapping positions with access to promoter elements. It is believed that changes in anisotropic DNA bending or flexibility due to epigenetic modification of DNA sequence could be the cause of nucleosome exclusion (Banyay and Graslund, 2002; Derreumaux *et al.*, 2001; Meints and Drobny, 2001; Nathan and Crothers, 2002; Virstedt *et al.*, 2004). In spite of this, other studies concluded that only a small subset of nucleosome positions seems to be affected by cytosine methylation, whereas the residual positions seem unaffected by CpG methylation (Davey and Allan, 2003; Davey *et al.*, 2003).

A study provided evidence for the influence of the DNA sequence on chromatin structure, by demonstrating that *in vitro* assembly of the yeast HIS3 locus (Korber *et al.*, 2004) into chromatin repeated some aspects of the *in vivo* structure.

Recent studies addressed the question of sequence-determined nucleosome positioning using bioinformatic approaches based on the computational extraction of nucleosome positioning and nucleosome excluding DNA sequences from *in vivo* nucleosome positions (Ioshikhes *et al.*, 2006; Peckham *et al.*, 2007; Segal and Widom, 2009a; Yuan and Liu, 2008) and using this as training set to determine DNA sequence patterns in nucleosomal DNA segments. Predicted nucleosome positions were then compared to available nucleosome position maps. A nucleosome positioning sequence (NPS) of AA/TT/TA dinucleotides every 10 bp was discovered for yeast (Ioshikhes *et al.*, 2006) with abundance at the nucleosome edges, what was also observed in chicken nucleosomes and in sequences isolated from nucleosomes reconstituted from random synthesized DNA *in vitro* (Segal *et al.*, 2006). Furthermore these studies revealed that NPS in TATA-less genes is uniform. Promoter regions are depleted of nucleosomes relative to transcribed regions. Nucleosome free regions (NFR) are just upstream of the transcription start site (TSS). The results obtained by scanning the yeast genome did also indicate that the first nucleosome downstream of the TSS (+1) is strongly localized. *In vivo* "nucleosome free regions" (NFR) had the strongest anticorrelation with NPS occurrence (Ioshikhes *et al.*, 1996; Ioshikhes *et al.*, 2006).

Additionally, a discrepancy between *in vitro* and *in vivo* nucleosome positioning was reported, suggesting that *in vivo* histones do not always position to the most stable location. These data indicate that as little as 15 % of yeast nucleosome positions might be established by sequence (Segal *et al.*, 2006).

Further analysis of the k-mer (k=1-6) distributions in 1000 highest and 1000 lowest scoring nucleosomes from the dataset of Yuan *et al.* (Yuan *et al.*, 2005) discovered AT or GC rich k-mers as nucleosome inhibiting or nucleosome favoring sequences. Only a subset of positions could be predicted with this k-mer distribution and the author suggested that only 22-25 % of nucleosome positions were determined by DNA sequence (Peckham *et al.*, 2007). The additional inclusion of linker regions or antinucleosomal sequences obtained better prediction rates (Field *et al.*, 2008). Though none of the described methods can globally predict the nucleosome positions, common features are apparent: nucleosomes clearly show some sequence preference *in vitro*, whereas the *in vivo* situation is different. Further, AT-rich sequences are good predictors of nucleosome-depleted regions (Field *et al.*, 2008; Yuan *et al.*, 2005).

A different genome-wide approach to address the question if the genome sequence directs the *in vivo* chromatin structure consists in the *in vitro* reconstitution of genomic DNA into nucleosomes. The comparison of the *in vitro* nucleosomal map to the *in vivo* map revealed a correlation of 0.74 indicating that much of the nucleosomal organization seems to be due to *cis* factors. *In vivo* and *in vitro* derived 3' NFR profiles were superimposable whereas *in* vivo 5' NFRs showed a higher degree of nucleosome depletion than *in vitro* ones, suggesting a further role for proteins in promoter nucleosome depletion (Kaplan *et al.*, 2009). TSS aligned averages of chromatin profiles *in vivo* revealed a strongly positioned +1 nucleosome downstream of the NFR (Field *et al.*, 2008; Kaplan *et al.*, 2009; Mavrich *et al.*, 2008a; Mavrich *et al.*, 2008b; Yuan *et al.*, 2005), (Kaplan *et al.*, 2009; Mavrich *et al.*, 2008a; Mavrich *et al.*, 2008b; Yuan *et al.*, 2005), whereas the corresponding *in vitro* average demonstrates a strong NFR but no positioned +1 nucleosome (Kaplan *et al.*, 2009).

Furthermore, chromatin maps obtained from other organisms showed similar results in terms of dinucleotide periodicity patterns, but further suggest that nucleosome exclusion sequences only occurs in a subset of organisms like yeast, *C. elegans*, whereas in *D. melanogaster* this was not found (Valouev *et al.*, 2008), (Kaplan *et al.*, 2008), (Kaplan *et al.*, 2009; Mavrich *et al.*, 2008b). In human cells, nucleosome-depleted regions occur upstream of transcribed genes, but are uncommon in uninduced genes (Ozsolak *et al.*, 2007; Schones *et al.*, 2008).

In summary, the major outcome of these genome-wide studies is that positioned nucleosomes seem to be much more frequent than initially expected (Albert *et al.*, 2007; Ozsolak *et al.*, 2007; Yuan *et al.*, 2005; Schnitzler *et al.*, 2008). In spite of this, not all nucleosomes were well positioned in these studies. The results suggest that the genome naturally encodes for a stable nucleosome positioning in order to obtain a repressed chromatin conformation to avoid a persistent gene expression. Nucleosomes adapt to preferred positions within a Gaussian distribution; these positions tend to be 10 bp apart (Albert *et al.*, 2007). Delocalized nucleosomes are enriched at locations distant from promoters (Yuan *et al.*, 2005), and in fact variability in nucleosome positioning increases with increasing distance from NFRs (Mavrich *et al.*, 2008a). These results are consistent with the "barrier model of statistical positioning", which proposed that barriers along the chromosome prevent nucleosome binding and nucleosomes are packed between these barriers at some average spacing (Kornberg and Stryer, 1988).

Altogether, the *in silico* models do not correctly predict the bulk of nucleosome positions, suggesting that *trans* positioning factors dominate global positioning. Statistically, there is clearly some enrichment of intrinsically bendable DNA that correlates with *in vivo* nucleosome positions. But this seems to play a minor role in translational positioning of nucleosomes *in vivo.* It has been suggested by many authors (Jiang and Pugh, 2009; Mavrich *et al.*, 2008b) that the dinucleotide periodicity contributes to "rotational positioning" and that *trans* acting factors play the major role in positioning the center of the nucleosome to within ~ 5 bp. Additional mechanisms like chromatin modifications and chromatin remodeling complexes are required to render specific genes and specific transcription factor sites accessible (Field *et al.*, 2008; Ioshikhes *et al.*, 2006; Mavrich *et al.*, 2008a; Peckham *et al.*, 2007; Segal *et al.*, 2006; Yuan and Liu, 2008).

3.2. Nucleosome positioning by chromatin remodeling enzymes

The imprecise predictability of the sequence-based nucleosome positioning algorithms indicates the involvement of additional *trans* acting factors. The evidence that *in vitro* reconstitution of the PHO5 promoter solely failed to repeat the *in vivo* nucleosome positioning, whereas the addition of ATP-dependent remodeling activity recreated the *in vivo* chromatin state suggests a major role for chromatin remodeling factors in the *in vivo* positioning of nucleosomes (Korber *et al.*, 2004)

The yeast chromatin remodeling complex RSC binds to approximately 700 target sites in the yeast genome and is predominantly located over Pol III genes and over a subset of Pol II promoters. RSC has a nucleosome positioning activity (Damelin *et al.*, 2002; Ng *et al.*, 2002). Conditional mutants of a RSC subunit (Sth1) display an increase of nucleosome occupancy at Pol III genes (Parnell *et al.*, 2008). A slight gain of nucleosome occupancy upon RSC loss was also detected at Pol II promoters (Badis *et al.*, 2008; Parnell *et al.*, 2008). The mechanism responsible for this increase in nucleosome occupancy seems to be a combination of nucleosome sliding and binding of new nucleosomes.

The yeast Isw2 is capable to move a nucleosome from its sequence-directed site towards a nucleosome free region of the POT1 promoter (Whitehouse and Tsukiyama, 2006). Isw2 is associated with tRNA genes and RNA Pol II genes. In wild-type Isw2 cells nucleosomes are positioned over TSS and NFR where most transcription factor

binding sites are located (Whitehouse *et al.*, 2007). The yeast Isw2 remodeling complex repositions nucleosomes onto unfavorable DNA sequences to generate tightly packed, inaccessible arrays. Furthermore, upon deletion of Isw2, the chromatin adopts a DNA-directed positioning based on dinucleotide rich elements that facilitates genomic access (Whitehouse and Tsukiyama, 2006). The yeast RNR3 gene requires for precise nucleosome positioning the Isw2 chromatin complex in addition to the global corepressor complex Ssn6-Tup1 (Cooper *et al.*, 1994; Kastaniotis *et al.*, 2000; Weiss and Simpson, 1997), (Fleming and Pennings, 2001; Li and Reese, 2001).

The yeast α2-MCM1 complex seems to actively position nucleosomes at repressed genes, which requires the histone H4 tail (Clapier *et al.*, 2001; Roth *et al.*, 1990; Shimizu *et al.*, 1991).

Active and silent rDNA copies are characterized by distinct epigenetic marks as well as by different nucleosome positions. The rDNA associated remodeling complex NoRC induces nucleosome movement of 25 bp, both *in vivo* and *in vitro*. It also moves the promoter bound nucleosome into the silent position on the inactive rDNA copies. This results in placing the UBF binding site and the functionally important CpG residue at nucleotide – 133 into one region (Li *et al.*, 2006).

Initial *in vitro* studies on the remodeler-mediated nucleosome positioning showed that the intrinsic sequence preference for remodeling is influenced at least by the effects of nearby DNA ends. All analyzed SWI/SNF members tended to move nucleosomes on linear fragments towards the end (Aoyagi *et al.*, 2002; Flaus and Owen-Hughes, 2003b; Jaskelioff *et al.*, 2000; Kassabov *et al.*, 2003; Lorch *et al.*, 2001; Ramachandran *et al.*, 2003), whereas most ISWI complexes catalyzed the mobilization away from the ends (Corona *et al.*, 1999; Eberharter *et al.*, 2001; Hartlepp *et al.*, 2005; Längst *et al.*, 1999; Schwanbeck *et al.*, 2004; Stockdale *et al.*, 2006; Yang *et al.*, 2006). Interestingly, these studies revealed some sequence specificity. Remodelers that move nucleosomes away from ends do not place them in the exact centers of the DNA, but prefer certain sequences (Flaus and Owen-Hughes, 2003b; Gutierrez *et al.*, 2007a; Kassabov *et al.*, 2002a). Distinct nucleosomal positions seem to be controlled by the DNA sequence. To eliminate the DNA end effects, remodeling studies were performed on three different circular mononucleosomal templates. In such a system hSWI/SNF moves the nucleosomes away from initially favored nucleosome positioning sequences to positions favored by the remodeling complex. Furthermore, hSWI/SNF seems to translocate

nucleosomes also on sequences that posses some intrinsic affinity for the histone octamer. These data suggests that each remodeler might have some degree of sequence preferences (Sims *et al.*, 2007).

The chromatin remodeler-mediated nucleosome spacing is a good example supporting the major role for chromatin remodeling in nucleosome positioning. Interestingly, different complexes are capable to promote distinct nucleosomal repeat lengths. The nucleosome repeat length, the 146 bp of DNA associated with a histone octamer plus the linker DNA between adjacent nucleosomes varies with species, cell type, physiological state, and developmental stage, due to variability in the length of the linker DNA (Van Holde, 1989). Yeast Isw1 and Isw2 complexes promote 175 bp and 200 bp repeat length (Tsukiyama *et al.*, 1999) whereas other complexes including the SWI/SNF subfamily and ISWI containing complexes removed regular spacing from chromatin *in vivo* (Guyon *et al.*, 2001; Schnitzler, 2001; Tsukiyama and Wu, 1995). Recent studies have demonstrated that some remodeling complexes require a certain length of DNA on one or both sites of the nucleosome for complete activity (Dang *et al.*, 2006; Gangaraju and Bartholomew, 2007a; He *et al.*, 2006; Kagalwala *et al.*, 2004; Yang *et al.*, 2006; Zofall *et al.*, 2004).

3.3. Additional factors influencing nucleosome positioning

In vivo additional factors, which are present on chromatin, could influence the intrinsic sequence specificity of remodelers. Furthermore the end-product of the remodeler-specific nucleosome position could be a combination of the DNA sequence, the remodeler specificity and also transcription factors, histone tail modifications, variant core histones and other chromatin proteins such as linker histone H1, HP1 and HMGs. Remodeling complexes make use of sequence-specific DNA binding factors to establish preferred nucleosome positions (Kang *et al.*, 2002; Pazin *et al.*, 1997). Additionally, histone H1 reverses the intrinsic preference of SWI/SNF to move nucleosomes to DNA ends, instead repositioning away from ends (Ramachandran *et al.*, 2003). Interestingly, different studies also demonstrated that exchange of canonical H2A for its variants macroH2A or H2A.Z in yeast might also block remodeler-mediated nucleosome repositioning. Another two major classes of *trans* factors have been implicated in nucleosome positioning: Transcription factors and RNA polymerases. They are described elsewhere in detail (Shim *et al.*, 1998; Taylor *et al.*, 1991; Varga-Weisz and

Becker, 1995), (Yarragudi *et al.*, 2004); (Field *et al.*, 2008; Mavrich *et al.*, 2008a; Schones *et al.*, 2008).

4. DNA methylation

Conrad Waddington (1905-1975) is given credit for coining the term "epigenesis". He defined this as the study of how genotypes give rise to phenotypes during development (Waddington, 1942). The contemporary usage of the word "epigenetics" is now to describe the study of heritable changes in genome function that occur without any changes in DNA sequence (Holliday, 2006).

Epigenetic processes play an important role in development and cellular differentiation but they can also occur in mature mammals, either by random change or under the influence of the environment (Issa, 2000). On the way understanding the mechanisms of how the genome adapts to developmental and environmental signals, postsynthetic modifications of the DNA itself and of associated proteins have been identified. Through a highly complex interplay between chromatin modifying proteins, distinct patterns of histone modifications and DNA methylation are established, resulting in specific gene expression profiles. However, the spatial and temporal coordination of this protein network is not yet completely understood.

4.1. DNA methylation – Enzymes and mechanism

Before the structure and function of DNA as genetic material was discovered, Rollin Hotchkiss identified 5-methylcytosine in calf thymus DNA using paper chromatography in 1948 (Hotchkiss, 1948). Research in the field of DNA methylation was based on the solving of the genetic code by Nirenberg and Matthei (Nirenberg, 1963; Nirenberg *et al.*, 1963).

Evolutionary, DNA methylation can be found in bacteriophages, bacteria, fungi and plants as well as in animals. In bacteria, DNA methylation is part of the restriction modification system that protects the host genome against foreign DNA such as bacteriophages (Wilson and Murray, 1991). It occurs at the C-5 and the N-4 of cytosine as well as at the N-6 of adenine, whereas DNA methylation in mammals exclusively takes place at the C-5 of cytosines in CpG dinucleotides (Bird, 2002; Hermann *et al.*, 2004b). Methylated C-5 is therefore often referred to as a 5th base (Bonfils *et al.*, 2000; Delaval and Feil, 2004).

DNA methylation is maintained through the catalytic process of DNA methyltransferases. Since 1964, when the first DNA methyltransferase was discovered in *E.coli* (Gold and Hurwitz, 1964), DNA methyltransferases have been purified and identified in various organisms ranging from bacteria to man (Roy and Weissbach, 1975), (Gruenbaum *et al.*, 1982). The mammalian DNA methylation machinery is composed of Dnmt1, Dnmt2 Dnmt3a, Dnmt3b and Dnmt3L as independently encoded DNA methyltransferases (Dnmts) (Figure 13).
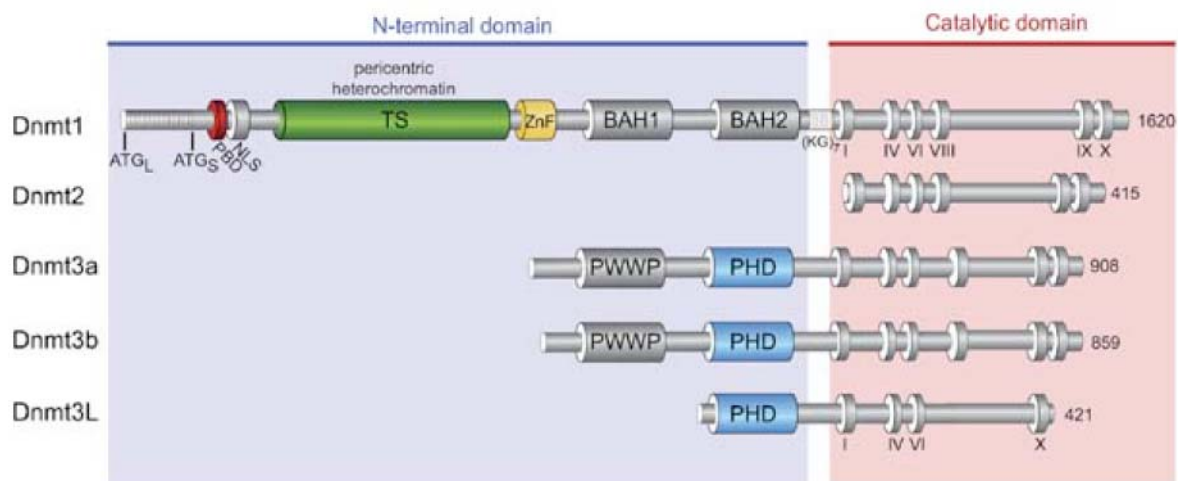
Figure 13: Graphical illustrations of the mammalian DNA methyltransferase domain organization
Mammalian DNA methyltransferases are divided into a N-terminal regulatory part and a C-terminal catalytic part. Conservative motifs that are involved in catalysis (PC), nuclear localization (NLS) or other functions (HRX-like region; ATR-X-like region or PWWP) are shown as boxes. Dnmt3a and Dnmt3b additionally contain a plant homeodomain (PHD) and a PWWP domain, which are required for targeting to pericentromeric heterochromatin and contribute to protein-protein interactions. The protein size is indicated in amino acids (aa). The key functional domains as well as the protein-protein interaction domains are indicated. All active DNA methyltransferases contain the motif IV in the carboxyterminal region. Dnmt1 harbors a cysteine rich HRX-like region and a lysine-glycine repeat ((KG)5) region in its aminoterminal region (Rottach *et al.*, 2009).

4.1.1. CATALYTIC DOMAINS AND REACTION MECHANISM OF DNA METHYLTRANSFERASES

The process of catalyzing the methylation of a cytosine on C5 is similar in all DNA methyltransferases due to their conserved catalytical domains (Kumar *et al.*, 1994). Interestingly, the catalytic domain of Dnmt1 has to be allosterically activated by regions of its aminoterminal domain (Fatemi *et al.*, 2001). DNA methyltransferases have to recognize a specific target sequence in order to catalyze the transfer of a methylgroups from S-adenosyl methionine to the C5 position of cytosine.

In studies on prokaryotic DNA methyltransferases, 10 conserved sequence motifs of the catalytic domain could be identified, six of which are highly conserved (Posfai *et al.*, 1989): I, IV, VI, VIII, IX and X.) These motifs were also characterized in mammalian

Dnmts (Cheng et al., 1993; Posfai et al., 1989) and encompass the SAM binding pocket (I, IV, V, X) and the active site of the DNA methyltransferase (IV). The region between motifs VIII and IX is variable in different Dnmts and is believed to account for sequence specificity (Balganesh *et al.*, 1987; Trautner *et al.*, 1988).

DNA methyltransferases use S-adenosyl-L-methionine as methylgroup donor (AdoMet) for the transfer to the DNA base. The reaction of methyl transfer is described as follows (Figure 14A): The DNA methyltransferase first binds nonspecifically to its substrate DNA, then recognizes the methylation site and finally binds its co-substrate AdoMet.

The enzyme needs to bring the target cytosine to its catalytic pocket (Figure 14B). This is achieved by a process called "base flipping", initially identified in uracil-DNA glycosylase (Klimasauskas *et al.*, 1994). During this process, the cytosine is flipped 180° out of the backbone by rotation around the axis of its phosphodiester backbone into an active site pocket of the enzyme reviewed in (Jeltsch, 2002).

A
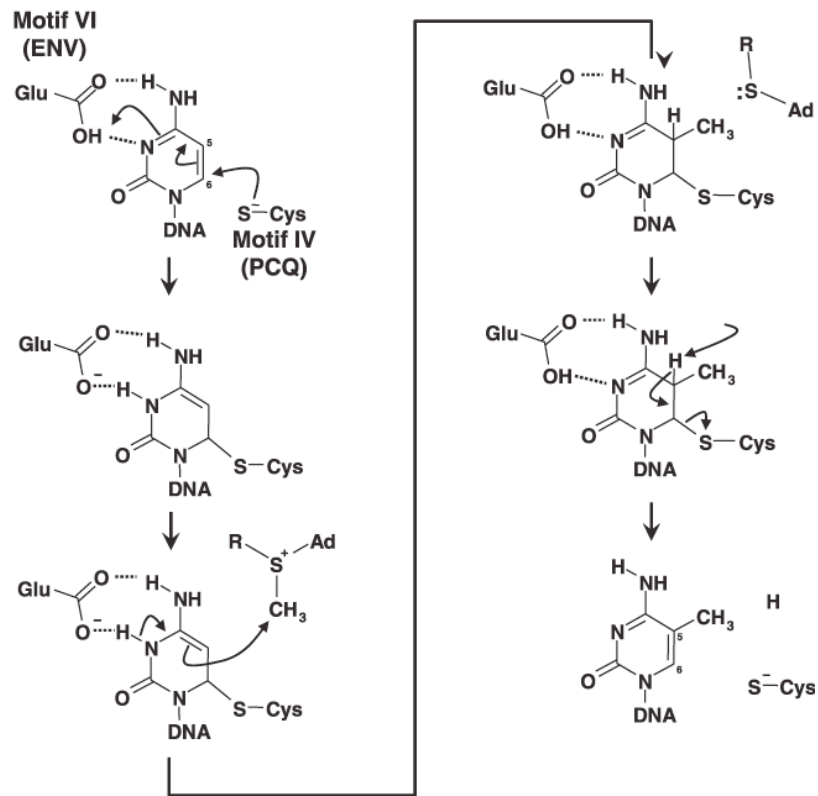
B
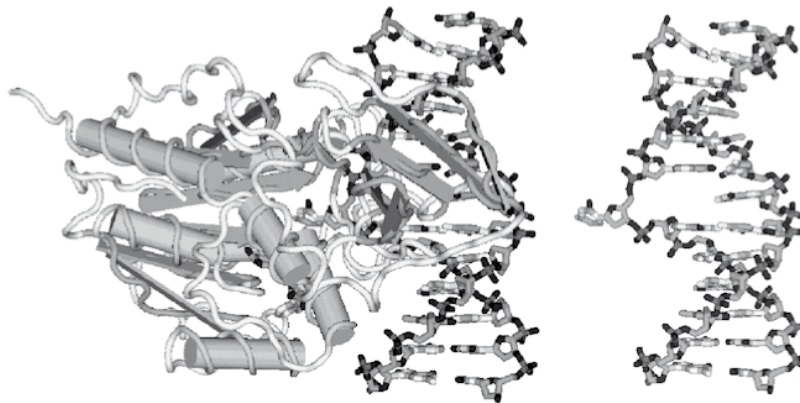
Figure 14: Catalytic mechanism of methylgroup tranfer by DNA methyltransferases
A) The figure is based on the structure of the M.HhaI ± DNA complex. Dihydrocytosin, which binds covalently to the enzyme and S-adenosyl-L-homocystein are formed as intermediates of the DNA methylation reaction. The covalent bond is resolved in the second step, what results in methylated cytosine. The cysteine residue originates from motif IV (PCQ), whereas the glutamic acid residue is from motif VI (ENV) of the DNA methyltransferase (Enzyme-COOH indicates the Glu 119 of motif VI, S-Cys indicates the Cys 81 of the catalytic center in motif IV). B) Structure of the prokaryotic M.HhaI – DNA complex. On the left-hand site the protein is illustrated in schematic view, whereas on the right-hand site the DNA alone is shown, to elucidate the rotation of the target base out of the DNA helix (adapted from (Jeltsch, 2006)).

The reaction proceeds with a cystein SH group from the active site of the enzyme making a nucleophilic attack at the C6 position of the target cytosine (see Fig. 14A). This results in a covalent complex intermediate between the enzyme and DNA. All known DNA methyltransferases include the conserved motiv IV, where the attacking cystein residue is located. Transient protonation of the cytosine ring at the endocyclic nitrogen, N3, by a glutamyl residue in motif VI, leads to the formation of a reactive enamine. This covalent intermediate activates the C5 of cytosine for a nucleophilic attack on the sulphonium-linked methyl group of SAM, finally transferring the methyl group to the cytosine. Following this transfer, the enzyme is finally released by ß-elimination (Pradhan and Esteve, 2003a) (Chen *et al.*, 1991; Randerath *et al.*, 1983) (Santi *et al.*, 1983; Santi *et al.*, 1984; Yoder *et al.*, 1997).

4.2. DNA methylation in mammals

In mammals, DNA methylation is predominantly found at cytosine residues located within CpG dinucleotides. The CpG dinucleotides of both DNA strands are methylated, resulting in a palindromic methylation (reviewed in (Jeltsch, 2002)). The distribution of CpG dinucleotides in the genome is uneven and non-random (Cooper and Krawczak, 1989). In general CpG sites are underrepresented except in specific genomic regions of ~ 1kb, where enrichment can be found (Bird *et al.*, 1985). These small regions, within which the dinucleotide CpG occurs almost at its expected frequency are designated as "CpG islands" and are mainly located within the first exon and promoter of numerous genes (Bird *et al.*, 1985; Jones, 1999) (Takai and Jones, 2003). While CpG islands cover less than 1 % of the whole genome and contain only 5.5 % of the total CpG sites (Rollins *et al.*, 2006), they include over 50 % of the non-methylated CpG sites. It is estimated that 45.000 "CpG" islands are associated with the 5' ends of most house-keeping genes and many regulated genes (Antequera *et al.*, 1990) (Bird, 1996), (Larsen *et al.*, 1992). A small but significant proportion of all CpG islands become methylated during development with the consequence of a stably silenced promoter. This kind of CpG island methylation that is linked to development is involved in genomic imprinting as well as X- chromosome inactivation. A significant fraction of all human CpG islands is prone to progressive methylation during aging (reviewed in (Issa, 2000), in transformed cells (cancer cells, reviewed in Baylin and Herman, 2000). Further it is notable that CpG islands are characterized by an accessible chromatin structure, lacking the linker histone H1 and containing a high

degree of H3 and H4 acetylation (Tazi and Bird, 1990); reviewed in (Razin, 1998). The depletion of CpG dinucleotides is restricted to organisms, which contain methylated genomes. This can be explained by the fact that methylated cytosine is a major mutational hotspot, due to its spontaneous deamination to thymine (Coulondre and Miller, 1978; Coulondre et al., 1978). The C $\rightarrow$ T transition results in the progressive elimination of cytosine sites from the coding sequence during evolution (Bird, 2002; Januchowski et al., 2004; Nakao, 2001).

4.2.1. BIOLOGICAL ASPECTS OF CPG METHYLATION

For mammalian development and normal function of the adult organism properly established and maintained DNA methylation patterns are essential. DNA methylation is a potent mechanism for both silencing gene expression and maintaining genome stability in respect to the repetitive DNA elements, which can otherwise lead to illegitimate recombination events and cause transcriptional deregulation of nearby genes (Yoder et al., 1997). DNA methylation plays a crucial role in normal mammalian development and has a major role in gene expression, X-chromosome inactivation in females and genomic imprinting (Bird, 2002; Li, 2002).

The spectrum of methylation levels and patterns shows a huge variety in different animals. The nematode worm Caenorhabditis elegans does not encode a conventional DNA methyltransferase. In contrast, Drosophila melanogaster posses a DNA methyltransferase-like gene (Hung et al., 1999; Tweedie et al., 1999) and contains extremely low levels of DNA methylation mostly located in the CpT dinucleotide (Gowher et al., 2000; Lyko et al., 2000). The vertebrate genomes posses the highest level of DNA methylation, which is dispersed over the global genome ("global methylation"). This variety of DNA methylation patterns in animals highlights the possibility that different distributions reflect different functions for the DNA methylation system (Colot and Rossignol, 1999).

DNA methylation is a stable epigenetic mark that regulates chromatin structure and gene expression through the modification of interaction between DNA and DNA binding proteins (Li, 2002). DNA methylation is associated with gene silencing. The following sequential order that finally leads to gene repression was described: Primarily, changes in interaction between DNA and DNA binding proteins are triggered by DNA methylation. For instance, binding of specific transcription factors (e.g. NFκB; E2F) to

their DNA target site can be impaired by the methylation of single or few CpG sites. On the other hand, DNA methylation recruits 5-methyl-cytosine binding proteins (MBDs, MeCP) that function as transcriptional co-repressors and other associated proteins, such as histone deacetylases (HDACs), which subsequently leads to transcriptional repression (Bird, 2002). Histones of methylated nucleosomes are mostly deacetylated facilitating additional H3K9 methylation. This leads to an even stronger condensation of chromatin *via* the transition of an active chromatin domain (euchromatin) to a repressive chromatin state (Cameron *et al.*, 1999). Furthermore, interactions with other chromatin-associated proteins such as histone methyltransferases, heterochromatin protein 1 (HP1) and chromatin remodeling factors contribute to this regulation (Robertson, 2002).

The vast majority of genes can be expressed from either the maternal or the paternal allele. "Genomic imprinting" is a process by which genes are selectively expressed by the maternal or paternal homologue of a chromosome reviewed in (Reik and Walter, 2001b) (Li, 2002). In this small subset of genes (~84 identified in mice until the end of 2007: http://www.har.mrc.ac.uk/mousebook/?by=imprinting), differences in expression levels can be observed when maternal and paternal alleles are measured separately. DNA methylation was found as a key molecular mechanism of imprinting. Due to methylation the imprinted genes are differently marked in egg and sperm and inheritance of these epigenetic marks leads to differential gene expression (Reik *et al.*, 1987; Sapienza *et al.*, 1987; Swain *et al.*, 1987). In mammals, approximately 80 % of imprinted genes exist in close proximity to each other or even in imprinted clusters (3-10 genes), the so-called "differentially methylated region" (DMR) (Reik *et al.*, 2001; Reik and Murrell, 2000; Reik and Walter, 2001a; Reik and Walter, 2001b; Verona *et al.*, 2003). A prominent example for "genomic imprinting" is the DMR at the *Igf2/H19* locus (Figure 15).
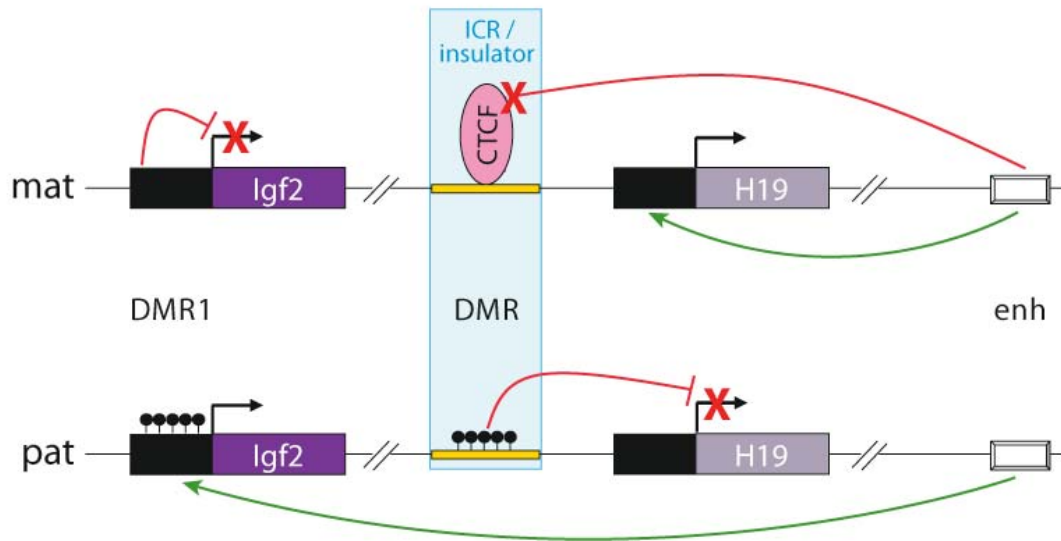
Figure 15: Imprinting control at the *Igf2/H19* differentially methylated region (DMR)
Allele-specific expression happens at the *Igf2/H19* locus. The DMR that controls parental expression at the *Igf2/H19* cluster (yellow bar) distinguishes from DMR1, another *cis*-acting element at this locus. Maternally, when bound by CTCF, DMR acts as an insulator and inhibits activation of the maternal *Igf2* promoter by the downstream enhancer. On the paternal chromosome, CTCF binding is inhibited by methylation at the DMR, what allows the activation of the paternal *Igf2* promoter by the enhancer (Enh).The transcription direction is indicated by black arrows (adapted from(Sha, 2008)).

The process of "dosage compensation" is also closely linked to DNA methylation. In female mammals, one of the two X-chromosomes is functionally silenced during embryogenesis in order to ensure that the stoichiometry of X-chromosomal and autosomal gene products remains the same in male and female organisms. The inactivation of the female X chromosome is achieved by selectively converting one female X chromosome into facultative heterochromatin by different repression mechanisms such as histone deacetylation, histone methylation and ubiquitylation that recruit repressor proteins such as HP1 and Polycomb group complexes and are associated with the enrichment of the histone variant macroH2A1 and finally DNA methylation (reviewed in (Heard and Disteche, 2006; Straub and Becker, 2007).

DNA methylation is also involved in protecting the genome from transposons, retrotransposons and viruses. These repetitive sequences ("parasitic elements") make up approximately 40 % of the human genome. The fact that these repetitive sequences contain many CpG dinucleotides and are methylated above-average, substantiate this hypothesis (Smit, 1999; Yoder *et al.*, 1997).

The importance of DNA methylation is highlighted by the increasing number of human diseases that are known to occur when the epigenetic information is not properly established and maintained (reviewed in (Robertson, 2005), (Baylin *et al.*, 2001; Baylin and Herman, 2000). The best-known links between changes in DNA methylation, gene expression, and disease have been described for cancer. Studies in tumors and cultured cell lines have shown that a general genome-wide demethylation that affects repeated sequences (Mays-Hoopes *et al.*, 1986) and a more gene-specific hypermethylation (Liang *et al.*, 1998) are characteristic for cancer progression. Abnormal methylation at the transcription start site of cancer cells can repress the expression of essential tumor suppressor genes, e.g. p16 (Gonzalez-Zulueta *et al.*, 1995), Rb (Sakai *et al.*, 1991); reviewed in (Momparler and Bovenzi, 2000). The resulting genomic instability that is a hallmark for cancer (Chen *et al.*, 1998) can subsequently cause mutations in genes, thereby representing an indirect way to change gene expression.

Several genetic disorders have been related to mutations in genes that appear to be either involved in DNA methylation itself or in methylation-mediated gene regulation. Among the best characterized are the ATRX syndrome (X-linked alpha-thalassaemia/mental retardation syndrome) ICF syndrome (Immunodeficiency, Centromeric instability, Facial abnormalities) and Rett syndrome (Amir *et al.*, 1999; Bienvenu *et al.*, 2000; Gibbons *et al.*, 2000; Hansen *et al.*, 1999). Imprinting disorders like Beckwith-Wiedemann and Prader-Willi/Angelman syndrome are well characterized (Nicholls *et al.*, 1998; Reik and Maher, 1997). Defects in imprinting are also related to the development of a number of cancers (e.g. Wilms' tumor, Rhabdomyosarcoma) (reviewed in (Falls *et al.*, 1999). Various reviews discuss DNA methylation in disease, including the silencing of tumor suppressor genes in cancer (Baylin *et al.*, 1998; Jones, 1999); genomic imprinting deficiencies (Jaenisch, 1997); heart diseases and ageing (Brown and Strathdee, 2002).

During early mammalian development, DNA methylation profiles are dynamically changed, reaching the final methylation level around gastrulation (Jaenisch, 1997). In somatic differentiated cells, genomic methylation patterns are generally stable and heritable. However, in mammals, at least two developmental periods are known - in germ cells and in preimplantation embryos - in which methylation patterns are reprogrammed genome-wide, generating cells with a broad developmental potential.

Typically, a substantial part of the genome is demethylated and remethylated subsequently in a cell- or tissue-specific pattern to consequently achieve a vast change in the methylation pattern (Reik *et al.*, 2001).

4.3. Mammalian DNA methyltransferases

The mammalian DNA methyltransferases consist of Dnmt1, Dnmt2, Dnmt3a, Dnmt3b, Dnmt3L and can be further classified into two subtypes according to their structure and function (Fig. 13). The Dnmt3 family establishes the initial CpG methylation pattern, therefore termed *de novo* methyltransferases, whereas Dnmt1 maintains the methylation pattern during replication (Chen and Li, 2006) and repair (Mortusewicz *et al.*, 2005). The Dnmt3 family includes two active *de novo* Dnmts (Dnmt3a, Dnmt3b) and one regulatory factor Dnmt3-Like factor (Dnmt3L). All DNA methyltransferases generally comprise two domains: a conserved catalytic domain in the carboxy-terminal part of the protein and a more variable regulatory domain in the amino-terminal region. All characterized mammalian DNA methyltransferases modify DNA at CG sites. They all differ in the degree of specificity for target sequences and the preference for different methylation states of the target sites. Structure and function of the different DNA methyltransferases will be described in more detail in the following section.

4.3.1. DNA METHYLTRANSFERASE 1

Dnmt1 was isolated as first eukaryotic methyltransferase and further identified by chromatographic methods (Bestor, 2000). Human Dnmt1 comprises 1616 amino acids, forming a large N-terminal domain and a C-terminal catalytic domain. C-and N-termini are connected via a lysine-glycine $(GK)_7$ repeat hinge region.

The aminoterminal region harbors different motifs and regulates the activity of the carboxyterminal region (Figure 16). The N-terminal domain harbors several subunits: at least three nuclear localization signals (NLS) (Leonhardt and Cardoso, 2000), a PCNA binding domain (PBD, (aa) 159-178) for interactions with the loading platform PCNA (Proliferating Cell Nuclear Antigen) (Leonhardt *et al.*, 1992). During S phase Dnmt1 is targeted by its PBD to the replication machinery where it associates with PCNA. PCNA increases the affinity of Dnmt1 for DNA and stimulates the methylation activity but is not essential for *maintenance* methylation (Chuang *et al.*, 1997; Iida *et al.*, 2002;

Schermelleh *et al.*, 2007; Spada *et al.*, 2007). PCNA also targets Dnmt1 to DNA repair sites in order to restore epigenetic information (Mortusewicz *et al.*, 2005). The aminoterminal targeting sequence (TS, aa 310-629) is important for recruiting Dnmt1 to heterochromatin, in a process that is independent of replication, the presence of H3K9 trimethylation, the interacting histone methyltransferase SUV39H1 and HP1 (Easwaran *et al.*, 2004; Leonhardt *et al.*, 1992). Furthermore, Dnmt1 forms dimers in a head-head conformation through its targeting sequence (TS) (Fellinger *et al.*, 2009). Moreover, the N-terminus mediates other protein-protein interactions (Robertson, 2001) and contains a cysteine-rich Zn^{2+} binding domain of the CXXC type (Bestor *et al.*, 1992), which comprises eight conserved cysteine residues in two CXXCXXC clusters and two isolated cysteines. The zinc finger in Dnmt1 is capable of binding two zinc ions, what has been implicated in DNA binding (Chuang *et al.*, 1996). The zinc finger was described to be essential for allosteric activation of the catalytic domain of Dnmt1 (Fatemi *et al.*, 2001). It was further shown that it binds specifically to unmethylated CpG sites, whereas deletion of the CXXC domain lead to decreased activity *in vitro* (Pradhan *et al.*, 2008).
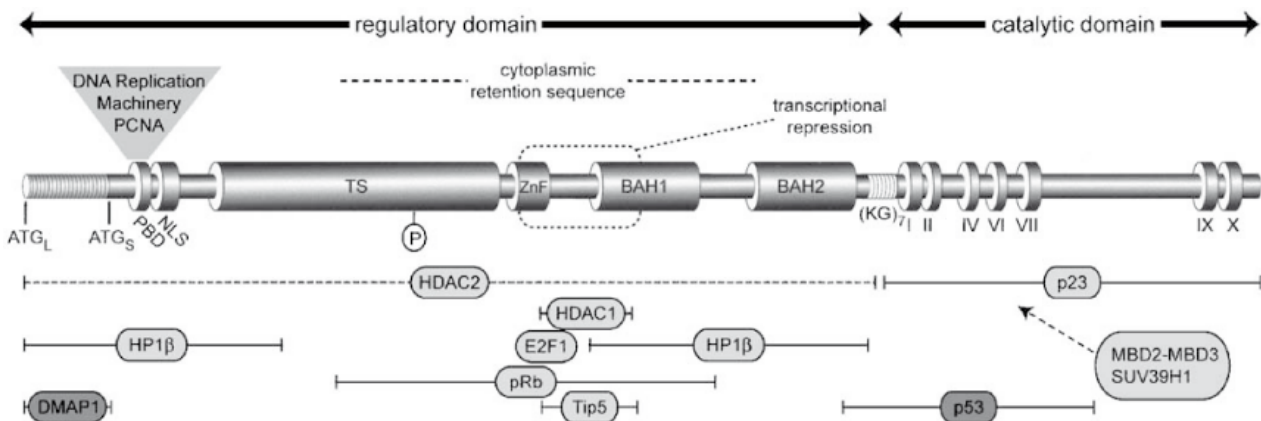
Figure 16: Most prominent interaction partners of Dnmt1
Structure of Dnmt1 and a summary of its interacting factors. The C-terminal domain includes the ten conserved sequence motifs of pro- and eukaryotic C5-cytosine methyltransferases. The aminoterminal regulatory domain exists in two variants generated by alternative transcriptional start sites and translation initiation at either ATG-L (long isoform) or ATG-S (short isoform). Functional domains are indicated: A Zn binding region (ZnF), a nuclear localization sequence (NLS), a targeting sequence (TS), a phosphorylation site, two bromo homology domains (BAH), a transcriptional repression domain and a cytoplasmic localization sequence. Several proteins reported to interact with Dnmt1, which are not shown. The interacting regions are indicated (adapted from (Spada *et al.*, 2006)).

Additionally, the aminoterminal part comprises two bromo adjacent homology (BAH) domains. The PHD domain and the two BAH-domains seem to play a role in targeting Dnmt1 to replication foci (Liu *et al.*, 1998).

The C-terminal domain of Dnmt1 contains all conserved motifs that are characteristic for DNA methyltransferases and harbors the active center of the enzyme (Bestor, 1988). Its primary structure suggests that the entire catalytic site is composed of about 500 aa (Pradhan and Esteve, 2003a; Pradhan and Esteve, 2003b). The catalytic domain *per se* lacks catalytic activity and needs the intramolecular interaction with the regulatory N-terminus for enzymatic activity.

The mRNA of Dnmt1 is ubiquitous and could be detected in all analyzed cell lines. *In vivo*, different splicing variants as well as alternative start codons have been discovered (Mertineit *et al.*, 1998; Pradhan *et al.*, 1997). The Dnmt1b isoform carries 16 additional amino acid residues in the N-terminal part (Bonfils *et al.*, 2000). Dnmt1b protein possesses enzymatic properties that are comparable to Dnmt1 *in vitro* (Bonfils *et al.*, 2000; Liu *et al.*, 2003). Dnmt1o and Dnmt1p are produced by alternative splicing of 5' exons. Dnmt1o is a shorter isoform of Dnmt1 which lacks the first N-terminal 118 amino acids and displays an increased stability against degradation *in vivo* (Ding, 2002). It is detected in growing oocytes and during preimplantation (Carlson *et al.*, 1992). The translocation of Dnmt1o from the cytoplasm to the nucleus during embryogenesis could be essential for the development of normal methylation patterns in imprinted regions (Cardoso and Leonhardt, 1999) (Doherty *et al.*, 2002). The aminoterminal 120 aa of Dnmt1o seem to be involved in ubiquitin dependent proteasomal degradation (Zhou *et al.*, 2008). Dnmt1p is a larger form of Dnmt1, but does not seem to be translated (Mertineit *et al.*, 1998). It can be exclusively found in pachytene spermatozytes and skeletal muscle (Mertineit *et al.*, 1998). Its biological function is still under discussion but it could play a role in oogenesis, gamatogenesis or myogenesis (Aguirre-Arteta *et al.*, 2000).

Dnmt1 is able to methylate CpG sites *in vitro* (Fatemi *et al.*, 2001). DNA methyltransferase isolated from mammalian cells, later identified as Dnmt1, displayed a high preference for hemimethylated target sites (Gruenbaum *et al.*, 1982). Using DNA methyltransferase activity isolated from mouse erythroleukemia cells, an inefficient methylation towards unmethylated in comparison to hemimethylated DNA was observed, arguing for a *maintenance* function (Bestor and Ingram, 1983). This

maintenance methyltransferase activity could be substantiated both *in vitro* and *in vivo* (Hitt *et al.*, 1988; Pradhan and Esteve, 2003b). This specificity of Dnmt1 for hemimethylated DNA has been investigated *in vitro* by several groups using oligonucleotide substrates and preferences ranging from 2 to 50-fold were published (Fatemi *et al.*, 2001; Flynn, 1996; Pradhan, 1999; Tollefsbol and Hutchison, 1995). These discrepancies could be due to factors like differences in length and sequence of the substrates, the experimental test system or the enzyme preparation (Fatemi *et al.*, 2002; Fatemi *et al.*, 2001; Flynn *et al.*, 1996; Tollefsbol and Hutchison, 1997; Tollefsbol and Hutchison, 1995; Pradhan *et al.,* 1999; Fatemi *et al.*, 2002). In the context of longer hemimethylated DNA the preference of the enzyme for hemimethylated *versus* unmethylated DNA was clearly stronger (15 to 24-fold) (Hermann *et al.*, 2004b; Jeltsch, 2006), which enables the enzyme to work as a *maintenance* methyltransferase *in vivo.* The flanking sequence preference of Dnmt1 can also play a role in the activity of Dnmt1. The two bases recognition sequence of DNA methyltransferases is shorter than typical DNA interaction sites, which normally range from 8-14 base pairs. Protein-DNA interactions could therefore occur also outside of the central CG site. Dnmt1 exhibited a clear preference for CCGG motifs in a recent study (Goyal *et al.*, 2006).

During replication Dnmt1 is the major enzyme responsible for maintenance of the DNA methylation patterns. In the newly synthesized DNA strand hemimethylated CpG dinucleotides become accurately methylated, whereas non-methylated sites are omitted. To implement this, Dnmt1 is associated during S-phase with the so-called "replication foci", the sites where replication takes place.

The fact that Dnmt1 interacts with PCNA at the DNA replication fork suggests that Dnmt1 methylates DNA in a processive manner. First evidence for an essential processive methylation of DNA came from a study where a higher methylation rate was demonstrated on longer DNA molecules in comparison to shorter ones (Bestor and Ingram, 1983). Later this processivity was confirmed in different studies using hemimethylated substrates and poly(dI-dC). It was concluded that Dnmt1 is capable to introduce up to 30 methyl groups in a processive manner. Two studies observed that processive methylation of the DNA can only take place in one DNA strand, which implies that Dnmt1 does not switch between DNA strands during processive methylation of DNA (Hermann *et al.*, 2004a; Hermann *et al.*, 2004b; Vilkaitis *et al.*, 2005). For the duration of the diffusional walk, Dnmt1 stays in intimate contact with the DNA, thereby

keeping its orientation and accurately copies the existing methylation pattern (Hermann *et al.*, 2004b). This implies that Dnmt1 moves along the DNA after each turnover of substrate, which suggests involving a sliding mechanism.

The N-terminal part of Dnmt1 has an important role in controlling the activity of the protein and could be considered as a kind of "regulatory domain". About half of the N-terminal region is required to obtain an active enzyme (Bacolla *et al.*, 2001; Fatemi *et al.*, 2001; Margot *et al.*, 2000; Zimmermann *et al.*, 1997). It has been proposed that the catalytic domain is transformed through intramolecular interactions into its active conformation (Pradhan and Esteve, 2003a). The hypothesis that Dnmt1 could exist in different conformational states is further supported by the fact that its catalytic center is stimulated allosterically by existent DNA methylation (Bacolla *et al.*, 1999; Fatemi *et al.*, 2002; Fatemi *et al.*, 2001). Interestingly, Dnmt1 bears at least two separate DNA binding sites, one in the N-terminal and one in the C-terminal domain (Araujo *et al.*, 2001; Fatemi *et al.*, 2001; Flynn and Reich, 1998). The enzyme can interact with its target DNA and additionally with a second DNA molecule that function as an allosteric regulator. Furthermore, different groups observed, that Dnmt1 has reduced specificity for hemimethylated DNA in the presence of methylated DNA (Bacolla *et al.*, 1999; Fatemi *et al.*, 2002; Fatemi *et al.*, 2001). As consequence the methylation rate increases for unmodified DNA and decreases for hemimethylated substrates (Fatemi *et al.*, 2001; Goyal *et al.*, 2006). The aminoterminal domain seems to be involved in this allosteric mechanism (Bacolla *et al.*, 1999; Fatemi *et al.*, 2002). Additionally, substrate inhibition was demonstrated in studies using unmethylated DNA (Bacolla *et al.*, 1999; Flynn *et al.*, 2003; Svedruzic and Reich, 2005a). Binding of the substrate to the N-terminal region of Dnmt1 is sequence and methylation dependent (Flynn *et al.*, 2003) and the binding sites for the observed substrate inhibition could be narrowed down to the first 501 amino acids (Bacolla *et al.*, 2001). These effects are consequences of the stimulatory or inhibitory influence of the amino terminal.

The *de novo* methylation rate of Dnmt1 that is observable *in vitro* as well as *in vivo* suggests a role for Dnmt1 in *de novo* methylation. Biological evidence shows Dnmt1-mediated *de novo* methylation of CpG islands (Jair *et al.*, 2006) (Feltus *et al.*, 2003) (Grandjean *et al.*, 2007). Besides the regulation of Dnmt1 activity by DNA substrates, it is proposed that binding of RNA molecules might contribute to the regulation (Svedruzic and Reich, 2005b).

Knockout studies demonstrated that Dnmt1 is essential during development. Dnmt1 knockout mice die in early stages of embryogenesis (Li *et al.*, 1992). Additionally, Dnmt1 knockouts of embryonic stem cells showed that Dnmt1 is essential for cell viability. Knockdown experiments using small interfering RNAs resulted in decreased cell viability as well as DNA hypomethylation (Egger *et al.*, 2006). In an inducible knockout system it was observed that Dnmt1 deficient cells exhibited an 80 % reduction in methylation activity, coupled with activation of the G2/M checkpoint, leading to G2 arrest. Cells showed severe mitotic defects and underwent apoptosis (Chen *et al.*, 2007). These studies indicated that Dnmt1 is required to maintain cell viability, what seems to be conserved between human and mouse and between normal and tumor cells (Egger *et al.*, 2006; Spada *et al.*, 2007).

The N-terminal domain of Dnmt1 seems to serve as a platform for assembly of various proteins involved in chromatin condensation and gene regulation (Figure 16). Dnmt1 interacts with a network of proteins. Interaction partners are histone modifying proteins like HDAC1 (Fuks *et al.*, 2000; Robertson *et al.*, 2000), HDAC2 and the histone methyltransferase SUV39H1 (Fuks *et al.*, 2003). Histone deacetylation goes along with transcriptional repression and the respective histone deacetylases further recruit Dnmts to establish DNA methylation marks. SUV39H1 or its resulting H3K9 trimethylation further recruits HP1, which also binds to Dnmt1 via its chromodomain (Fuks *et al.*, 2003; Geiman *et al.*, 2004b) (Lehnertz *et al.*, 2003). The H3K9 methyltransferase G9a can be found in euchromatin, where it is associated with Dnmt1, Dnmt3a and Dnmt3b (Epsztejn-Litman *et al.*, 2008; Esteve *et al.*, 2006). Interestingly, it was recently shown that G9a is recruited to chromatin via the noncoding RNA *Air*. The interaction with the transcriptional co-repressor DMAP1 (Dnmt1 associated protein1) takes place during S-phase and is suggested to mediate repression (Rountree *et al.*, 2001). Interactions with chromatin remodeling factors will be discussed in section B.III.1. Dnmt1 interacts with Methyl CpG binding domain proteins (MBD) that bind to methylated CpG, thereby amplifying transcriptional silencing, such as MeCP2, MBD2, MBD3 (Kimura and Shiota, 2003; Tatematsu *et al.*, 2000). Furthermore, interactions of Dnmt1 with the chromatin factors ICBP90 (inverse CAAT box binding protein of 90kDa) also termed NP95 or UHRF1), EZH2 and G9a were shown to be essential for maintenance of DNA methylation (Bostick *et al.*, 2007; Sharif *et al.*, 2007; Vire *et al.*, 2006). Dnmt1 interacts with the SET and RING associated domain (SRA domain) of ICBP90 via its TS domain

(Achour *et al.*, 2008; Bostick *et al.*, 2007; Leonhardt *et al.*, 1992), which then recruits it to replication foci. ICBP90 was found to be involved in DNA methylation during replication (Li *et al.*, 1992; Miura *et al.*, 2001) and was subsequently discovered to exhibit strong binding affinity to newly replicated hemimethylated DNA, thereby recruiting Dnmt1 (Bostick *et al.*, 2007; Sharif *et al.*, 2007). ICBP90 seems to recognize hemimethylated 5-methylcytosines by a base flipping mechanism (Arita *et al.*, 2008; Avvakumov *et al.*, 2008; Hashimoto *et al.*, 2009) and recent studies suggest that ICBP90 confers Dnmt1 its increased activity and accuracy on hemimethylated DNA. Dnmt1 interacts also with the cell-cycle regulatory proteins Rb and E2F1 that were identified in a Dnmt1 complex together with HDAC1 by chromatographic fractionation from Hela nuclear extracts (Robertson *et al.*, 2000). Interestingly, global DNA methylation was inhibited by overexpression of Rb, irrespective of the phosporylation status (Pradhan and Kim, 2002) and Rb was further shown to bind to allosteric sites of Dnmt1 (Pradhan and Esteve, 2003a). Dnmt1 also interacts with p21WAF1, an inhibitor of cyclin-dependent kinases (CDKs) (Chuang *et al.*, 1997).

Finally, direct interactions between Dnmt1 and the *de novo* methyltransferases Dnmt3a and Dnmt3b were found *in vivo* and *in vitro* (Kim *et al.*, 2002). In summary, these observations build a complicated but coordinated network of connections between Dnmt1 and several cellular proteins involved in gene regulation and epigenetic signaling that could mediate methylation-dependent as well as independent functions of Dnmt1 at different cell stages.

Interacting protein	Potential function	Reference
PCNA	Targeting to replication foci and repair sites	(Chuang *et al.*, 1997) (Mortusewicz *et al.*, 2005)05)
HDAC1	Transcription inhibition and chromatin remodeling	(Fuks *et al.*, 2000)
HDAC2 DMAP1 SUV39H1 HP1	Transcription inhibition and chromatin remodeling Maturation of chromatin following replication, Mediates repression Histone H1 methyltransferase Binds to H3K9 methylated chromatin	(Rountree *et al.*, 2000) (Fuks *et al.*, 2003)
pRb	Transcription inhibition and chromatin remodeling	(Robertson *et al.*, 2000)

HDAC1	Targeting of methylation	
E2F1	Cell cycle regulator	
MBD2 MBD3 MeCP2	Targeting to DNA and replication foci	(Kimura *et al.*, 2003; Tatematsu *et al.*, 2000)
MeCP2	Transcription inhibition	(Kimura *et al.*, 2003)
p23	Chaperone protein: Folding; Recruitment to nuclear matrix.	(Zhang and Verdine, 1996)
Annexin	Recruitment to nuclear matrix	(Ohsawa *et al.*, 1996)
hSnf2H	Both are subunits of NoRC Chromatin remodeling	(Robertson *et al.*, 2004)
Tip5	Transcription inhibition, rDNA specific inhibitor	(Santoro *et al.*, 2002) (Zhou and Grummt, 2005)
ICBP90	Recruitment to replication foci	(Bostick *et al.*, 2007; Sharif *et al.*, 2007)
p21WAF1	Inhibitor of CDKs	(Chuang *et al.*, 1997)
LSH	Essential for maintenance methylation	(Myant and Stancheva, 2008)
EZH2 and G9a	Essential for maintenance methylation	(Esteve *et al.*, 2006; Vire *et al.*, 2006)
Dnmt3a / Dnmt3b	Cooperation in maintenance de novo methylation	(Kim *et al.*, 2002)
RGS6	Inhibitor of DMAP1	(Fisher and Merkenschlager, 2002)
PML-RAR	Oncogenic transcription factor	(Di Croce *et al.*, 2002)
PARP-1	Poly-ADP-ribose polymerase1: Inhibition of DNA methyltransferase activity	(Reale *et al.*, 2005)
Hsp90	Forms complex with Dnmt1, probably stabilization	(Zhou *et al.*, 2008)
RIP140	Scaffold for DNA methyltransferase activity.	(Kiskinis *et al.*, 2007)
CFP1	CXXC finger protein: Intersection of the cytosine methylation machinery	(Butler *et al.*, 2008)

Table 1. Dnmt1 interacting proteins

4.3.2. DNA METHYLTRANSFERASE 2

The Dnmt2 gene is conserved among eukaryotes (Yoder and Bestor, 1998). With 391 amino acids it lacks the aminoterminal regulatory domain, thereby resembling prokaryotic methyltransferases. Dnmt2 harbors a conserved Cys-Phe-Thr motif, which is not found in other DNA methyltransferases (Dong *et al.*, 2001). At first no methylation

activity could be detected (Okano *et al.*, 1998b), but later it was shown that Dnmt2 is a RNA methyltransferase for tRNA$_{Asp}$, though it showed low methylation activity (Goll *et al.*, 2006). It was shown to act through a DNA methyltransferase-like catalytic mechanism (Jurkowski *et al.*, 2008).

4.3.3. DNA METHYLTRANSFERASE 3 FAMILY

The mammalian Dnmt3 family consists of three different proteins, Dnmt3a, Dnmt3b and Dnmt3L (Okano *et al.*, 1998a). Though Dnmt3a and Dnmt3b are highly related one to another, they are encoded by separate genes (Xie *et al.*, 1999). The general architecture of both Dnmt3 enzymes is consistent with the C-terminal catalytic domains of Dnmt1 that harbor all motifs (Gowher and Jeltsch, 2002). Structurally, Dnmt3a and 3b also share two conserved domains in the N-terminal region: the proline- and tryptophan-rich PWWP domain (named after the characteristic Pro-Trp-Trp-Pro motif) and the cysteine-rich PHD domain (Plant HomeoDomain), also called ATRX domain, because of its homology to the PHD region of the ATRX gene (Herman, 2004). This ~ 50 amino acid motif is mainly found in proteins that are involved in transcription regulation. The PHD domain has been described to interact with various chromatin proteins like HDACs, HP1 and SUV39H1 (Fuks *et al.*, 2001).

The PWWP domain, whose structure has been solved, interacts with DNA (Qiu *et al.*, 2002). In the Dnmt3 family it is required for the targeting to pericentromeric heterochromatin as well as for protein-protein interactions (Aapola *et al.*, 2000; Bachman *et al.*, 2001; Chen *et al.*, 2004; Fuks *et al.*, 2003; Ge *et al.*, 2004). However, the PWWP domain of Dnmt3a binds nonspecifically to DNA (Qiu *et al.*, 2002), whereas that of Dnmt3b possesses little DNA binding ability (Chen and Li, 2004).

Dnmt3a transcripts are expressed in the majority of adult and embryonic tissues, most tumor-cell lines and embryonic stem cells (Robertson *et al.*, 1999; Xie *et al.*, 1999). The expression seems to be independent of the cell cycle (Robertson, 2002) and it is assumed to be crucial for imprinting of paternal and maternal genes (Kaneda *et al.*, 2004). In contrast, the expression levels of Dnmt3b are very low in most tissues, except for the testis, indicating an important role in spermatogenesis (Okano *et al.*, 1998a; Xie *et al.*, 1999).

Two splice variants for Dnmt3a are known, namely Dnmt3a1 and Dnmt3a2, of which the latter lacks the N-terminal 219 aa. The splice variant Dnmt3a2 as major form during

embryogenesis is catalytically active and is localized to euchromatin propably due to its lacking aminoterminal domain (Chen and Li, 2004). Several Dnmt3b isoforms that result from alternative splicing of exons 10,21, 22 are described: Dnmt3b1, 3b2, 3b3 (Okano *et al.*, 1998a). Dnmt3b1 and Dnmt3b2 are enzymatically active, whereas Dnmt3b3 seem to be inactive. They were shown to be expressed in a tissue-specific manner (Robertson *et al.*, 1999). Dnmt3b1 is the longest form and is usually regarded as the typical gene product of Dnmt3b. Dnmt3b4 and Dnmt3b5 encode truncated proteins, and are predominantly expressed in testis (Hansen *et al.*, 1999).

Dnmt3a and Dnmt3b establish DNA methylation patterns *de novo* in early development. Members of the Dnmt3 family methylate CpG dinucleotides without any preference for hemimethylated DNA both *in vitro* (Gowher and Jeltsch, 2001; Hsieh, 1999) and *in vivo* (Lyko *et al.*, 1999). As consequence of this fact they were assigned as *de novo* methyltransferases. Both enzymes are capable to methylate cytosine bases outside the context of CpG dinucleotides, but the biological function of this activity remains unclear (Aoki *et al.*, 2001; Gowher and Jeltsch, 2001; Gowher and Jeltsch, 2002; Handa and Jeltsch, 2005; Hsieh, 1999; Ramsahoye *et al.*, 2000). The catalytic domain of Dnmt3 family members itself is active, independently of the aminoterminal domain (Gowher and Jeltsch, 2002). Despite significant amino acid sequence and biochemical similarities, both enzymes execute distinct biological roles. Dnmt3a works distributively (Gowher and Jeltsch, 2002; Yokochi and Robertson, 2002) has been associated with the methylation of single copy genes and retrotransposons (Bourchis and Bestor, 2004; Bourchis *et al.*, 2001; Hata *et al.*, 2002) and seems to be required for the establishment of genomic imprinting during germ cell development (Kaneda *et al.*, 2004). Structure and mutagenesis experiments suggest that an interaction with Dnmt3L is required for full Dnmt3a activity (Jia *et al.*, 2007). Dnmt3b is responsible for methylation of pericentromeric satellite regions (Hansen *et al.*, 1999; Okano *et al.*, 1999a; Okano *et al.*, 1999b; Xu *et al.*, 1999). Mutations within the Dnmt3b gene can result in the ICF syndrome. Patients usually carry alleles with a mutation in the C-terminal domain, which leads to completely unmethylated DNA in pericentromeric regions of specific chromosomes (Hsieh, 1999; Kondo *et al.*, 2000). In contrast to Dnmt3a, Dnmt3b is a processive DNA methyltransferase and its activity has been observed both in vivo and in vitro (Aoki, 2001; Okano *et al.*, 1998a; Qiu *et al.*, 2002; Tuck-Muller *et al.*, 2000).

The critical role of Dnmt3a and Dnmt3b during development was elucidated by studies on transgenic mice lacking Dnmt3a and Dnmt3b singly or in combination. Dnmt3a knockouts show post-natal mortality, whereas Dnmt3b knockouts die in the embryonic stage (Okano *et al.*, 1999a) (Li *et al.*, 1992). Double knockout of Dnmt3a and Dnmt3b embryos show a phenotype similar to the Dnmt1 knockout embryo. The fact that the consequence of a double *knockout* is more severe than any single knockout suggests that they have overlapping functions.

Dnmt3a and Dnmt3b interact with various transcriptional repressors proteins. Both proteins are capable of repressing transcription of a reporter gene mediated by the PHD domain in a HDAC dependent way. Dnmt3a was found to interact with HDAC1, RP58, a sequence specific transcriptional repressor, H3K9 metyltransferase Suv39 and p53. Both methylation-dependend and independent co-repression by Dnmt3a can occur (Datta *et al.*, 2003; Fuks *et al.*, 2000; Fuks *et al.*, 2003; Wang *et al.*, 2005). Dnmt3b interacts with histone modifying enzymes like HDAC1, HDAC2, Suv39H1, chromatin remodeling enzymes like Snf2H, histone binding proteins like HP1α and components of the condensing complex (Geiman *et al.*, 2004a). A recent study showed that the transcription factor SALL3 inhibited interaction of Dnmt3a with DNA via the PWWP domain (Shikauchi *et al.*, 2009).

Dnmt3a and Dnmt3b can undergo posttranslational modifications like SUMOylation (Kang *et al.*, 2001; Ling *et al.*, 2004) and Dnmt3a interacts with the SUMOylation machinery and the SUMOylation mark inhibits the interaction with HDAC1 and HDAC2, thereby abolishing transcriptional repression (Ling *et al.*, 2004).

Dnmt3L as the third member of the Dnmt3 family shows a clear homology to Dnmt3a and Dnmt3b (Aapola *et al.*, 2000). Its aminoterminal domain only contains the PHD domain and carries mutations within all conserved DNA methyltransferase motifs. This suggests that it does not have catalytic activity. It was shown to repress transcription by recruitment of HDAC1 (Aapola *et al.*, 2002; Deplus *et al.*, 2002). Dnmt3L directly interacts with Dnmt3a and 3b via its C-terminus, thereby inducing a conformational change that facilitates DNA and AdoMet binding (Gowher *et al.*, 2005a; Hata *et al.*, 2002; Suetake *et al.*, 2004). Dnmt3L stimulates the activity of Dnmt3a and Dnmt3b up to 15-fold (Gowher *et al.*, 2005a). The crystal structure of a Dnmt3L-3a-3a-3L-tetramer revealed that Dnmt3L-3a interface stabilizes the conformation of the active site loop of Dnmt3a (Jia *et al.*, 2007). This dimer formation suggest the observed periodicity of 8-10

bp in methylation of maternally imprinted genes. Moreover, Dnmt3a-3L complexes were shown to multimerize on DNA, forming protein-DNA filaments (Jurkowska *et al.*, 2008). Dnmt3L seems to respond to states of histone modification to regulate *de novo* DNA methylation. For instance, Dnmt3L binds directly to unmethylated lysine 4 of histone H3 (H3K4) through its N-terminal PHD domain; thereby recruiting or activating Dnmt3a to induce *de novo* methylation (Ooi *et al.*, 2007).

The expression of Dnmt3L is similar to Dnmt3a and 3b, highly expressed during gametogenesis and embryonic stages (Bourchis and Bestor, 2004) but Dnmt3L *knockout* mice display a normal phenotype. Apart from this Dnmt3L was found to be essential for embryonic development due to the establishment of maternal imprints (Bourchis *et al.*, 2001; Hata *et al.*, 2002).

The active methyltransferases (Dnmt1, Dnmt3a and Dnmt3b) have been shown to closely interact with each other (Datta *et al.*, 2003; Kim *et al.*, 2002). This cooperation of *de novo* and *maintenance* methyltransferases ensures proper methylation patterns, while deficiency of one of the methyltransferases results in hypomethylation. Dnmt1 interacts with Dnmt3a and Dnmt3b via their N-terminal domains (Kim *et al.*, 2002). The activity of the *de novo* methyltransferases is enhanced by the presence of Dnmt1. Thus it is hypothesized that Dnmt1 supports the introduction of new methylation marks. Because of this tight interaction and complementation between the Dnmts it is proposed to use the terms "*de novo*" and *"maintenance"* to define the processes at the DNA rather than solely the methyltransferases (Fatemi *et al.*, 2002).

III. INTERPLAY BETWEEN CHROMATIN REMODELING AND DNA METHYLATION

The enzymatic processes and properties of DNA methyltransferases have been analyzed intensively in several *in vitro* studies with purified enzymes (Aoki *et al.*, 2001; Bacolla *et al.*, 2001; Bacolla *et al.*, 1999; Bestor and Verdine, 1994; Cheng and Roberts, 2001; Gowher and Jeltsch, 2001; Gowher and Jeltsch, 2002; Pradhan *et al.*, 1999) (Suetake *et al.*, 2003; Yokochi and Robertson, 2002). However, most of these studies were carried out on free and often artificial DNA substrates, though the physiological substrate of eukaryotic cells is chromatin. Far less is known about the mechanism of DNA methylation within chromatin. The tight cooperation between the DNA methylation machinery and epigenetic chromatin modifications was already described in the section B.II.4.2. (reviewed in (Geiman and Robertson, 2002).

1. *In vitro* studies on DNA methylation in chromatin

Though Dnmt1 is capable to rapidly methylate a large number of CpGs behind the replication fork, a fraction of CpG dinucleotides also shows delayed DNA methylation (Liang *et al.*, 2002; Woodcock *et al.*, 1986). Interestingly, Dnmt1 was shown to act in a biphasic process in respect to the timing of methylation, with 10-20 % of the methylation delayed, extending beyond post-replication.

Different spontaneous mechanisms could enhance the activity of DNA modifying proteins by facilitating the access to their sites within nucleosomes (Anderson *et al.*, 2002). One is spontaneous site exposure that rather occurs through the spontaneous transient dissociation of short DNA stretches which starts at one end of the nucleosome and extends inward (Anderson *et al.*, 2002; Polach and Widom, 1995).

The question if this holds true for DNA methylation in chromatin was addressed in several studies: The first *in vitro* study on mononucleosomal templates showed that DNA methylation is at least restricted within a chromatin environment (Okuwaki and Verreault, 2004). Dnmt1, though slightly inhibited, seemed to posses an intrinsic ability to modify CpG dinucleotides on the surface of nucleosomes. This activity was highly dependent on the sequence of the DNA substrate: CpG sites on the surface of 5 S rRNA gene or the H19 promoter were completely methylated (100 % methylation efficiency), whereas nucleosomes containing the Air promoter were refractory (< 10 % methylation) (Okuwaki and Verreault, 2004). Another study used a 208 bp DNA derived from the sea urchin 5S rDNA sequence (Flaus *et al.*, 1996; Ura *et al.*, 1995) that is a well-characterized nucleosome positioning sequence (Robertson *et al.*, 2004). The Dnmt1 and Dnmt3a activities on naked DNA were 8-fold and 17-fold, respectively, higher in comparison to the activities on the same sequences assembled into mononucleosomes. Interestingly, the ability of both enzymes to bind the substrate was not significantly altered by the chromatin structure (Robertson *et al.*, 2004).

Takeshima and coworkers analyzed the methylation characteristics of Dnmt3a and Dnmt3b in nucleosome core particles that differed in sequence and the length of overhanging DNA (Takeshima *et al.*, 2006). In this assay setup the methylation activity of both *de novo* methyltransferases was strongly inhibited. Furthermore the methylation activity towards the naked DNA region was much higher for Dnmt3a than Dnmt3b, whereas Dnmt3b showed higher methylation activity towards the DNA within the nuclesome core region. Interestingly, the increase in length of overhanging DNA

enhanced the methylation efficiency for Dnmt3a but not for Dnmt3b (Takeshima *et al.*, 2006). A similar study elucidated the methylation activity of Dnmt3a towards the nucleosome core region and linker DNA using oligonucleosomes and especially analyzed the effect of linker histone H1 on the activity (Takeshima *et al.*, 2008). The Dnmt3a activity was higher towards oligonucleosomes depleted of histone H1 than that with H1. The assembly of histone H1 inhibited the activity of Dnmt3a towards the linker DNA region. The C-terminal and the central globular domain of H1 together seem to mediate inhibition (Takeshima *et al.*, 2008).

Taken together, these results argue against the sufficiency of a spontaneous site exposure to relieve methylation of nucleosomal core particles and chromatin higher order structures. Chromatin in the eukaryotic cell is even more compacted than in the mononucleosome, which may further restrict access to certain CpGs sites *in vivo*. Therefore, methylation of nucleosomal CpG may require the involvement of ATP-dependent nucleosome remodeling factors. Different studies provided evidence for this hypothesis.

2. *In vivo* studies on DNA methylation in chromatin

Interestingly, mutations of genes encoding chromatin remodeling factors, such as *DDM1* in Arabidopsis*, ATRX* in human, Lsh in mouse induce hypomethylation in certain genomic regions (Dennis *et al.*, 2001; Fan *et al.*, 2005b; Gibbons *et al.*, 2000; Jeddeloh *et al.*, 1999). Mutations in DDM1 lead to a 70 % decrease of whole genomic 5-methylcytosine, primarily at repetitive elements like satellites and rDNA regions (Martienssen and Henikoff, 1999). Further indications are that DDM1 could play a role in the replication-dependent maintenance methylation (Jeddeloh *et al.*, 1999). Lsh (lymphoid-specfic helicase, Hells, PASG) is highly expressed in lymphoid tissues and thought to be involved in recombination (Jarvis *et al.*, 1996). *Knockout* of the Lsh gene resulted in hypomethylation, mainly in repetitive regions with a general reduction of genomic 5-methylcytosine in 50-60 % in all tissues (Dennis *et al.*, 2001). Mutations in the PHD region that show high homology to the PHD regions of Dnmt3a and Dnmt3b of the ATRX gene cause the ATRX-syndrome (Gibbons *et al.*, 1997). ATRX localizes to pericentromeric heterochromatin and was proposed to act as transcriptional regulator (Berube *et al.*, 2000). Mutations in ATRX result in both aberrant losses and gains of DNA methylation in the genome.

A study demonstrated direct association between Dnmt1 and Snf2H by co-localization as well as by co-immunoprecipitation (Robertson *et al.*, 2004). Immunofluorescence microscopy revealed that a significant fraction of both proteins co-localized in heterochromatic regions of HeLa cells. Furthermore, the addition of recombinant Snf2H enhanced the binding affinity of Dnmt1 to nucleosomes by 3-fold in an ATP-independent manner *in vitro*, but had no effect on the enzymatic activity of Dnmt1 on mononucleosomal substrates (Robertson *et al.*, 2004). We could also find an association between Dnmt1 and human Snf2H by co-immunoprecipitation assays on human 293 cell extracts (Anna Schrader, diploma thesis). Co-immunoprecipitation assays and GST-pulldowns revealed that Dnmt3b interacts with Snf2H and other chromatin-associated proteins. Additionally, these two proteins co-localize in heterochromatic regions of HeLa cells (Geiman *et al.*, 2004b). Further studies demonstrated a direct interaction between Dnmt3a and components of Brg1 complex. These proteins were associated with transcriptionally silent methylated metallothionein promoter in mouse lymphosarcoma cells and are involved in its repression (Datta *et al.*, 2005). Interestingly, the catalytic function of Dnmt3a was dispensable for silencing, whereas that of Brg1 was crucial for it indicating involvement of chromatin remodeling in this process (Datta *et al.*, 2005).

The nucleolar remodeling factor, NoRC, is involved in promoting the methylation and silencing at the rDNA gene region. NoRC interacts with Dnmt1 and Dnmt3a *in vivo* (Santoro *et al.*, 2002), where methylation directly affects transcriptional repression (Santoro and Grummt, 2001).

Lsh is primarily involved in *de novo* methylation but seems to be dispensable for *maintenance* methylation (Yan *et al.*, 2003; Zhu *et al.*, 2006). Lsh was shown to cooperate with Dnmt1 and Dnmt3b and also HDAC1 and HDAC2 to silence transcription. Repression by Lsh and interactions with HDACs are lost in Dnmt1/3b knockout cells. These data suggest that Lsh might serve as "recruiting factor" for Dnmts and HDACs to establish transcriptionally repressive chromatin. Interestingly, transcriptional repression and recruitment of DNA methyltransferases did not immediately result in DNA methylation (Myant and Stancheva, 2008).

Together, these studies provide evidence for a tight interplay between chromatin remodeling and DNA methylation. However, the functional mechanisms linking these processes are far from being understood. The interaction with a variety of other DNA

binding proteins and the burden of the nucleosomal chromatin structure suggest that chromatin-associated factors could probably dictate the targeting of DNA methyltransferases to specific DNA sequences. For example Dnmt1 and Dnmt3a are known to interact with HDAC1 and HDAC2, but the functional consequence of this interaction remains unclear (Fuks *et al.*, 2001; Ling *et al.*, 2004; Robertson *et al.*, 2000; Rountree *et al.*, 2000).

C. Objectives

Two main research objectives of this doctoral thesis have been defined:

I. Study the molecular mechanisms of nucleosome positing directed by chromatin remodeling.

II. Examine the biochemical properties of the *maintenance* methyltransferase Dnmt1 in the context of chromatin.

1. Nucleosome positioning by chromatin remodeling enzymes

Recent results of numerous, mainly *in silico* studies suggest the participation of additional trans-acting factors besides the DNA sequence, such as chromatin remodeling complexes in positioning nucleosomes (Ioshikhes *et al.*, 2006; Peckham *et al.*, 2007; Segal *et al.*, 2006) (see section B.II.3). Nevertheless, it is unclear to which extend nucleosome positions are determined by histone-DNA interactions or are mediated by chromatin remodeling activities. To gain insight into the role of chromatin remodeling enzymes in the process of nucleosome positioning, I compared the nucleosome positioning properties of different chromatin remodeling enzymes, such as Snf2H, ISWI, Brg1, Mi-2 and the ACF and NURF complex. Furthermore, I analyzed specific DNA features that are recognized by chromatin remodeling enzymes to elucidate the molecular characteristics.

2. *Maintenance* methylation in the context of chromatin

Packaging of CpG sites into mononucleosomes and higher levels of chromatin compaction could represent an obstacle for Dnmt1 to reach its target sites for methylation. The functional properties of DNA methylation by Dnmt1 within the context of chromatin are poorly defined: While interactions of Dnmt1 with chromatin remodeling enzymes have been demonstrated (Geiman *et al.*, 2004b; Robertson *et al.*, 2004), it is unclear whether these proteins affect DNA methylation activity. Efficient DNA methylation could require additional participation of remodelers. To shed light onto the role of chromatin remodeling in maintenance methylation by Dnmt1, I initially studied the DNA and nucleosome binding properties of Dnmt1. To further extend these analyses, I then investigated Dnmt1 mediated DNA methylation in mononucleosomes. Finally, to determine the influence of chromatin remodelers in this process, I tested different chromatin remodeling enzymes such as Brg1 and ACF in my experimental set-up.

D. Material and methods

I. MATERIAL SOURCES

All common chemicals and materials were ordered by Merck (Darmstadt), Pharmacia (Freiburg), Pierce (Bonn), Promega (Mannheim), Roche (Penzberg), Roth (Karlsruhe), Serva (Heidelberg), and Sigma (Deisenhofen), unless otherwise stated. Radioactive materials were ordered by Amersham Pharmacia (Braunschweig).

1. Laboratory chemicals and biochemicals

Acrylamide (Rotiphorese Gel® 30)	Roth, Karlsruhe
Agarose (ME, LE *GP* and low melting)	Biozym, Hessisch Oldenburg
Ampicillin	Roth, Karlruhe
Aprotinin	Sigma, Taufkirchen
ATP	Sigma, Taufkirchen
[γ-32P]- ATP	GE Healthcare, Munich
Bacto Agar	BD, France
Bacto Peptone	BD, France
Bacto Trypton	BD, France
Blue Gal	Invitrogen
BSA (Bovine serum albumin), 98% pure	Sigma, Taufkirchen
BSA, purified	NEB, Frankfurt/Main
Bromphenolblue	Serva
β-Mercaptoethanol	Sigma, Taufkirchen
Chloramphenicol	Roth, Karlsruhe
Coomassie G250	Serva, Heidelberg
[α-32P]-dCTP	GE Healthcare
DEAE Sepharose	GE Healthcare, Munich
dNTP-Mix	NEB, Frankfurt/Main
dNTP-Set	Roche, Mannheim
DMSO (Dimethylsulfoxid)	Merck
DTT (Dithiothreitol)	Merck
EDTA	Sigma, Taufkirchen
EGTA	Sigma, Taufkirchen
Ethidium bromide	Sigma, Taufkirchen
Fetal bovine serum	Sigma, Taufkirchen
3-glycerophosphate	Sigma, Taufkirchen
Glycogen	Roche, Mannheim
Guanidium-Cl	Sigma, Taufkirchen
Hepes	Roth, Karlsruhe
Hydroxyl apatite	Bio-Rad, Munich
IPTG	Roth, Karlsruhe

Kanamycin	Sigma, Taufkirchen
Leupeptin	Sigma, Taufkirchen
NP40 (Igepal CA-630)	Sigma, Taufkirchen
Orange G	Sigma, Taufkirchen
Paraformaldehyde	Sigma, Taufkirchen
Pepstatin	Sigma, Taufkrichen
Phenol/ Cholorform/ Isoamylalcohol 25/ 24/ 1	Roth, Karlsruhe
Polyethyleneglycol 8000	Roth, Karlsruhe
PMSF (Phenylmethylsulfonylfluoride)	Roth, Karlsruhe
S'adenosly methionine (SAM)	Sigma, Taufkirchen
Salmon Sperm DNA	Invitrogen
SYBR Safe	Invitrogen
N,N,N',N'-Tetramethylethylendiamine (TEMED)	Roth, Karlsruhe

2. Enzymes

Enzymes	Company
Creatin phoshate kinase	Boehringer
DNaseI	Roche
Klenow enzyme	New England Biolabs
Iproof high fidelity DNA polymerase	BiooRAD
MNase (S7 Nuclease)	Roche, Sigma Aldrich
Proteinase K	Merck
Restriction endonucleases (e.g.MspI, HpaII)	Fermentas, New England Biolabs, Promega, Roche
RNase A	Promega
M.SssI-Methylase	New England Biolabs
T4 DNA ligase	New England Biolabs
T4 polynucleotide kinase (PNK)	New England Biolabs
Taq DNA polymerase	Promega, AG Längst (University of Regensburg)

Table 2: Used enzymes and respective company

3. Buffers and solutions

Stock solutions like PBS, TBE, TE, DNA sample buffer or SDS-PAGE-running- and sample buffer and several other buffers were prepared according to „Lab FAQS" (Hoffmann-Rohrer, 2000). Additional buffers and solutions are described in the individual sections. The most common solutions are listed below:

Buffers and solutions	Components
DNA Sample buffer (10x)	50 % glycerol; 50 mM Tris-HCl, pH 7.6; 10 mM EDTA; 0.05 % bromphenolblue und xylenecyanol or 0.05% orange G
SDS protein sample buffer (6x)	300 mM Tris/HCl pH 6.8, 10 % SDS, 50 % glycerin, add 0.05 % Bromphenolblue and 5 % β-Mercaptoethanol later
EX- X buffer	20 mM Tris-HCl, pH 7.6; 1.5 mM MgCl2; 0.5 mM EGTA; 10 % glycerol; X mM KCl
Stop mix	4 % SDS; 100 mM EDTA
Phosphate buffered saline (PBS)	140 mM NaCl; 2.7 mM KCl; 8.1 mM Na2HPO4; 1.5 mM KH2PO4, pH adjusted to 7.4 with HCl
TBE buffer	90 mM Tris; 90 mM Boric acid; 2 mM EDTA
TE buffer	10 mM Tris-HCl, pH 7.6; 1 mM EDTA
Stacking buffer (4x)	0.5 M Tris-HCl; 0.4 % SDS, pH adjusted to 6.8 with HCl
Resolving buffer (4x)	1.5 M Tris-HCl; 0.4 % SDS, pH adjusted to 8.8 with HCl
SDS-PAGE running buffer	3.5 mM SDS; 25 mM Tris; 190 mM glycine

Table 3: Common buffers and solutions

4. Kits

Kit	Company
Enhanced chemiluminescence Kit	Amersham
EpiTect Bisulfite Kit	Qiagen
Plasmid purification Kit	Qiagen
Plasmid isolation kit	Qiagen Invitrogen
QIAquick PCR purification Kit	Qiagen
pGEM-T-EASY cloning Kit	Promega

Table 4: Kits with the respective company

5. Radioactive material

All radioactive material was either supplied by Amersham Pharmacia ([^{3}H]-S-adenosyl methionine , 37 MBq/ml, 1 mCi/ml; (α-^{32}P) dCTP (3000 Ci/mmol, 10 mCi/ml) or by NEN (γ-^{32}P)-ATP (3000 Ci/mmol, 10 mCi/ml).

6. Medias

Mammalian cells were cultured in DMEM (Dulbecco's Modified Eagle Medium, Gibco) supplemented with glucose (100 mg/l), pyruvat und L-glutamine. 1 % penicillin-streptomycin (10 mg/ml Gibco) and 10 % fetal calf serum (Gibco) was added prior to use. *Sf21* and *Sf9* cells were maintained in Sf900II-media (Invitrogen), containing 4 mM N-acetyl-L-alanyl-L-glutamin, 63 mg/l penicillin, 50 mg/l streptomycin and 10 % fetal calf serum (FCS), heat-inactivated. Liquid and solid LB-medium (Luria-Bertani) was prepared according to standard protocols by (Sambrook *et al.*, 1989)

7. Antibodies

The following table gives an overview of the utilized primary and secondary antibodies and their individual dilutions:

Name	Description/ Dilution / Supplier
α-GFP (mouse)	monoclonal antibody (IgG2a)/1:200/ Mobitec, #A-11120
α-His (mouse)	Monoclonal Penta-histidin- antibody/1:1.000/Qiagen, #34660
α-hSnf2H (6929) (rabbit)	Polyclonal antibody/1:2.000/provided by P. Varga-Weisz (Poot *et al.*, 2000a)
α-IgG (rabbit)	Secondary antibody, goat, Horseradish Peroxidase (HRP-conjugated)/1:10000/Biozol, #12348
α-IgG (mouse)	Secondary antibody, goat, (HRP-conjugated)/1:5000/Amersham Pharmacia, #NA931
α-IgG (rat)	Secondary antibody, goat, (HRP-conjugated)/1:5000/Amersham Pharmacia, #NA931
α-IgG+IgM (rat)	Secondary antibody (HRP-conjugated)/1:5000/Dianova, #111-116
α-Flag (mouse)	Secondary antibody, goat, (HRP-conjugated)/1:1000/Sigma
α-Dnmt1 (2E8)	Monoclonal antibody (IgG2b), rat / 1: 2000/ E. Kremmer, Helmholtz Gesellschaft
α-tubulin (mouse)	Monoclonal antibody (DM1a) / 1:3000/Abcam

Table 4: Utilized antibodies

8. Eukaryotic tissue culture cell lines

For growth conditions see ATCC: http://www.lgcstandards-atcc.org.

Cell line	Derivation
HeLa	human adenocarcinoma cell line (epithelial cells)
HEK 293	human renal carcinoma cell line (epithelial cells)
NIH/3T3	murine embryonic fibroblast cell line
Sf21/Sf9	Insect cell line (*Spodoptera frugiperda*)

Table 5: Utilized mammalian and insect cell lines

9. Bacteria

XL1 blue (Novagen), DH5α E. coli strains (Novagen), Pir+ 8B (Imre Berger, EMBL Grenoble) were used for DNA plasmid amplifications.

10. DNA-constructs

Name	Cloning strategy
pPCRScript_slo1-gla75 insert (Sloning DNA)	slo1-gla75 insert consisting of NPSs rDNA-601-*Hsp70* dimer; Sloning
pBluescript(BsmI)	pBluescriptSK(+)backbone.HindI/EcoRI fragment. (Oligonucleotides: BsmHE_F/ BsmHE_R); Längst Lab
pT7K3	PT7Blue3(Novagen) backbone with K3rDNA fragment insert. Blunt end cloning with EcoRV (see (Rippe *et al*., 2007); Längst Lab
pCpGLbasic	R6P origin, only in cells with pir gene (Rehli group); Cloning strategy described in (Klug and Rehli, 2006)
pGA4 BN-601-m1	Vector of mod. 601 sequence for Bisulfite sequencing; the modified 601 NPS sequence can be amplified (Oligonucleotides: MF77/78), Mr Gene
rDNA constructs	The construct pT7blue3-LP7/LP2 was used to generate hemimethylated DNA that was constructed of the pT7-blue-3vector (Novagen). The 248 bp-rDNA-promotor-fragment was synthesized by PCR (Oligonucleotides: LP2 and LP7) and inserted by the EcoRV-restriction site of the plasmid

601 construct	p601-construct, which was inserted into the pGEM3Z-plasmid was kindly provided by Jon Widom (Lowary and Widom, 1998).
CpGless601	BamH1/HindIII fragment (Oligonucleotides: Bam_fw_new/HindIII_rev_new) inserted into pCpGLbasic
Dnmt1 construct pEGFPC1-Dnmt1 human full length	Mammalian expression vector EGFP, N-terminal GFP-tagged murine Dnmt1Unknown cloning strategy (Leonhardt group)
pEGFP Dnmt1 mouse full length	Mammalian expression Vector EGFP, N-terminal GFP-tagged, XmaI/SmaI - SpeI NotI fragment (Leonhardt group)
Dnmt1 construct pEGMT1LdeltaZnF mouse	pEGMT1Delta-ZnF : Deletion in Zn-finger (aa 655-696), Integration of SacII site (Ala-Ala-Ala); Leonhardt group
Dnmt1 construct GFP-Znf mouse	GFP-ZnF (aa 643-700): Zn-finger Dnmt1 Leonhardt group

Table 6: DNA constructs with cloning strategy

Plasmid	Supplier
pCMV14	Stratagene
pBluescript SK(+)	Stratagene
pUC19	Novagen
pBR322	Novagen

Table 7: Common DNA plasmids with supplier

11. Oligonucleotides

All oligonucleotides were purchased from Eurofins MWG Operon and diluted to a final solution of 100 µM with MilliQ-water.

Oligonucleotide	Sequence		T_m	Purpose
Air1_met.up	TGCGGAAT5GTCTAA5G5GTGGAAT5GTCCCCTTG	fw	69,5°C	Generation AIR fragment
Air1_nomet.do	CAAGGGGACGATTCCACGCGTTAGACGATTCCGCA	rev	74,2°C	Generation AIR fragment
AP1	ATCTTTTGAGGTCCGGTTCTTT	fw	56°C	77-WID
AP2	GATCTTAGTACAGAGAGGGAGAGTCAC	rev	65°C	77-WID-77
AP3	CATGGTATGACTTCCAGGTATGG	fw	60,6°C	22-WID
AP4	GGAGGTGGCCCAAACATATG	rev	59,6°C	Not used here
AP5	ATGTTTGGGCCACCTCCCC	fw	61°C	40-WID

AP6	GACCCCATAACGAAAAGAACCG	rev	60,3°C	Not used here
AP7	GATCCAGAATCCTGGTGCTGAG	fw	62,1°C	WID
AP8	TGTATATATCTGACACATGCCTGGA	rev	59,1°C	WID
AP9	GGCCTTAAGAGAAATTTCTCGAG	rev	58,9°C	22-WID-22
AP10	CTAGAGAATAACGGCCTTAAGAGA	rev	59,3°C	40-WID40
AP11	TCTTTTCGTTATGGGGTCATAT	fw	54,7°C	60-WID
AP12	AAACGAATCTAGAGAATAACGGC	rev	57,1°C	60-WID-60
AP13	TTTCTCGAGTTTTCTTTGCTAGCT	rev	57,6°C	22-WID-22
AP14	TAACGGCCTTAAGAGAAATTTCT	rev	55,3°C	40-WID-40
AP15	GTACAGAGAGGGAGAGTCACAAAAC	rev	63,0°C	77-WID-77
AP16	TGACTTCCAGGTATGGATCCAG	rev	60,3°C	15-WID
AP17	AGTTTTCTTTGCTAGCTAGCTGTATA	rev	58,5°C	15-WID-15
601_m1	TCTTCACAC^{m}CGGGTTCATCCCTTATGTGC^{m}CGGAC	fw	70.7 °C	601 DNA fragment (hemimet.)
601_nm1	TCTTCACACCGGGTTCATCCCTTATGTGCCGGAC	fw	73.1 °C	601 DNA fragment (unmeth.)
601_nm2 rev	GTCCGGCACATAAGGGATGAACCCGGTGTGAAGA	rev	73.1 °C	601 DNA fragment
LP2	GGACAGCGTGTCAGTACCTATCT	fw	62.4 °C	rDNA fragment
LP7	GAAAGCTATGGGCGCGGTT	rev	58.8 °C	rDNA fragment
MF77	AGATCTTTTGAGGTCCGGTTCTT	fw	60°C	BN601
MF78	ATCTTAGTACGGAGAGGGAGCG	rev	60°C	BN 601
MF79	GAATTGGGTACCAGATCTTTTGAG	fw	60°C	BN601 no CpG, 342 bp
MF80	GGGAACAAAAGCTGGAGCTC	rev	60°C	BN 601 no CPG, 342 bp
MF81	GAATTGGGTATTAGATTTTTTGAGGTT	fw	60°C	BN601 (+)strand Bisultfite with MF82
MF82	AAAAACAAAAACTAAAACTCAAATCTTAATA	rev	60°C	BN 601 (+) Bisultfite, with MF81
MF 112	GGGAATAAAAGTTGGAGTTTAGATTTTA	fw	60°C	BN 601 (-) strand Bisulfite with MF113
MF113	AAATTAAATACCAAATCTTTTAAAATCC	rev	60°C	BN 601 (-) strand Bisulfite with MF112
MF124	GATCCCGAATCCCGGTG	fw	60°C	pGA BN601 147bp fragment

MF125	CTAGCTGTATATATCTGACACGTGCC	rev	60°C	pGA BN601 147bp fragment
pBR322_hm_rev	CATTCACAGTTCTCCGCAAGAATTG	rev	61,3°C	T4 DNA poly reaction, Oligo at Nb.BsmI site
CMV_14_rev	CATTCATTTTATGTTTCAGGTTCAGGGGGGAGGTGTGGGA	rev	71,6°C	Nb.BsmI site in CMV14
BsmHE_F	AGCTTGCGGAGAACTGTGAATGCGC	fw	66,3°C	Generation BsmI site in pBluescript
BsmHE_R	AATTGCGCATTCACAGTTCTCCGCA	rev	63,0°C	Generation BsmI site in pBluescript
BamH1_fw	GCTGACTACAAAGACCATGACGGTGATT	fw	60°C	Insertion of nicking site BamHI
BamH1-rev	GATCCTCTAGAGTCGACTGGTACCGATATC	rev	60°C	Insertion of nicking site HpaI
Nb.BbvCI_fw	GCCTCCCGAGTTGTTGGGATTCCAGG	fw	69,5°C	Generation hm DNA after ss-nick via PCR
Nb.BbvCI-rev	GAGAATCGCTTGAACCCAGGAGGCGGCGA	rev	70,9°C	Generation hm DNA after ss-nick via PC
pT7_3765.fw	GCTCGTATGTTGTGTGGAATTGTGAG	fw	60°C	Generation of pT7k3 border frame
pT7_190.rev	GGCCAGTGAATTGTGCGGCC	rev	60°C	Generation of pT7k3 border frame
pT7_3801.fw	TTTCACACAGGAAACAGCTATGACCATG	fw	60°C	Generation of pT7k3 central frame
pT7_226.rev	GCCAGGGTTTTCCCAGTCACG	rev	60°C	Generation of pT7k3 central frame
Bam_fw_new	GGTACGACTTCCAGGTACGGATC	fw	61,7°C	Cloning 601 sequence in CpG less vector
HindIII_rev_new	CGAGTTTTCTTTGAAGCTTGCTG	rev	61,4°C	Cloning 601 sequence in CpG less vector
601_CpGless_fw	GAGCAAACAGCAGATTAAAAGGAAT	fw	60 °C	Primer to check correct insertion of 601 into CpG less

Table 8: Oligonucleotides with indicated name, sequence, orientation, melting temperature and respective purpose

12. Fluorescence labeled Oligonucleotides

Oligonucleotide	Sequence		T$_m$ (°C)	Purpose
BglII_A647_fw	ATCTTTTGAGGTCCGGTTCTTT	fw	56,5 °C	Labeled 77-WID-77 (Alexa)
15f_A647	TCAGGTCGACCAGTT	fw	47,8	Dnmt1 EMSA free DNA Labeled 15-mer (Alexa)
15rev	AACTGGTCGACCTGA	rev	47,8	Dnmt1 EMSA free DNA 15-mer
30f_A488	CTCCGGGTTGTCAGGTCGACCAGTTGTTCC	fw	72,2	Dnmt1 EMSA free DNA Labeled 30-mer (Alexa)
30r	GGAACAACTGGTCGACCTGACAACCCGGAG	rev	72,2	Dnmt1 EMSA free DNA 30-mer
45f_A555	ATCAGTTCTCCGGGTTGTCAGGTCGACCAGTT GTTCCTTTGAGGT	fw	>75	Dnmt1 EMSA free DNA Labeled 45-mer (Alexa)
45r	5ACCTCAAAGGAACAACTGGTCGACCTGACAA CCCGGAGAACTGAT	rev	>75	Dnmt1 EMSA free DNA 45-mer
60f_A647	5TCGGTCTTATCAGTTCTCCGGGTTGTCAGGTC GACCAGTTGTTCCTTTGAGGTC	fw	>75	Dnmt1 EMSA free DNA Labeled 60-mer (Alexa)
60r	GAACCGGACCTCAAAGGAACAACTGGTCGACC TGACAACCCGGAGAACTGATAAGACCGA	rev	>75	Dnmt1 EMSA free DNA 60-mer
AP1_fw_FAM	ATCTTTTGAGGTCCGGTTCTTT-	fw	56,5	5'Fluorescein (FAM) labeled for 77-WID-77 Footprint
AP15_revHEX	GTACAGAGAGGGAGAGTCACAAAAC	rev	63°C	5'HEX (HEX) labeled for 77-WID-77 Footprint

Table 9: Fluorescence labeled oligonucleotides with indicated name, sequence, orientation, melting temperature and respective purpose

13. Recombinant Baculoviruses for *Sf9* or *Sf21* cells

Recombinant viruses, encoding the following proteins were available in the department. Penta histidin-taggted Dnmt1 (human) was kindly provided by Dr. Keith Robertson (Yokochi and Robertson, 2002).

ISWI	Gernot Längst
Flag-ISWI	Gernot Längst
Flag-ACF1	Gernot Längst
Flag-Snf2H	Ralf Strohner
Flag-Mi-2	Gernot Längst
Flag-Brg1	Robert Kingston
Flag-Chd1	Alexandra Lusser

14. *Drosophila melanogaster*: maintenance, embryo collection and extracts

Fly maintenance and embryo collection was performed according to the rules established fly facility in the department of Peter Becker, Adolf-Butenandt-Institute. *Drosophila* embryo extracts were prepared as described by Peter Becker. Recombinant histones were a common reagent, produced routinely in the department of Peter Becker, Adolf-Butenandt-Institute.

15. Chromatographic material

Material	Company
Nickel-NTA agarose (Ni^{2+} beads)	Qiagen
M2 agarose (Flag-beads)	Sigma
Sephadex G 25/50 spin columns	Roche

Table 10: Chromatographic material

16. Blotting material

Material	Company
Hybond N+ membrane	Amersham
Whatman 3MM paper	Whatman
PVDF membrane (Immobilon) 0.4 µm	Amersham/ Millipore

Table 11: Material used for Western blotting

17. Instruments

Instruments	Supplier
37 °C shaker	Heraeus Instruments, Kendro
37°C plate incubator	Memmert
-80 °C freezer	Sanyo
Agarose gel chamber	Werkstatt University of Regensburg
Autoclave	Verioklav
Autoclave LTA 25B2	Zirbus
Balance	Sartorius, Kern
Centrifuge 5415R	Eppendorf
Centrifuge Centrikon T-324	Kontron Instruments
Centrifuge 3-16K/ 1-14/ 4-15	Sigma
Centrifuge rotator A. 0.9 / A. 8.24	Heralab / Kontron
Cell Spinner bottles	Integra Bioscience
Drying Cabinet	Mammert
Fireboy plus	IBS
Fluorescence Image reader BAS 1000	Fuji
GelMax UV imaging system	Intas
Laminar flow hood	Antair BSK
Liquid nitrogen can	Union Carbide, UK
Ice machine	Ziegren
Incubator SafeCell UV	Sanyo
Cooled Incubator (27°C)	LMS
Magnetic stirrer MR HEI-Mix L/ MR 3001	Heidolph
Microscope IX50	Olympus
Microwave	Sharp, MDA
Millipore machine	ELGA
Nanodrop UV Spectrometer ND-1000	PeqLab
Overhead shaker	Biosan
PAA gel chamber (Novex Mini cell)	Invitrogen
PCR machine Primus 96 advanced	PeqLab
Peristaltic pump	Heidolph

pH electrode + meter	Knick
Photometer	Amersham Biosciences
Pipetman "Pipetboy comfort"	Integra Biosciences
Polymax 1040 gel shaker	Heidolph
Rotorshake Genie	Scientific Instruments
RS 24 Rotating wheel	Biosan
SafeImager	Invitrogen
Shaker Unimax 2010 (insect cells)	Heidolph
Shaker incubator (Minitron)	Infors HT
Digital Sonifier Model 250-70	Branson
Tabletop balance	Acculab
Thermomixer comfort	Eppendorf
TS 100 Thermo shaker	PeqLab
Unigeldryer 3545D	Biosan
Western Blot apparatus	PeqLab /
Power-Supplier Power Pac 3000	BioRad
Protein gel chamber Novex mini-Gel	Invitrogen
LE-80K ultracentrifuge	Beckman Coulter, Optima^{TK} 6000
Agarose UV imaging system	Gelmax, Intas
BAS 1000 Raytest	Fujix
PCR machine (old)	Perkin Elmer
PCR machine	Peqlab
Real Time PCR machine	Corbett Research, Rotor Gene RG-3000
Trans – Blot® SD Semi-dry transfer cell	BioRAD

Table 12: List of instruments

18. Free software and online tools

Application	Author
NEB double digest finder	New England Biolabs (http://www.neb.com)
Reverse Complement	(http://www.bioinformatics.org)
Netprimer	Premierbiosoft (http://www.premierbiosoft.com)
VectorNTI	Invitrogen (http://www.invitrogen.com)
BiQ Analyzer	Christoph Bock (http://biq-analyzer.bioinf.mpi-sb.mpg.de)

Table 13: List of used software

II. M ETHODS

1. Biochemical methods (DNA-specific methods)

1.1. Standard procedures

The generation of competent cells and the transformation of electro-, or chemically competent bacteria with DNA and cultivation of bacteria were both performed according to standard protocols (Sambrook, 1989). The preparation of plasmid DNA was done by using the Qiagen or Invitrogen Midi-/Maxi-Preparation kit according to the manual. Purification, concentration determination, ethanol precipitation, restriction enzyme digestion, ligation of DNA fragments, analysis of DNA on agarose and polyacrylamide gels and amplification of DNA by polymerase chain reaction (PCR) were all performed according to standard protocols (Ausubel, 1999; Hoffmann-Rohrer, 2000; Sambrook and Russell, 2001). Isolation of DNA from agarose gels was done using the Qiagen gel extraction kit.

1.2. Determination of DNA concentration

The DNA concentration of single and double stranded DNA was determined by absorption measurement at 260 nm using a NanoDrop ND1000 spectrophotometer (Peqlab). The purity of the DNA could be judged by the ratio A260/280.

1.3. Analysis of DNA quality and quantity

Restriction enzymes were used in reaction conditions according to the manufacturer's recommendations concerning buffer, addition of BSA and temperature (see NEB). Different experimental set-ups were used in dependence on preparative or analytical scale: For the analytical digest 0.1-1 µg DNA were incubated using 5 u of the respective restriction endonuclease in a total volume of 50 µl. The preparative restriction digest was done with 20 µg DNA using 20 u restriction endonuclease in a total volume of 30 µl. To check the completion of the digest, DNAs were electrophoretically separated using 0.8-2.0 % TBE-agarose gels supplemented with SybrSafe.

1.4. Hybridization of Oligonucleotides

Similar quantities of complementary single strand oligonucleotides (300 pmol each) were mixed in reaction buffer (0.1 M KCl and 1 mM $MgCl_2$) in a final volume of 100 µl, denatured in a thermocycler (Perkin Elmer; 95°C for 10min) and slowly (1-2 hours) chilled to room temperature to allow complete oligonucleotide hybridization.

1.5. Radioactive and fluorescent labeling of DNA

For radioactive labeling, DNA was either labeled by incorporation of radioactive dNTP during PCR ("body labeling") or by labeling of an oligonucleotide with T4 PNK ("endlabeling"). For "body labeling", a standard PCR reaction was performed, to which (α-^{32}P) dCTP was added: 100 ng DNA template, 500 pmol of each primer, 100 nmol of dATP, dGTP, dTTT, 20 nmol dCTP and 16.7 pmol (α-^{32}P) dCTP in 1ml. Purification and removal of non-incorporated nucleotides was done by ethanol precipitation with subsequent gel isolation. Oligonucleotides were alternatively end labeled with γ-^{32}P-ATP using T4 PNK according to the manufacturer's protocol. Non-incorporated nucleotides were separated from the labeled DNA using Sephacryl G25 spin columns (Roche).

DNA was 5' fluorescently labeled by PCR with oligonucleotides harboring a 5' fluorescence tag (see section D.I.12. for oligonucleotides). For the footprint template a forward 5' FAM and a reverse 5' HEX labeled oligonucleotide was used. The PCR reaction was performed following standard PCR protocols (see section D.II.1.8) with the indicated annealing temperature. The DNA quality was analyzed on a 5 % polyacrylamide gel and the DNA purified using ethanol precipitation. Non-incorporated oligonucleotides were removed using a Sephacryl G50 spin column (Roche, GE Healthcare).

1.6. Precipitation and isolation of radioactive DNA fragments

DNA fragments were precipitated from the supernatant by adding 0.5 volumes of 7.5 M ammoniumacetate (pH 7.7) and 2.5 volumes of 100% ethanol, vortexed briefly and incubated on ice (10min). Precipitates were span (4°C, 13000 rpm, 15 min), washed with 70% ethanol and dissolved in 100 µl EX-100. Depending on the purpose and purity of the amplified DNA, the probe was either used directly or gel purified.

For gel purification, DNA was separated by polyacrylamide gel electrophoresis in 0.4 x TBE. The wet gel was exposed on an X-Ray film, and the DNA fragment was excised from the gel. The gel piece was incubated with 1000 µl EX-300 and the DNA fragment eluted by vigorous shaking for at least 3 h at RT. Gel pieces were pelleted in an Eppendorf mini-centrifuge (RT, 16000 g, 1 min). The eluted DNA was precipitated again and finally dissolved in 100 µl EX-100. This DNA was subsequently used for nucleosome assembly reactions.

1.7. Generation and analysis of hemimethylated and methylated DNA

Generally, DNA was methylated using the bacterial methyltransferase M. SssI according to the manufacturer's instructions (NEB). Briefly, 1µg of DNA was incubated with 5 u enzyme in the respective reaction buffer in the presence of 160 µM S-adenosyl methionine at 37°C for at least 4 h or O/N with freshly added SAM every hour. The enzyme was inactivated at 65°C for 20 min.

The final protocol used to prepare hemimethylated DNA was the following:

At first the 6.3 kb pCMV14 plasmid was linearized with a single cutter restriction endonuclease (here HindIII) according to the manufacturers' recommendations. 1/3 of the linearized DNA was methylated with M.SssI methyltransferase and then incubated with 2/3 non-methylated linear pCMV14 DNA for 10 min at 95°C and hybridized by slowly cooling down. Subsequently, the mixture was applied to MspI/HpaII digest and analyzed on a 1.3 % agarose gel to check the quality of hemimethylated DNA.

To prepare hemimethylated DNA a variety of different methods were tested:

In each experimental setup 20 µg pCMV14 were first methylated with 12.5 u M.SssI. A single-strand nick was inserted by incubating with the nicking endonuclease Nb.BbvCI (3 u/µg) for 4 h at 65°C and heat inactivated according to the manufacturers' recommendations. After heat inactivation for 20 min at 80°C the DNA was phenol-chloroform extracted and precipitated by ethanol precipitation.

ExonucleaseIII digest was carried out in 200 µl volume using ExonucleaseIII (60 u/µg DNA) for at least 4 h at 37°C and heat-inactivated afterwards. Hybridization of 3 µg Primer Nb. BbvCI_rev (300 pmol/10 µg DNA) was done by incubation for 5 min at 95°C and a constant cooling down to 37°C.

The extension was performed using 10 µg pCMV14 (in buffer 1); 200-500 µM dNTP-mix and 10 u T4 polymerase in 200 µl volume by incubation at 37°C for at least 90 min. The DNA was extracted with phenol-chloroform and precipitated using ethanol and ammonium acetate.

A method based on nick translation using Taq polymerase was carried out as follows: 10 µg nicked DNA were incubated with 5 u Taq polymerase, 4 µl dNTP-mix (2.5 mM each) in 100µl volume for 2h at 37°C. Alternatively, *E.coli* DNA polymeraseI was used: 10 u DNA polymerase I; 500 µM dNTPs for 2h30 at 16°C. The DNA was extracted with phenol-chloroform and ethanol precipitated.

1 µg nicked DNA was applied to 100 µl reactions using 1.5 u, 2.5 u and 5 u Taq Polymerase. The DNA was extracted with phenol-chloroform and precipitated using ethanol and ammonium acetate. PCR using oligonucleotides Nb. BbvCI_fw and Nb. BbvCI_rev that hybridize next to the nick to generate circular and linear hemimethylated DNA in one reaction was performed. The PCR reaction was done following standard protocols with 3 cycle rounds:

Cyclestep (Programm number #)	Temperature (°C)	Time
Denaturation	95°C	5 min
Annealing	67°C	8 min
Extension	72°C	15 min

Table 14: Used PCR protocol

1.7.1. ANALYSIS VIA RESTRICTION ENZYME DIGEST (MSPI / HPAII OR GLAI)

Methylation efficiency was determined by restriction digest with the methylation sensitive restriction endonucleases MspI/HpaII according to the manufacturers' recommendations (NEB). Alternatively, GlaI (SibEnzyme) a restriction endonuclease that cuts methylated DNA in dependence on the number and position of methylated nucleotides in its recognition sequence was used.

1.7.2. TIME COURSE EXPERIMENT TO ANALYZE HEMIMETHYLATED **DNA**

The quality of hemimethylated DNA was also checked by performing a kinetic approach:

40 nM Dnmt1 were incubated either with the hemimethylated substrate or a 1:3 mixture of SssI methylated and unmetylated substrate in a 400 µl reaction volume with 63 nM ^{3}H-SAM, 4 µl BSA. Aliquots were taken at different time points (5 min-3 h) and the reactions stopped by shock-freezing on a dry ice/ethanol bath. The methylation activity of Dnmt1 was analyzed as described in section D.II.6.1.

1.7.3. METHYLATION BY **D**NMT1

1 µg pCMV14 DNA was methylated with 10-80 nM Dnmt1 O/N at 37°C with 160 µM SAM in the optimized 10 x reaction buffer. Subsequently the DNA was ethanol precipitated and quality analyzed by restriction digest.

1.8. Preparation of DNA fragments for the assembly of mononucleosomes

1.8.1. GENERATION OF **601** FRAGMENTS

The 601 DNA templates (WID) for the Dnmt1 EMSAs were generated by different preparative restriction digests of the Sloning DNA (pPCRScript_slo1-gla75 insert). Figure 17 illustrates the Sloning construct with the respective restriction sites indicated. Prior to large-scale reactions analytical test reactions were performed. The different fragments were amplified via PCR (see below). Quality of the restriction digests and the PCR amplification were analyzed on a 1.2 % agarose gel and DNA concentration was determined. Subsequently these different fragments were assembled into chromatin using salt gradient dialysis (see section D.II.4.1). The efficiency was analyzed on a 6 % PAA gel. By using this strategy asymmetrical and symmetrical nucleosomal positions with different overhanging DNA lengths were generated.
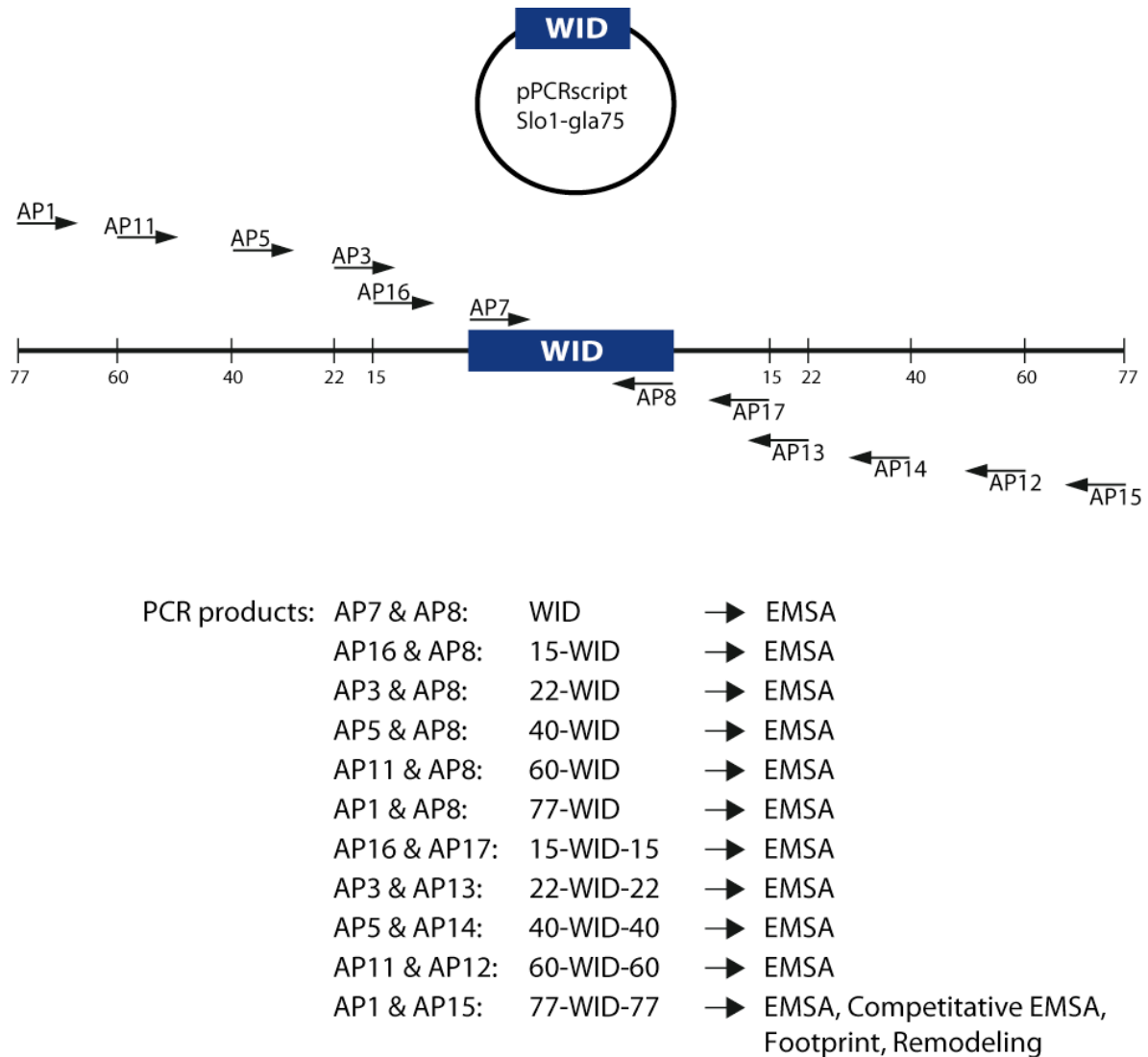
Figure 17. Generation of different 601 DNA templates
The different 601 DNA fragments were generated by PCR using the plasmid pPCRscript Slo-1-gla75 as DNA template. By using different combinations of oligonucleotides (AP1-AP17), DNA fragments containing the 601 nucleosome positioning sequence (referred to as WID, 147 bp) and different length of flanking DNA (0-77 bp), either symmetric or asymmetric were generated. The PCR products were either used directly as nascent DNA or reconstituted into chromatin using the salt gradient dialysis method. The different 601 DNA and nucleosomal substrates were then applied to the specific functional assays as indicated (EMSA, Competitive EMSA, DNaseI footprint assay or Nucleosome remodeling assay).

Restriction endonuclease digest in 30 µl volume with 20 µg Sloning construct, 3 µl 10x NEB restriction Buffer, 20 u restriction endonuclease at 37°C O/N.Ethanol Precipitation O/N at -20°C with glycogen as carrier.

1. Test PCR in analytical scale (50 µl):

   50 ng DNA template (see below), 5 µl 10x Taq-Buffer (Genaxxon S), 1 µl of each Oligonucleotide (10 pmol/µl stock), 1 µl dNTP-Mix (10 mM), 1 µl Taq Polymerase (Elisa).

   Run PCR in old Perkin Elmer cycler (0.5 ml reaction tubes) or old PeqLab cycler (0.2 ml reaction tubes).

2. Large scale PCRs in 10 ml:

   10 µg DNA template (see below), 1 ml 10x Taq-Buffer (Genaxxon S), 20 µl of each Oligonucleotide (100 pmol/µl stock), 20 µl dNTP-Mix (10 mM), 200 µl Taq Polymerase (Elisa).

   Mix well and aliquot 200-300 µl to 0.5 ml reaction tubes. Run PCR in old Perkin Elmer cycler.

Cycle step (Programm number #)	Temperature (°C)	Time	Number of cycles
# 18 Initial denaturation	94	2 min	1
# 19 Denaturation	94	40 s	35
Annealing	55-58°C according to table ($T_{(Ann.)}$)	40 s	
Extension	72	40 s	
# 20 Final Extension	72	10 min	1
# 21 Cool down	4	forever	1

Table 15: Used PCR protocol for 601 fragments

Template	Primer_fw	Primer_rev	RE template
15-WID	AP16	AP8	NcoI/NheI
15-WID-15	AP16	AP17	NcoI/AflII
22-WID-22	AP3	AP13	NcoI/AflII
40-WID-40	AP5	AP14	NdeI/XbaI
60-WID	AP11	AP8	BglII/NheI
60-WID-60	AP11	AP12	BglII
77-WID-77	AP1	AP15	BglII
22-WID	AP3	AP8	NcoI/NheI
40-WID	AP5	AP8	NdeI/NheI
77-WID	AP1	AP8	BglI/NheI
WID	AP7	AP8	BamHI/NheI

Table 16: 601 DNA templates (WID)

Ethanol Precipitation O/N at -20°C with glycogen as carrier.

The quality was analyzed on a 1.2 % agarose gel and concentration determined at the nanodrop.

Output: ~ 20-50 µg / 1 ml PCR reaction.

1.8.2. GENERATION OF 601-BASED DNA FRAGMENTS

The 342 bp template used for the Bisulfite sequencing assay harboring the 601 sequence and 27 CpG sites was prepared by PCR of the pGABn601_mod DNA as described in section D.II.1.8 using the oligonucleotides MF79 and MF80 with 56°C as annealing temperature.

The 147 bp 601 template was prepared by PCR of the pGABn601_mod DNA as described in section D.II.1.8 using oligonucleotides MF124 and MF125 with 56°C as annealing temperature.

The 345 bp 601 CpG less flanking region template was prepared by PCR of the Bn601CpGless DNA as described in section D.II.1.8 using oligonucleotides CH01 and CHO2 (see Lablife) with 50°C as annealing temperature.

These templates were all precipitated using 10 % PEG and 30mM MgCl2. ½ sample Vol PEG solution was added to the probe and incubated for 30 min on ice. Centrifugation at 13000 rpm for 30 min at 4°C and two washing steps using 70 % ethanol (13000 rpm for 30 min at 4°C). The pellet was air-dried and dissolved in 50 µl H2O. The concentration was determined on a Nanodrop spectrophotometer.

2. Molecularbiological methods (Protein-specific methods)

2.1. Standard procedures in protein analysis

All protein analysis were performed according to standard protocols (Ausubel, 1999; Ausubel and et al., 1994; Hoffmann-Rohrer, 2000; Sambrook *et al.*, 1989; Sambrook and Russell, 2001). Generally, proteins were kept on ice, in the presence of protease inhibitors (either Roche Complete® or Leupeptin, Pepstatin, Aprotinin (all 1 µg/ml,Genaxxon) and PMSF (0.2-1 mM) added separately). 1 mM of reducing agents DTT or ß-mercaptoethanol was also added.

2.2. Protein quantification

Protein concentration was determined using the colorimetric assay described by Bradford (Bradford, 1976). The concentration of purified proteins was also estimated according to protein standards (e.g. BSA) with known concentration in SDS-PAGE followed by Coomassie blue staining.

2.3. SDS-polyacrylamide gel electrophoresis (SDS-PAGE)

Pouring and electrophoresis of SDS-polyacrylamide gels were both performed using the Invitrogen Novex Mini cell chamber or the BioRad gel system. Separating and stacking gels were prepared according to standard protocols (Sambrook and Russell, 2001) using ready-to-use polyacrylamide solutions from Roth (Rotigel, 30 %, 49:1). For electrophoresis, protein samples were mixed with SDS-PAGE sample buffer, heat-denatured for 5 min at 95°C and directly loaded onto the gel. Proteins were separated at 90 V until the samples had passed through the stacking gel and then at 150 V until the dye front had reached the end of the gel. By running pre-stained marker proteins (PeqLab gold IV) the molecular weight of proteins could be estimated. Following electrophoresis, proteins were either stained or subjected to Western blotting.

2.4. Coomassie blue staining of protein gels

Following electrophoresis, polyacrylamide gels were fixed for 30 min in fixation solution (50 % methanol/ 10 % acetic acid) and stained for 60 min on a rocking platform with Coomassie staining solution (0.025 % Coomassie Blue R in 10 % acetic acid). Destaining was performed in 10 % acetic acid (tissue added to accelerate destain). After documentation, gels were dried onto a Whatman paper at 80 °C for 2 h on a gel dryer (BioRad).

2.5. Semi-dry Western Blot

Proteins were first separated by SDS-PAGE and transferred to nitrocellulose or PVDF membranes using a Bio-Rad "Trans-Blot SD Apparatus" or a "PeqLab Semi-Dry blotting apparatus" for 90 min at 50 mA/membrane or for 1h at 24V. For the protein transfer, the gel was sandwiched between gel-sized Whatman papers, either soaked in anode or cathode buffer (1 piece in each buffer) or in the subsequent blots just soaked in transfer buffer (6 pieces). The PVDF membrane was equilibrated for 30 min in methanol. The blot sandwich was assembled in the following order (bottom-up): 1 Whatman paper in anode buffer 1, 1 Whatman paper in anode buffer 2, SDS-PAA gel with the separating gel removed, PVDF membrane in methanol, 1 Whatman paper in cathode buffer or using the transfer buffer (Towbin buffer: 192 mM glycine, 25 mM Tris, 20% methanol, 0.05 % SDS): 1. 3 Whatman papers, PVDF membrane in methanol, SDS-gel, 3 Whatman papers. Care was taken not to trap air-bubbles between the layers.

2.5.1. DETECTION BY PONCEAU S STAINING

Transfer of the proteins was confirmed by staining the PVDF membrane for 5 min at room temperature with Ponceau S solution. The membrane was then destained by several 1 min washes in water.

2.5.2. IMMUNODETECTION

Nitrocellulose filters were incubated for at least 30 min in blocking solution (1x PBS, 5% dried milk and 0.2% Tween-20) after protein transfer in order to reduce non-specific background. Membranes were sealed in a plastic bag and incubated for 1h at RT or O/N at 4°C with the appropriate dilution of the primary antibody directed against the protein of interest. Dilutions of the used antibodies are listed in section D.I.7. The

membrane was than washed three times in PBS-Tween (10 min each) and incubated for an additional hour with the horseradish peroxidase-coupled secondary antibody. After 3 washes with PBS-Tween the antigen-antibody complex was detected using Enhanced Chemi-Luminescence Kit (ECL, Amersham) or Roche Chemiluminescence Substrate (POD) and autoradiographed according to the manuals. Visualization was performed by using the Fuji LAS3000 Fluorescence Image Reader. All steps were performed at RT.

3. Isolation of chromatin remodeling complexes and the DNA methyltransferase Dnmt1

3.1. Expression of recombinant proteins with the baculovirus system

The baculovirus system allows high expression levels of large eukaryotic proteins. Furthermore, this system reflects eukaryotic cells as the proteins are processed and posttranslational modified.

3.1.1. MAINTENANCE OF *SF21* / *SF9* CELLS

Sf21 and *Sf9* cells were cultivated in Sf-900 II medium (Invitrogen), supplemented with 4 mM N-acetyl-L-alanyl-L-glutamine, 63 mg/l penicillin, 50 mg/l streptomycin and 10 % fetal calf serum (inactivated by incubation at 56°C for 20 min). Cells were grown in suspension or as monolayers at 27°C. The suspension culture was maintained either in spinner bottles at 80 rpm or in Erlenmeyer flasks on a rotating shaker at 90 rpm. The vessels were then sterilized by autoclaving twice (spinner bottles) or by heating to 220°C (Erlenmeyer flasks). Cell density of spinner cultures was kept between $5x10^5$ and $2x10^6$ cells/ml.

3.1.2. AMPLIFICATION OF RECOMBINANT BACULOVIRUSES

Virus amplification was undertaken to preserve the virus stock and to gain a high titer of virus (typical 10^7-10^8 plaque forming units (pfu/ml)). Expansion of viral stocks was carried out at rounds of low MOI infections (e.g. 0.1 or less) in order to select for intact virus particles over several generations of virus replication.

For virus amplification, $1x10^8$ *Sf21* or *Sf9* cells (*Spodoptera frugiperda*) in 100 ml Sf 900II medium were infected with 500µl of either initial or already expanded virus stock in Erlenmeyer flasks at 27°C. Cell growth was thereafter monitored twice a day and

cells were split to maintain a constant cell density of 1×10^6 cells/ml. After the estimated time point of growth arrest, cells were further incubated for 24 hours. The cell suspension was then centrifuged for 5 min at 4000 rpm and the viral supernatant was recovered sterilely and stored at 4 °C, protected from light.

3.1.3. TESTEXPRESSION

The protein test expression serves as method to experimentally determine the amount of virus stock needed for high levels of heterologous gene expression. 1×10^6 *Sf21* cells growing in logarithmic phase were seeded to each well of a 6-well plate in 3 ml fresh medium. Alternatively, 12×10^6 *Sf9* cells/150 mm plate were seeded in 5 ml media. After leaving the plate for 15 min at room temperature to allow attaching of the cells, several dilutions of the virus stocks were made (in the range: 1-50 µl for *Sf21* or 50-1000 µl for *Sf9*) and added. As a mock control, one well was left uninfected. The plate was sealed with parafilm and incubated for 72 h at 27 °C. Cells were then detached with a cell scraper and pelleted (500 rpm for 5 min at RT). The pellets could be either stored at -80°C or analyzed for protein expression:

All following steps were carried out on ice. Cell pellets were resuspended in 200 µl B-PER reagent (Thermo Scientific), incubated for 10 min on ice and vigorously vortexed twice during this time. The suspension was then centrifuged (25.000 g, 15 min at 4°C) and the supernatant diluted 1:2 in 20 mM Tris-HCl pH 7.5. Cell lysate was incubated for 1 hour on a rotating wheel with equilibrated affinity resin according to the affinity tag of the protein to be purified and the company's recommendations. Beads were recovered by centrifugation (500 g, 5 min at 4°C) and washed three times with 20 bed volumes of its respective binding buffer. One bed volume of SDS-PAGE sample buffer was added to the washed resin, the suspension was then heated to 95 °C for 5 min. 10-15 µl of this sample were analyzed on a SDS-PAA gel of appropriate percentage. The amount of virus per cell number that produced the maximal protein yield was determined and used for subsequent large-scale infections in suspension cultures.

3.1.4. VIRUS INFECTION OF *SF21/ SF9* CELLS

For the 20 times scaled-up reaction 2.4×10^4 *Sf21* cells were transferred to 50 ml Sf900II media in tissue culture flasks (Rollerbottle Cell-master, Greiner-Bio-one). Cells were incubated with the respective virus (2 ml/10x reaction) on a rocking platform (1 h,

27° C). 150 ml fresh Sf900II was added and further incubated for 48 -72 h at 27° C. Cells were harvested, washed twice with 1x PBS and stored at -80°C, or proceeded to protein purification.

3.1.5. CELL HARVESTING

Cells were detached from the tissue culture vessels using a cell scraper and transferred to centrifuge bins. Cells were pelleted and washed twice with 1xPBS (800 rpm, 10 min, RT). Subsequently, the cell pellet was shock-frozen in liquid nitrogen and stored at -80°C or directly proceeded to protein purification.

Alternatively, $2x10^8$ *Sf21* cells in 100 ml of medium were transferred to a new culture vessel. The appropriate amount of virus stock was added to the culture. After 3 hours of incubation, 100 ml of fresh medium were added to the vessel and it incubated for 3 more days.

3.2. Purification of recombinant proteins using affinity chromatography

Expression and purification by affinity chromatography (Cuatrecasas *et al.*, 1968) was optimized for each specific protein as described in the following sections. Different tags were used in present study: a penta-histidine tag and a flag-tag. Purifications were done according to a common scheme, simply buffer conditions varied with the tags (see below). All buffers contained protease inhibitors.

At first, cell lysates were prepared as described previously using the appropriate lysis buffer: A cell pellet (~$2x10^8$ cells) was thaw on ice or harvested cells were directly resuspended in 20 ml of the lysis buffer corresponding to the affinity tag. This suspension was snap frozen in liquid nitrogen and thawed in cold water. The freeze-thaw procedure was repeated twice and cells were further lysated by sonication (3 times using the large tip for 30 s at 50 % amplitude and 50 % duty cycle with a cooling period of 30s in between). The insoluble fraction was pelleted by centrifugation (Sorvall: 20000 g, 30 min 4°C). The supernatant was subsequently used for protein purification. The amount of affinity resin was applied according to the manufacturers' recommendations. The required amount of slurry (300 µl for FLAG and His) was transferred into a reaction tube and equilibrated in the respective binding buffer by adding 5-10 volumes of buffer, resuspending, spinning down the resin (500 g, 5 min). The supernatant was removed carefully. This equilibrating step was repeated twice and

the beads were added to the cleared lysate and incubated in 10 ml binding buffer on the rotating wheel for 3 h at 4 °C. After this period, the beads were collected by centrifugation (500 g, 5 min, 4°C). The beads were washed three times as described above in 3 x 20 volumes wash buffer. The washed beads were resuspended in 150-300 µl elution buffer and incubated on a rotating wheel at 4°C. The suspension was then transferred to either a MoBiCol or a BioRad spin column and centrifuged for 1 min at 100 g. The eluted protein was recovered and two more elution steps were carried out in the spin columns. Samples for SDS-PAGE were taken from the flow-through fractions, wash fractions and all elution fractions. After the third elution step, the beads were resuspended in an equal volume of SDS-PAGE sample buffer and heated to 95 °C for 10 min. Purification and protein purity were then evaluated on a SDS gel. If necessary, the purified protein was dialysed against a storage buffer. Two steps of dialysis (1. 1 h, 2. O/N) into 1 L of storage buffer were carried out using dialysis tubes with a MWCO of 6-8.000; Spectrapor®. Purified protein was then snap frozen in liquid nitrogen and stored at -80 °C. Please see Figure 18 for purified Dnmt1 (A) and Remodelers (B).
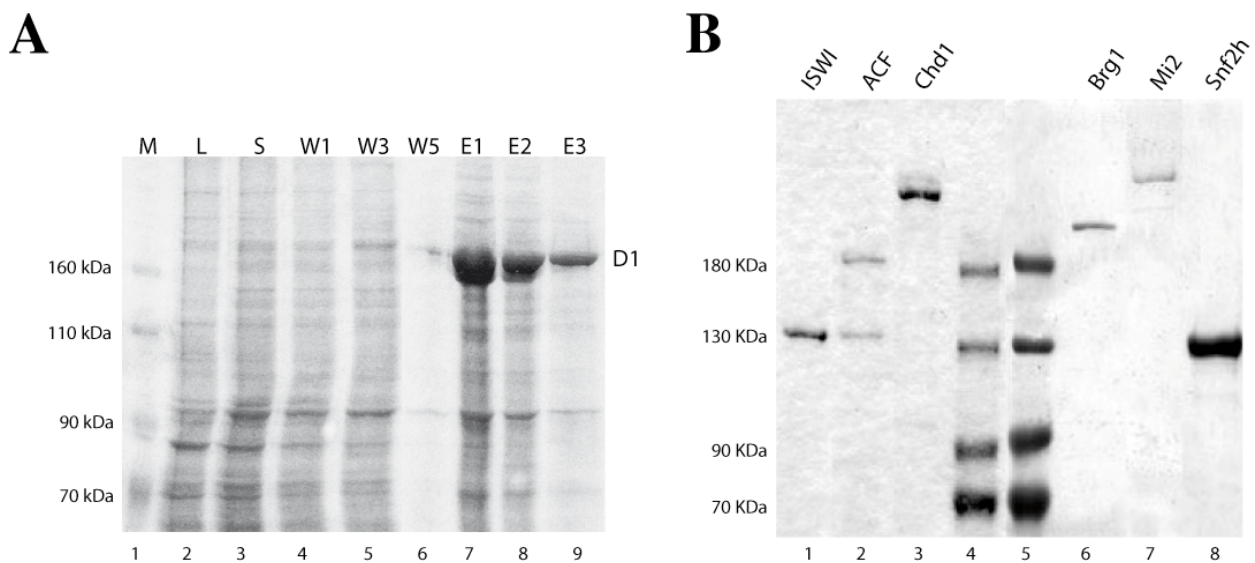
Figure 18. Expression and purification of recombinant DNA methyltransferase 1 and chromatin remodeling enzymes

A) Penta-His-tagged Dnmt1 (D1) was expressed in *Sf 9* cells and purified via "Ni-NTA-agarose-beads". The beads were washed five times with wash buffer (W1, W3, W5, lane 4-6; W2 and W4 are not shown). Proteins were eluted four times with elution buffer (E1-E3, lanes 7-9; E4 is not shown). Analysis was done on a 6 % SDS-PAA gel, using Coomassie blue staining for visualization. Similar amounts of lysate (L, lane 2) and supernatant (S, lane 3) were analyzed. A size standard was run in lane 1 (peqGold Protein marker IV, Peqlab). B) The indicated proteins were expressed in *Sf 21* cells using the baculo-virus system, purified according to the respective affinity tag and analyzed by SDS-PAGE. Proteins were visualized by Coomassie blue staining. Relative protein sizes are indicated.

Affinity-Tag	Protein	Lysis-and binding buffer	Washbuffer	Elution	Storage
Flag	Snf2H Brg1 ISWI Mi-2 Chd1	EX-50; 0.1 % NP-40	Wash 1+2: EX-500; 0.05 % NP40 Wash 3+4: EX-1000;0.05% NP40 Wash 5+6: EX-500;0.05 % NP40 Wash 7+8: EX-300;0.05 % NP40	EX-300; 400µg/ml FLAG peptide (1.: 2 h; 2.:O/N)	EX-300
His	Dnmt1	20mMNaH2PO4 250mM NaCl 1 mM Imidazole 2 mM ß-ME 1 % NP-40 10 % Glycerole pH 8.0	Wash 1+2: 20mM NaH2PO4 500mM NaCl 10 mM Imidazole 10 % Glycerole pH 8.0 Wash 3+4: 20mM NaH2PO4 100mM NaCl 10 % Glycerole pH 8.0	20mM NaH2PO4 200mM NaCl 250 mM Imidazole 10 % Glycerole pH 8.0	20mM Tris 200mM NaCl 1mM EDTA 1.5mMMgCl$_2$ 10%Glycerole 1 mM DTT pH 7.6

Table 17: Purification by affinity chromatography

4. Chromatin – Assembly and analysis of arrays

4.1. Chromatin reconstitution using the salt gradient dialysis technique

Reconstitution of chromatin from DNA and purified histones was carried out by salt gradient dialysis according to Rhodes (Rhodes and Laskey, 1989). The histones, stable as monomers at high salt conditions, assemble onto the DNA during dialysis to low salt conditions.

The assembly reaction was performed in the lid of siliconized 1.5 ml reaction tubes (Biozym) (see Figure 19 for experimental setup). Preparation of the assembly chamber: The bottom of the tubes was removed using a claw trimmer. A hole was melted into the lid using a heated metal rod. Any remaining sharp plastic protrusions were removed using scissors. 6.0-8.0 kDa dialysis membranes (Spectrapor) were pre-equilibrated for 5 min in High salt buffer (Hi-buffer) and clamped between lid and remaining bottom of the

tube in a single layer. Prepared tubes were placed in a styrofoam floater into a 3-5 l beaker filled with 300 ml Hi-buffer (containing a magnetic stirrer). Air bubbles below the membrane were removed with a bent Pasteur pipette.
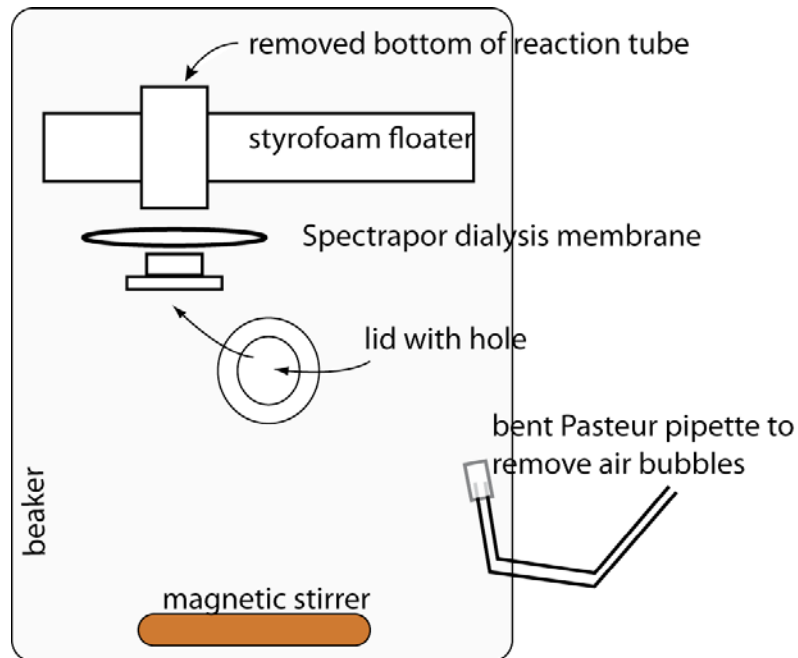
Figure 19. Chromatin assembly by salt gradient dialysis
Schematic illustration of chromatin assembly by the salt gradient dialysis (kindly provided by Gernot Längst).
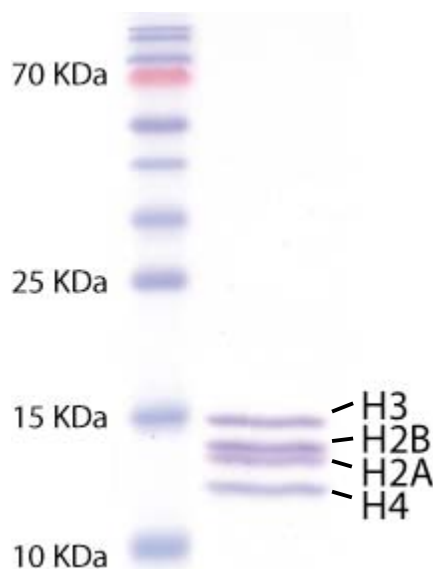
Figure 20. Recombinant *Drosophila* histones
Purified *Drosophila* histones. Core histones were purified from *Drosophila* embryos. Proteins were resolved by 17.5 % SDS-PAGE and stained with Coomassie blue. A size standard was run in lane 1 (peqGold Protein marker IV, Peqlab).

Finally the assembly reaction was pipetted into the lid:

A typical assembly reaction contained 5 µg DNA with varying amounts of histone octamer in 50 µl volume. To estimate the optimal histone to DNA ratio, rising amounts of histones were tested compared to a fixed amount of DNA. The assembly was done in High salt buffer (salt concentration was adjusted with 5 M NaCl if required) supplemented with 200 ng/µl BSA. For mononucleosomes assembly, 250 ng pCpGbasic or pCMV14 (see section D.I.10) were used as competitor DNA in free form.

The salt gradient dialysis was done by continuous addition of low salt buffer (3 l in total) into the beaker over a period of 16-20 h at room temperature. The high salt buffer was then diluted with 3 l low salt buffer, adding 150 ml low salt buffer per hour. The nucleosomes were then assayed on a 5 % TBE gel and stored at 4°C.

Name	Components
High salt buffer	10 mM Tris/HCl, pH 7.6; 2 M NaCl; 1 mM EDTA; 0.05 % NP40; 2 mM β-Mercaptoethanol
Low salt buffer	10 mM Tris/HCl, pH 7.6; 50 mM NaCl; 1 mM EDTA; 0.05 % NP40; 2 mM β-Mercaptoethanol

Table 18: Buffers used for salt gradient dialysis

4.2. Chromatin assembly using the *Drosophila* embryo extract (DREX)

Assembly using *Drosophila* embryo extract (DREX) was performed as described (Becker and Wu, 1992). A standard assembly reaction contained 900 ng of circular DNA, 12 µl McNAP buffer (30 mM $MgCl_2$, 30 mM ATP, 300 mM creatine phosphate, 10 µg/ ml creatine phoshate kinase, 10 mM DTT) and varying amounts of *Drosophila* embryo extract (20-80 µl). The volume was increased with EX-100 to a final volume of 120 µl. The assemblies were performed in 0.5 ml PCR tubes for 6 h at 26°C (Perkin Elmer PCR cycler). The quality was analyzed by MNase digestion.

4.3. Chromatin analysis by Micrococcal Nuclease (MNase) digest

Chromatin arrays were analyzed via Micrococcal nuclease (MNase) digest. MNase preferentially cleaves DNA in the linker region between individual nucleosomes, leading to the characteristic nucleosomal ladder. The MNase digest provides a method to analyze both the quality and periodicity of the chromatin assembly. Chromatin was

partially digested with MNase (depending on the assembly method, MNase concentration had to be optimized):

- 120 µl of reconstituted chromatin from *Drosophila* embryo extract was incubated with 50 u MNase in EX100-buffer (5 mM CaCl2). The reaction was stopped after 30, 90, 300 s with 0.2 Vol. stop-mix (4 % SDS, 0.1 M EDTA) and incubated for 1h at 37°C with 10 µg RNase A.
- 1 µg of the chromatin reconstituted by salt gradient dialysis was incubated for 10, 40 and 240 s with 25 u MNase in a total volume of 20 µl EX80 (supplemented with 3 mM CaCl$_2$ and 4 µg CEA). The reaction was stopped with 0.2 vol. stop-mix.

10 µg proteinase K were added and the reaction was incubated for 1 h at 45 °C. Subsequently the DNA was ethanol precipitated and the purified DNA analyzed on a 1.3 % agarose gel.

5. Chromatin – Preparation of positioned mononucleosomes

Mononucleosomes were reconstituted on 247 bp rDNA promoter fragments; *Hsp70* promoter fragments and the artificial 601 nucleosome positioning (designed by Jon Widom) sequence either using salt gradient dialysis as assembly method (see section D.II.4.1) or with the HP-Mix method (Stein *et al.*, 1979). Nucleosomes assembled onto the 601 sequence preferentially occupied one visible position. In contrast, nucleosomes assembled onto the 247 bp rDNA promoter fragment and the *Hsp70* fragment displayed multiple distinct positions that could be separated by native gel electrophoresis. Faster migrating nucleosomes are located at the periphery of the DNA fragment, whereas the slower migrating nucleosomes occupy positions at the center of the DNA. Positioned nucleosomes were separated using native gel electrophoresis, gel-purified and further used.

5.1. Assembly of mononucleosomes using HP-Mix

5.1.1. PREPARATION OF HP-MIX

For radioactive labeled DNA and/or small amounts of material the assembly method developed by Stein and colleagues is convenient (Stein *et al.*, 1979). Poly-L-glutamic acid (PGA) is a negatively charged polymer, which can force histones to form octamers in low salt conditions. The PGA polymers then progressively exchange with DNA molecules allowing nucleosome assembly.

2-fold weight excess of PGA (10 mg/ml PGA (Sigma) stock) was given to the histones and the reaction was mixed by flicking the tube. The salt concentration was adjusted to 150 mM NaCl with TE (pH 8.0) and gradually filled up with TE containing 150 mM NaCl (TE150) to a final histone concentration of 50-100 ng/µl. The reaction was gently pipetted up and down and incubated at room temperature for 1 h. Aggregates were pelleted at 13000 g for 10min and supernatants (= HP-Mix) transferred into fresh tubes and stored at -20°C.

5.1.2. RECONSTITUTION OF CHROMATIN WITH HP-MIX

First, test assemblies with different ratios of DNA and HP mix were performed to determine optimal conditions. 50 ng of labeled DNA (in 10 µl EX-100 supplemented with 200 ng/µl CEA) was incubated with increasing amounts of HP-Mix for 90 min at 30°C and analyzed using native polyacrylamide gel electrophoresis. The optimal condition of the test assembly reaction were scaled up for a large preparative assembly (x 160).

5.2. Isolation of positioned mononucleosomes

Following nucleosome assembly in preparative scale, the different translational positions were separated on 4.5 % polyacrylamide gels in 0.4 % TBE at RT for 3-4 h (120 V). The gel was exposed for 10-15 min to an X-Ray film and the different translationally positioned nucleosomes (and free DNA) were isolated: Nucleosome positions were precisely marked on the autoradiogram and the gel slices corresponding to the separated nucleosomes were cut out. Gel slices were transferred into a siliconized 1.5 ml reaction tube and 500 µl EX-50 buffer (supplemented with 200 ng/µl CEA, 1 mM DTT, PMSF) were added. The nucleosomes were shake-eluted from the gel pieces at 37°C O/N.

6. In vitro analysis of DNA methylation in chromatin

The incorporation of radioactively [3H]-labeled methyl groups of S-adenosyl-methionine into different free DNA and chromatin templates was measured to determine the enzymatic activity of purified DNA methyltransferases.

6.1. Methylation activity assay on free DNA

The reaction was performed in 50 µl reaction buffer (10 mM Tris pH 7.6, 100 mM KCl, 1 mM EDTA, 1 mM DTT) containing 150 pmol- 2 nmol free DNA or 25-50 pmol of the AIR DNA fragment as positive control (free DNA 50-500 nM CpG sites, AIR fragment 0.5-5 µM CpG sites) and BSA at 0.2 µg/µl. Dnmt1 was applied at a concentration of 50-100 nM, [3H]-SAM at 60-320 nM. The reaction was incubated for 60-90 min at 37°C. The reaction was stopped by addition of 10 µl 10 mM unlabeled SAM and the whole reaction onto DE81 filter (2,5 cm diameter; Whatman). Filters were transferred into 0.2 M ammonium carbonate solution and washed for 10 min. This washing step was repeated twice with 0.2 M ammonium carbonate, once with water and once with 70% ethanol. Filters were dried for approximately 30 min at 37 °C and transferred into Mini-Poly-Q vials. 5 ml Gold-LSC scintillation cocktail were added and decays of incorporated [3H]-SAM measured for 1 min using a scintillation counter.

6.2 Methylation activity assay on mononucleosomes and chromatin arrays

The assay was performed as described in C.II.6.1. with slight modifications due to the chromatin template:

The reaction volume of 50 µl comprises of 200-300 ng nucleosomal DNA, 50-100 nM of Dnmt1 in the special reaction buffer and BSA at 0.2 µg/µl. The experiment in chromatin was performed in the presence of 160 nM [3H]-SAM. The reaction was incubated at 26 °C for 1h using a thermoblock.

The chromatin array substrate was treated differently: Due to observed inhibition by high salt concentrations, the reaction buffer was optimized (10 mM Tris pH 7.6, **25 mM KCl**, 1mM EDTA, 1mM DTT) and the reaction was stopped by addition of 0.2 Vol. stop-mix, 1 mM SAM, 10 µg RNase A, 20 µg Glycogen and incubation at 37°C O/N. 10 µg Proteinase K and 1 µg competitor-DNA were added and the reaction then incubated for 1 h at 45°C. The filter spotting and washing steps were performed as described in section D.II.6.1.

6.3. Bisulfite genomic sequencing

To analyze the changes in cytosine methylation at specific sequences, genomic DNA samples can be modified with bisulfite. When DNA is incubated in the presence of bisulfite at acid pH, cytosine residues are deaminated to uracil, but, if the cytosine ring is methylated in the 5' position, the reaction is slow enough to be stopped it after conversion of the non-methylated cytosine moieties and before the transformation of the methylated ones (Wang *et al.*, 1980). This selective modification allows the analysis of cytosine methylation at specific DNA sequences by different techniques, some of them based on PCR since uracil residues will be amplied as thymines whereas the methylated cytosines will remain as cytosine in the PCR product.

Since the strands of dsDNA are not fully complementary anymore after cytosine deamination, primers must be designed to amplify selectively one of both strands. Bisulfite genomic sequencing reveals the methylation status of the sequence in between the primers.

For bisulfite sequencing both methylated and unmethylated alleles are amplified in the same PCR reaction. Thus, only one pair of oligonucleotides is required and the primers should not encompass any CpG. When this is not possible, degenerated oligonucleotides considering both the presence and absence of methylation must be used to avoid a possible bias in the experiment (Frommer *et al.*, 1992).

6.3.1. METHYLATION AND BISULFITE CONVERSION

To analyze the methylation efficiency of Dnmt1 in the mononucleosomal context, a 342 bp mononucleosomal DNA harbouring a modified 601 nucleosome positioning sequence was used. The 342 bp fragment harbours 27 CpG sites of which 16 are located within the 601 positioning sequence. The template was amplified by PCR as described in section C.II.1.8 with the indicated primers. The purified template DNA was then assembled into chromatin using salt gradient dialysis. For the Dnmt1 methylation, the 601 substrate was applied in free and nucleosomal form:

Components	Volume (µl)	Final concentration
10x reaction buffer	4 µl	1x
DNA	1 µl (5 ng naked DNA) 1 µl (10ng Nuc. DNA)	16 nM CpG sites
SAM	1 µl	250 nM
Dnmt1	1.25 µl	100-400 nM
H2O	Ad 40 µl	

Table 19: Methylation reaction for bisulfite sequencing

The reactions were mixed and incubated for 1 h at 37°C using an incubator. The addition of 250 nM SAM was repeated every hour (4 times) and the reaction stopped by heat inactivation for 20 min at 65°C.

The bisulfite conversion was carried out using the EpiTect Kit (Qiagen) according to the manual. Two elutions of 20 µl were combined in one tube.

6.3.2. PCR AMPLIFICATION OF BISULFITE CONVERTED DNA

The purified bisulfite converted DNA was applied to PCR amplification using two different primer pairs to distinguish between the (+) and (-)- DNA strands. The PCR was performed with 2-8 µl of the bisulfite treated DNA using standard protocols with an annealing temperature of 56°C and 40 amplification cycles. For analysis the amplicons were loaded on a 1.2 % agarose gel.

6.3.3. CLONING THE PCR FRAGMENT AND ANALYSIS

Afterwards, the PCR product was ligated into a standard cloning vector (pGEM-T-EASY) by TA cloning according to the manual. Briefly, an insert:vector ratio of 6:1 was used for overnight ligation. 4 µl of the ligation reaction were transformed in 50 µl *E.coli XI1* blue competent cells. 250 µl pre-warmed LB medium was added and incubated for 1h at 37°C, 300 rpm. 200 µl of the cell suspension were plated on LB plates supplemented with ampicillin and X-gal according to Invitrogen BlueGal manual and incubated for 24h in the 37°C incubator. Positive clones were identified by Blue-white screening and re-streaked onto LB/Amp plates. The selected clones were amplified using a Miniprep kit (Invitrogen) and CpG sites of the DNA analyzed by DNA

sequencing using Sangers dideoxy method with the M13_fw and M13_rev standard oligonucleotides. The obtained sequences were then evaluated using a specific software for evaluation of bisulfite treated DNA (Bock *et al.*, 2005). The results were illustrated using Excel (Microsoft).

7. Chromatin – functional assays

7.1. Nucleosome mobilization assay

By using the nucleosome mobility assay one can visualize nucleosome movement catalyzed by ATP dependent nucleosome remodeling factors on single molecule level (Längst *et al.*, 1999). The nucleosome sliding assay relies on the fact that the location of a histone octamer on a DNA fragment affects its electrophoretic mobility in native polyacrylamide (PAA) gels. Centrally positioned nucleosomes migrate slower than nucleosomes positioned at one end of a DNA fragment. DNA templates between 200 bp and 300 bp are a preferred substrate because this fragment size should allow the formation of essentially one nucleosome per template. Longer DNA fragments would require a nucleosome assembly at lower histone:DNA ratios to avoid the assembly of more than one nucleosome per DNA template. This would result in lower mononucleosome assembly yields. All reactions were performed in siliconized tubes (Biozym). A reaction contained 100 ng mononucleosomes (50-100 fmol) in a total volume of 10 µl in EX50-buffer containing 1 mM ATP, 1 mM DTT and 200 ng/µl BSA. The nucleosomes were then incubated with the remodeling proteins (2-20 fmol) indicated in the individual figures for 90 min at 26°C. The reaction was stopped by adding 250-500 ng of competitor DNA (plasmid DNA or PCR fragment) and further incubated for 5 min. Nucleosome positions were analyzed by native gel electrophoresis using 4.5 – 5.0 % polyacrylamide gels in 0.4 % TBE buffer. Gels were pre-electrophorized for 30 min-1 h and run for 90 min- 3 hours at 80-130 V. Optimal migration was controlled by using Orange G DNA loading dye as a marker. After separation the nucleosomal DNA was visualized by staining with ethidium bromide. Documentation was performed with the gel documentation system. Assays using radioactive nucleosomes were performed similarly with slight modifications for detection.

7.2. ATPase assay

ATPase assays were performed in the presence of γ-^{32}P-ATP (3000 Ci/mmol, 10 mCi/ml) using different substrates to analyze the specific activity. A typical reaction contained 150 ng of either naked DNA or chromatin in 10-15 µl reaction buffer (20 mM-50 mM Tris pH 7.6, 1.5 mM MgCl2, 50 mM KCl, 0.5 mM EGTA, 0.5 mM ß-mercaptoethanol, 10 % glycerol, 0.2 mg/ml BSA), in the presence of 10 µM ATP together with 0.1 µl of γ-^{32}P-ATP. The reaction was incubated at 26°C after the addition of the proteins. At different time points (30 min, 60 min), 1 µl of the reaction was spotted on a thin layer chromatography cellulose plate (PEI Cellulose F25 20x20, Merck) and air-dried. The hydrolyzed phosphate was separated from unconsumed ATP using thin layer chromatography in 0.5 M LiCl/ acetic acid buffer. Samples were separated until the buffer reached the top of the plate. The plate was dried at 60°C for 5 min and exposed on a Phospho Imager. ATP and hydrolyzed phosphate spots were quantified using AIDA software. Percentage of hydrolyzed ATP was determined (Eberharter *et al.*, 2004):
$$(\gamma\text{-}^{32}P_{Hydrolyzed})/(\gamma\text{-}^{32}P_{Hydrolyzed} + \gamma\text{-}^{32}P_{unhydrolyzed})$$

Alternatively, the ATPase activity was measured using a Luminescence assay. ATP can be rapidly detected by light emission through combined use of Luciferase and a Luminometer:

$$ATP + d\text{-}Luciferin + O_2 \longrightarrow Oxyluciferin + AMP + Pyrophosphate + CO_2 + Light_{(560nm)}$$
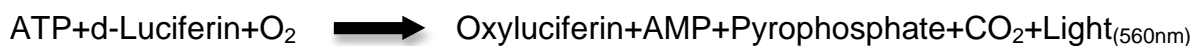
The assay was performed as follows: At first an ATP standard curve was prepared and measured. The linear range was between 10^{-7}- 10^{-10} M/l ATP. 150-200 ng template (Buffer, DNA or Chromatin) were added to EX40 buffer supplemented with 200 ng/µl BSA. The protein of interest was given to the reaction (10 pmol) in the presence of 13 µM ATP. After the reaction was incubated for 30 min at 26°C the 1:10.000 diluted sample was measured in the Luminometer according to the company's instruction.

7.3. Electrophoretic mobility shift assay (EMSA)

Positioned mononucleosomes were used to study protein-DNA and protein-nucleosome interactions. The interactions were analyzed by electrophoretic mobility shift assays (EMSA). A typical reaction contained 10-50 fmol of DNA or nucleosome in a total volume of 10-12 µl EX-50 buffer containing 200 ng / µl BSA and 1 mM DTT. For the EMSAs using the "601"-fragments as DNA substrates, 100-500 nM Dnmt1 were titrated to 50-200 nM nucleosomal DNA. Proteins (as indicated in figure legends) were

incubated with the DNA or nucleosomal template for 15-30 min at 26°C. Afterwards the protein-DNA (protein-nucleosome) complexes were separated from free DNA (nucleosome) by native gel electrophoresis. The reactions were loaded on pre-electrophoresed 4.5-5 % PAA gels in 0.4x TBE buffer and run for 90 min-3h at 80-100V. Orange G DNA loading dye was used to monitor the optimal running time. After separation the nucleosomal DNA was visualized by staining with ethidium bromide. Documentation was performed with the gel documentation system.

To test the influence of Snf2H in the presence and absence of ATP (1 µM) on the binding characteristics of Dnmt1 to mononucleosomes, electromobility shift assays in the presence of Snf2H were performed. For this an EMSA reaction was performed as described before with the exception that 90 nM Snf2H were added to the 12 µl Dnmt1 reaction in EX-50-Hepes buffer with or without 1 µM ATP (10 mM HEPES (pH 7.6), 50 mM KCl, 2.5 mM MgCl2, 10 % Glycerol, 1 mM DTT). The reaction was incubated for 1 h at RT and analyzed on a native 4.5-5 % polyacrylamide gel as described before.

7.4. Competition assays

To analyze the stability of the Dnmt1-mononucleosome complex, competition experiments were carried out. 100-500 ng naked plasmid DNA (here pCMV14) were titrated to the totally shifted Dnmt1-mononucleosome complex and the stability analyzed on a 5 % polyacrylamide gel.

7.5. Dnmt1 binding assay using small DNA fragments

To analyze the binding characteristics of Dnmt1 to small DNA fragments, binding assays using an ultra low range DNA marker (Fermentas) was carried out:

Different concentrations of Dnmt1 (100 nM-0.5 µM) were titrated to the DNA substrates (65-125 ng ultra low range DNA ladder). The reaction was incubated for 30 min at 26°C in binding buffer and DNA-protein complexes analyzed on a 15 % PAA gel. Low range DNA ladder was loaded in rising concentrations.

To further analyze the DNA binding properties of Dnmt1 5' Alexa fluor labeled oligonucleotides were annealed with their complement oligonucleotide for 10 min at 95°C in equivalent ratio and cooled down slowly. 5-50 pmol of the short DNA fragments were analyzed on a 10.5 % polyacrylamide gel and visualized using the Fuji FLA 5000 system. The Dnmt1 EMSA reactions using the DNAs of different length could be

performed in one reaction due to the different fluorescence labels that could be discriminated using the specific filters / lasers for detection: 4 pmol annealed Oligonucleotide (15bp, 30bp, 45 bp and 60 bp) supplemented with 0.2 µg Poly(dI-dC) were incubated in EX-50 buffer with 100 nM-0.5 µM Dnmt1 for 15 at 37°C. After addition of 5 % glycerol and analysis of protein-DNA complexes on a 5 % or 15 % PAA gel, the reactions were visualized using the Fuji FLA 5000 with specific filters to detect the individual DNA.

7.3. DNaseI protection assays ("DNaseI footprinting")

Protein-DNA and protein–nucleosome interactions were further studied by DNaseI footprinting assays. Fluorescence labeled DNA was either applied directly or assembled into nucleosomes. The endlabeling of DNA was performed as described in section C.II.1.5. For the optimization of DNaseI digests, purified DNA and positioned mononucleosomes (50-100 ng, 12-25 nM) were incubated with DNaseI (0.1 u-0.5 u) for 10-240 s in 1x DNaseI buffer or Ex-50 (with 5 mM $CaCl_2$ final concentration). DNaseI was inactivated by the addition of EDTA to a final concentration of 5 mM. The reaction was purified by using the Qiagen purification kit.

DNaseI footprint with Dnmt1 was performed with purified, end labeled 301 bp nucleosomal template (77-WID-77) harboring the 601 nucleosome positioning sequence. This template was generated by PCR using 5'fluorescence labeled primers followed by assembly into mononucleosomes (see section D.II.1.5.) After incubation for 30 min allowing formation of the Nucleosome - protein complex, the samples were treated partially with DNaseI, the reaction stopped and the completion of the digest analyzed on a native 5 % SDS-gel. The localization of Dnmt1 was mapped by using capillary electrophoresis sequencing as readout method (Zianni *et al.*, 2006).

Labeled nucleosomal 77-WID-77 template, 100 ng (25 nM final), was incubated with varying amounts of Dnmt1 protein ranging from 0 to 250 nM in binding buffer (the 1x DNaseI buffer or Ex-50 buffer supplemented with 5 mM $CaCl_2$). After several optimization experiments, the nuclease digestion was found to work best with 0.1 units of DNase I (Roche) for 100 ng DNA per 20 µl reaction for 90 s at 26°C. The reaction was stopped with 0.25 M EDTA. The DNA fragments were purified with the QIAquick PCR Purification kit (Qiagen, Valencia, CA) and eluted in 30 µl H_2O to eliminate salts that can interfere with capillary electrophoresis.

The visualization was performed in collaboration with the "Institut für funktionelle Genomik, Universität Regensburg", Prof. Dr. Peter Oefner. Sophie Hinreiner performed the read-out with the capillary electrophoresis instrument under following conditions: Approximately 1 ng (250 pM) purified DNA was loaded onto a 3730 capillary electrophoresis instrument (G5 dye set). The injection was 2 kV and injection time 15 s. The electropherogram of FAM (blue)- and HEX (green)-labeled DNA as well as free oligonucleotides are shown. The intensity was measured in relative fluorescence units (RFU). As size standard a 1:2 mixture of GeneScan- LIZ120 and LIZ500 was used.

8. Mammalian tissue culture

All work with mammalian tissue cultures was performed according to standard protocols with standard precautions. For maintenance the mammalian cells were propagated in their recommended medium according to ATCC, containing 10 % FCS and 1 % penicillin / streptomycin. The medium of the cultures was changed every 2-3 days depending of the confluence of the cells. According to the growth properties and the respective assays, cells were split at an estimated confluence of 70 % to different ratios. For splitting, the medium was aspirated and for adherent cells trypsin/EDTA solution was added to the cells (1/10 of tissue culture dish) and incubated for 5min at 37°C. The process of detachment was monitored under the microscope and the reaction was stopped by adding culture medium. For splitting an appropriate volume of cells was transferred to a new flask and filled with medium to the final volume. Cells were incubated in an incubator at 37 °C and 5 % CO_2.

Mammalian tissue cultures can be cryopreserved and stored over long time periods at -80 °C. This procedure allows to discontinue a cell culture and to repeatedly work with cells of low passage, as a cell line may change properties and loose viability at high passages due to ageing, selection and, in the worst case, contamination.

For cryopreservation, a cell line of a low passage number at 60-70 % confluence, was detached from the flasks with Trypsin/EDTA. The reaction was stopped by adding 10 ml medium to a 15 cm plate and cells were spun down at 500 rpm for 5 min. The supernatant was removed and cells were gently resuspended in 2.5 ml FCS containing 5% DMSO. The suspension was then aliquoted to 1 ml in sterile cryo-tubes precooled to -20 °C. The closed tubes were put into the centre of a paper towel roll which was

transferred to the -80 °C freezer. The insulation layer provides slow cooling to -80 °C, which improves the viability of the frozen cells.

For unfreezing cryo-cultures of mammalian cell lines were removed from the -80 °C freezer and warmed in the hand until the thawed cell suspension could be poured into a T7 tissue culture flask containing 7 ml of the appropriate cell culture medium supplemented with penicillin/streptomycin and 10 % FCS. The flask was transferred to a tissue culture incubator and incubated at 37 °C and 5% CO_2 O/N. The medium was changed to remove remaining DMSO.

E. Results

I. NUCLEOSOME POSITIONING BY CHROMATIN REMODELING COMPLEXES

The diversity of different chromatin remodeling factors in the cell on the one hand and their high abundance on the other hand give evidence for the assumption that chromatin remodeling complexes establish specific chromatin configurations. To address whether chromatin remodeling enzymes provide a regulatory level of chromatin structure, the nucleosome positioning properties of different chromatin remodeling enzymes have been dissected.

1. Chromatin remodeling factors determine specific nucleosome positions

To analyze the sequence dependency for nucleosome positioning by chromatin remodeling factors (see Fig. 18 for purified recombinant proteins), the nucleosome mobilization direction of five different chromatin remodeling motors and two remodeling complexes have been compared. In initial experiments I made use of a well-characterized nucleosome positioning sequence, the 248 bp murine rDNA promoter. Briefly, the template was prepared by PCR using "body labeling" for radioactive labeling with [α^{32}P]dCTP. Subsequently, the gel purified DNA fragments were assembled into chromatin using a histone-poly-l-glutamic acid-mix (HP-mix) for assembly as described by Stein and coworkers (Stein *et al.*, 1979) (see section D.II.5.1) for the detailed DNA substrate preparation protocol).

The nucleosome assembly gave rise to two nucleosome positions, one at a major border position N1 and one at a minor central position N2 (Fig. 21A). The experiments were either performed with the N1 or N2 position alone or with a mixture of both positions. The outcome of the nucleosome remodeling reaction revealed significant differences (see figure legend for a detailed assay description). By comparing the nucleosome positions of the ISWI- and Snf2H-catalyzed chromatin remodeling reaction it became apparent that ISWI translocates the central N1 nucleosome preferentially to N2, whereas Snf2H repositions the nucleosomes to positions evenly between N1 and N2 (see Fig. 21A, lanes 2 and 3). The experiments with Snf2H on the border-positioned N2 nucleosomes also show a distribution of nucleosome positioning between positions N1 and N2 (see Fig. 21A, lane 8). The ACF complex preferentially places both N1 and
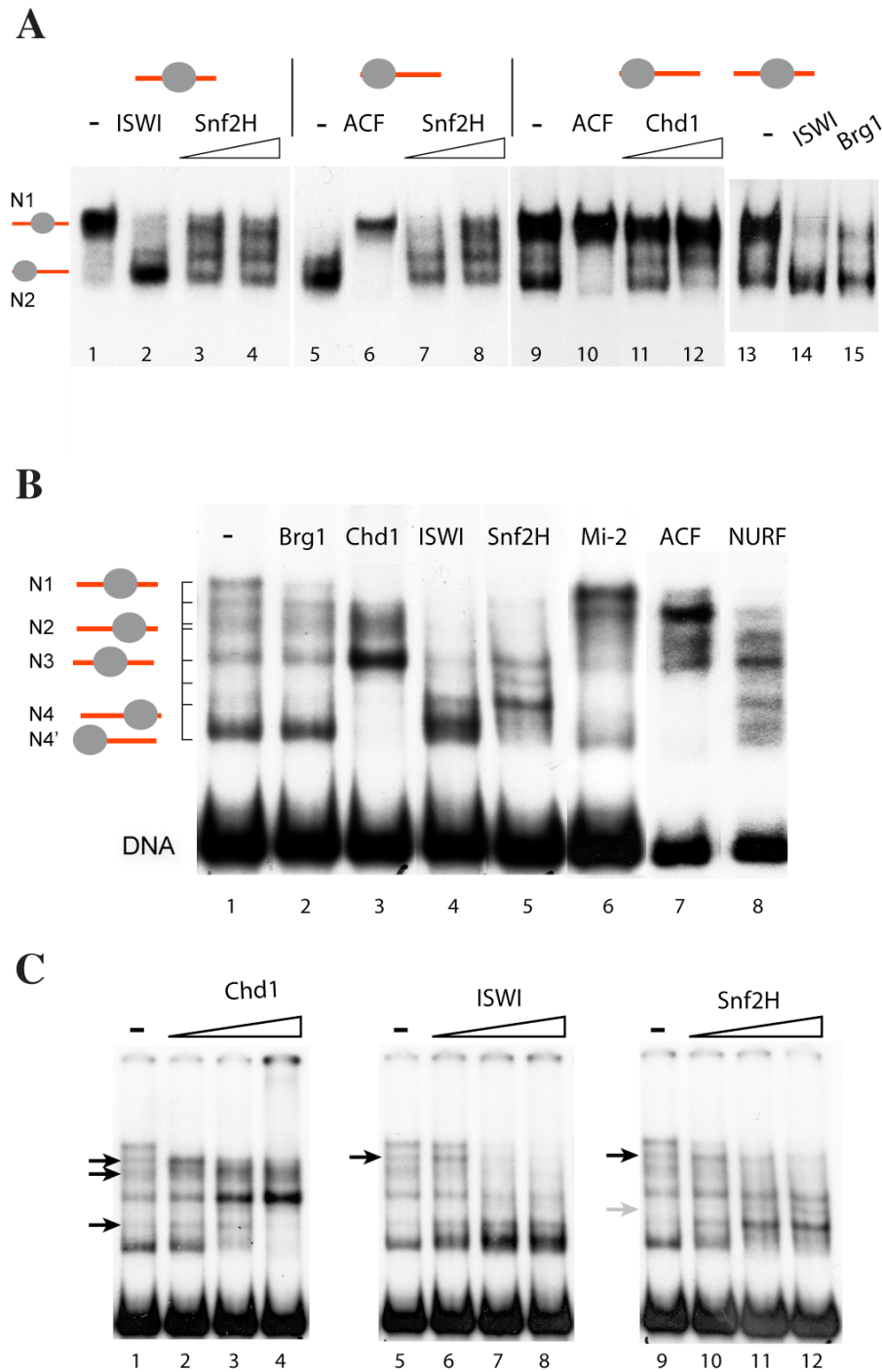
Figure 21. Chromatin remodeling complexes position nucleosomes in dependence on the underlying DNA sequence.

A) *Drosophila* histones were reconstituted on a radioactively labeled 248 bp long rDNA promoter fragment that is a well-characterized NPS using HP-mix for assembly (Please find detailed protocols for DNA labeling, DNA purification and nucleosome assembly in section D.II.1-5). Briefly, after the assembly of the radiolabeled DNA fragment the nucleosomes adopt two positions, a major central (N1) position and a less dominant border position (N2). The chromatin remodeling reaction was carried out using the isolated central N1 position (lane 1-4), the border N2 position (lane 5-8) or a mixture of both positions (lane 9-15). The indicated remodelers (~ 5-10 fmol) were given to the central or border nucleosome or the mixture of both and incubated for 90 min at 26°C in the presence of 1 mM ATP.

B) The chromatin remodeling reaction on the 348 bp DNA fragment harboring the *hsp70* promoter was carried out with slight variances to that described in A). A heterogeneous nucleosome population of a single nucleosome at five different translational positions (indicated as N1, N2, N3, N4, N4') was obtained. This mixed nucleosome population (lane 1) was used for the nucleosome mobility assay. Therefore approximately 50 fmol radioactive labeled DNA fragment were incubated with ~ 5-10 fmol of the indicated chromatin remodeling machines (Brg1, Chd1, ISWI, Snf2H; lane 2-6) or remodeling complexes (ACF, NURF; lane 7 and 8) in the presence of 1 mM ATP. The reactions were incubated for 90 min at 26°C and stopped by the addition of 0.5- 1 μg competitor DNA. The end point of the nucleosome mobility reaction was analyzed on a native 4.5 % PAA gel and visualized by autoradiography. C) In order to monitor the progression of nucleosome translocation, nucleosomes were assembled onto the *hsp70* promoter fragment as described in A). The remodeling reaction was carried out by the addition of increasing amounts (2-10 fmol) of the indicated remodeling machines (Chd1, ISWI or Snf2H). All following steps were carried out as described in A). The intermediate nucleosome positions are marked by arrows.

N2 positioned nucleosomes to the central N1 position (Fig. 21A, lane 6 and lane 10). Chd1 translocates the mixed N1 and N2 nucleosomal substrate to the central position (Fig. 21A, lanes 11 and 12), while ISWI and Brg1 translocate the nucleosomes at N2 (Fig. 21A, lane 15).

To further characterize this phenomenon, a more complex substrate has been used to address this question. A 350 bp fragment, derived from the gene coding for *Hsp70* in *Drosophila*, another well-defined nucleosome positioning sequence has been used. Nucleosome assembly on this DNA fragment led to five distinct nucleosome positions (Fig. 21B). These positions were generated by a single nucleosome adopting five major positions. Chromatin remodeling experiments ("nucleosome sliding assays") testing seven different chromatin remodeling enzymes clearly showed that every individual remodeling enzyme positions the nucleosomes at a different site on the 350 bp DNA fragment (see Fig. 21B). ACF and NURF, two chromatin remodeling complexes tested in this experimental set-up consist both of the ATPase ISWI and specific additional subunits. Interestingly, the nucleosome sliding reactions catalyzed by these complexes obtained different results: whereas ACF positions the nucleosomes efficiently to the N2 position (see Fig. 21B, lane 7), catalyzes NURF the reposition of the nucleosome to N3 (Fig 21B, lane 8). Additionally, the different individual molecular motors (Brg1, Chd1, ISWI, Snf2H, Mi-2) have different nucleosome positioning properties: *Drosophila* ISWI the ATPase subunit of the ACF and NURF complex positions the nucleosomes to the N4 and N4' position (Fig. 21B, lane 4). Human Snf2H preferentially places the nucleosomes to 3 sites between position N3 and a position above N4 (Fig. 21B, lane 5). Supplementing the remodeling reaction with Brg1 does not change the nucleosome distribution significantly, just displacement away from the central N1 position was observed (Fig.

21B, lane 2). Contrary, nucleosome sliding reactions using other individual motor proteins lead to the formation of different nucleosomal end-points. Chd1 almost completely translocates the nucleosomes to the N3 position (Fig 21B, lane 3), whereas Mi-2 catalyzes the nucleosome mobilization primarily to the N1 end-position (Fig. 21B, lane 6). These different nucleosome end positions cannot be explained by differences in the underlying DNA sequence.

The addition of increasing amounts of Chd1, ISWI or Snf2H to the *Hsp70* DNA substrate made it possible to track the progression of the nucleosome mobilization reaction (Figure 21C). This experimental setup allows observing intermediate nucleosome positions and not only the determination of the reaction endpoint. The experiments revealed that the nucleosome remodeling reaction seems to occur in several steps, forming intermediate nucleosome positions (see Fig. 21C, indicated by arrows) until reaching its terminal position. This was observed for all three tested remodelers. The intermediate positions were predominantly those positions that showed a higher intrinsic histone-DNA affinity. These positions were already obtained in the initial chromatin reconstitution by salt gradient dialysis, which indicates a translocation from one stable nucleosome position to the next.

These results suggest that the outcome of the reaction is also determined by the type of ATPase and the composition of the multi-subunit complex in which it is assembled.

2. Specific DNA features that direct nucleosome positioning

According to the results obtained by the nucleosome remodeling reaction one can conclude that every individual chromatin remodeling factor does interpret the DNA sequence and structural information differently. In initial experiments we could show that ACF moves the nucleosomes of a 253 bp rDNA fragment from the border positions to two rotationally spaced nucleosomes, corresponding to positions 46/56 and 196/206 (N1) on the 248 bp rDNA fragment (Fig. 21A). Previous studies detected that the rDNA promoter exhibits a conserved structure based on its underlying sequence (Längst *et al.*, 1997) (Marilley and Pasero, 1996). A strong correlation between ACF-mediated nucleosome positioning and the presence of an intrinsically curved DNA region has been described. Further studies demonstrated that ACF translocates the nucleosome with its dyad axis close or over a DNA bending peak, which was shown for the rDNA

promoter, *Hsp70* DNA as well as the 601 DNA fragment (see manuscript Fig. 3 in (Rippe *et al.*, 2007).

In order to test the hypothesis whether a DNA sequence encodes information on the positioning of nucleosomes, a DNA sequence element derived from the rDNA promoter that was shown to direct nucleosome positioning was inserted into an unspecific DNA context (see manuscript Fig. 3A). The insertion of a 40 bp highly curved region of the rDNA promoter into a sequence independent environment, revealed that ISWI does not simply translocate the nucleosomes to the ends of a DNA fragment, but instead recognizes some sequence or structure-dependent DNA features. Interestingly, ACF places the nucleosomes again close to the highest DNA bending region, indicating that ACF-dependent nucleosome positioning could be directed by the features of the DNA structure (see manuscript Fig. 3C and 3D). In order to exclude the possibility that this effect is only a consequence of the preference of ACF for sufficiently long (30 bp) protruding DNA, two additional substrates were tested for their positioning properties mediated by ACF (Fig 22A). The experimental design also ensured that the nucleosome flanking regions had the length required for ACF mediated remodeling. They differed in the position of the 40 bp curved DNA fragment (border or central position), which was confirmed by *in silico* analysis (Fig. 22B). The comparative chromatin remodeling reactions with ACF on both DNA substrates revealed that the curved DNA element is sufficient to direct nucleosome positioning even to a border position closer to the DNA end (Fig. 22C, "K3-b" or "K3-c"). If the sequence element was located at the border ("K3-b"), nucleosomes are translocated to the more peripheral positions (see Fig. 22B, left), whereas the central location ("K3-c") shifts the nucleosomes to the more central positions (Fig. 22B, right).
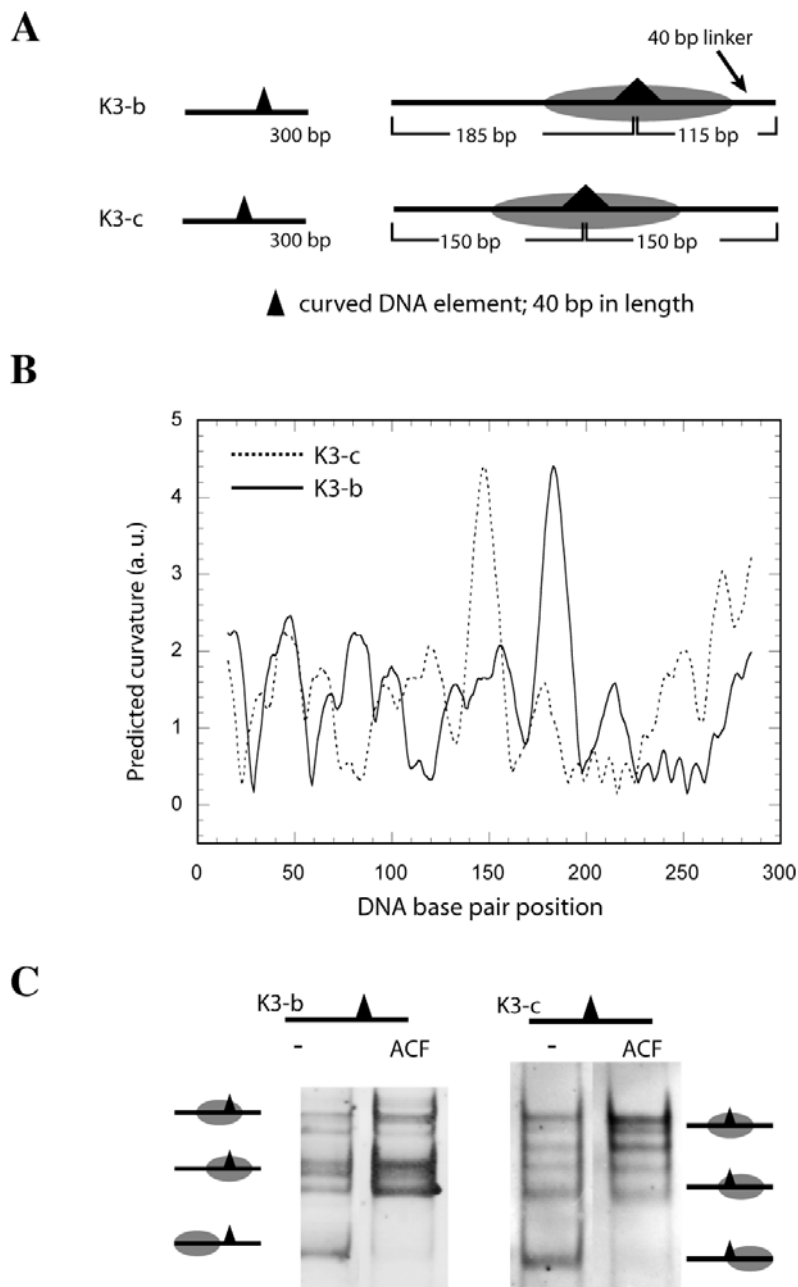
Figure 22. A curved DNA fragment guides remodeler-dependent nucleosome positioning
A) Left hand side: Schematic illustration of the two nucleosomal 300 bp substrates that contain the 40 bp curved DNA fragment either centrally (K3-c) or close to the border (K3-b). The curved DNA fragment is indicated as triangle. Right hand side: The location of the 40 bp fragment is indicated. Both DNAs are 300 bp long with the K3-c DNA carrying the curved DNA element at the center whereas in the K3-b it is located 115 bp from one and 185 bp from the other DNA end. The estimated nucleosome positions are indicated as grey ellipses. B) Graphic illustration of the predicted DNA curvature for the two rDNA promoter fragments based on biophysical properties of the DNA. This was predicted according to the parameter set published by (Bolshoy *et al.*, 1991). C) Analysis of the nucleosome positioning properties of both K3 DNA fragments in the ACF-mediated chromatin remodeling reaction. Left: The remodeling reaction with ACF using the K3-b fragment. Right: The nucleosome mobilization on the K3-c fragment. *Drosophila* histones were used to reconstitute nucleosomes on these fragments using salt gradient dialysis as described by(Rhodes and Laskey, 1989). The nucleosome positions relative to the 40 bp elements are indicated. The remodeling reaction was performed as described before, with ACF and ATP and the endpoint of the reaction visualized by PAA gel electrophoresis and EtBr staining.

3. Two models explaining remodeler directed nucleosome positioning

The results obtained in the comparative chromatin remodeling experiments revealed that the end product (nucleosome position) of the nucleosome translocation reaction is determined by two factors, namely the DNA sequence as well as the type of chromatin remodeling "motor" and potentially its additional subunits. The kinetic model presented in Figure 23A and B was used to explain specific nucleosome positioning directed via a chromatin remodeling enzyme. This approach is based on a Michaelis-Menten like kinetic of the nucleosome translocation. Consequently, "good" substrates (nucleosome positions on a given DNA) for the chromatin remodeling enzyme are characterized by a high binding affinity. This high affinity of the remodeler to its nucleosomal substrates implies a low K_M value and a high K_{cat} (catalytic conversion rate) of the remodeler-nucleosome complex to the end product of the reaction (the positioned nucleosome). A catalytically efficient reaction would hence be characterized by a high K_{cat}/K_M ratio, while a "bad" nucleosomal substrate shows the opposite (a high K_M value and a low K_{cat} that results in a low K_{cat}/K_M ratio).

Our two proposed models suggest the following reaction process (23A):

Nucleosomes can adopt three positions *i, i+1* or *i-1* to which the remodeling enzyme R can bind. All nucleosomes are at position *i* when the reaction starts. The remodeling complex R now binds its substrates to form the RN_i complex and can translocate the nucleosome by a remodeler-specific number of bp to the other nucleosome positions (*i+1* or *i-1*) with the rate constant k_{i+1} or k_{i-1} Alternatively, the RN_i complex can dissociate with dissociation constant $K_{d,i}$ into nucleosome N_i and free remodeler R with $K_{d,i} = [R] \times [N_i] / [RN_i]$. Equivalent reactions can occur at nucleosome positions *i+1* or *i-1*. In order to place nucleosomes at a specific position, we suggest that certain DNA sequences harbor intrinsic features that provide "bad" substrates for the nucleosome remodeling complex. This implies a low escape rate from theses sites thereby forming the preferred end points of the nucleosome positioning of the reaction.

Figure 23B illustrates the remodeling reaction for a remodeling factor that preferentially positions the nucleosomes at position *i+1*. According to the above described processes, the escape rate $k_{esc,i+1}$ from the nucleosome position N_{i+1} (determined by the translocation rate constant $k_{-i} \times [RN_{i+1}]$ that is in turn determined by the corresponding dissociation constant $k_{d,i+1}$) is proportional to $k_{-i} / k_{d,i+1}$. Based on these assumptions, either the translocation rate k_{-i} away from this position or the binding affinity of the

remodeler to the nucleosome at position *i+1* in order to position the nucleosome at *i+1* (equivalent to increase value of $k_{d,i+1}$) has to be reduced. The latter case is described by the "release model" that shows analogies to the transcription termination of RNA polymerase by specific DNA terminator sequences (Greive and von Hippel, 2005; von Hippel and Yager, 1992). The other model referred to as "arrest model" implies a low translocation rate k_{-i} away from the nucleosome position, again showing analogy to the transcription reaction, where pausing/arrest can occur due to a rearrangement of the active site of the enzyme (Landick, 2006).

In summary, the "release model" predicts a reduced affinity of the remodeler to the nucleosome at the end point of the reaction, while the "arrest model" would lead to a specific intermediate that inhibits further translocation without lowering the binding affinity at the terminal nucleosome position. This hypothesis was tested for the remodeling machines Chd1 and ACF by EMSAs with the *Hsp70* and rDNA fragment (Fig. 24A and B). The binding affinities of Chd1 to the initial, heterogenous population of *Hsp70* nucleosome positions were compared to the binding events obtained by the addition of the chromatin remodeling factor (24A, left). The binding experiments lead to the formation of a nucleosome-protein complex with increasing amounts of Chd1 (Fig. 24A, lanes 4 to 7). Quantification of the relative DNA stain intensities corresponding to the individual nucleosome positions revealed that positions N1, N2 and N3 are preferred substrates of Chd1 to form a nucleosome-protein complex (Fig. 24A, right). Interestingly, the affinity to the N3 position increased only to a lower extend. By comparing those results to the results obtained in the nucleosome remodeling reaction (Fig. 21B) it becomes visible that Chd1 positions the nucleosomes to N3, exactly the position with the lowest binding affinity for Chd1. These results support a mechanism of remodeler mediated nucleosome translocations according to the "release model". The results could be confirmed with the mixed nucleosome positions (central and border) of the rDNA fragment (Figure 24B). Both tested remodeling factors (ACF and Chd1) bind preferentially to positions located at the border of the DNA fragment and show weaker binding affinities to the central nucleosome position (Fig. 24B, lanes 3 and 5). The central position is the position to which the nucleosomes are shifted during the remodeling reaction. Summarizing, my results suggest a nucleosome positioning mechanism mediated by remodeling factors (ACF and Chd1) according to the " release model".
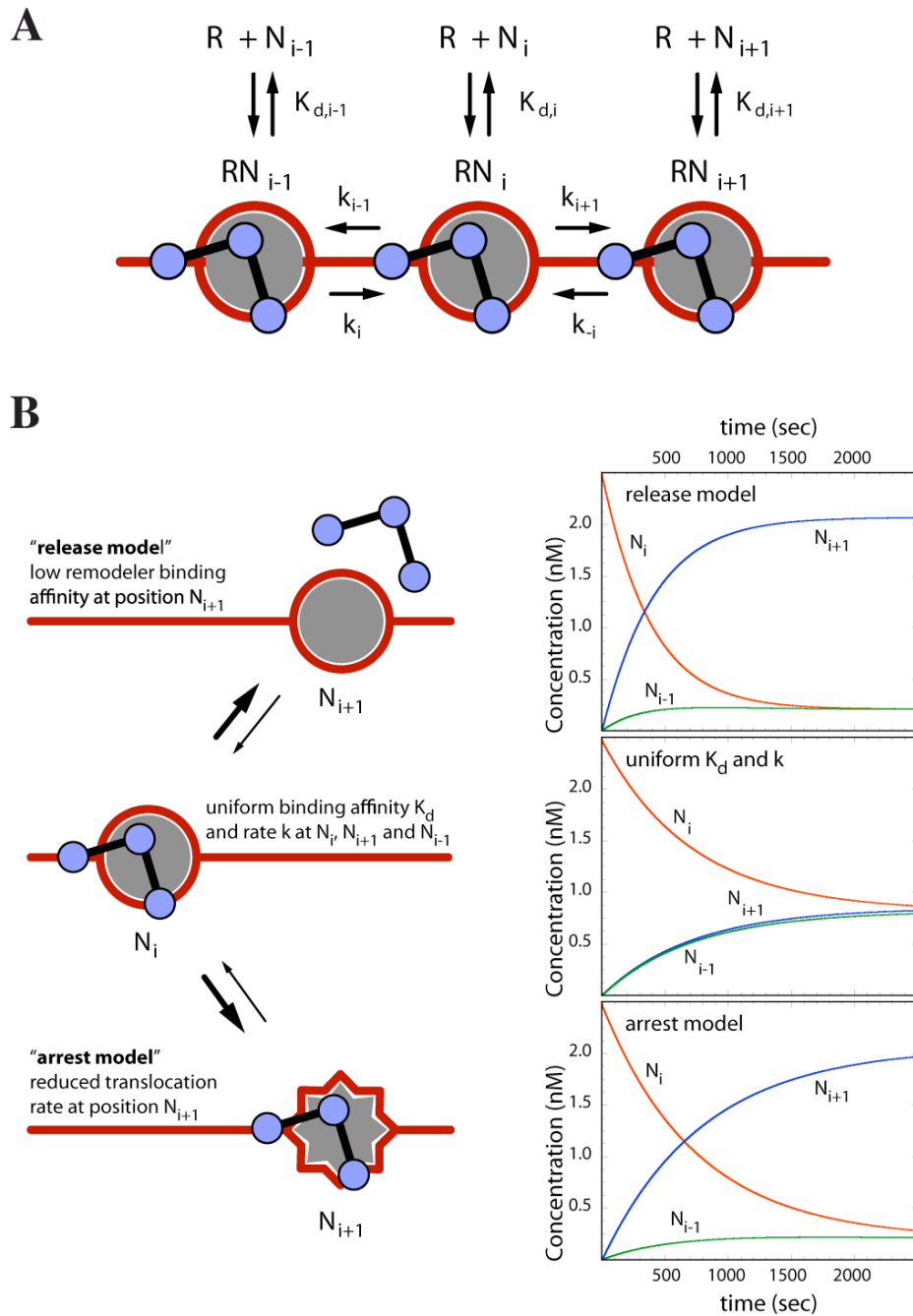
Figure 23. Schematic representation of the remodeler-dependent nucleosome translocation reaction

A) Simplistic scheme for the nucleosome remodeling reaction. Three possible nucleosome positions on the DNA (i-1; i and i +1) are considered. The chromatin remodeling factor (R) could bind to a nucleosome (N) at each of the three positions with a dissociation constant (k_d). Nucleosome translocation to or from these nucleosome positions could occur with specific rate constants (k). A detailed description can be found in the text. B) Two models could explain the remodeler-dependent nucleosome translocation reaction. The corresponding time course of the concentrations of nucleosomes is illustrated on the right hand side. The chromatin remodeling reaction starts at nucleosome position N_i at a concentration of 2.5×10^{-9} M. According to the "release model" the binding affinity to the nucleosome at position N_{i+1} is reduced 10-fold as compared to positions i and i-1. This leads to a distribution in which about 80 % of the nucleosomes are at this site when the equilibrium is reached. When all binding constants and translocation rate constants are identical a homogenous distribution of nucleosome positions is obtained in equilibrium (uniform k_d and k). For the "arrest model" the rate constant k_{-1} that translocates the nucleosome from position i+1 back to position i is ten times reduced as compared to the other translocation rates. At the steady-state again 80 % of the nucleosomes will be at site N_{i+1}.
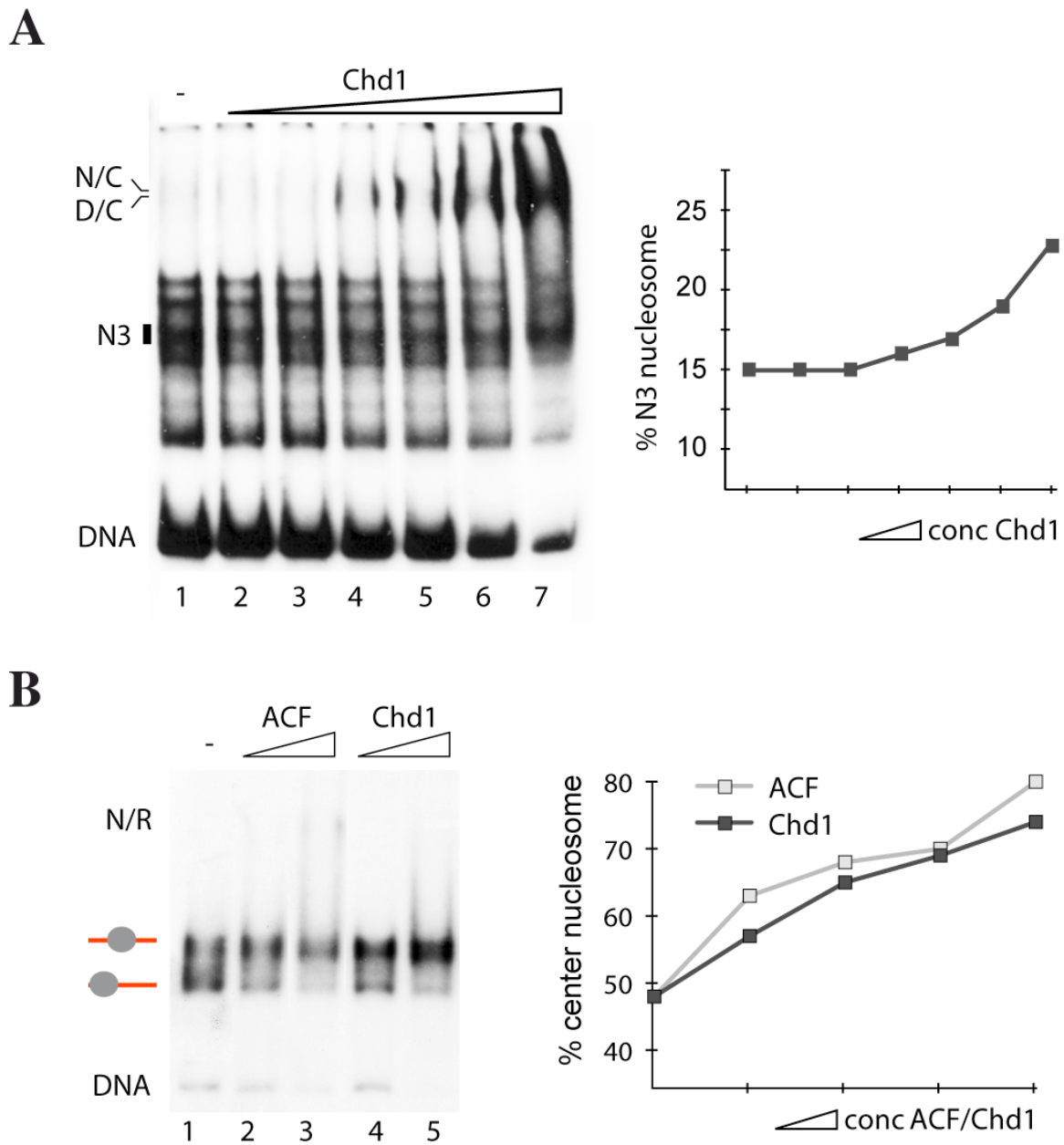
Figure 24. Evidence for a nucleosome positioning according to the "release model"
EMSAs were performed to analyze the binding affinities of Chd1 and ACF to the nucleosomal substrates. A) The radiolabeled *hsp70* promoter fragment was assembled into chromatin (lane 1) as described for Fig. 21A and B. Chd1 was added in rising amounts (20-200 fmol, lane 2-7) to the DNA substrate (10-50 fmol) without ATP. The reaction was incubated for 30 min at room temperature and analyzed by PAA gel electrophoresis and visualized using autoradiography. The positions of the formed DNA-protein (D/C) and the nucleosome-protein (N/C) complexes are indicated. Additionally, a box marks the N3 position. The diagram shown at the right hand side illustrates the percentage of nucleosomes at N3 plotted versus the Chd1 concentration. B) Nucleosomes were assembled onto the radiolabeled rDNA promoter fragment. The nucleosome bandshift assays with ACF (lane 1-3) and Chd1 (lane 4-5) were performed with a gel-purified mixture of the nucleosome border and center position derived from the rDNA fragment. The position of the nucleosome-protein complex is indicated. The graph at the right hand side represents the nucleosome population at the center position in dependence on increasing ACF or Chd1 concentration.

4. Nucleosome positioning on "601"-NPS DNA substrates

In an additional comparative nucleosome mobilization experiment I analyzed the nucleosome positioning properties of different remodelers using several nucleosomal templates, all based on the "601"-DNA sequence. Four different DNA fragments have been reconstituted into mononucleosomes using salt gradient dialysis: 1) The 342 bp modified 601 substrate harboring 27 evenly distributed CpG sites (as used in the bisulfite assay, see section D.II.1.8), 2) A similar 342 bp DNA fragment harboring the modified 601 sequence and flanking regions without CpG-dinucleotides (see section D.II.1.8), 3) The 77-WID-77 DNA fragment, 4) The 22-WID-22 DNA fragment.

The experiments illustrated in Figure 25A show 601 nucleosomes harboring CpG less flanking regions that have been tested in nucleosome sliding assays with Snf2H (lanes 1 to 8), ISWI (lanes 9 to 16) and the ACF complex (lanes 17 to 24) with and without ATP. It has been observed that Snf2H and ISWI translocate nucleosomes to border positions, while this effect is most pronounced for ISWI (compare lanes 8 and 24 with lane 16). Contrary, nucleosome mobilization with ACF does not show a significant effect. Similar experiments have been performed with the 342 bp DNA fragment used in the bisulfite assay (Fig. 25B): again a conversion of the slow migrating central positioned nucleosome to the faster migrating forms has been observed. This is due to the relocation of the histone octamer from the central position to the more peripheral position of the DNA fragment. ISWI shows the strongest nucleosome sliding (see Fig. 25B, lane 18), with all nucleosomes mobilized towards the end of the DNA fragment. As previously detected, ACF shows just a marginal effect (lane 26).

Experiments comparing the 22-WID-22 and the 77-WID-77 substrates, revealed that both Snf2H and ISWI require a minimal length DNA protrusions for catalyzing the nucleosome translocation reaction (Fig. 25C and D). Using the 22-WID-22 mononucleosome as substrate did not show any effect for neither Snf2H nor ISWI (compare Fig. 25C and D, lanes 6). Contrary, with the 77-WID-77 substrate, nucleosome translocations towards more peripheral positions have been observed as for the previously analyzed substrates (compare lane Fig. 25C and D, lanes 12).

In summary, these results confirm our previous data on the *hsp70 DNA* and rDNA promoter fragments and additionally suggest that every single chromatin remodeling enzyme reads and interprets the underlying DNA sequence and or its structure differently, leading to a distinct nucleosome positioning.
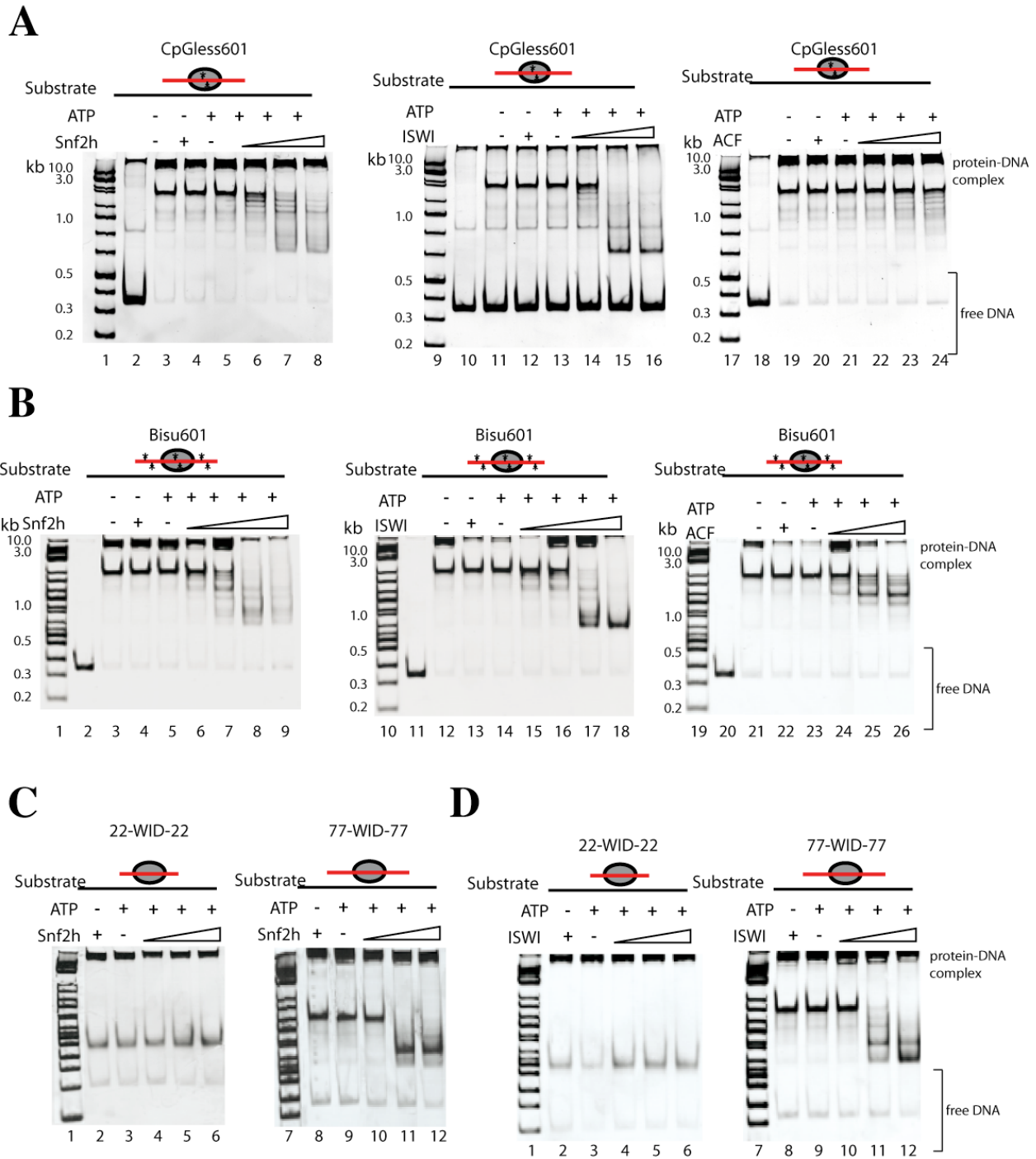
Figure 25. Comparative nucleosome mobilization assays on different 601 nucleosomal substrates
A) "Nucleosome sliding" assays with different chromatin remodeling factors (Snf2H, ISWI, ACF complex, 2-40 fM) using the 601 template lacking CpG sites in the protruding DNA (approximately 50 fmol) revealed a preferred shift to the border positions (see section D.II.1.8 for DNA fragment description). Positioned mononucleosomes were incubated at 26° C with increasing amounts of the indicated remodeller in the presence or absence of ATP as indicated (* represents the presence of CpG sites). The reaction was stopped after 90 min with competitor DNA, separated on a native 4.5 % polyacrylamide gel and visualized by ethidium bromide staining. B) Chromatin remodeling reaction with Snf2H, ISWI, ACF as described in A) with the 342 bp substrate used in the bisulfite assay C) and D) Nucleosome mobilization with Snf2H (C) and ISWI (D) on the 22-WID-22 in comparison to the 77-WID77 substrate: Affinity purified Snf2H (C) or ISWI (D) was incubated with 50 fmoles of nucleosomes in the presence or absence of ATP as indicated. Nucleosome positions were analyzed by electrophoresis on native polyacrylamide gels as described above.

II. MAINTENANCE METHYLATION IN THE CONTEXT OF CHROMATIN

The molecular mechanisms of DNA methylation in the context of chromatin are still ambiguous. Recent data provide evidence for a restricted DNA methylation by Dnmt1 in chromatin (Okuwaki and Verreault, 2004). However, the published results are conflicting. To elucidate the properties of Dnmt1 on DNA packaged into chromatin in detail, I have performed studies on the binding and methylation characteristics of Dnmt1. Furthermore, I have addressed the influence of chromatin remodeling on the DNA methylation and binding efficiency of Dnmt1.

1. DNA and nucleosome binding properties of Dnmt1

By comparing the binding properties of Dnmt1 to different DNA substrates either in free form or packaged into mononucleosomes, the basic unit of chromatin, I wanted to determine the structural effects on the binding characteristics of Dnmt1.

1.1. DNA binding characteristics of Dnmt1

To determine the binding affinity of Dnmt1 for free DNA I used the technique of electrophoretic mobility shift assay (EMSA). This method facilitates the visualization of DNA-protein interactions due to differences in migration behavior in the gel: higher molecular DNA-protein complexes migrate slower in native gel electrophoresis than free DNA and can hence be distinguished. Please see Figure 18 for the purification of recombinant Dnmt1.

In initial experiments, I compared binding of Dnmt1 to free DNAs of different length (Fig. 26A). Increasing amounts of Dnmt1 (Fig. 26A, lane 3-6; 100 nM-0.5 µM) were titrated to a low range DNA ladder consisting of 10-250 bp DNA fragments (Fig. 26A, lane 1 and 2). The addition of increasing amounts of Dnmt1 showed that the protein binds preferentially to longer DNA substrates (> 35 bp), visible as DNA-protein complexes stuck in the gel well. The affinity to smaller DNA fragments (< 35 bp) was much lower and higher protein concentrations even lead to discrimination of fragments shorter than 35 bp in length (Fig. 26A, lane 5 and 6). According to this assay, only longer (> 35 bp) free DNA substrates are stably bound by Dnmt1.
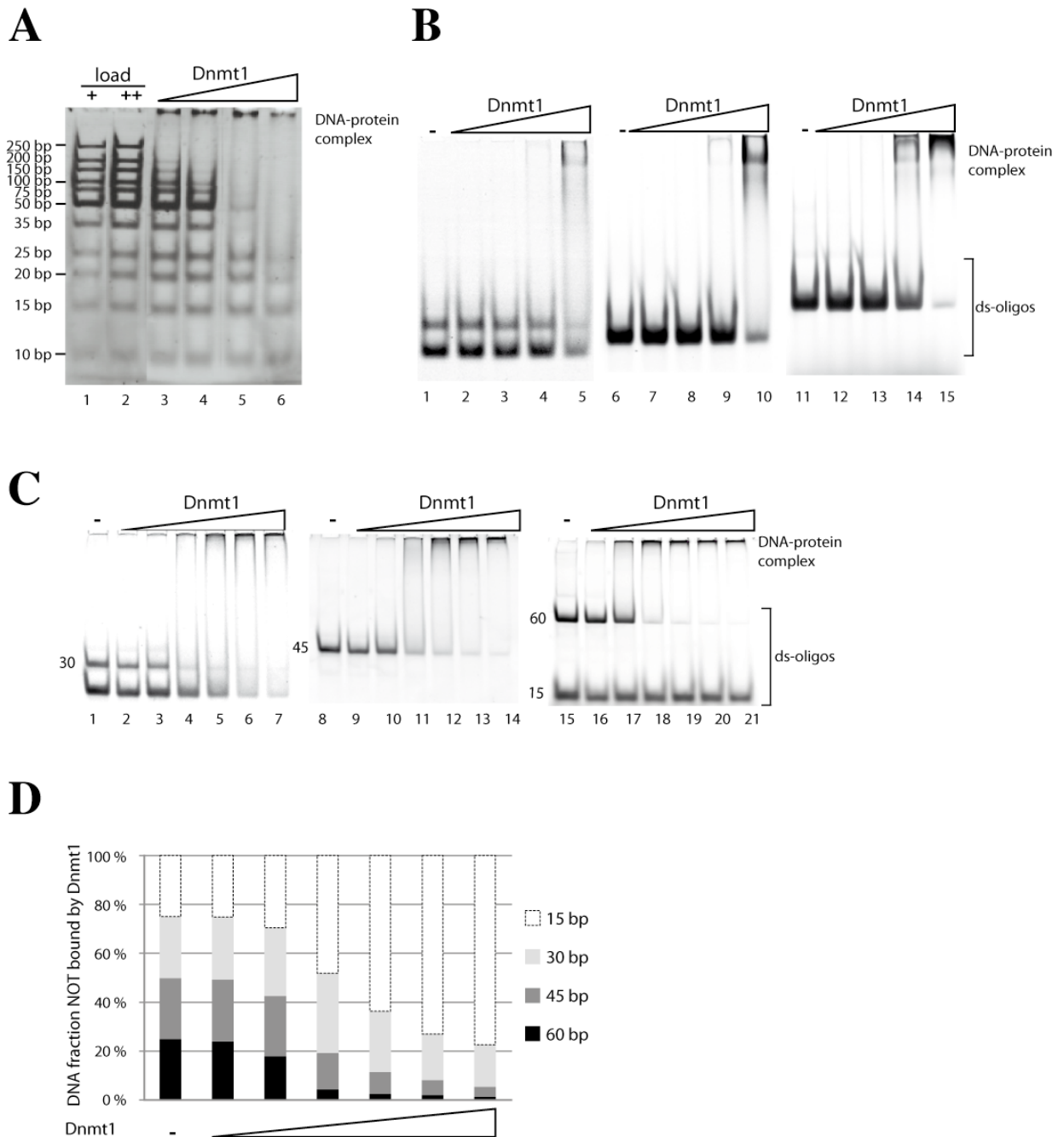
Figure 26. Dnmt1 requires a DNA substrates length > 45 bp for efficient DNA binding

A) Electrophoretic mobility shift assays. Ultra low range DNA ladder (DNA size (bp) indicated on the left) was loaded in rising concentrations (62 and 125 ng, lane 1-2). Different concentrations of Dnmt1 (100 nM-0.5 µM) were added to 125 ng of the DNA (lanes 3-6) and the DNA-protein complexes were analyzed on a 15 % PAA gel.

B) Fluorescence labeled oligonucleotides of different lengths (30 bp (A488, lane 1-5), 45bp (A555, lane 6-10), 60 bp (A647, lane 11-15) were hybridized in similar quantities to their complementary strand. EMSA was performed in a 12 µl volume containing the mixture of different Alexa-labeled ds-oligonucleotides (4 pmol of each ds-oligonucleotides), 0.2 µg poly(dIdC) and the reaction was incubated without (lane 1, 6, 11) or with Dnmt1 (final 100 nM- 1 µM, lane 2-5; lane 7-10; lane 12-15) in Ex50 Buffer for 15 min at 26°C and analyzed on a 5 % native polyacrylamide gel. The Fuji FLA 5000 system was used for visualization of the DNA-protein complexes.

C) Similar procedure as in B). Fluorescence labeled oligonucleotides of different lengths (15 bp (A647, lane 15-21), 30 bp (A488, lane 1-7), 45bp (A555, lane 8-14), 60 bp (A647, lane 15-21)) were hybridized in similar quantities to their complementary strand. A 12 µl reaction contained the mixture of different Alexa-labeled ds-oligonucleotides (4 pmol of each ds-oligonucleotides), 0.2 µg poly(dIdC) and was incubated without (lane 1) or with Dnmt1 (final 100 nM- 0.5 µM, lane 2-3) in Ex50 buffer for 15 min at 26°C and analyzed on a 15 % native polyacrylamide gel. The Fuji FLA 5000 system was used for visualization. D) Relative quantification of Dnmt1 binding properties comparing DNA molecules of different lengths (see C).

Dissection on the binding affinity of Dnmt1 to small DNA fragments in more detail, EMSAs with fluorescently labeled oligonucleotides that were hybridized to their complementary strand were performed (Fig. 26B and 26C). Fluorescently labeled ds-oligonucleotides (4 pmol each) of different lengths (15-60 bp), harboring different labels on their 5'end, were incubated with increasing amounts of Dnmt1 (100 nM-0.5 µM; 30 bp: lane 2-5, 45 bp: lane 7-10; 60 bp: lane 12-15) and complex formation was analyzed on a 6 % PAA gel (Figure 26B). A similar experiment is shown in Figure 26C with the exception that the Dnmt1 affinity to a 15 bp ds-oligonucleotide was also tested (30 bp: lane 2-7, 45 bp: lane 8-14; 15 bp and 60 bp: lane 15-21). These experiments confirmed that Dnmt1 requires a minimal DNA length of > 30 bp to efficiently bind its substrates. The observed higher affinity for longer DNA substrates suggests either a cooperative binding of Dnmt1 or a DNA-binding domain within the protein that requires longer DNA to bind.

1.2. Nucleosome binding characteristics of Dnmt1

The initial experiments suggested that the affinity of Dnmt1 to DNA requires a specific minimal length of free DNA. This observation provided the basis for interaction studies of Dnmt1 with different mononucleosomal substrates. Firstly, EMSAs on reconstituted mononucleosomes varying in the length of the DNA overhang were conducted. Figure 27A shows an illustration of the DNA substrate design used for the nucleosome binding assay (please find a detailed description of the template design in D.II.1.8). The different DNA substrates as generated by the use of respective restriction enzyme digests on the pPCRScript_slo1-gla75 are represented in Figure 27B. The resulting DNA fragments were amplified using PCR (Figure 27C, a selection of PCR products is shown) to generate the respective DNA substrates for nucleosome assembly (see Figure 17 in section D.II.1.8. for illustration of DNA substrate design). Subsequently the different fragments, ranging from 147 bp to 301 bp were reconstituted
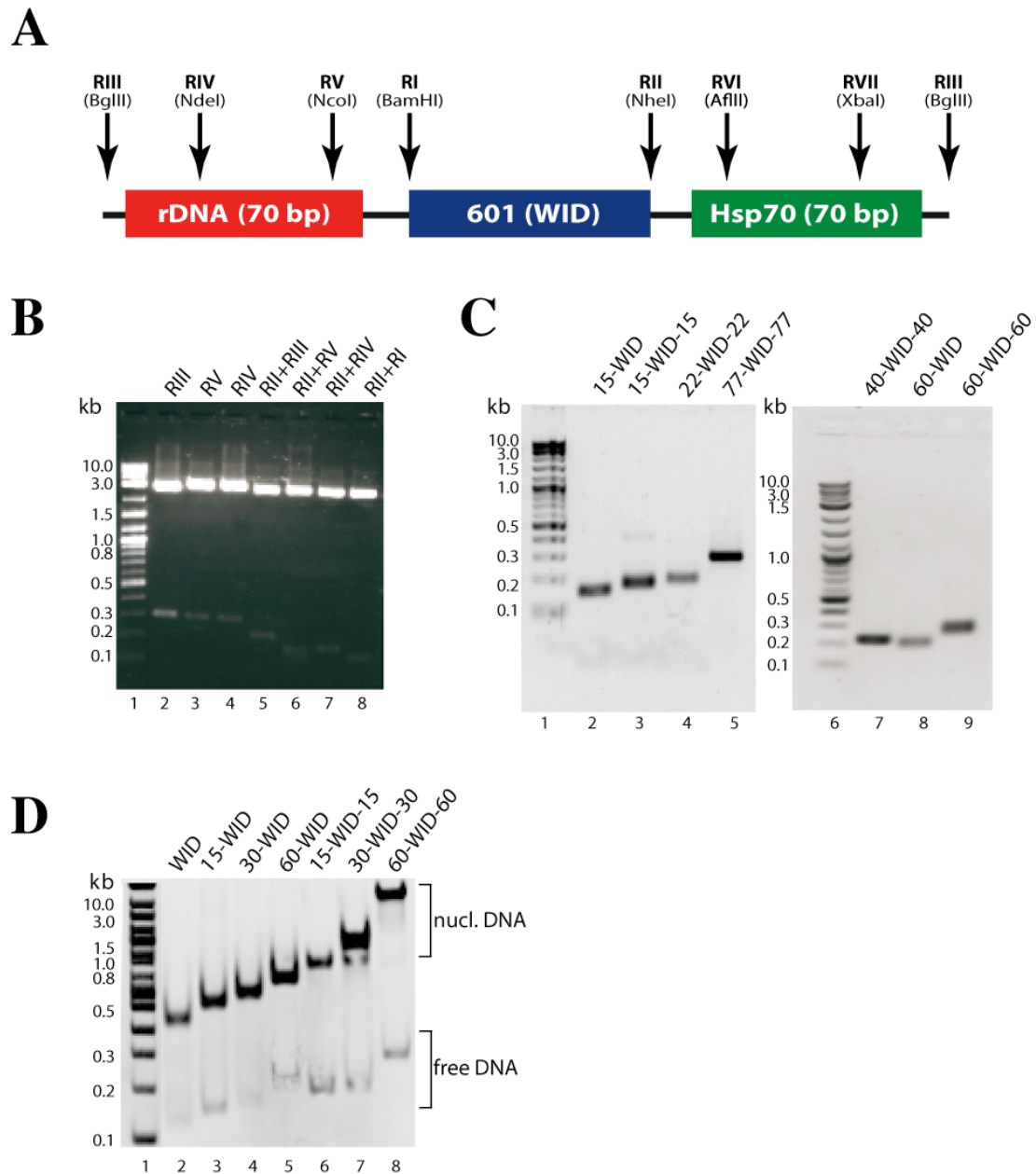
Figure 27. Nucleosome assembly on modified 601 fragments

A) Ilustration of the nucleosomal substrate design used for the 601 nucleosome mobility shift assays. Central 147 bp 601 nucleosome positioning sequence and flanking rDNA (70 bp) and Hsp70 (70 bp) sequences are presented as blue, red and green rectangles, respectively. Restriction sites for the separation of different fragments are indicated as arrows. B) The 601 NPS was used to generate nucleosomal templates with different lengths of overhanging DNA by restriction digest of the DNA construct and analyzed on a 1.3 % agarose gel. The different restriction endonucleases (RI-RV) used here are indicated on top of the different lanes (lane 2-8). By combination of different restriction endonucleases, symmetrical and asymmetrical DNA overhangs of variable lengths, relative to the WID sequence could be prepared. C) Following restriction digest, the templates were amplified by PCR. The used oligonucleotides to generate the specific WID DNA templates are described in Fig. 17 and section D.II.1.8. Not all PCR products are shown. D) Subsequently these different fragments were assembled into chromatin using salt gradient dialysis. The nucleosome positions were separated on a 5 % polyacrylamide gel (lane 2-8, free DNA and nucleosomes are indicated). A size standard (2-log DNA ladder) was run in lane 1.

119

into mononucleosomes by salt gradient dialysis (Figure 27D) as described before (Rhodes and Laskey, 1989) (see Figure 19 for the salt assembly experimental set-up and Figure 20 for recombinant *Drosophila* histones). Nucleosome assembly with the different "601-DNAs" resulted in the appearance of a single band that could be visualized on a native PAA gel (Fig. 27D, lane 2-8). Using this strategy a variety of asymmetrical and symmetrical "601-nucleosome positions" with different linker length are generated. The DNA protrusions of the mononucleosomes range from 0-77 bp either asymmetric or symmetric from both sides of the nucleosome. The different nucleosomal substrates could be separated according to their migrating characteristics in the PAA gel: border positioned nucleosomes migrate faster as compared to more centrally positioned nucleosomes.

To characterize the binding characteristics of Dnmt1 to nucleosomes, I compared the affinity of Dnmt1 to the 601 nucleosomal substrates with different length of protrusions. The nucleosomal substrates (50-200 nM) were incubated without or with increasing amounts of Dnmt1 (100 nM – 0.5 µM). The resulting DNA-protein complexes were analyzed in gel retardation assays (Fig. 28A-C). Figure 28A shows the binding of Dnmt1 to symmetrical templates whereas Figure 28B compares asymmetrical templates. Dnmt1 fails to stably interact with nucleosomes assembled on the 147 bp DNA (WID, fast migrating band, e.g. lane 2-5), even at high Dnmt1 concentrations (0.5 µM), no stable Dnmt1-nucleosome complex with the 147 bp nucleosome was formed (see Fig. 28A, lane 5). Dnmt1 shows weak interactions with the symmetrical 22-WID-22 substrate (see Fig. 28B, lane 3-5). The binding of Dnmt1 to the 40-WID-40 template results in a clear shift (Fig. 28B, lane 2-5 or 7-9). Interestingly, Dnmt1 shows low binding affinities to the asymmetric templates (22-WID, 40-WID, 77-WID) (Fig. 28A). Along this line, Dnmt1 shows the strongest interactions with the 77-WID-77 nucleosome, whereas it shows only weak affinity to the asymmetric counterpart (77-WID) (Figure 28C, lane 2-4).

The binding affinities to the free DNA substrates could also be estimated in these experiments. Free DNA of 300 bp (77-WID-77) is preferentially bound in comparison to shorter DNA fragments (< 200 bp, WID) (see Fig. 28B or C, fast migrating band). Comparing the longest symmetrical mononucleosome (77-WID-77) to its histone-free DNA it becomes apparent that Dnmt1 shows similar affinities to both substrates (see Fig. 28C, lane 3 and 4). For all shorter symmetrical and also asymmetrical substrates, Dnmt1 prefers the free DNA form compared to the mononucleosomal form (see Fig.
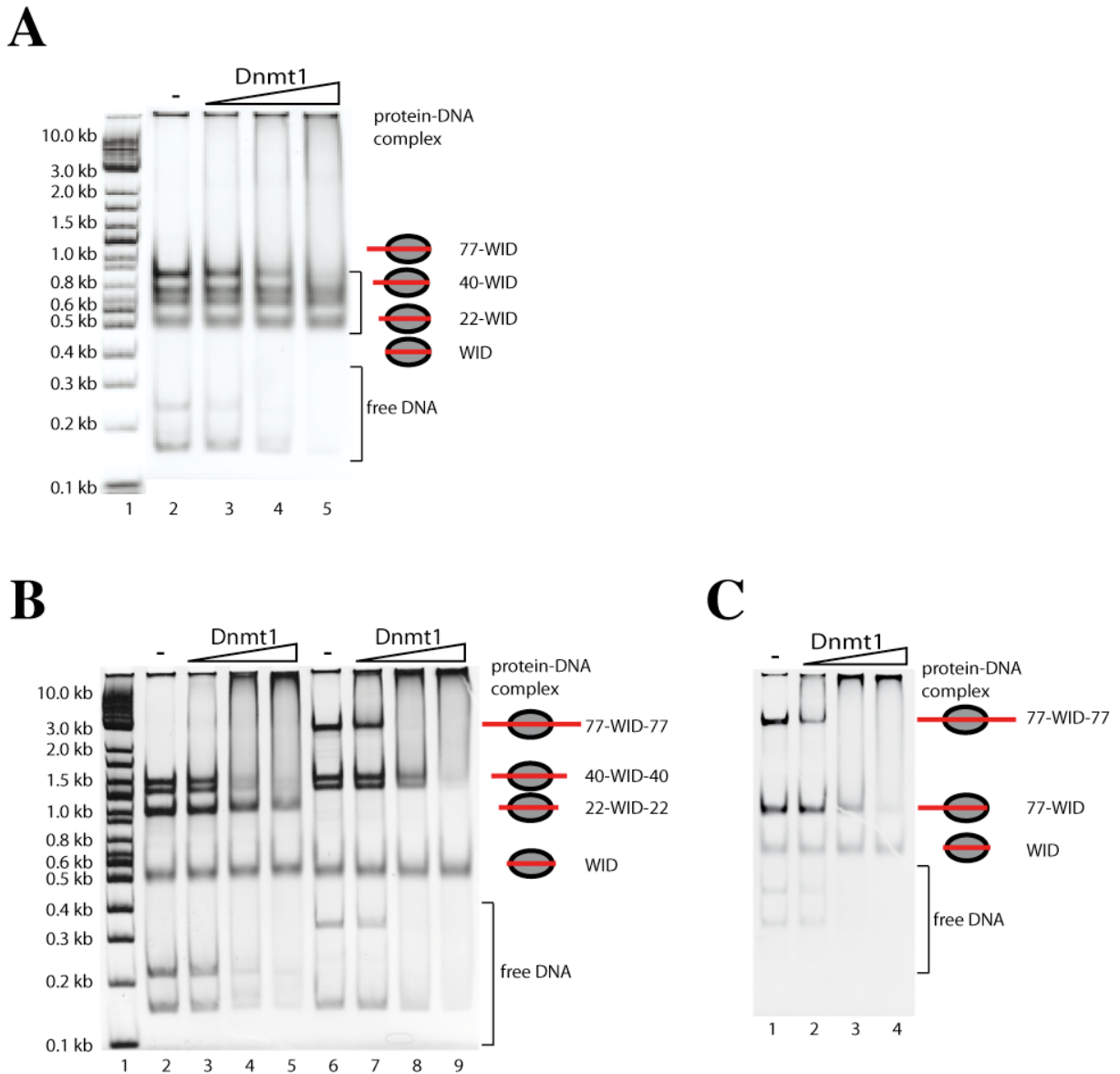
Figure 28. Characterization of the Dnmt1 binding affinity to mononucleosomal substrates differing in the length of protruding DNA

A) to C) The different symmetrical (A) and asymmetrical (B) nucleosomal templates (100-150 ng; 50 – 200 nM) (linker length of the WID sequence indicated by cartoons) were incubated in a 12 µl reaction volume without (lane 2 and 6) and with 100 nM-0.5 µM Dnmt1 (lane 3-5 and 7-9) for 30 min at 26°C in binding buffer (10 mM HEPES (pH 7.6), 50 mM KCl, 2.5 mM MgCl2, 10 % Glycerol, 1 mM DTT). C) A comparison of the Dnmt1 affinity to the 77-WID-77 asymmetrical and symmetrical mononucleosomes is shown. Potein-DNA and Protein-nucleosome complexes were analyzed on 6 % polyacrylamide gels. A size standard (2-log ladder) was run in lane 1.

28A and B). This suggests that Dnmt1 preferentially recognizes and stably associates with free DNA instead of nucleosomal DNA. It further demonstrates that a minimal DNA length of 40-80 bp flanking the nucleosome positioning site is needed for an efficient Dnmt1 binding. Additionally, preferential binding is observed to the symmetrical nucleosomes harboring 40-80 bp flanking sequences. Notably, Dnmt1 preferentially binds to the symmetrical 40-WID-40 substrate over the asymmetrical 77-WID substrate, though they harbor the same amount of binding sites (data not shown). Titration of Dnmt1 to the 77-WID-77 substrate led to the formation of several retarded DNA bands, suggesting that more than one Dnmt1 molecule can associate with the DNA (see Fig. 29A). The results of these binding experiments indicate the formation of a stable Dnmt1 – nucleosome complex (Fig. 29A, lane 3-5 (left) or lane 2-4 (right)).

In order to test the stability of the Dnmt1-nucleosome complex more accurately, competitive binding assays were performed (Fig. 29B). As competitor, a 6 kb free DNA plasmid was used (Fig. 29B, lane 2). The 77-WID-77 nucleosome (50 nM) was first incubated with amounts of Dnmt1 (150 nM) appropriate to form the stable nucleosome–Dnmt1 complex as described before (Fig. 29B, lane 3). The stable complex was subsequently incubated with rising amounts of competitor DNA (20-100 nM) and analyzed by native PAA gel electrophoresis (PAGE). It was observed that even after the addition of low amounts of competitor DNA, the Dnmt1–nucleosome complex started to disassemble (Fig. 29B, lane 5). This effect was potentiated by adding more competitor DNA (Fig. 29B, lane 6 and 7). These observations demonstrate that, although the formed complex of Dnmt1 and the 77-WID-77 nucleosome seems stable, it can be disintegrated by the addition of low concentrations of competitor DNA. Similar results were obtained in a time course experiment with addition of a fixed amount of competitor DNA (data not shown). These results indicate a complex formation that is highly dynamic. Figure 29C summarizes the Dnmt1 binding characteristics with respect to the different nucleosomal templates.
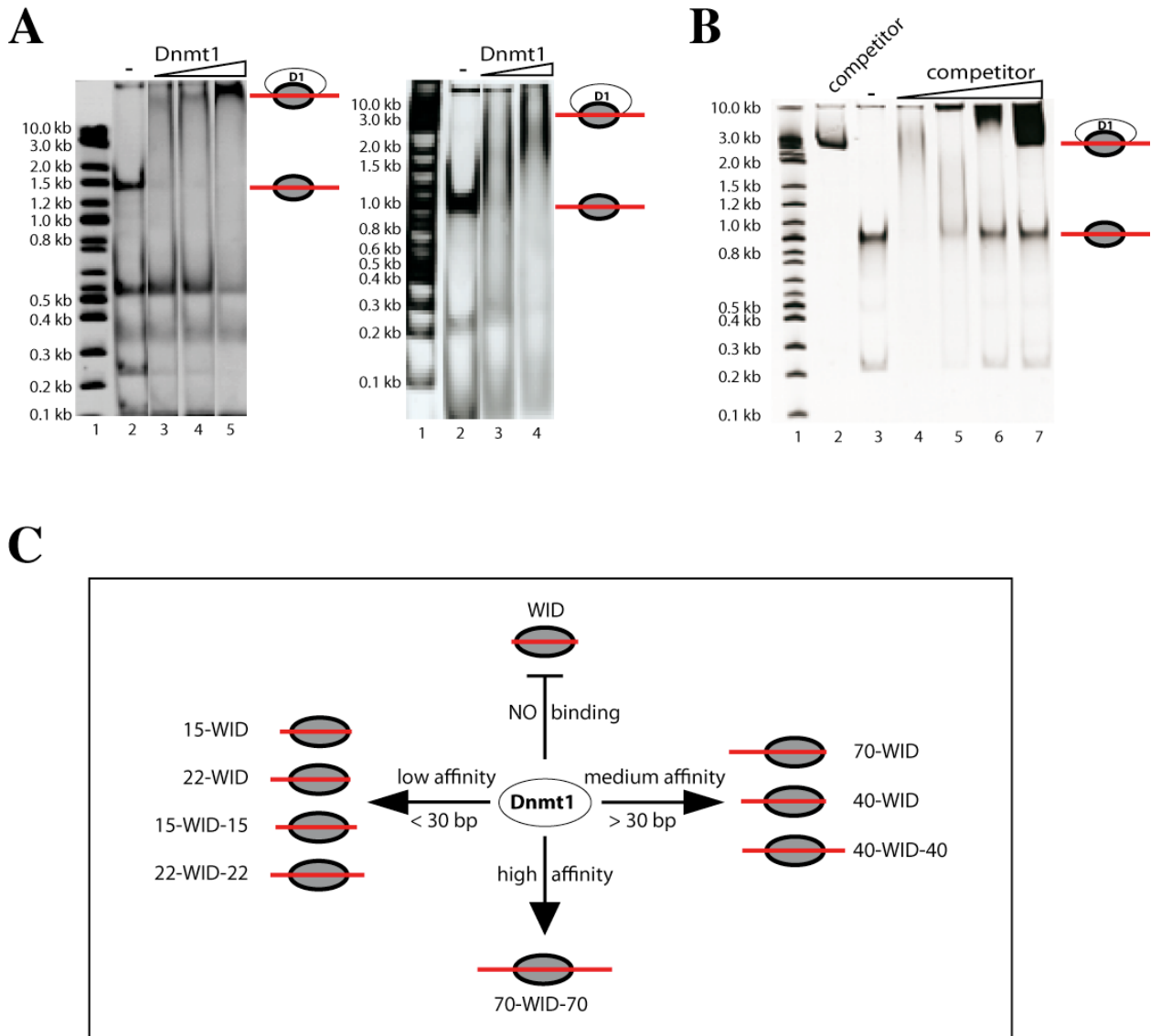
Figure 29. The binding of Dnmt1 to nucleosomes occurs on symmetrical nucleosomes harboring 30-80 bp DNA overhangs on entry and exit sites of the nucleosome

A) Electromobility shift assays using the symmetrical 77 bp linker nucleosome (77-WID-77) as substrate indicate a stable Dnmt1-nucleosome complex (please see Fig. 28A for assay procedure). Dnmt1 was titrated to the 77-WID-77 nucleosomal substrate. The protein-DNA complex was visualized on a 4.5 % native PAA gel. B) Competitive binding assays. Lane 2 shows the 6 kb competitor plasmid DNA. 100 ng (50 nM) of the 77-WID-77 nucleosome (lane 3) were first incubated with appropriate amounts Dnmt1 (150 nM) to form the stable nucleosome–Dnmt1 complex (lane 4). The stably formed complex was subsequently incubated with rising amounts of competitor DNA (100-500 ng (20 nM-150 nM), lane 5-7) and analyzed on a 6 % native polyacrylamide gel. A size standard (2-log ladder) was run in lane 1. C) Conclusion of the Dnmt1 EMSAs using the different 601 nucleosomal fragments. Dnmt1 (centrally) discriminates nucleosomal substrates without DNA overhangs (WID, on top). It shows low affinity to asymmetrical and symmetrical mononucleosomes with < 30 bp flanking DNA (left side), whereas its affinity to templates > 30 bp is medium (right side). The highest affinity was observed on templates harboring 40-80bp of symmetrically DNA overhangs.

1.3. Mapping the localization of Dnmt1 on the 77-WID-77 nucleosome

1.3.1. SET-UP OF THE DNASEI FOOTPRINTING ASSAY

The read-out of EMSAs is limited to the single information of a DNA–protein complex formation and does not allow specifying the precise localization of the protein on the DNA substrate. To further analyze whether binding of Dnmt1 to the 77-WID-77 nucleosome occurs exclusively via contacts of free DNA or requires additional nucleosomal contacts, DNaseI protection (DNaseI "footprint") experiments were performed. While the read-out method has been described before (Yindeeyoungyeon and Schell, 2000; Zianni *et al.*, 2006) I at first had to set up the assay conditions, in order to identify protected sites and hypersensitive regions of the DNaseI digest on an automated capillary DNA analyzer.

Fluorescently labeled 301 bp 77-WID-77 DNA was generated by PCR using oligonucleotides that were 5' labeled (see section D.II.1.5 for detailed description). The quality of the amplified DNA was then analyzed on a native PAA gel and 5'-Fluorescein phosphoramidite (6-FAM) or 5'-Hexachloro-Fluorescein- Phosphoramidite (HEX) labels visualized using the Fuji Fla-5000 system or ethidium bromide staining (Fig. 30A). The visualization clearly shows that the amplification of the 301 bp DNA substrate works and efficiently labels. However, a big amount of unincorporated oligonucleotides remains in the probe (Fig. 30A lane 3 and 4). The quality of the labeled DNA fragment was analyzed using an automated capillary electrophoresis instrument (Fig. 30B). This was done by Sophie Hinreiner at the "Institute of functional genomics" (see section D.II.7.6). The results of the fragment analysis showed the most significant peak at approximately 300 bp, which represents the detection of the DNA fragment at the correct size. Peaks smaller than 50 bp correspond to free oligonucleotides.

Fluorescently labeled 77-WID-77 DNA was subsequently assembled into nucleosomes using salt gradient dialysis (Fig. 31A).

Though DNaseI has a sequence preference it randomly hydrolyzes the phosphodiester bonds of DNA between the 3′ oxygen on the deoxyribose of one nucleotide and the 5′ phosphate of the next nucleotide. Generally, a low DNase I concentration is used so that on average each DNA molecule is cleaved just once. In initial experiments I determined the optimal DNaseI concentration for the footprinting reaction (31B). To this end, DNA and positioned nucleosomes (12.5-25 nM) were treated with DNaseI (0.1 u)
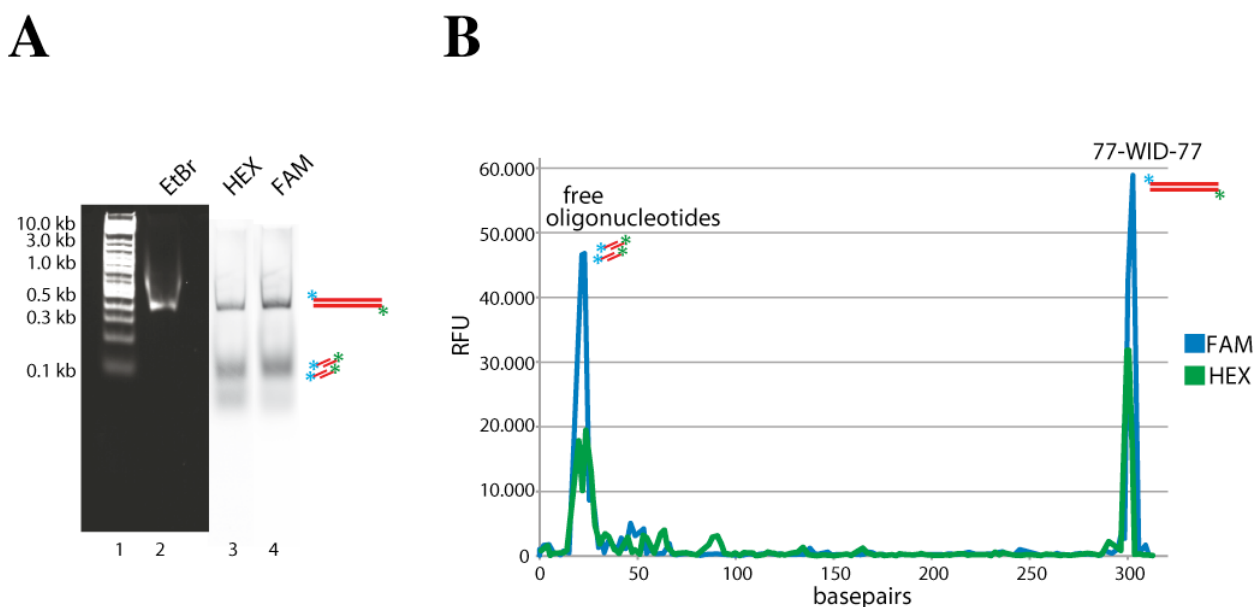
Figure 30. Labeling of the 77-WID-77 DNA substrate using fluorescently labeled oligonucleotides

A) The 77-WID-77 template was fluorescently labeled by PCR ("body labeling") using 5' labeled oligonucleotides (FAM: Em519 = green and HEX: Em556 = yellow) as described in section D.II.1.6. The labeled DNA was purified by ethanol precipitation and analyzed on a 5 % native polyacrylamide gel. EtBr or the respective laser (FAM: 473 nm; HEX: 473) was used to visualize the labeled DNA. Free oligonucleotides and the labeled 77-WID-77 DNA are indicated as bars. B) For visualization approximately 1 ng (2.5-5 nM) purified DNA was loaded onto a 3730 capillary electrophoresis instrument. The injection was 2 kV and injection time 15 s. The electropherogram of FAM (blue)- and HEX (green)-labeled DNA as well as free oligonucleotides are shown. The intensity was measured in relative fluorescence units (RFU). As size standard a 1:2 mixture of LIZ 120 and LIZ500 was used.
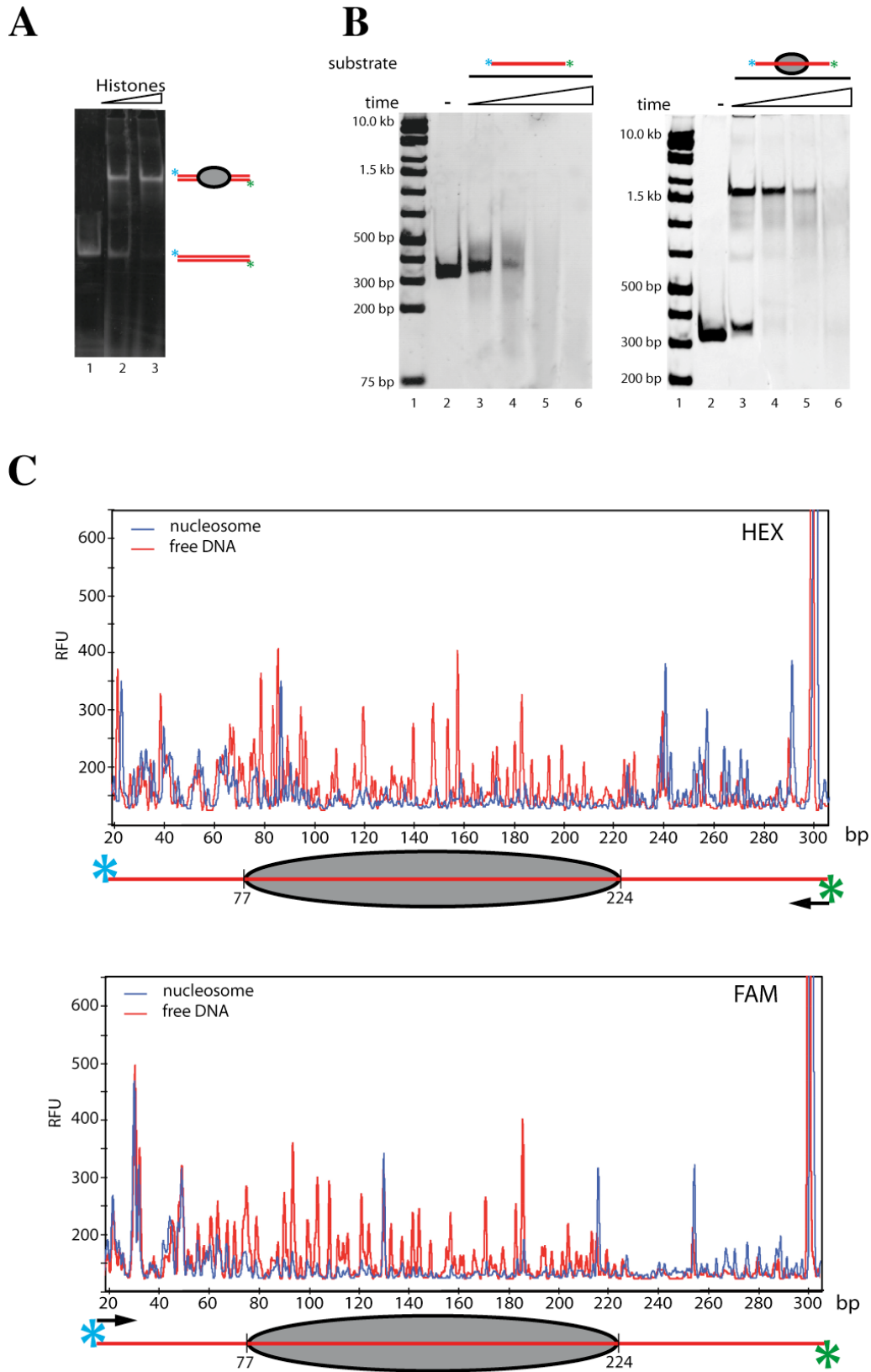
Figure 31. Setting up the DnaseI protection assay using a capillary electrophoresis instrument

A) Reconstitution of mononucleosomes using salt gradient dialysis. Labeled DNA (lane 1) incubated with *Drosophila* histones was assembled by salt gradient dialysis into chromatin (lane 2 and 3). Different ratios of histones to DNA were used in salt assembly and tested for nucleosome occupancy using a 5 % native polyacrylamide gel. Free DNA and nucleosome positions are indicated. A size standard (2-log ladder) is indicated.

B) Partial DNaseI digests of free DNA and central positioned mononucleosomes are shown. DNaseI digestion was performed using the 77-WID-77 DNA fragment in free and nucleosomal form. The 301 bp 5'fluorescently labeled DNA was assembled into nucleosomes by salt gradient dialysis as described in A) 50 ng (12,5 nM) free DNA, (red bar on the left) and positioned nucleosomes, grey ellipse on the right were treated with 0.1 u DNaseI for several time points (0, 60,120, 240 s, as indicated). The reaction was stopped by the addition of 5 mM EDTA to inactivate the DNaseI. DNA was subsequently analyzed for complete digestion on a 5 % native polyacrylamide gel. A DNA size standard (2-log ladder) was run in lane 1. C) Comparison of the electropherograms originating from 1. DNaseI digest of free DNA (red line) 2. DNaseI digest of nucleosomal DNA (blue line). The position of the central nucleosome is indicated (ellipse). The DNaseI digest was performed using the 77-WID-77 DNA fragment in free and nucleosomal form. The 301 bp 5'fluorescently labeled DNA was assembled into nucleosomes by salt gradient dialysis. 50 ng (250 nM) free DNA and positioned nucleosomes were treated with 0.1 u DNaseI for several time points (0, 60,120, 240 s). The reaction was stopped by the addition of 5 mM EDTA to inactivate the DNaseI. DNA was subsequently loaded onto a capillary electrophoresis instrument as described in 30B. The electropherograms for both directions (5'HEX: on top and 5'FAM: on bottom) are compared for free DNA (red line) and nucleosomal DNA (blue line). The nucleosome core is illustrated by an ellipse.

and the reaction was stopped at several time points (0, 60, 120, 240 s) by the addition of EDTA. Digestion products were analyzed on a native PAA gel (Fig. 31B). The partial DNaseI digest results in a characteristic cleavage pattern that differs between the free DNA and nucleosomal DNA (Fig.31B, compare left to right hand site). Longer incubation times lead to the accumulation of smaller fragments (Fig. 31B, lane 4 and 5). The optimal DNaseI concentration for 25 nM free DNA (50 ng DNA) was determined as 0.1 u for 60 s, resulting in a partial DNaseI digest (Fig. 31B (left), lane 2). The DNaseI digest of the nucleosome (50 ng) was incubated longer compared to the free form, thereby generating longer products (Fig. 31B (right), lane 3 and 4). The optimal DNaseI concentration was determined as 0.1 u for an incubation time of 120 s (Fig. 31B (right), lane 4). One major criterion of the DNaseI footprinting analysis using the capillary electrophoresis instrument is the DNaseI concentration. Therefore, several optimization experiments testing DNaseI on the nucleosomal template have been analyzed on the capillary electrophoresis instrument (data not shown). Zianni and coworkers reported that the electropherogram of optimal DNaseI digestion should show peak heights that are I) evenly distributed and II) show a distribution along the complete size of the fragment (Zianni *et al.*, 2006). These characteristics were implemented at DNaseI concentrations of 0.5 u and incubation times of 120 s for 25 nM DNA (data not shown). Further, DNaseI protected fragments of both DNA forms free and the nucleosomal form, were analyzed on the automated sequencer (Fig. 31C). The analysis of both sites (FAM/ HEX) reveals a protected region between ~ 80 and 230 bp, exactly the nucleosome positioning sequence (78 bp- 224 bp), known as the "601" NPS.

1.3.2. DNMT1 FOOTPRINTING ASSAY

Next, I intended to map Dnmt1-nucleosome interactions using the DNaseI protection assay. A flow-chart of the DNaseI protection ("footprinting") assay and its read-out by capillary electrophoresis is depicted in Figure 32 (for a detailed description see section D.II.7.3): Briefly, Dnmt1-nucleosome complex was prepared in large scale. Prior, the optimal ratio of Dnmt1 (150 nM) to 77-WID-77 (25 nM) nucleosomes that barely forms a Dnmt1-nucleosome complex was determined by EMSA (Fig. 33A, lane 4).

Subsequently, the reaction was subjected to a partial DNaseI digest and stopped at the multiple time points (0-240 s). Additionally, Both DNaseI digests (with/without Dnmt1) were compared and checked for completion (Fig. 33B). After purification from proteins and free oligonucleotides the DNA was finally loaded onto the capillary electrophoresis sequencer instrument (Fig. 33C). The resulting peak pattern was compared to the pattern obtained after DNaseI digest of the nucleosomal DNA in the absence of Dnmt1.

The comparison of the two fragment patterns showed clear differences at the nucleosome entry and exit sites. This indicates that Dnmt interacts with both, overhanging DNA and nucleosomal DNA. The protected sites between basepairs 40 to 80 of both nucleosome sites suggest that Dnmt1 might bind ~ 30-40 bp of free DNA and an symmetric region surrounding the nucleosome dyad axis. Another interpretation is that Dnmt1 binds bilaterally to the 77-WID-77 nucleosomal substrate. Furthermore Dnmt1 could also posses a very long DNA binding domain. Figure 33 D shows the DnaseI protected regions on both sites of the nucleosome (left) and a hypothetical cartoon in 3D, how Dnmt1 could bind on the nucleosome entry/exit sites (right).

In conclusion, the EMSAs on DNA in free and nucleosomal form have shown, that Dnmt1 requires DNA overhangs to stably interact with mononucleosomes. Furthermore this interaction seems to occur at both sites of the nucleosome as suggested by the results of the footprinting assay.
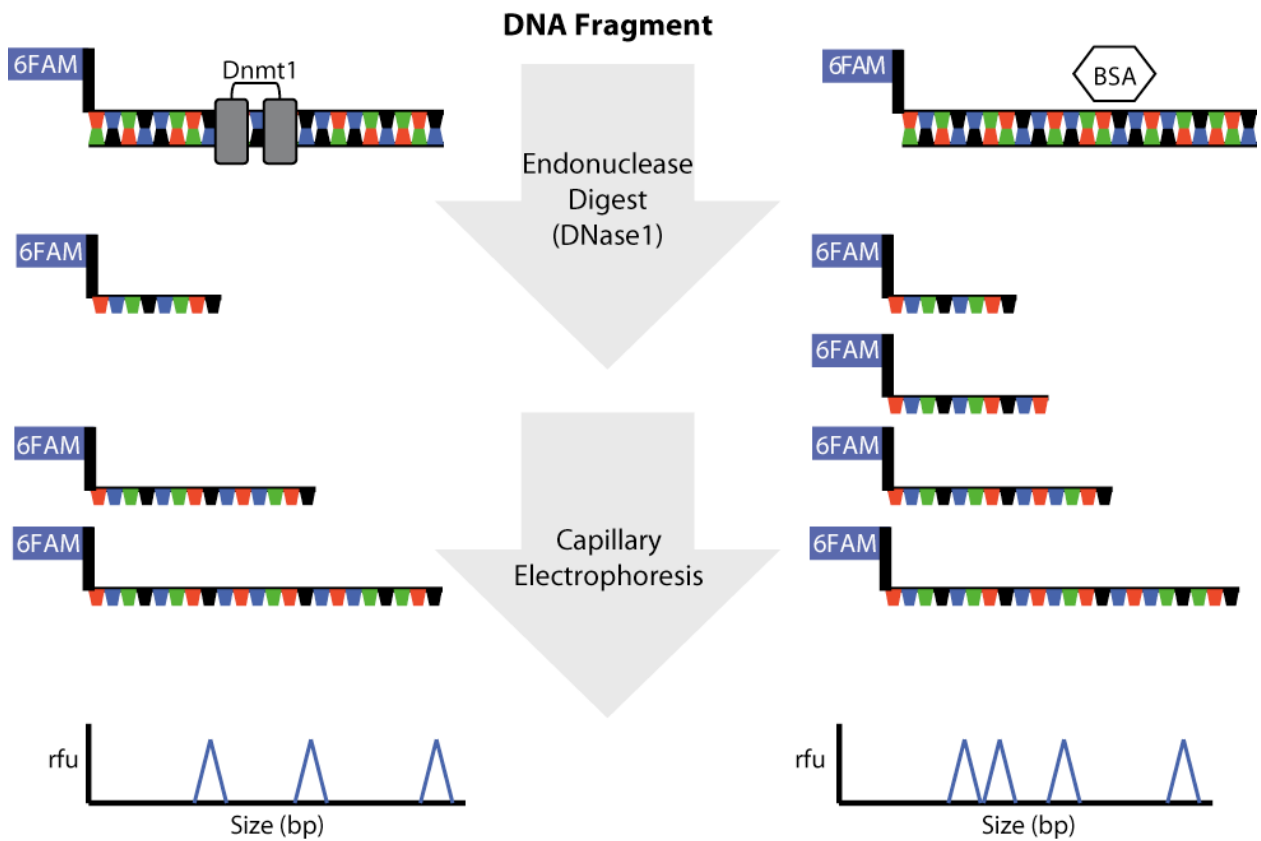
Figure 32. Scheme of the DNaseI protection assay ("Footprint")

A) Schematic representation of the DNaseI footprinting assay (please find detailed protocol in section D.II.7.3). Briefly, fluorescence labeled DNA was incubated without (right side) or with (left side) the protein of interest (Here: Dnmt1). Subsequently, DNA was partially digested with DNaseI. The DNaseI protected fragments were analyzed by Maxam-Gilbert DNA-Sequencing using an automated capillary electrophoresis system for the read-out. The electropherograms reveal the location of the protein of interest by "footprints".
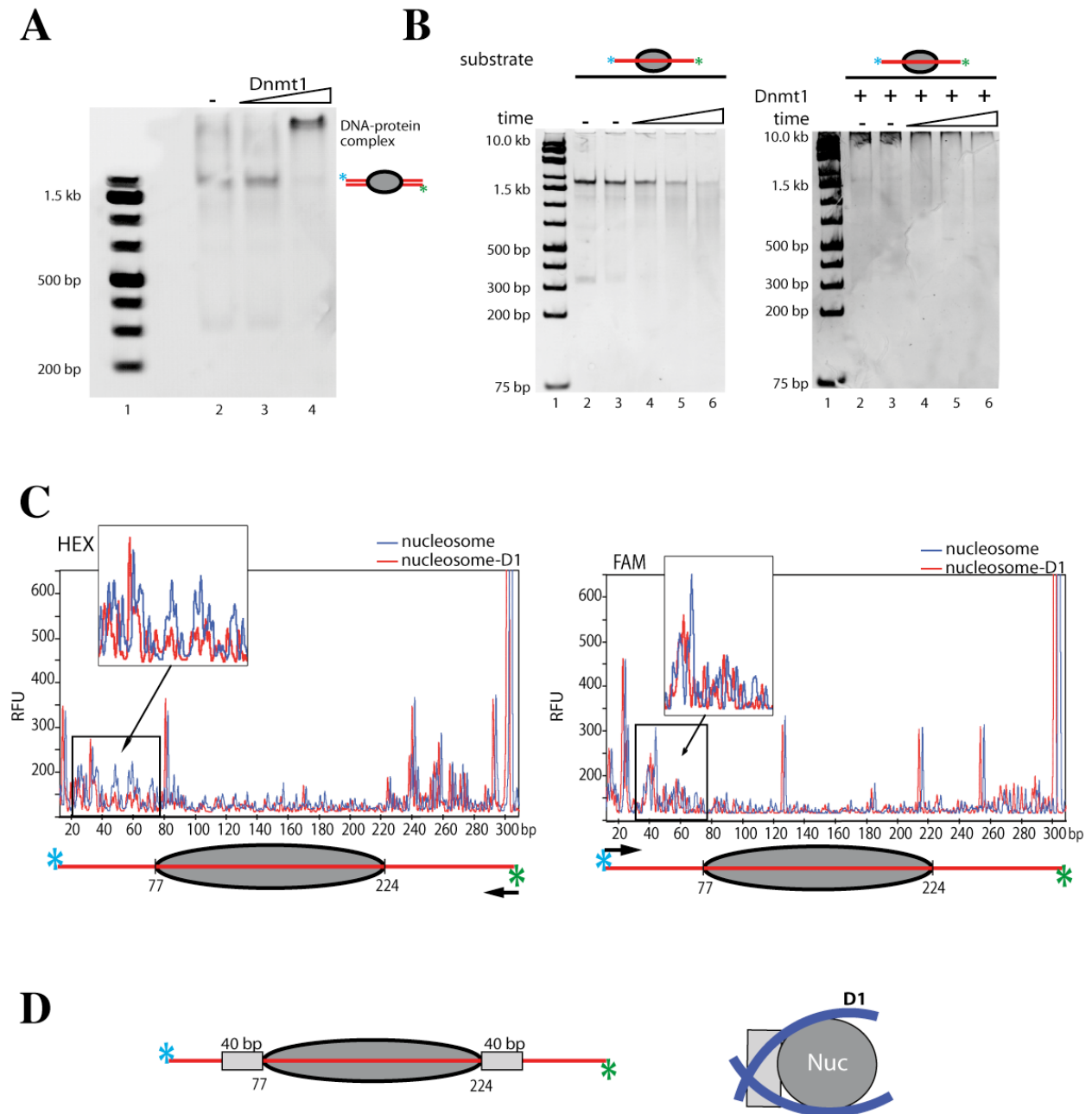
Figure 33. DNaseI protection ("Footprinting") assay to map the localization of Dnmt1 at the preferred mononucleosomal template

A) Analytical EMSA to test the Dnmt1 affinity prior to the footprint reaction. 150 nM Dnmt1 were titrated to 100 ng (25 nM) nucleosomal DNA (77-WID-77) to monitor Dnmt1-nucleosome complex formation in the DNaseI reaction buffer and incubated for 30 min at 26°C. Complexes were separated on a 5 % PAA gel. The positions of the nucleosome (ellipse) and Dnmt1-nucleosome complexes are indicated. B) Quality analysis of the DNaseI protection assay ("footprinting assay") in the absence (left side) or presence (right side) of Dnmt1. Recombinant Dnmt1 (150 nM) was incubated with the 77-WID-77 nucleosomal template (25 nM) and partially digested with DNaseI (10 sec, 30 sec, 60 sec, 90 sec, 120 sec). The reaction was stopped by the addition of 5 mM EDTA to inactivate the DNaseI. Subsequently the nucleosome-Dnmt1 complexes were analyzed on a 5 % polyacrylamide gel. C) Read-out of DNaseI protection assay. The position of Dnmt1 was mapped using an automated sequencing machine. DNA was purified using the PCR purification kit (Qiagen) prior to loading onto the capillary electrophoresis instrument. A comparison between the nucleosomal DNA alone (blue line) and the Dnmt1 bound nucleosomal DNA (red line) is shown. The electropherograms for both directions (5'HEX: on top and 5'FAM: on bottom) are compared are

represented. The nucleosome position (ellipse) and the flourescence labels are indicated. An enlarged region, showing the protected region is highlighted in the box. D) Conclusion of the Dnmt1 "footprinting" assay. Left: A schematic illustration of the nucleosome and its DNaseI protected regions (indicated as grey boxes on the entry/exit sites of the nucleosome) is shown. Right: Cartoon illustrating how Dnmt1 (blue) could hypothetical bind to the exit and entry site of the nucleosome (3D-view).

2. Methylated CpG site analysis in the mononucleosomal core

The accessibility of a DNA sequence packaged into a mononucleosomes could influence the methylation of specific target CpG sites by Dnmt1 depending on their specific position within the nucleosome. To examine the distribution of CpG dinucleotides methylated by Dnmt1, I performed bisulfite sequencing experiments. For this purpose a 342 bp DNA substrate (based on the "pGA4 BN-601-m1"-DNA) consisting of a central modified 601 nucleosome positioning sequence and 27 CpG sites evenly distributed over the entire DNA fragment was used (see section D.II.1.8 for detailed description of DNA substrate preparation). This substrate was assembled into chromatin by salt gradient dialysis as described before (Figure 34A, lane 3). The estimated nucleosome position was verified by restriction endonuclease digest (data not shown). A flow-chart of the bisulfite sequencing assay is shown in Figure 34B: After incubation of free DNA or mononucleosomes (16 nM CpG sites applied) with Dnmt1 (120 nM final concentration) and SAM (250 nM) the DNAs was converted via bisulfite treatment. This treatment deaminates unmethylated cytosines but does not react with methylated ones. Next, the resulting DNA sequences were amplified by PCR and the products subsequently cloned and sequenced. After bisulfite treatment the DNA strands are not complementary anymore, therefore two primer pairs are needed to discriminate between the sense and the antisense DNA strands. The efficiency of the PCR amplification was verified on an agarose gel (Fig. 34C): It was clearly shown that all DNA fragments had the expected size and therefore were successfully amplified (Fig. 34C, lane 2-6).

Figure 34D and 34E shows the methylation efficiency of Dnmt1 at individual CpG sites on the modified 601 nucleosome substrate.
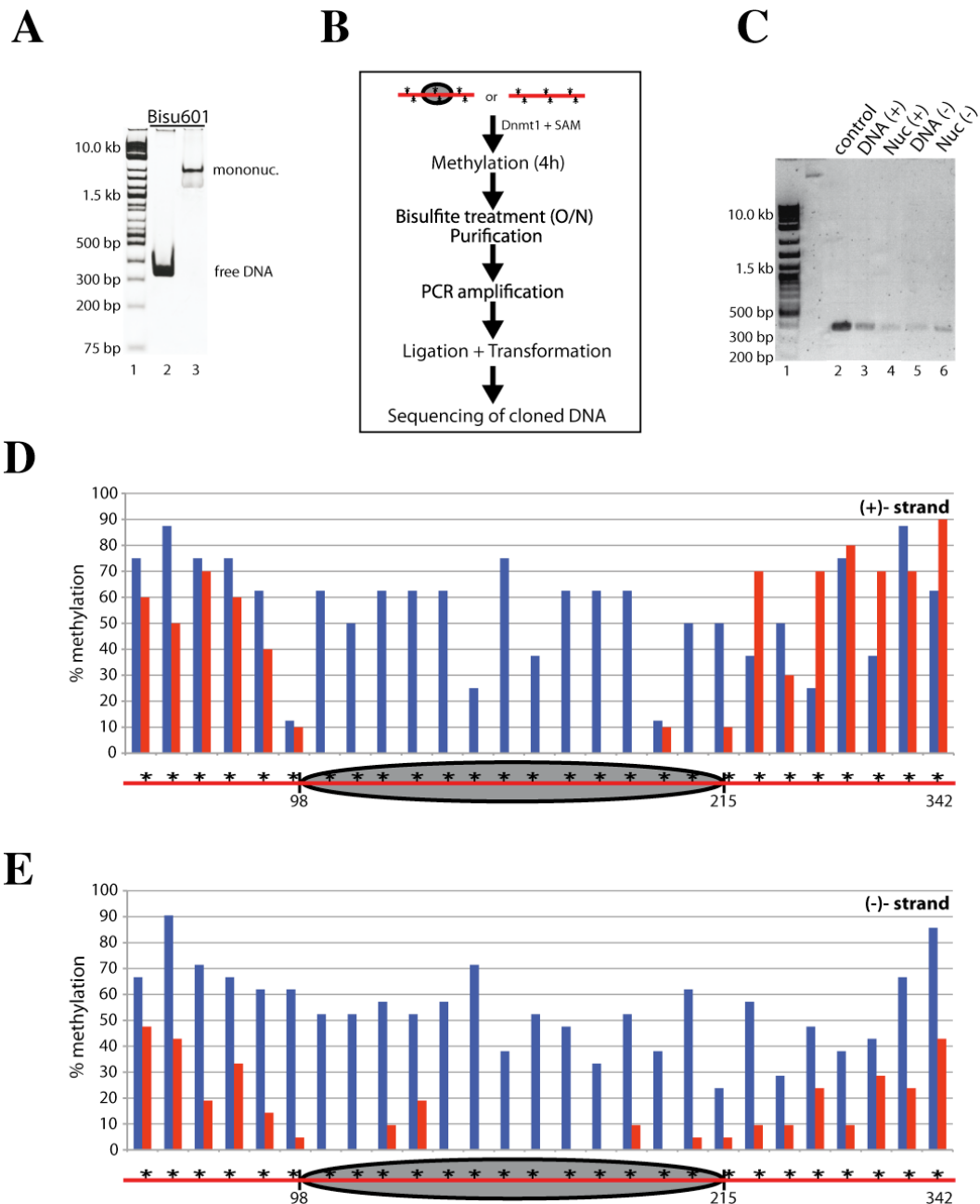
Figure 34. Bisulfite sequencing of Dnmt1-methylated mononucleosomal templates

A) Reconstitution of 601Bisulfite mononucleosome (342 bp fragment, harbouring 27 CpGsites) using salt gradient dialysis. DNA incubated with histones was assembled by salt gradient dialysis into chromatin. Different ratios of histones to DNA (lane 2 and 3) were used in salt assembly and tested for nucleosome occupancy. A size standard (2-log DNA ladder) was run in lane 1. Free DNA and mononucleosomes (both indicated) were visualized by agarose gel electrophoresis and ethidium bromide staining. B) Flow-chart of the bisulfite assay. Localization of methylated CpG sites in the 601 mononucleosome in comparison to free DNA is shown. 601 mononucleosome and free DNA templates (both 16 nM CpG sites applied in final reaction) were incubated with Dnmt1 (120 nM final concentration) and S-adenosyl methionine (250 nM) in a 40 µl reaction. The DNA was treated with bisulfite, purified and subsequently applied to PCR with specific oligonucleotides to discriminate between the (+) and (-) strand. The PCR products were then cloned into the pGEMTeasy vector and the clones analyzed by bisulfite sequencing. C) PCR products of the Bisulfite 601 free and nucleosomal DNA fragments following bisulfite conversion. (+) and (-) represents the respective amplified DNA strand. In D) and E) Evaluations of the Dnmt1 methylated CpG sites (in percent) according to their position in the 601 free DNA (blue bars) form or on mononucleosomes (red bars). (+) and (-) strands are shown. The red bar on the bottom represents the DNA fragment with the CpG sites (marked as stars). The ellipse illustrates the 601 nucleosome position.

132

Whereas on both strands the CpG sites within the regions flanking the nucleosome can be efficiently methylated, the methylation efficiency rapidly decreases towards the nucleosome core. This effect is more drastic on the sense strand. In contrast Dnmt1 is capable to methylate all CpG sites distributed over the free DNA substrate. This counted for the (+) strand as well as for the (-) strand. Interestingly, Dnmt1 seems to methylate specific CpG sites more efficiently even in free DNA substrates. On the sense strand CpG 6, 12, 18, 23 are barely methylated (Fig. 34D), whereas this phenomenon is less pronounced for CpG 20, 22 on the antisense strand (Fig. 34E).

To analyze the DNA substrates more precisely, I compared the activity of Dnmt1 on different free DNA and nucleosomal substrates without or with DNA protrusions (Fig. 35A and C). The substrates that were analyzed in this assay are shown in Fig.35A and described in section D.II.1.8.

The catalytic activity of Dnmt1 on the different free DNA and nucleosomal substrates was analyzed in the radioactive DNA methylation activity assay:

The transfer of tritium-labeled methyl groups from S-adenosyl methionine ($[^3H]$-SAM) onto the different free DNA and chromatin reconstituted DNA substrates by Dnmt1 was analyzed with little modifications from a published protocol (Pradhan *et al.*, 1999). A flow-chart of this assay is outlined in Figure 35B. Briefly, free DNA or corresponding chromatinized DNA (480 nM CpG sites) was incubated for 60-90 min at 26°C with rising amounts of purified Dnmt1 (50 nM final concentration) enzyme in the presence of $[^3H]$-SAM (60-360 nM final). Tritium incorporation was counted using a liquid scintillation system.

As can be seen in panel 2 and 4, Dnmt1 methylates the two free DNA substrates (Fig. 35C). Surprisingly, the 147 bp free DNA substrate (panel 4) was more efficiently methylated as compared to the 342 bp DNA (panel 2). This could be due to local differences in the higher order structure of the DNA. Vast differences were detected for nucleosomal substrates: the modified 601 substrate that was used in the bisulfite assay proved to be a good substrate for Dnmt1 (panel 3). In contrast, Dnmt1 could barely methylate the 147 bp nucleosome substrate without protruding DNA (panel 5). These results strengthen the conclusion that Dnmt1 needs DNA overhangs for both, binding and methylation events.
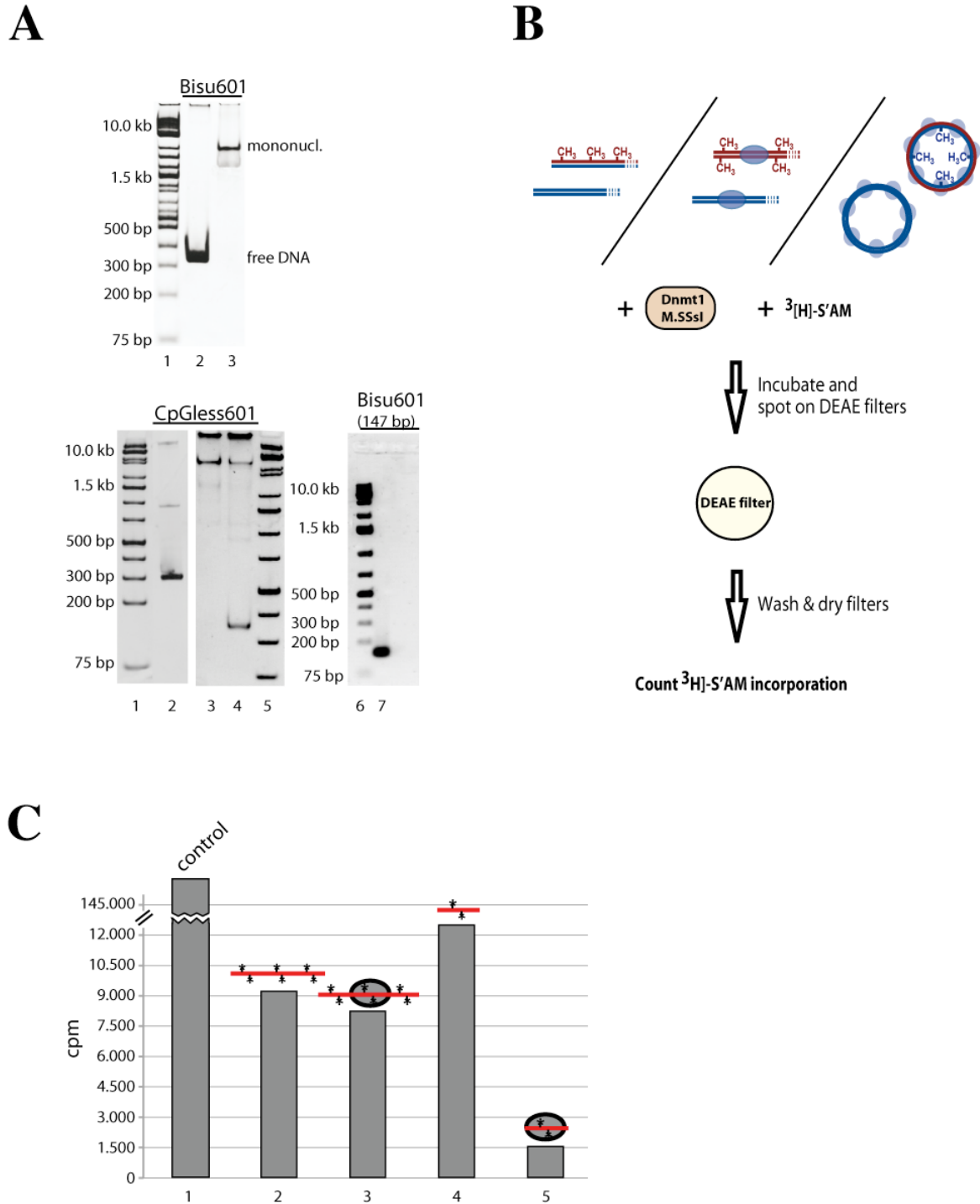
Figure 35. Analysis of Dnmt1 activity on different mononucleosomal templates

A) Agarose gel analysis of free DNA and nucleosomal 601 templates used in B). The different DNA templates are described in section D.II.1.8. On top: The 342 bp DNA fragment (Bisu601), here shown in free (lane 2) and nucleosomal (lane 3) form, was used for bisulfte sequencing. Below: The 346 bp DNA fragment harboring a CpG less nucleosome flanking region is shown in free (lane 2) and assembled form (lane 3). The 147 bp 601 DNA fragment is shown only as free DNA (lane 7). Approximately 200 ng DNA were loaded onto the gel and were visualized by agarose gel electrophoresis and ethidium bromide staining. B) Graphic representation of the DNA methyltransferase activity assay. Hemimethylated and unmethylated free DNA or chromatinized substrates were incubated for 60-90 min at 26°C (for chromatin templates) or 37°C (for naked DNA templates) in the presence of 3[H]-SAM and Dnmt1. The reaction was subsequently spotted onto DEAE filters and the incorporated 3[H]-CH3 was measured (please find a detailed description in section D.II.6.1).

C) Enzymatic activity of Dnmt1 at the different DNA templates analyzed in the radioactive methylation activity assay. The 601 bisulfite template (as free DNA and nucleosomal template) was applied to the Dnmt1 (80 nM Dnmt1) methylation efficiency assay and compared with a 147 bp fragment (both 480 nM CpG sites in final reaction) harboring no linker DNA in the mononucleosomal form. The incorporation of 3H-SAM (360 nM final) was measured. The different DNA substrates are illustrated as bars, the ellipse represents the nucleosome position marked. The AIR DNA fragment was applied as positive control. CpG sites are shown as stars.

3. Generation of hemimethylated DNA as a substrate for Dnmt1

Dnmt1 has been described to catalyze maintenance methylation. Thus, one major objective was to generate long hemimethylated DNA for subsequent analyses. I compared different procedures of DNA preparation, because of the lack of standard protocols. Initial experiments were performed using the strategy depicted in Fig. 36A. First, fully methylated DNA was generated by treating a circular plasmid with the bacterial CpG methyltransferase M.SssI. In the following, a single strand nick was introduced using Nb.BsmI. Exonuclease III was then used to remove mononucleotides from the 3'-hydroxyl terminus of the nicked strand. Following primer annealing the DNA was repaired by DNA ligase and analyzed on an agarose gel (Fig. 36B): After M.SssI methylation of the plasmid DNA the methylated DNA was incubated with the methylation sensitive restriction enzymes MspI and HpaII to analyze the methylation efficiency. MspI and HpaII are isochizomeres with the recognition palindrom CCGG. The methylation efficiency can be analyzed due to the features of the enzymes: MspI is active on unmethylated as well as metylated DNA, whereas the activity of HpaII is inhibited by methylation. Therefore different restriction patterns do correlate with the degree of DNA methylation. The restriction digests with MspI and HpaII showed that the methylation reaction was efficient: in comparison to the MspI restriction pattern HpaII was inhibited by the successful methylation (Fig. 36B). Finally, the methylated and nicked plasmid DNA rendered single-stranded by the incubation with Exonuclease III. The nicked-DNA can be distinguished due to its slower migration.

Due to precipitation efficiency problems of single-stranded DNA or degradation in case of primer extension, only about 50 % of the input DNA could be recovered after exonuclease III digestion. To increase the yield, variations of the above described methods were tested (data not shown). One was to use T4 polymerase instead of Taq
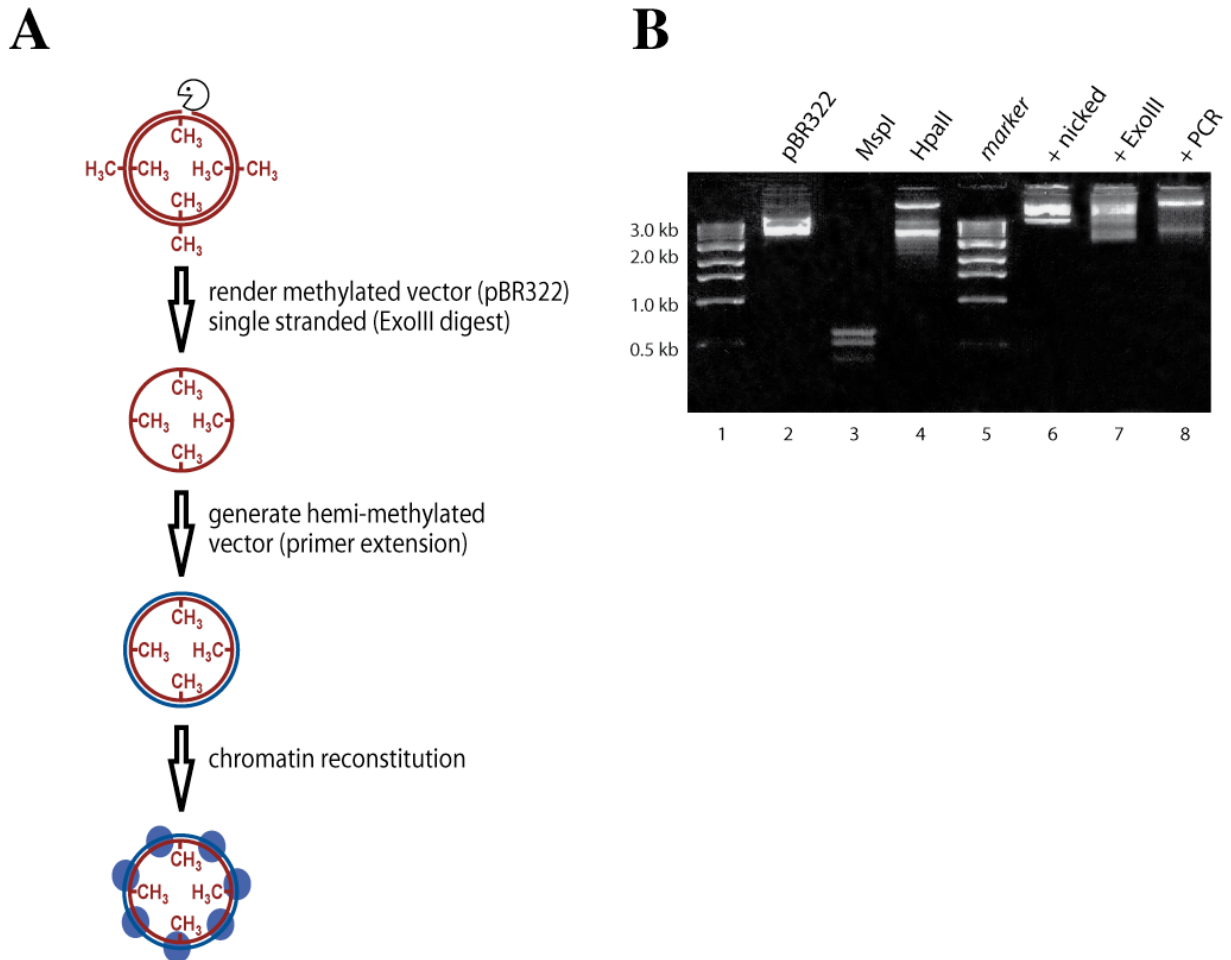
Figure 36. Preparation of hemimethylated DNA

A) Schematic illustration of the strategies used to generate hemimethylated chromatin (please find a detailed description in text). A single-strand nick was inserted into a M.SssI-methylated 6 kb plasmid using a restriction endonuclease. Subsequently the nicked strand was digested with ExonucleaseIII and the complementary strand hybridized by primer extension reactions. The plasmid was then re-ligated and packaged into chromatin using salt gradient dialysis. B) Qualitative agarose gel analysis of the different educts and products to generate hemimethylated DNA as substrate for Dnmt1. Methylation efficiency was analyzed by restriction digest using the methylation sensitive isochizomers MspI/HpaII.

polymerase for the primer extension reaction, because the 5'-3' exonuclease activity of Taq polymerase might have been the cause of DNA degradation.

Because none of the above variations proved very efficient in generating hemimethylated DNA, the protocol was redesigned (Fig. 37A). The circular plasmid DNA was linearized with a restriction endonuclease (HindIII). One third of the linearized DNA was methylated by M. SssI and mixed with two third of linearized unmethylated DNA. Following denaturation at 94°C and re-annealing, the quality of this hemimethylated DNA product was analyzed on an agarose gel (Fig.37B and 37C): Estimations of the amount of produced hemimethylated DNA were determined by restriction digest using MspI and HpaII. The fragment patterns produced by HpaII in unmethylated compared to hemimethylated DNA were clearly different (Fig. 37C compare lanes 6 and 8). The methylated DNA inhibits HpaII activity, whereas in the hemimethylated fraction additional higher molecular weight bands come up (Fig. 37C, lane 8). This could be due to the heterogenous DNA mixture that is generated by this method.

The purified DNA was re-circulated by DNA ligase (Fig. 37B, lane 8) and assembled into chromatin by salt gradient dialysis (data not shown).
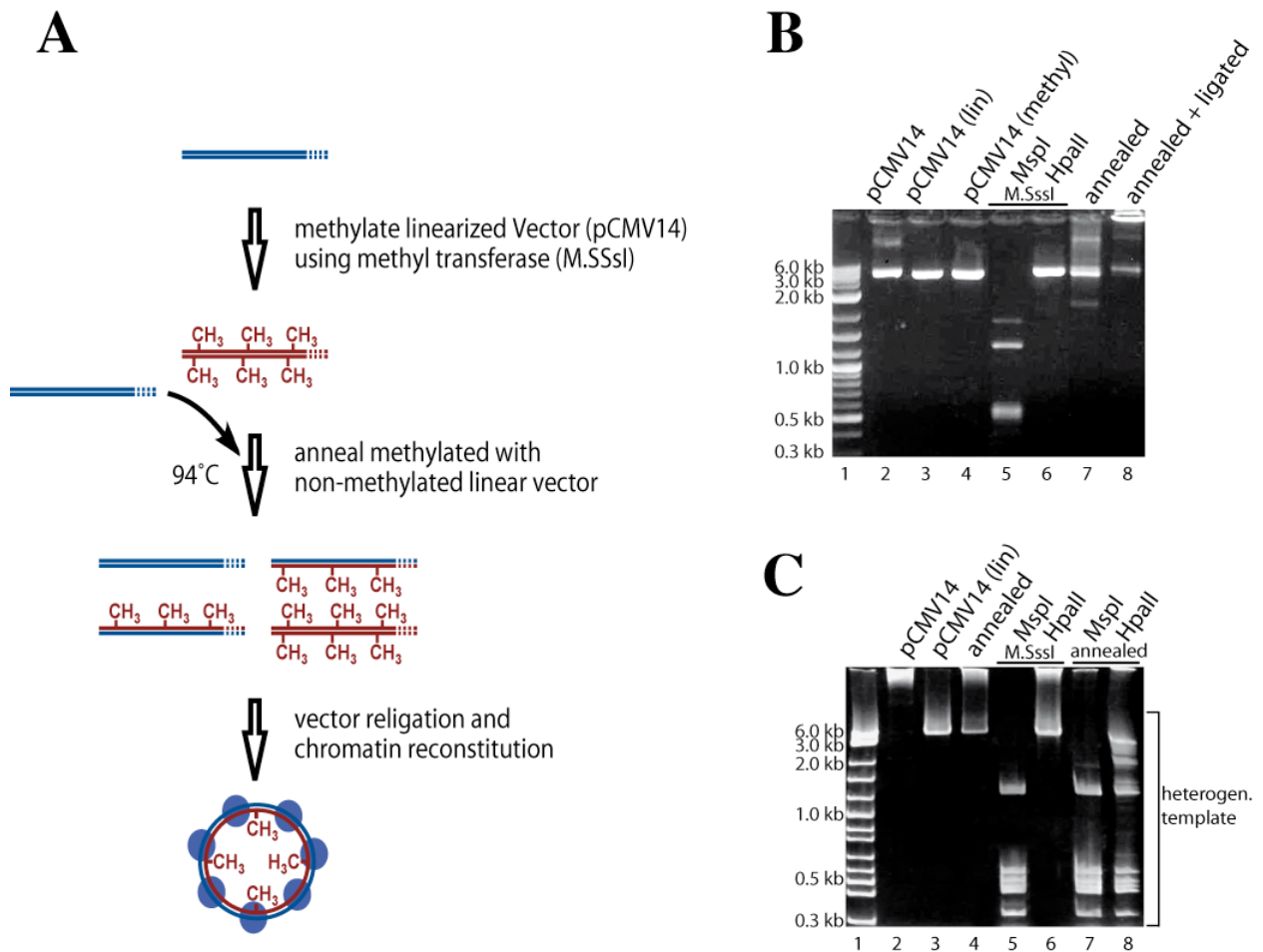
Figure 37. Effective generation of hemimethylated DNA

A) Graphic illustration of the method used to effectively generate hemimethylated chromatin. The linearized (HindIII) 6 kb plasmid was methylated using the bacterial methyltransferase M.SssI. 2/3 untreated DNA was mixed with 1/3 methylated DNA and subsequently annealed (10 min at 95°C denaturation, slowly cool down for annealing). The DNA was re-circulated using DNA ligase and then assembled into chromatin. B) and C) The different educts and products used to generate hemimethylated DNA as depicted by scheme A) were analyzed as described in Fig. 36 by agarose gel electrophoresis. Methylation efficiency was analyzed by restriction digest using the methylation sensitive isochizomers MspI/HpaII. The heterogeneous template is indicated. A 1 kb size standard (1 kb ladder NEB) was run in lane 1.

3.1. Analysis of the hemimethylated substrates

The analysis of the hemimethylated DNA via restriction digest suggests a successful generation of hemimethylated DNA. However, this method is not quantitative. To examine the hemimethylated DNA more precisely, I analyzed the catalytic activity of Dnmt1 on this template in a sensitive radioactive assay. To inspect the quality of the hemimethylated DNA, the DNAs described above were applied to the radioactive methylation assay (Figure 38A). As positive control, the 34 bp hemimethylated AIR DNA fragment (15 pmol CpG sites), harboring 5 CpG sites was used in the assay. This well-characterized fragment is derived from the AIR promoter, which is regulated by methylation (Sleutels and Barlow, 2002; Zwart *et al.*, 2001). The activity of Dnmt1 on the hemimethylated substrates is about 1.25 times lower (80 % of catalytic activity on AIR fragment) than on the hemimethylated AIR fragment (Fig. 38A, panel 1 and 5). This could be due to the quality of the hemimethylated DNA, because as a consequence of the preparation method it is a heterogeneous mixture that contains unmethylated and methylated DNA in addition to hemimethylated DNA.

To further characterize the hemimethylated DNA, same amounts of the prepared DNA (hemimethylated substrate) or a 1:3 mixture of fully methylated and unmethylated template (mixed substrate) were subjected to the radioactive methylation assay and a time-course experiment was performed. A graphic illustration of the applied DNA substrates (hemimethylated substrate versus mixed substrate) is depicted in the diagram 38B, while Figure 38C shows an agarose gel analysis of the different DNA substrates. The linearization of the circular pCMV14 plasmid worked (Fig. 38C, lane 3), but there is some circular plasmid left after the digest as can be seen by a faster migrating band. Differences between the mixed substrate and the hemimethylated substrate are clearly visible: the hemimethylated substrate shows higher-molecular weight bands that could be due to different DNA structures after hybridization (Fig. 38C,lane 5).

The time course experiment (Fig. 38D) shows an incorporation of $[^3H]-CH_3$ that is almost 4 times higher in the hemimethylated substrate as compared to the mixed substrates. The reaction shows linearity up to two hours, where the maximum of the reaction velocity is reached and rapidly decreases afterwards. The mixed template shows almost constant counts (~ 1000 cpm). This suggests an inhibition of Dnmt1 caused by unmethylated and methylated DNA substrates.
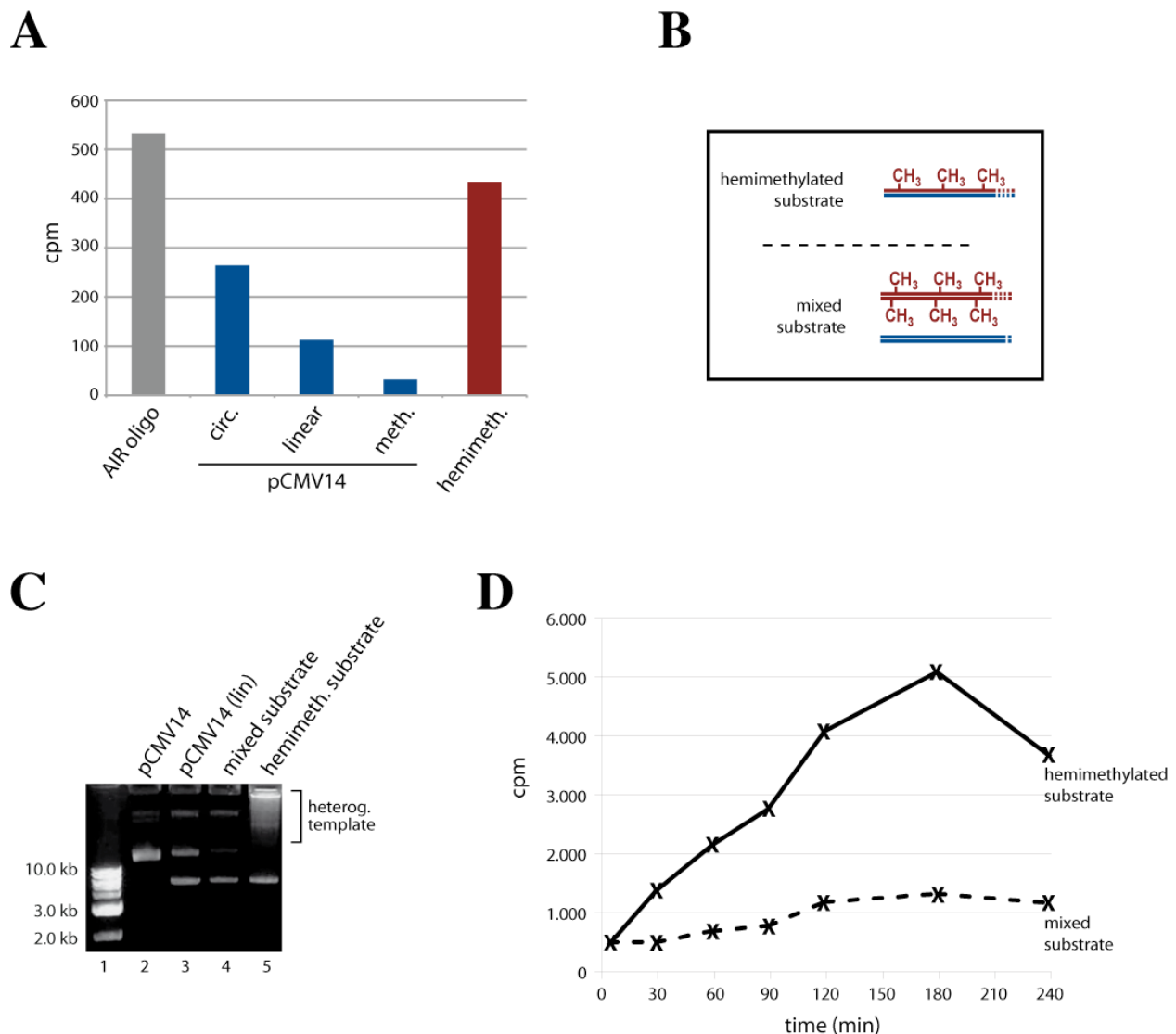
Figure 38. Analysis of DNA methylation efficiency in chromatin

A) The hemimethylated DNA templates as shown in Figure 37 were tested in the radioactive methyltransferase activity assay for further qualitative analysis. A hemimethylated 34 bp AIR DNA fragment (15 pmol CpG sites applied) was used as positive control (panel 1). The circular (panel 2), linear (panel 3) and linear methylated (panel 4) templates (15 pmol CpG sites applied) are shown. Identical amounts of CpG sites (15 pmol) of the hemimethylated DNA were applied (panel 5). The reaction was performed in the presence of 50 nM Dnmt1 and 60nM [3H]-SAM. B) Schematic illustration of the DNA substrates tested in the methylation time-course experiment. The hemimethylated substrate was generated as described in Fig. 37 A). The mixed substrate was prepared by mixing the M.SssI methylated and untreated DNA in a 1:3 ratio. C) Agarose gel analysis of the different templates used in D). A size standard (1 kb) was run in lane 1. D) Monitoring the time-kinetics of the putative hemimethylated DNA template. The enzymatic activity of Dnmt1 was analyzed on the re-annealed hemimethylated substrate (referred to as "hemimethylated substrate") in comparison to the 1:3 mixture of methylated to untreated template (referred to as "mixed substrate") in the methylation assay. Aliquots were taken after indicated time points and the reaction stopped using a dry ice/ethanol bath.

4. Dnmt1 methyltransferase activity on nucleosome arrays

4.1. Activity in the absence and presence of chromatin remodeling factors

I tested whether the presence of chromatin remodeling complexes can enhance the activity of Dnmt1 on chromatin arrays.

First the hemimethylated substrate was assembled into chromatin by salt gradient dialysis. The optimal reconstitution ratio between histones and DNA was determined as 0.8 :1 as analyzed by partial MNase digest (Figure 39A).

Assembled chromatin, unmethylated and hemimethylated (200 ng), was incubated without or with ATP and/or recombinant chromatin remodeling complex ACF (20 to 70 fmol) in the presence of Dnmt1 (60 nM) and [^{3}H]-SAM (60 nM) under standard conditions and the incorporation of tritiated methyl groups was determined (Figure 39B). Interestingly, Dnmt1 showed no activity on unmethylated chromatin; even the presence of ACF did not complement this inhibition (see Fig. 39B, panel 2-5). Contrary, on hemimethylated chromatin Dnmt1 alone was capable to methylate the chromatin array (see panel 7). The addition of ACF complex showed a marginal increase in the activity (see panel 8). In the presence of both ATP and ACF there was a 3.5 fold increase in the methylation rate (see Fig. 39B, panel 9). This ATP-dependent effect could not be significantly enhanced by increased ACF additions (panel 10). Interestingly, the methylation efficiency was as high as on the naked hemimethylated control.

The basal methylation rate, which was also observed in the absence of ACF could be explained by methylation activity in the linker regions. Salt-assembled chromatin has a compact structure, which however still comprises gaps. In comparison, chromatin derived from *Drosophila* embryo extract (DREX*)* yields a higher degree of compaction. It could hence be observed that chromatin generated by salt gradient dialysis is more accessible (diploma thesis, Anna Schrader).

Similar results were obtained in the presence of the ATPase Brg1 as molecular motor (Figure 39C). I compared the methylation efficiencies of Dnmt1 on unmethylated, hemimethylated and methylated chromatin. In contrast to the experiments with ACF, a basic catalytic activity of Dnmt1 could be observed without Brg1 and ATP on all three forms of methylated chromatin, with the highest activity on hemimethylated chromatin (~ 2 times higher than on unmethylated chromatin) (compare Fig. 39C panel 2, 6 and 19). The influences of Brg1 on Dnmt1 methylation in chromatin were similar as for the ACF
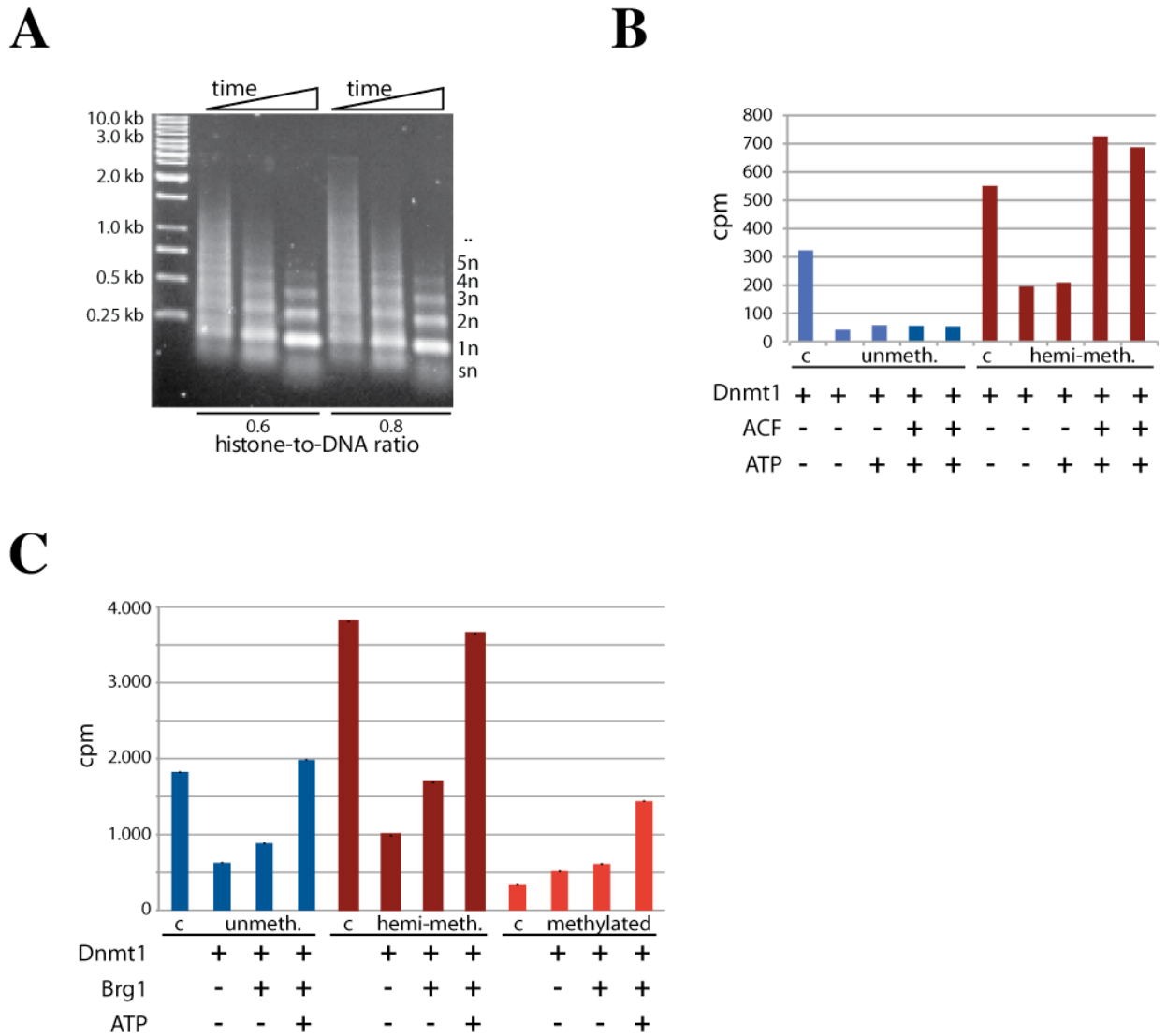
Figure 39. Remodeling factors are required for efficient DNA methylation in chromatin
A) Reconstitution of chromatin arrays using salt gradient dialysis. DNA incubated with histones was assembled by salt gradient dialysis into chromatin. Different ratios of histones to DNA were used for chromatin assembly and tested for nucleosome occupancy. Nucleosome arrays were analyzed using partial MNase digestion at different time points (10, 40, 240 sec). The purified DNA was visualized by agarose gel electrophoresis and ethidium bromide staining. The regular fragment ladder indicative for nucleosomal arrays is shown (sn: subnucleosomal DNA, 1n-5: mono-, di-, tri-, tetra-, pentanucleosomal fragments). A size standard (1 kb) was run in lane 1. B) Unmethylated (blue bars) or hemimethylated (red bars) nucleosomal DNA (200 ng) was subsequently incubated for 6h at 26°C either in the absence or presence of Dnmt1 (60 nM), ATP and ACF (20-70 fmol) (components listed below the diagramm). DNA was isolated and the incorporation of 3[H]-labeled CH3 determined. The DNA accessibility for Dnmt1 was restored (panel 3/5) by addition of the recombinant remodeling complex ACF and ATP to chromatin. C) Brg1 (50-90 fmol) was also tested in the radioactive methylation activity assay. This was performed as described in B) with minor variations: The methylation efficiency of Dnmt1 (60 nM) was analyzed on non-methylated (panel 1-4), hemimethylated (panel 5-8) and methylated (panel 9-12) chromatin templates (200 ng). As positive control the AIR fragment was used (referred to as "c").

complex. The addition of the ATPase Brg1 solely enhanced the tritium incorporation marginally, again showing the highest effect on hemimethylated chromatin (~ 1.6 times in comparison to the catalytic activity without Brg1, panel 7). In the presence of both Brg1 and ATP, the methylation efficiency of Dnmt1 increased significantly on all three substrates. The most significant effect (~ 2.5 times higher) was observed on hemimethylated chromatin in comparison to the methylation efficiency without ATP (panel 8).

In contrast to the experiments with ACF, I observed that the methylation efficiency on hemimethylated DNA was generally higher in the presence of both Brg1 and ATP (compare Fig. 39B panel 9 with 39C panel 8). This could be the consequence of the different chromatin remodeling mechanisms used by Brg1 and ACF1.

Thus, DNA methylation in the context of chromatin arrays is enhanced in the presence of ACF and Brg1 in an ATP-dependent manner. Furthermore this suggests that chromatin remodeling could play a crucial role in the process of DNA methylation within nucleosomes. Finally these findings suggest that DNA methylation is more efficient in a dynamic chromatin system.

5. Binding properties on mononucleosomes in the presence of the chromatin remodeling enzyme Snf2H

The presented bisulfite sequencing data demonstrate that the catalytic activity of Dnmt1 is inhibited by the first level of chromatin compaction, the mononucleosome. CpG sites within the nucleosomal core are refractory to methylation by Dnmt1. Due to this fact it becomes apparent that DNA methyltransferases require additional factors to gain access to their target CpG sites within the nucleosome core. My previous analyses of the methylation activity of Dnmt1 in chromatin arrays showed that remodeling enzymes are required for an efficient DNA methylation in chromatin in an ATP-dependent manner. To shed a light on the question whether chromatin remodeling factors, modify the binding characteristics of Dnmt1, binding studies on mononucleosomes in the presence of Snf2H were conducted.

It has been previously reported that the binding efficiency of Dnmt1 to mononucleosomes is enhanced in the presence of the remodeling factor Snf2H (Robertson *et al.*, 2004). It was shown that this effect is ATP-independent. To address this question of Dnmt1 binding in the context of the optimal nucleosomal substrate (77-

WID-77), EMSAs were performed. In initial experiments I determined the amount of Snf2H that barely did not bind to the nucleosomes (Figure 40, marked with a star), in order to rule out a Snf2H triggered nucleosome translocation. Subsequently, Dnmt1 binding assays with or without Snf2H supplemented with or without ATP were performed as indicated in Figure 40. My results do not confirm an increased binding affinity of Dnmt1 to mononucleosomal substrates without ATP (Fig. 40, compare lanes 9 and 10 with 13 and 14). Regarding protein-nucleosome complex formation one might speculate that there is a marginal increase of Dnmt1 binding affinity caused by the presence of both ATP and Snf2H (lanes 17 and 18). Further investigations will be required to address this question.
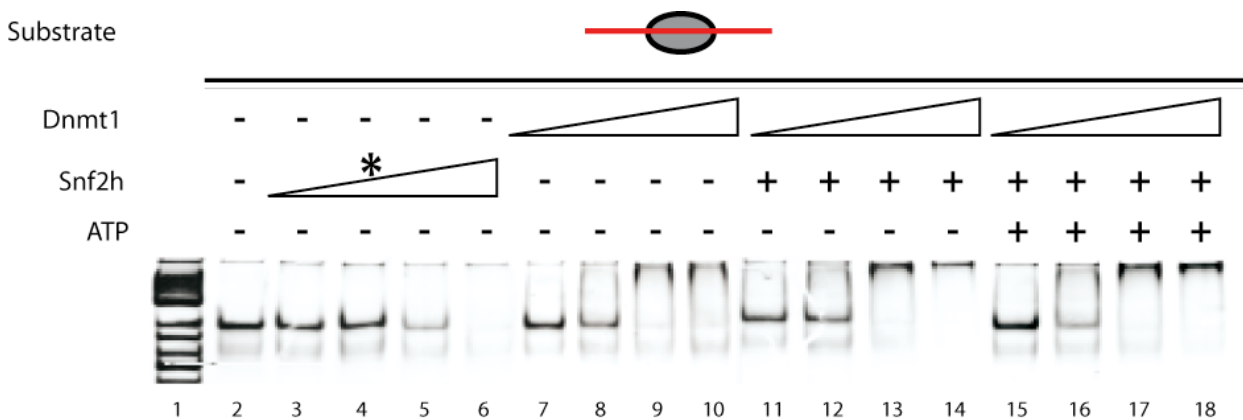
* = this Snf2h concentration has been used in reactions deposited in lanes 11 to 19

Figure 40. Analysis of the DNA binding characteristics of Dnmt1 in the presence of Snf2H
A) Electromobility shift assays were performed using the optimal Dnmt1 nucleosomal template as substrate (77-WID-77: lane 2, as described in the text). Mononucleosomes were incubated with the respective protein alone (Snf2H: lane 3-6, (30-120 nM); Dnmt1: lane 7-10, (50-150 nM)). To test the influence of Snf2H in the presence or absence of 1 μM ATP (as indicated) on the binding characteristics of Dnmt1, Snf2H (90 nM) was added to the reaction (absence of ATP: lane 11-14; presence of ATP: lane 15-18). The black star indicates the amount of Snf2H that was added to the reaction.

F. Discussion and Perspectives

I. Nucleosome positioning by chromatin remodeling complexes

The understanding of how nucleosome positions and dynamics regulate gene expression has increased enormously in recent years. Different studies provided evidence on the influences and mechanisms behind nucleosome positioning (see section B.II.3). In the course of my studies it became apparent that the positioning of nucleosomes is a multifactoral process. For example it had been demonstrated, that in a promoter region, nucleosomes frequently adopt specific positions (Sekinger *et al.*, 2005). Other studies suggest that the DNA sequence plays a major role in determining the nucleosome position (Ioshikhes *et al.*, 2006; Satchwell *et al.*, 1986; Segal *et al.*, 2006). Additionally, it has been shown that ATP-dependent chromatin remodeling complexes are in large parts involved in the direction of nucleosomes to specific positions (Cooper *et al.*, 1994; Weiss and Simpson, 1997), a result that we were especially interested in and which I followed up during my PhD. I could show that chromatin remodeling complexes establish distinct chromatin structures in the cell, providing a higher order regulatory level.

1. Do remodelers position nucleosomes in a sequence-dependent manner?

The pivotal question we asked was, for what reason does the cell possess such a variety of different remodeling complexes? Our working hypothesis was that these numerous remodeling complexes recognize distinct DNA-nucleoprotein signals that are then translated into a remodeler-specific chromatin structure. The suggestion that each individual chromatin remodeling enzyme posses a specific function is more likely than simply maintaining an unspecific dynamic and accessible chromatin, because of too high energetic costs for the cell.

To test this hypothesis I performed comparative chromatin remodeling assays by using different recombinant molecular motors (Brg1, Chd1, Mi-2, ISWI, Snf2H) and two recombinant complexes (ACF, NURF). The results of the nucleosome remodeling reaction on the rDNA promoter fragment as well as the *Hsp70* DNA fragment revealed, that every individual remodeling factor displays different nucleosome translocation properties (see Fig. 21A and B). Due to the fact that the nucleosomal substrates used here were the same for each protein, one can conclude that each individual remodeling

factor translates the recognized signals of the nucleosomal substrate differently. Consequently, each remodeling enzyme establishes its specific chromatin structure, visible as a specific nucleosome position in my assay. The *Hsp70 DNA* fragment (Hamiche *et al.*, 1999) is a more complex substrate compared to the rDNA promoter NPS. Due to the formation of five major nucleosome positions, I could bypass the reported DNA end effects with this DNA fragment. Studies have demonstrated that most SWI/SNF chromatin remodeling complexes, the yeast Isw1b and the NURF complex preferentially translocate the nucleosomes towards DNA ends (Hamiche *et al.*, 1999; Jaskelioff *et al.*, 2000; Kang *et al.*, 2002; Lorch *et al.*, 2001; Ramachandran *et al.*, 2003; Stockdale *et al.*, 2006; Aoyagi *et al.*, 2002a;Aoyagi *et al.*, 2002b; Flaus and Owen-Hughes, 2003b; Kassabov *et al.*, 2003).

My comparative nucleosome mobilization experiments using four different mononucleosomal templates have confirmed the results discussed above (see Fig. 25 A to C). With the exception of the 22-WID-22 DNA fragment, all fragments seem to be good substrates for chromatin remodeling enzymes. This suggests that the protruding DNA ends of 22 bp at both sites of the nucleosomal core seem to be below the minimal length required for catalysis of the remodeler. Interestingly, this phenomenon has been reported before (He *et al.*, 2006; Yang *et al.*, 2006; Zofall *et al.*, 2004; Gangaraju and Bartholomew, 2007a; Kagalwala *et al.*, 2004). All other 601-related DNA substrates showed a translocation of the nucleosomes to a more border position, while this effect was most pronounced for ISWI. Contrary, nucleosome mobilization using ACF did not show a significant effect. In summary, these results confirm our previous results on the *hsp70 DNA* and rDNA promoter fragment and further suggest that every single chromatin remodeling enzyme recognizes and translates the underlying DNA sequence and or structure differently into a distinct nucleosome positioning patter.

But which properties of the nucleosome remodeling complex direct this specific nucleosome positioning? In our study, the same molecular motor (ISWI) assembled with different additional protein subunits (ACF and NURF complex) resulted in different nucleosome positioning. This elucidates that the outcome of the reaction is dependent on the ATPase and the type of subunits that form a multiprotein complex. A previous study demonstrated that the biochemical function of a chromatin remodeling enzyme can be modified by the addition of protein subunits, e.g. the addition of hACF1 altered the remodeling pattern of Snf2H (Fan *et al.*, 2005a). Due to these results one can

assume that chromatin remodeling factors do translate the combination of DNA sequence and structural information differently, thereby establishing specific nucleosome positions. Of special interest are the DNA binding domains that could directly influence the DNA binding manner. My data suggest that different DNA binding domains could account for the direction of the nucleosome positioning. This is supported by the fact that the assembly of additional protein subunits to the ATPase changes the end position of the nucleosome. This can be nicely observed by comparing the results of the chromatin remodeling reactions catalyzed by ISWI and ACF. Another conceivable explanation for these significant differences could be that the assembly of additional subunits leads to intramolecular interactions, thereby changing the protein conformation. This could in turn modify the DNA binding properties of the protein due to the exposure or occlusion of DNA binding domains.

Therefore the DNA binding affinity of the separate binding domains should be tested in comparison to the complete complex. Sequences at which certain subunits bind tightly could result in pausing of the remodeling reaction and *vice versa* the remodeler could move nucleosomes away from the sequences that facilitate recruitment of the complex. In addition, sequence and structural features of the nucleosome could be responsible for the altered remodeler-nucleosome binding affinity. Future experiments are needed to elucidate the mechanisms behind this altered binding affinity and the possible enrichment of certain intermediates.

While monitoring the progression of the nucleosome mobilization reaction on the *hsp70* promoter fragment I could see that the nucleosome remodeling reaction seems to proceed in several sequential nucleosome positions, forming intermediate nucleosome positions until reaching their terminal position (see Fig. 21C). Interestingly, the adopted intermediate positions were predominantly the positions that had already been obtained in the initial chromatin reconstitution by salt gradient dialysis, due to a higher intrinsic histone-DNA affinity. This is an indication for a translocation from one stable nucleosome position to the next one during the process of chromatin remodeling and further suggest that the nucleosome position is at least in part determined by interactions of the histone octamer with the underlying DNA.

But to what extent is nucleosome positioning determined by the underlying sequence and how do additional factors influence the final nucleosome position? Numerous studies have addressed these questions and revealed the existence of specific

nucleosome positioning DNA sequences (NPS) (Ioshikhes *et al.*, 2006; Satchwell *et al.*, 1986; Segal *et al.*, 2006; Wang and Widom, 2005) (please see section B.II.3.1 for a detailed discription). The major outcome of these studies was that individually positioned nucleosomes seem to be much more frequent than initially expected (Albert *et al.*, 2007; Ozsolak *et al.*, 2007; Yuan *et al.*, 2005) The data suggest that NPSs are characterized by AA, TT and TA dinucleotides occurring every 10 bp. Additionally, a 10 bp periodicity of GC dinucleotides has been found, that is offset by 5 bp compared to the other dinucleotides. This periodical presence of dinucleotides provides a certain rotational setting: AA / TT extend the major groove, whereas GC contract the minor groove, what might facilitate DNA wrapping (Albert *et al.*, 2007; Field *et al.*, 2008; Mavrich *et al.*, 2008a; Mavrich *et al.*, 2008b). Despite of these findings, the presence of the reported dinucleotide patterns in an individual nucleosome only occurs modestly above a random distribution and is largely limited to the first nucleosome upstream of the 5' nucleosome free region (-1 nucleosome) and the first nucleosome downstream of the nucleosome free region (+1 nucleosome) (Mavrich *et al.*, 2008a; Segal *et al.*, 2006). Therefore, one can conclude that sequence dependent nucleosome positioning might only be a subtle force and positioning could involve a combination of these favorable positions and unfavorable nucleosome free regions. Further it has been suggested that additional factors are needed to establish specific nucleosome positions, which are observed *in vivo.*

With respect to my studies on DNA methylation in chromatin, I will briefly discuss the impact of DNA methylation on the positioning of nucleosomes. Several studies detected a strong link between CpG methylation and nucleosome positioning (Davey and Allan, 2003; Davey *et al.*, 2003). Though some results were conflicting, one can conclude that CpG methylation decreases the ability of DNA to bend into the major groove at the methylated CpG site, thereby influencing nucleosome positioning. Other studies have shown a decreased DNA bending flexibility (Nathan and Crothers, 2002) and a hindrance of forming bent structures mediated by CpG dinucleotides (Tippin and Sundaralingam, 1997). Additionally, a decreased nucleosome affinity was also detected (Pennings *et al.*, 2005). In summary, numerous studies suggest that CpG methylation can directly influence the DNA bendability and thereby nucleosome positioning. This reciprocal interaction between DNA methylation and nucleosome positioning is a very interesting fact, which implies that not only nucleosome positioning could influence the

accessibility of DNA methyltransferases to specific CpG sites but also points on the exclusion of histone octamers to adopt a CpG dinucleotide position. Moreover, this NFR could consequently be accessible for other chromatin associated factors such as methylated cytosine binding proteins (MBDs,MeCPs), HDACs, HMTs or transcription factors.

Despite of these observations it has been observed that nucleosomes are in general positioned, allowing access for transcription factors for proximal promoter regions (Sekinger *et al.*, 2005). TF binding sites in yeast were shown to be ~ 7 times more frequent situated in linker DNA sequences than in nucleosomal regions (Yuan *et al.*, 2005). High-resolution position mapping of nucleosomes containing the histone variant H2A.Z revealed that TF binding sites are most frequently found near the edges of nucleosome (Albert *et al.*, 2007).

Though many studies computationally predicted nucleosome positions based on the properties of the underlying DNA sequence and were valuable from a statistical perspective, they miss some important additional factors that contribute to the *in vivo* nucleosome position in the cell (Field *et al.*, 2008; Gupta *et al.*, 2008; Ioshikhes *et al.*, 2006; Mavrich *et al.*, 2008b; Peckham *et al.*, 2007; Segal *et al.*, 2006; Yuan and Liu, 2008).

Chromatin remodeling complexes seem to provide such a major factor that determines nucleosome positioning besides the underlying DNA sequence. This hypothesis is supported by my studies. I could show that although the same DNA substrate was utilized, the outcome of the chromatin remodeling reaction differed for each protein analyzed.

Different lines of evidence support this asumption. A good example is the nucleosome spacing controlled by chromatin remodelers. Interestingly, different complexes are capable to promote distinct repeat length. Yeast Isw1 and Isw2 complexes for example generate repeat length of about 175 bp and 200 bp (Tsukiyama *et al.*, 1999). Contrary, other complexes including the SWI/SNF subfamily and ISWI containing complexes alleviate regular spacing from chromatin *in vivo* (Guyon *et al.*, 2001; Schnitzler *et al.*, 2001; Tsukiyama *et al.*, 1995; Tsukiyama and Wu, 1995) Recent studies provided evidence that some remodeling complexes require a given length of protruding DNA to one or both sites of the nucleosome to be sufficiently active (Dang *et al.*, 2006;

Gangaraju and Bartholomew, 2007a; He *et al.*, 2006; Kagalwala *et al.*, 2004; Yang *et al.*, 2006; Zofall *et al.*, 2004). These characteristics could also account for the differences in recognizing DNA sequences as observed in my studies. Furthermore, one recent study analyzed how specific DNA sequence elements influence the nucleosome positions promoted by spacing remodeling complexes (Whitehouse and Tsukiyama, 2006). The authors showed that the yeast Isw2 remodeling complex repositions nucleosomes onto unfavorable DNA sequences to generate tightly packed, inaccessible nucleosomal arrays. In addition, the authors demonstrated, that upon deletion of Isw2 chromatin adopts a DNA directed nucleosome positioning based on dinucleotide rich elements that facilitate genomic access. Maier *et al.* demonstrated that ACF moves regularly positioned nucleosomes of 12 "601" NPSs away from this high affinity sites to a random end-position with respect to each 601 repeat (Maier *et al.*, 2008).

Further experiments have to be done to elucidate the mechanism that directs nucleosome positioning. For example it would be crucial to identify the responsible signals or features that are encoded by the DNA and direct individual remodelers to distinct nucleosome positions. This could be done by mapping the nucleosome positions via MNase digests of the nucleosomal DNA and subsequently determine the nucleosome boundaries by primer extension reactions. Afterwards it would be necessary to analyze the sequence and structural information of the underlying DNA to get an idea about some important DNA features and to find similarities and differences between positioning sequences. This could be done by *in silico* analysis to yield information on biophysical properties of the DNA, such as curvature, flexibility, dinucleotide content and bending ability. Additionally, it would be necessary to compare the nucleosome positioning abilities of various motor proteins on different nucleosome positioning sequences, determining their high combinatory diversity.

2. Is remodeler directed nucleosome positioning determined by the DNA?

Previous studies have shown that specific DNA sequences are capable to direct nucleosome positioning (Albert *et al.*, 2007; Ozsolak *et al.*, 2007; Yuan *et al.*, 2005). My data obtained by nucleosome mobility assays suggest that the diversity of chromatin remodeling complexes generates distinct nucleosome "patterns". To further analyze this phenomenon, I have tested the nucleosome positioning capability of a specific DNA fragment (see manuscript Fig. 3). For this assays the 248 bp rDNA fragment was used.

Firstly, gel permutation assays experimentally verified that the rDNA fragment contained an intrinsically curved DNA (see manuscript Fig. SI 7C). Interestingly, several previous studies could demonstrate that the rDNA promoter of different organisms exhibits a conserved sequence-dependent structure (Längst *et al.*, 1997; Marilley and Pasero, 1996). In nucleosome remodeling assays we observed that ACF moves the nucleosomes from border positions to two rationally spaced positions of the rDNA fragment (see manuscript Fig. SI 7A and 3A) (Längst *et al.*, 1999; Strohner *et al.*, 2005). The fact that we could find a strong correlation between ACF-dependent nucleosome positioning and the presence of an intrinsically curved region was an indication for a possible nucleosome positioning element. Additional evidence is provided by the close vicinity of the nucleosome dyad axis and the DNA curvature peak (see manuscript Fig. 3C and D). Our experiments using nucleosomal substrates that have been generated by cloning a 40 bp curved DNA fragment into a sequence-unspecific DNA environment, reveals a distinct nucleosome positioning by ISWI and ACF (see manuscript Fig. 3A). ISWI seems to recognize specific DNA features and does not simply move nucleosomes to the extremities of DNA (Längst and Becker, 2001b).

Contrary, I could demonstrate for ACF that a 40 bp highly curved sequence element is sufficient to direct nucleosome positioning, again with the dyad close to the highest DNA curvature peak, indicating that ACF-dependent nucleosome positioning could be directed by the features of the DNA structure (see manuscript Fig. 3a). I could exclude the possibility that this effect is only a consequence of the preference of ACF for sufficiently long (30 bp) protruding DNA by choosing an appropriate experimental design that fulfils the required conditions (Fig. 22C). The curved DNA fragment was sufficient to direct nucleosome positioning even to a border position closer to the DNA end (Fig. 22C, "K3-b" or "K3-c").

Numerous studies provide at least minor evidence for a sequence specificity of the different remodeling enzymes: Studies performed on linear DNA substrates harboring one or two positioned nucleosomes have demonstrated that the inherent sequence preference for remodeling enzymes was at least influenced by the effects of nearby DNA ends, the effect that we could bypass by our experimental design For example all analyzed SWI/SNF members tended to move nucleosomes towards the end (Aoyagi and Hayes, 2002; Aoyagi *et al.*, 2002; Flaus and Owen-Hughes, 2003b; Jaskelioff *et al.*, 2000; Kassabov *et al.*, 2003; Lorch *et al.*, 2001; Ramachandran *et al.*, 2003), whereas

most ISWI complexes catalyzed the mobilization away from the end (Corona *et al.*, 1999; Eberharter *et al.*, 2001; Hartlepp *et al.*, 2005; Langst *et al.*, 1999; Schwanbeck *et al.*, 2004; Stockdale *et al.*, 2006; Yang *et al.*, 2006). Interestingly, it has been described that remodelers moving nucleosomes away from DNA ends do not place them in the exact centers of the DNA, but appear to favor certain sequences (Flaus and Owen-Hughes, 2003a; Flaus and Owen-Hughes, 2003b; Gutierrez *et al.*, 2007b; Kassabov *et al.*, 2002b). In our study I examined the mononucleosome positioning on long linear DNA substrates (*Hsp70*) to reduce the effects of DNA ends on the positioning. Using this substrate we concluded that the observed distinct nucleosomal positioning, seems to be controlled by the underlying DNA sequence and not by the DNA ends. Another study eliminated these DNA end effect entirely by examining human SWI/SNF remodeling on three different circular mononucleosomal substrates (Sims *et al.*, 2007). Similarly to our results, hSWI/SNF moved the nucleosomes away from initially favored nucleosome positioning sequences in such a way that these sequences become the least well-occupied positions of the substrate. The authors observed instead that nucleosomes were rather localized to positions favored by the specific remodeling complex used in the assay. Furthermore, hSWI/SNF seems to translocate nucleosomes also onto sequences that posses some intrinsic affinity for the histone octamer, in addition to just simply direct according to the enzym's own intrinsic sequence preferences (Sims *et al.*, 2007). These results are consistent with our observations and together they suggest that although the intermediate nucleosome positions clearly exhibits some histone octamer-DNA interaction, there is clearly some degree of sequence directed nucleosome positioning by chromatin remodeling enzymes. In summary my data show that at least some remodeling complexes, such as ACF are able to recognize the underlying DNA sequence and move nucleosomes to favored positions of the complex, which can differ, from the nucleosome positioning sequence.

Following the identification of specific DNA sequence elements that show a high positioning potential for the different motor proteins, it would be interesting to analyze the binding affinity of the remodeling enzymes. This could be addressed by the design of artificial DNA substrates on the basis of this nucleosome positioning sequence information in order to identify DNA features that direct nucleosome positioning. It is possible that the observed differences in the positioning potential are due to topological reasons, directing nucleosome translocations. Our laboratory could previously show that

chromatin remodeling enzymes can bind nucleosomes symmetrically or asymmetrically, like ACF that binds in a symmetrical manner, whereas the ISWI motor binds asymmetrically to nucleosomes (Längst and Becker, 2001b; Strohner *et al.*, 2005). Therefore DNaseI footprinting studies could give high resolution insight into the topology of the enzyme-nuclesome complex.

3. How can remodeler dependent nucleosome positioning be explained?

As desdibed above, we now know that the end product (nucleosome position) of the remodeling reaction is at least dependent on two factors: The type of chromatin remodeling enzyme with or without its additional subunits and the underlying DNA sequence. We proposed two theoretical kinetic models to explain the mechanisms of the nucleosome positioning reaction: the "arrest model" and the "release model" (see Fig. 23B). Generally, both models dissect the remodeling reaction in different steps and are based on changes in the binding affinity of the remodeling enzyme to the specific nucleosome position. My EMSA experiments revealed that the nucleosome movement proceeds by positions that show an intrinsic nucleosome affinity (see Fig. 21C). These data suggest that chromatin remodeling enzymes pass over high affinity nucleosome positioning sequences and rather establish sequence-independent positions. The observed effect cannot be explained by the underlying sequence or conformation of DNA, but is more likely determined by specific remodeling factors itself. Furthermore, this cannot be explained by the means of affinity, since the enzymes would simply catalyze the transfer to the highest and thereby most favorable affinity binding site, positioning all nucleosomes to the same end position. EMSAs with heterogeneous nucleosome positions provide evidences for ACF and Chd1 to follow the "release model" (see Fig. 24A and B) In analogy to the process of "transcription termination", during which specific sequence termination elements disrupt the binding of the RNA polymerase to its DNA substrate and therefore stop elongation, the binding affinity of the remodeler is reduced according to this model (Greive and von Hippel, 2005; von Hippel and Yager, 1992).

I could demonstrate for the two tested DNA substrates that the analyzed remodelers have weaker binding affinities to those nucleosome position to which the nucleosomes are finally translocated in the remodeling reaction (compare Fig. 21A and B with Fig. 24A and B). In accordance with the study of Sims *et al.* (Sims *et al.*, 2007) it can be

concluded that the different remodeling enzymes recognize the underlying DNA sequence and move nucleosomes to positions that are preferred by the respective remodeler. Interestingly the position can differ from the strongest nucleosome positioning sequence. The nucleosome is translocated away from initially favored NPSs to new positions preferred by the enzyme. These adopted positions are characterized by some intrinsic affinity for the histone octamer. Therefore one could speculate that each remodeler might possess low sequence preference.

My experiments have all been performed *in vitro*. Different lines of evidence suggest that nucleosome positioning by chromatin remodeling enzymes plays a major role *in vivo*. My results suggest that different remodeling enzymes could be targeted to specific genomic loci. The fact that functional TF binding sites are much more frequently found in linker regions compared to DNA covered by nucleosomes and that TSS are often devoid of nucleosomes suggest that promoter DNA sequences regulate transcription by arranging nucleosome positioning sequences according to TF binding site (Albert *et al.*, 2007; Allan *et al.*, 1980a; Narlikar *et al.*, 2007; Ozsolak *et al.*, 2007; Segal *et al.*, 2006; Yuan *et al.*, 2005).

Though regulatory regions of eukaryotic genes were shown to be organized by specifically positioned nucleosomes (Grunstein, 1990; Simpson, 1990; Simpson, 1991), it has been suggested that additional factors are required to establishment of NFRs and nucleosome positioning (Bernstein *et al.*, 2004; Li *et al.*, 1997).

 It was demonstrated that DNA sequences, that had been shown to position nucleosomes *in vitro* failed to do so *in vivo* (Li *et al.*, 1997) : For example the yeast Isw2 remodeling complex overrides the sequence preferences of nucleosomes, causing nucleosomes to move into the 5' and 3' NFR resulting in transcriptional repression (Whitehouse *et al.*, 2007; Whitehouse and Tsukiyama, 2006). Also in yeast, the α2-MCM1 complex seems to actively position nucleosomes at repressed genes. (Clapier *et al.*, 2001; Roth *et al.*, 1990; Shimizu *et al.*, 1991). The yeast *RNR3* gene requires precise nucleosome positioning by the Isw2 chromatin complex for transcriptional repression (Cooper *et al.*, 1994; Fleming and Pennings, 2001; Kastaniotis *et al.*, 2000; Li and Reese, 2001; Weiss and Simpson, 1997).

Interestingly, active and silent rDNA copies are characterized by distinct epigenetic marks as well as by different nucleosome positions. It was observed, that the rDNA

associated remodeling complex NoRC induces nucleosome movement of 25 bp, both *in vivo* and *in vitro* (Li *et al.*, 2006). In respect to silent rDNA copies, NoRC is the remodeling complex that moves the promoter bound nucleosome into the silent position. This results in placing the UBF binding site and the functionally important CpG residue into one region.

A recent study analyzed the relationship between CpG islands, nucleosome remodeling and nucleosome stability during inducible gene transcription (Ramirez-Carrozzi *et al.*, 2009). The authors discovered for the first time that specific genes displaying a high CpG dinucleotide degree are not associated with chromatin remodeling enzymes, whereas other genes lacking CpG sites are associated with SWI/SNF remodeling complexes. Characteristic properties of mammalian promoters are the presence of CpG islands (70 % of mammalian promoters) (Davuluri *et al.*, 2001), a low nucleosome occupancy (Yuan *et al.*, 2005) and preassociation of RNA polymerase II with inactive genes (Gilmour and Lis, 1986; Krumm *et al.*, 1992). The authors depleted Brg1 and Brm simultaneously in macrophages and revealed that only a subset of Toll-like receptor 4 (TLR4) induced genes requires SWI/SNF for regulation (Ramirez-Carrozzi *et al.*, 2009). Secondary response genes exhibited strong SWI/SNF dependence, whereas primary response genes could be divided into SWI/SNF dependent and independent regulatable genes. Interestingly, promoters of the SWI/SNF-dependent group exhibited inducible nuclease accessibility and inducible association of Brg1, whereas the independent ones were permanently accessible for nucleases. Although CpG-island promoters do not functionally require SWI/SNF complexes it was discovered that these are constitutively associated with Brg1 (Ramirez-Carrozzi *et al.*, 2006). The authors suggest that the high CpG content of SWI/SNF independent genes contributes to nucleosome instability. Contrary, SWI/SNF dependent genes lacked CpG-islands and assembled into stable nucleosomes (Ramirez-Carrozzi *et al.*, 2009). In respect to our study, these are interesting results. It is conceivable that SWI/SNF remodelers could recognize specific signals that are encoded in the underlying DNA sequence, thereby recruiting them to SWI/SNF dependent-genes, whereas they are kept away from CpG less genes due to the nucleosome instability. The exact functional role of SWI/SNF complexes in this process remains to be identified.

In vivo additional factors, which are present in chromatin, could influence the intrinsic sequence specificity of remodelers and thereby the outcome of chromatin remodeling

reaction. Furthermore, the end-product of the remodeler-specific nucleosome position could be a combination of the DNA sequence, the remodeler and also transcription factors, histone tail modifications variant core histones and chromatin proteins such as linker histone H1, HP1 and HMGs. It was demonstrated that remodeling complexes make use of sequence-specific DNA binding factors to establish preferred nucleosome positions (Kang *et al.*, 2002; Pazin *et al.*, 1997; Pazin and Kadonaga, 1997). Additionally it was shown that histone H1 reverses the intrinsic preference of hSWI/SNF to move nucleosomes towards DNA ends, instead repositions nucleosomes away from ends (Ramachandran *et al.*, 2003). Interestingly, other studies also demonstrated that some chromatin associated factors such as H2A variants macroH2A or yeast H2A.Z might also block remodeler-mediated nucleosome repositioning (Li *et al.*, 2005). Tom Owen-Hughes and coworker showed recently, that histone acetylation had regulating influence on the type and rate of remodeling by Isw2, Chd1, RSC complexes (Ferreira *et al.*, 2007a).

In conclusion the goal of this project was to elucidate the chromatin remodeler directed nucleosome positioning focusing on the underlying DNA sequence. To date it is unclear to which extend nucleosome positions are determined by histone-DNA interactions or mediated by chromatin remodeling activities.

By comparing the molecular mechanisms of different chromatin remodeling enzymes I could demonstrate that each tested remodeling enzyme possesses distinct nucleosome translocation properties. I could show that nucleosome positioning by two specific motor proteins is determined by a reduced affinity of the remodeling enzyme to the end product of the reaction. In summary, this study provides evidence that the end product of the remodeling reaction is determined by a combination of the underlying DNA sequence and the presence of additional protein subunits.

The identification of remodeler and DNA sequence/structure mediated nucleosome positioning suggests the existence of a "remodeler-dependent nucleosome positioning code". This process could establish a remodeler-specific chromatin structures at specific genomic loci. With respect to DNA dependent processes such as DNA methylation this might be an important regulatory process. One could image the following sequential order: A specific chromatin remodeling complex like NoRC could be targeted by specific DNA-based features and/or the recruitment by additional proteins to a genomic locus, e.g. the rDNA promoter. The remodeler-specific translation could then lead to the

establishment of new nucleosome positions, which in turn would allow DNA methyltransferases like Dnmt1 and Dnmt3a to gain access to their target sites.

In conclusion my results provide evidence for a new model of transcriptional control by the combined action of DNA sequences and chromatin remodeling complexes. Future research will have to elucidate the complex mechanisms of this combined regulation.

II. CHARACTERIZATION OF DNMT1 IN THE CONTEXT OF CHROMATIN

For several years the basic enzymatic mechanisms and functions of DNA methyltransferases have now been studied *in vitro* with purified enzymes (Bestor and Verdine, 1994; Cheng and Roberts, 2001). However, although the physiological DNA substrate of eukaryotic cells is packaged into chromatin, most of these assays have been carried out on free DNA substrates and DNA sequences that are not found in nature. Much less is known about the mechanism of DNA methylation within chromatin. Studies that did address this question obtained quite conflicting results (Gowher *et al.*, 2005b; Okuwaki and Verreault, 2004; Robertson *et al.*, 2004; Takeshima *et al.*, 2006; Takeshima *et al.*, 2008). Hence, to clarify the influence of chromatin on DNA methylation, I analyzed the DNA binding and enzymatic properties of Dnmt1 under these conditions. Additionally, I examined the impact of chromatin remodeling "machineries" on DNA methylation,

1. What are the DNA and nucleosome binding properties of Dnmt1?

To elucidate the binding properties of Dnmt1 on free DNA, I performed EMSAs using a low range DNA marker as substrate. The initial experiments on short free DNA fragments suggested that Dnmt1 preferentially binds to longer DNA substrates (> 35 bp) (see Fig. 26A). To narrow down these results, binding assays on fluorescently labeled hybridized oligonucleotide fragments of different length (15 to 60 bp) have been carried out. This method allows the direct comparison of different DNA substrates in competition. By choosing different fluorophores with distinct excitation and emission spectra, simultaneous substrate binding analysis were possible (Fig. 26B and C).

Quantification of the fractions that were not bound by Dnmt1 suggested that Dnmt1 requires a minimal binding length of ~ 45 to 60 bp for efficient DNA binding and discriminates shorter fragments (see Figure 26D). This binding affinity of Dnmt1 for

longer DNA substrates either suggests a cooperative binding mechanism or a DNA recognition/-binding domain that requires long DNA substrates. Recent studies on Dnmt3a showed an oligomerization for the isolated carboxyterminal domain of murine Dnmt3a on DNA (Jia *et al.*, 2007). Furthermore the C-terminal domain of Dnmt3a has been described to partially bind to DNA > 20 bp when bound in association with several Dnmt3a molecules (Jia *et al.*, 2007). These differences could be due to alterations in DNA binding characteristics mediated by the N-terminal regulatory domain. Both, DNA binding and allosteric control of the methyltransferase have been reported to be located in the N-terminal domain (Bacolla *et al.*, 2001; Bacolla *et al.*, 1999; Fatemi *et al.*, 2001).

Interestingly, my binding assays now reveal a narrow range of Dnmt1 concentrations that causes the probe to shift from unbound to completely bound, suggesting a cooperative binding mechanism (see Fig. 26B). This interpretation is supported by a recent publication determining Hill values to biochemically characterize the binding of Dnmt1 to DNA (Robertson *et al.*, 2004). The Hill equation describes the fraction of a macromolecule saturated by a ligand as a function of the ligand concentration and can be further used to determine the degree of cooperativity of ligand-enzyme binding (Hill and Flack, 1910). In accordance with our results, Robertson and coworkers calculated Hill plots with straight lines characterized by slopes > 1, indicating that Dnmt1 binds cooperatively to DNA (Robertson *et al.*, 2004).

Dnmt1 bears at least two separate DNA binding sites, one in the N-terminal and one in the C-terminal domain (Araujo *et al.*, 2001; Fatemi *et al.*, 2001; Flynn and Reich, 1998). The enzyme can interact with its target DNA and additionally with a second DNA molecule that functions as an allosteric regulator. The prominent N-terminal CXXC zinc finger motif of Dnmt1 has been reported as being essential for allosteric acivation of the catalytic domain of Dnmt1 (Fatemi *et al.*, 2001). Despite of this finding, recent data demonstrates that this domain is dispensable for the intramolecular N-C-terminal interaction (Fellinger *et al.*, 2009), but is instead important for DNA binding. It is therefore possible that intramolecular interactions between different domains change the binding property of Dnmt1 to DNA.

To further elucidate the binding properties of Dnmt1 on chromatin, I performed EMSAs on mononucleosomal substrates (see Fig. 28A to C).

A key aspect of this study was the analysis of different effects of DNA overhang lengths from the nucleosome core on the binding ability of Dnmt1. Therefore the well-defined 601 nucleosome positioning sequence (Lowary and Widom, 1998) was used to generate substrates that harbored a symmetrical or an unsymmetrical overhang from the nucleosome ends (15 bp, 22bp, 40 bp, 60s bp, 77 bp). For this comparative analysis I adjusted the amounts of free DNA and mononucleosomes to the intensity of EtBr intercalation, since intercalation scales differently between free DNA and the more condensed nucleosomal DNA. Like this it was possible to draw conclusions on differences in binding affinities between free DNA and nucleosomal DNA based on quantitative changes. Using this technique I could demonstrate that a minimal binding length of 30-80 bp of protruding DNA is needed for efficient binding of Dnmt1 to nucleosomes (see Fig. 28C and 29C). Furthermore binding to nucleosomes occurs preferentially on "symmetrical" nucleosomes harboring DNA overhangs on both sites (entry and exit site) of the nucleosome. The observed differences of binding between symmetric and asymmetric nucleosomes regarding DNA overhangs could be the consequence of different binding mechanisms. Furthermore it can be speculated that symmetrical flanking DNA just provides the 2-fold amount of binding sites or alternatively that DNA in direct contact to the entry and exit sites of the mononucleosome is preferentially bound. I could address this question by comparing a symmetrical substrate, harboring 40 bp of DNA overhang at both sites of the nucleosome with an asymmetrical nucleosome with 77 bp flanking DNA on only one side (data not shown). The results revealed that Dnmt1 preferred the symmetrical substrate over the asymmetrical one. This argues for the preferred binding of symmetrical nucleosomes due to specific DNA structures. The presence of DNA overhangs seems to enhance the interaction between Dnmt1 and the nucleosome. This characteristic has been described for various remodeling proteins before: Although SWI/SNF complexes bind to core mononucleosomes with little flanking DNA, flanking DNA is important for the ISWI protein to bind to mononucleosomes (Aalfs *et al.*, 2001; Kagalwala *et al.*, 2004; Strohner *et al.*, 2005; Whitehouse *et al.*, 2003). Longer nucleosomal DNA overhangs have also been reported to be essential for Snf2H to form a stable protein-nucleosome interaction (He *et al.*, 2006).

The putative optimal nucleosomal substrate for Dnmt1 binding in my study harbors 77 protruding basepairs on both sites of the nucleosome (77-WID-77; see Fig. 29A). This

suggests that the length of protruding DNA affects the binding productivity of Dnmt1 to DNA/nucleosomes and could also be important for an efficient methylation activity. The appearance of several retarded bands (Fig. 29A) suggests that multiple Dnmt1 molecules associate with the substrate to form a stable Dnmt1-nucleosome complex (see Fig. 29A). The narrowness of the range of Dnmt1 concentration within which the substrate shifted from not being bound to completely being bound by the methyltransferase, again indicates a cooperative binding mechanism to nucleosomes. The Hill plot data by Robertson *et al.* also suggest a cooperative binding manner of Dnmt1 to both, their 208 bp fragment from the sea urchin 5S ribosomal DNA in its free as well as in its nucleosomal form (Robertson *et al.*, 2004). Interestingly, in this study it was observed that Dnmt1 binds mononucleosomes with approximately the same affinity as free DNA. The discrepancy to my results could be due to a different DNA sequence analyzed in their EMSAs. They used the well-characterized 208 bp 5S rDNA NPS (Flaus *et al.*, 1996; Nilsen *et al.*, 2002; Tse *et al.*, 1998; Ura *et al.*, 1995) that is in contrast to the 601 DNA a physiologically relevant DNA methylation target sequence (Bird, 1978; Bird and Southern, 1978; Bird and Taggart, 1980; Grummt and Pikaard, 2003). The different DNA conformation could account for the conflicting results obtained by us.

I could further see that the addition of a DNA competitor of unspecific sequence to my Dnmt1 binding reaction dispersed the protein-mononucleosome complex (see Fig. 29B). Upon addition of competitor DNA the shorter nucleosomal DNA substrate is released and Dnmt1 forms a complex with the longer competitor plasmid DNA. Furthermore, time course experiments revealed that the dissociation of Dnmt1 from the nucleosomal substrate is a highly dynamic process (data not shown).

In contrast to my results for Dnmt1, a study analyzing the binding characteristics of Dnmt3a and Dnmt3b on different nucleosomal substrates obtained different results (Takeshima *et al.*, 2006). The authors observed that Dnmt3a binds equally well to nucleosomes regardless of the presence or absence of protruding DNA, whereas Dnmt3b does not bind nucleosomes without DNA overhangs. Their data for Dnmt3b are consistent with our data for Dnmt1 and suggest different binding mechanisms of these enzymes to nucleosomal DNA (Takeshima *et al.*, 2006).

My Dnmt1 DNA binding results on free DNA fragments are in accordance with my observations of Dnmt1 binding on nucleosomal substrates; together they suggest that

Dnmt1 needs at least a DNA substrate of 30-80 bp or alternatively symmetrical nucleosomal DNA overhangs of the same length for a strong interaction. I could confirm a cooperative binding mode of Dnmt1 for both DNA conformations, free DNA and nucleosomes. To further analyze the binding properties of Dnmt1, different approaches can be followed. Due to the maintenance methyltransferase activity of Dnmt1, it would be important to monitor the binding affinities of Dnmt1 on hemimethylated substrates of different length, DNA sequences and conformations (e.g. hairpin structure). It would be interesting to determine the K_M values in order to determine the ability of Dnmt1 to bind to different substrates. Moreover it would be attractive to monitor the binding properties of the isolated DNA binding domains or their mutants. One study addressed this question using the isolated catalytic domains of Dnmt3a and Dnmt1 (Gowher *et al.*, 2005b). The authors detect only a weak affinity of this domain to mononucleosomes in contrast to the full-length Dnmt3a / Dnmt1. This suggests that the N-terminal domain could play a critical role in nucleosome binding (Gowher *et al.*, 2005a). For other chromatin associated proteins, such as MENT, a cooperative binding was also shown (Springhetti *et al.*, 2003). This phenomenon of cooperativity could account for the appearance of "methylation spreading" and the aberrant de novo methylation of CpG islands that is often observed in tumor cells (Graff *et al.*, 1997).

2. Where does Dnmt1 bind on a nucleosome?

My results presented above have shown that Dnmt1 needs protruding DNA for stable binding to nucleosomes. However, whether binding occurs exclusively through contacts to free DNA or also through nucleosomal contacts had to be determined. In this context DNaseI protection assays gave precise information about the target sites of Dnmt1 at the 77-WID-77 mononucleosomal substrate. Presumably, Dnmt1 might need the interaction with both, protruding DNA and the core nucleosome, since it showed no affinity to the core nucleosome alone.

The comparison of the cleavage patterns for free and nucleosomal DNA revealed a protected region corresponding to the nucleosome positioning sequence (~ 80 to 230 bp) (see Fig. 31C). My results of the DNaseI footprinting assays imply that Dnmt1 interacts with overhanging DNA and nucleosomal DNA (see Fig. 33C).

The protected sites between 40 – 80 bp on both sites of the nucleosome indicate that Dnmt1 might bind ~ 40 bp of free DNA, a symmetric region surrounding the nucleosome

dyad. To precisely characterize the target sites of Dnmt1 it would be important to analyze the binding behavior of Dnmt1 on hemimethylated naked DNA substrates in comparison to nucleosomal DNA. Footprinting Dnmt1 onto hemimethylated DNA or nucleosomes would give detailed insight whether Dnmt1 needs to contact the DNA beyond the target CpG site. In order to study the interaction between Dnmt1 and its nucleosomal substrate cryo-electron microscopy studies would by a desirable complementing approach.

In conclusion, the EMSAs on DNA in free and nucleosomal form have shown, that Dnmt1 requires DNA overhangs to stably interact with mononucleosomes.

3. Does Dnmt1 methylate DNA within the nucleosome core region?

My results have demonstrated that Dnmt1 is able to bind to nucleosomal DNA only if the DNA is equipped with DNA protrusions. To further determine whether this basic repeating unit of chromatin is accessible to Dnmt1, I mapped the methylation sites in the 342 bp nucleosome, harboring the 601 nucleosome positioning sequence flanked by CpG less flanking sequences (Fig. 34 D and E). The bisulfite sequencing data clearly revealed that the enzymatic activity of Dnmt1 is inhibited within the nucleosome core region, leaving only the linker regions for Dnmt1 mediated methylation. This effect was more distinct for the sense-strand than the antisense-strand. Whereas the methylation activity decreased to 0 % for the sense strand there was a marginal catalytic activity for single CpG sites within the antisense strand. This difference could probably be due to discrepancies in the DNA conformation. It seems likely that DNA conformational flexibility, which varies along nucleosomal DNA, could also have an impact on base flipping of the target cytosine (Davey *et al.*, 2002; Nilsen *et al.*, 2002). Other enzymes that gain access to their target sites by base flipping are the DNA glycosylases. For two of them a severe inhibition by nucleosomal core particles has been shown (Beard *et al.*, 2002; Nilsen *et al.*, 2002). However it is not known whether base flipping is involved in inhibiting these factors within nucleosomes. Additionally, the path of DNA helix around the histone octamer has been shown to be dependent on the local DNA sequence (Richmond and Davey, 2003). This effect could influence the enzymatic activity of DNA methyltransferases. Furthermore, by mapping of methylation sites in the sense and antisense strand I could show that Dnmt1 methylates specific CpG sites more efficiently even in free DNA substrates. In the sense strand CpG 6, 12, 18, 23 have barely been

methylated and the same phenomenon could be observed for CpG 20, 22 in the antisense strand (though less pronounced). This may reflect the effect of the local DNA conformation rather than the linear DNA sequence, due to the relative sequence non-specificity of Dnmt1. Additionally; I could observe that the enzymatic activity of Dnmt1 escalated abruptly in the border region, near the nucleosome edge. It can be imagined that for CpG sites located near the edge of the nucleosome, the probability of site exposure by spontaneous transient dissociation is higher than within central sites of the nucleosome (Anderson *et al.*, 2002; Polach and Widom, 1995).

Another *in vitro* study obtained slightly different results: though Dnmt1 was inhibited in the context of chromatin, it still posses the ability to modify CpG dinucleotides on the surface of nucleosomes (Okuwaki and Verreault, 2004). Interestingly, the activity was highly dependent on the nature of the DNA substrate. CpG sites on the surface of 5 S rRNA gene or H19 promoter were methylated efficiently, whereas nucleosomes containing the *Air* promoter were refractory to methylation. This discrepancy in the methylation of equivalent positions in the *H19* and *Air* nucleosome core particle could be the consequence of the above mentioned sequence dependent variations in local DNA structure and/or conformational flexibility (Okuwaki and Verreault, 2004). To further analyze this hypothesis, it would be important to analyze natural DNA sequences and to compare their competence on methylation efficiency.

My Dnmt1 activity assays using different substrates of free DNA and nucleosomal DNA with or without extruding DNA revealed that Dnmt1 requires protruding DNA to exhibit an efficient methylation activity (see Fig. 35C). The fact that Dnmt1 barely methylates the 147 bp nucleosome substrate without DNA overhangs suggests that Dnmt1 needs linker DNA for an efficient methylation activity. In accordance with my EMSA data this reduced methylation activity suggest to be the consequence of a reduced binding affinity to nucleosomes without protruding DNA. The obtained results coincide with the bisulfite sequencing data and have revealed that Dnmt1 activity is inhibited within the nucleosomal core region and needs symmetrical DNA overhangs for an efficient methylation.

The experiments of Robertson *et al.* determined the kinetics of Dnmt1: The $K_M^{(CG)}$ value on mononucleosomes was 12-fold higher than that on free DNA (Robertson *et al.*, 2004). This could reflect the hindrance of CpG sites that are partially occluded by histones. In this study, Dnmt1 was also less catalytic efficient on mononucleosomes

than on free DNA (Robertson *et al.*, 2004), what again is consistent with our results and also with the data of Okuwaki and coworkers (Okuwaki and Verreault, 2004).

An interesting candidate protein for future Dnmt1 studies in the context of chromatin is histone H1. A recent study examined the methylation activities of Dnmt3a towards the nucleosome core region and linker DNA using oligonucleosomes, focusing especially on the effect of linker histone H1 (Takeshima *et al.*, 2008). As I could demonstrate for Dnmt1, Dnmt3a was shown to scarily methylate DNA in the nucleosome core region and preferentially methylates the adjacent linker DNA (Takeshima *et al.*, 2006). Interestingly, Dnmt3a methylation activity was higher towards oligonucleosomes depleted of histone H1 than those supplemented with H1. Both, DNA methylation and binding of histone H1 are signs of transcription inhibition *in vitro (Bird, 2002)* (Bouvet *et al.*, 1994; Schlissel and Brown, 1984; Zlatanova *et al.*, 2000). Therefore one can suggest that the binding of histone H1 could result in the decrease of DNA methylation *in vivo.* However, studies depleting histone H1 partially in different organisms did not show a global effect on DNA methylation or gene transcription, but rather showed local consequences for gene expression and DNA methylation *in vivo* (Barra *et al.*, 2000; Fan *et al.*, 2005c; Shen and Gorovsky, 1996; Wierzbicki and Jerzmanowski, 2005). Taken together, these studies indicate that histone H1 contributes to the regulation of DNA methylation of specific regions, either by increasing or by decreasing the methylation level.

In this context it would be very interesting to compare Dnmt1 mediated methylation activity on nucleosomal DNA in the presence of histone H1. Further experiments could then test for enzymatic activity of Dnmt1 when the reactions are supplemented with chromatin remodeling complexes.

4. Are chromatin dynamics required for Dnmt1 activity in chromatin?

To study the ability of Dnmt1 to preserve DNA methylation patterns in chromatin, hemimethylated DNA has been generated. The final method of use is based on the hybridization of unmethylated and methylated DNA and therefore produces a heterogeneous mixture of methylated products with a major proportion of hemimethylated DNA. Restriction endonuclease digests on the one hand and incorporation of radioactive CH_3-groups on the other hand have confirmed the heterogeneity of the generated products (see Fig. 37B and C).

Time-kinetic studies have verified the efficient generation of hemimethylated DNA: Dnmt1 activity on the mixed substrate (i.e. mixture of unmethylated and methylated DNA) remains at a low level (Fig. 38D). The low activity of Dnmt1 on un-and fully methylated DNA suggests that these substrates could have an inhibitory effect on the enzymatic activity. In contrast Dnmt1 shows efficient methylation activity on the corresponding hemimethylated substrate (i.e. hybridization of unmethylated and methylated DNA). The increase of activity within the first two hours of the experiment could be due to allosteric activation of Dnmt1 by methylated CpG sites (Bacolla *et al.*, 1999). The observed inhibition after two hours could be due to an accumulation of homocysteine, leading to a competitive product inhibition (Yokochi and Robertson, 2002; Yokochi and Robertson, 2004). Different studies have shown that Dnmt1 is subject to both allosteric activation and competitative product inhibition by methylated DNA (Bacolla *et al.*, 1999; Fatemi *et al.*, 2001; Yokochi and Robertson, 2002). It has been shown that the methylated cytosine is a more potent activator than inhibitor (Bacolla *et al.*, 1999). N-terminal parts of the enzyme interact with the C-terminal domain, inducing the activation of Dnmt1 due to a conformational change (Fatemi *et al.*, 2001; Margot *et al.*, 2003). Additionally, unmethylated substrates have been demonstrated to repress the enzyme activity of Dnmt1, what argues for a substrate inhibition (Flynn and Reich, 1998). These results highlight the complexity of enzymatic events and clearly show that the outcome is dependent on various factors. Hence, it would be interesting to analyze how these complicated effects depend on the sequence and methylation state of the DNA bound to the allosteric and catalytic sites. According to the data cited above, Dnmt1 could be inhibited by the accumulation of methylated CpG dinucleotides and/or the activity of the enzyme could be repressed by unmethylated substrates.

I could reproduce the reported preference of Dnmt1 for hemimethylated CpG sites *in vitro* (Hitt *et al.*, 1988; Pradhan and Esteve, 2003b) (Bestor and Ingram, 1983). The published preference of Dnmt1 for hemimethylated oligonucleotide substrates of different length and sequences ranged from 2 to 200-fold depending on the study (Fatemi *et al.*, 2001; Flynn *et al.*, 1996; Goyal *et al.*, 2006; Tollefsbol and Hutchison, 1997; Tollefsbol and Hutchison, 1995). In my experiments the methylation activity of Dnmt1 has been about 3.5 times higher on hemimethylated compared to unmethylated linear substrates (see Figure 38A). In previous assays using unmethylated and

hemimethylated short AIR-DNA fragments I could observe a 10-fold increase of Dnmt1 mediated methylation efficiency (Anna Schrader, diploma thesis). The lower increase of methylation activity observed in the present study could be due to the heterogeneity of the substrates.

In further studies, I have determined the catalytic activity of Dnmt1 on chromatin arrays both in the absence and presence of ATP-dependent chromatin remodeling activities (ACF, Brg1) (see Figure 39B and C). The assembly method via salt gradient dialysis (Rhodes and Laskey, 1989) (Längst *et al.*, 1999) generates a pure chromatin system of highly compacted nucleosomes with a regular spacing of ~ 160 bp (Fig. 39A). My previous data revealed that the methylation activity of Dnmt1 on chromatin generally decreases in comparison to naked DNA substrates. The reported preference of Dnmt1 for hemimethylated free DNA has also been confirmed for hemimethylated chromatinized DNA. Using my set-up the methylation activity of Dnmt1 increases roughly 2-fold comparing hemimethylated chromatinized DNA to unmethylated one (Anna Schrader, diploma thesis).

The efficiency of DNA methylation by Dnmt1 increases significantly in the presence of chromatin remodeling activity and ATP as tested with ACF and Brg1 (see Fig. 39B and C). In the non-dynamic chromatin system (the absence of both remodeler and ATP) a basal enzymatic activity of Dnmt1 in chromatin has been observed. This could be due to methylation in the linker regions. Other data of mine shows that in comparison to the dense chromatin confirmation derived from *Drosophila* embryo extract, the chromatin assembled via salt gradient dialysis harbors a less compact structure (data not shown). Free DNA stretches could be better exposed which would result in a higher DNA methylation degree of Dnmt1. Interestingly, I could observe an increase in the methylation efficiency of Dnmt1 also in the presence of the remodeler (Brg1 or ACF complex) without ATP. This could be the consequence of a conformational change of Dnmt1 through the interaction with the remodeler and thereby probably an increased binding of Dnmt1 to its substrate. Another possible explanation could be that remodeling proteins bind on the DNA substrate at first and subsequently co-recruit Dnmt1 onto the substrate, what could stabilize the binding of Dnmt1. Also conceivable is that remodeling complexes stabilize Dnmt1 on its DNA substrate.

The results further show that the nucleosomal DNA is not completely accessible since the addition of ATP and recombinant remodeling complexes had clear methylation

activity increasing effects. The most likely explanation is that that the remodeling complexes ACF and Brg1 render the DNA in salt assembled chromatin accessible for DNA methyltransferases. This is consistent with the general increase in DNA access that was reported for DNA binding factors by nucleosome remodeling complexes, like CHRAC (Varga-Weisz *et al.*, 1997). Moreover, CHRAC enhances the accessibility of nucleosomal DNA for transcription factors during replication (Alexiadis, 1998). Ito and colleagues have shown that ACF establishes the interactions of DNA binding proteins and nucleosomal DNA, thereby facilitating transcription *in vitro* (Ito *et al.*, 1997a). The nucleotide excision repair machine (NER) has been shown shown to be inhibited in the context of chromatin. Strong suppression of NER activity was observed on physiological spaced dinucleosomal substrates, even on the linker DNA (Ura *et al.*, 2001). Interestingly, NER regained its activity in the presence of the ACF complex, indicating an interaction with chromatin remodeling complexes.

As for methylation activity reactions supplemented with ACF, I obtained similar results with the catalytic subunit Brg1 of the SWI / SNF remodeling complexes (see Fig. 39 B). The dynamics mediated by the presence of Brg1 were also able to increase the methylation efficiency of Dnmt1 on hemimethylated chromatin. This increase was even higher when compared to the methylation efficiency with ACF, probably due to mechanistic differences of nucleosome mobilization (see below). Furthermore, the addition of ACF to the unmethylated chromatin substrate does not show an effect. Contrary, the addition of Brg1 stimulates the enzymatic activity of Dnmt1. The effect of the Brg1 activity on the catalytic activity of Dnmt1 is generally higher for Brg1 than for ACF. This could be the consequence of different biochemical and biological activities of the two remodeler classes. They use different strategies to make DNA accessible: Snf2H (as a model for the ISWI family) makes DNA accessible primarily by sliding the histone octamer away (Fan *et al.*, 2003; Hamiche *et al.*, 1999; Kassabov *et al.*, 2002b; Langst *et al.*, 1999), whereas Brg1 (as a model for the SNF2 family) generates DNA loops thereby making DNA accessible (Fan *et al.*, 2003; Fazzio and Tsukiyama, 2003), (Kassabov *et al.*, 2002b; Langst *et al.*, 1999). Nucleosomes remodeled by Brg1 contain DNA loops that are stably exposed within the bounds of the histone octamer (Fan *et al.*, 2003). Brg1 facilitates access to sites near the dyad of the nucleosome (Fan *et al.,* 2003). The two remodeling families also differ in their substrate specifities: Snf2 complexes can work on nucleosomes with little flanking DNA (Clapier *et al.*, 2001;

Guyon *et al.*, 2001), while ISWI cannot (Aalfs *et al.*, 2001; Whitehouse *et al.*, 2003). ISWI-based nucleosome remodelers can also assemble and space nucleosomes, whereas SNF2 cannot. The addition of ACF1 influences the remodeling strategy of Snf2H. ACF requires longer DNA overhangs for an optimal activity of the complex, which might be important for the ability to space nucleosomes (He *et al.*, 2006).

Brg1 has been described to be implicated in both, transcriptional activation and repression (Martens and Winston, 2003). Mutations or deletions of the Brg1 coding region or related genes result in altered gene expression in cancer cell lines through largely unknown mechanisms (Roberts and Orkin, 2004). It has been shown that the loss of SWI / SNF-mediated transcriptional activation can be regarded as a novel mechanism to increase DNA methylation in cancer cells (Banine *et al.*, 2005). Recently, Datta *et al.* demonstrated a direct interaction between Dnmt3a and Brg1 (Datta *et al.*, 2005). Furthermore in this study an association of these proteins with the transcriptionally silent, methylated metallothionein promoter in mouse lymphosarcoma cells has been shown. Dnmt3a seems to be involved in the inhibition of the transcriptional initiation on the methylated promoter, though its catalytic function was dispensable for suppression. Contrary, the catalytic activity of Brg1 seems to be necessary for the suppression, indicating involvement of chromatin remodeling in this process (Datta *et al.*, 2005). My studies now have shown that Brg1 also increases the activity of Dnmt1 in chromatin *in vitro*.

All previous published studies analyzing the methylation activity of DNA methyltransferases in chromatin were done on mononucleosomal substrates (Okuwaki and Verreault, 2004; Robertson *et al.*, 2004; Takeshima *et al.*, 2006; Takeshima *et al.*, 2008). In these publications a general reduction of DNA methyltransferase activity (Robertson *et al.*, 2004) that was highly sequence specific (Okuwaki and Verreault, 2004) was observed. Results by Okuwaki and co-workers further suggest that Dnmt1 methylates DNA even within the nucleosome core. They further describe that this does not account for DNA sequences that are not regulated by DNA methylation, like imprinting control regions (Okuwaki and Verreault, 2004).

However, in my present work I could observe a sequence-independent reduction of the Dnmt1 methylation activity using chromatin arrays. My studies were performed with a DNA sequence that is not naturally regulated by DNA methylation. Furthermore I could

demonstrate by *in vitro* approaches that the Dnmt1 methylation activity increases significantly in the presence of chromatin remodeling complexes and ATP.

It has been reported that different spontaneous mechanisms could influence the ability of DNA modifying proteins to gain access to their sites of action within nucleosomes, like direct recognition and spontaneous site exposure mediated by nucleosome sliding or transient dissociation (Anderson *et al.*, 2002; Felsenfeld, 1996; Lorch *et al.*, 1987; Polach and Widom, 1995; Widom, 1997). It has also been demonstrated that short-range nucleosome sliding under similar conditions as used in my assay set-up is negligible for proteins to get access but that site exposure rather occurs through the spontaneous transient dissociation of short DNA stretches. This process starts at one end of the nucleosomal core particle and extends progressively towards its interior (Anderson *et al.*, 2002; Polach and Widom, 1995). In spite of these phenomena my results and the studies of other groups on the characterization of DNA methylation on mononucleosomes and higher order chromatin level have shown that DNA methylation is less efficient in chromatin. This argues that spontaneous site exposure seems to be not sufficient to relieve methylation of nucleosomal core particles and chromatin higher order chromatin structures. Methylation of such CpG sites may require the involvement of ATP-dependent nucleosome remodeling factors. This hypothesis is further substantiated by studies mutating the genes encoding chromatin remodeling factors such as ATRX, LSH, DDM1 that lead to hyper- or hypomethylation (Dennis *et al.*, 2001; Fan *et al.*, 2005b; Gibbons *et al.*, 2000) (Jeddeloh *et al.*, 1999). Together, these studies provide evidence for a tight interplay between chromatin remodeling and DNA methylation. However, the mechanisms of these processes are far from being understood. The interaction with a variety of other DNA binding proteins and the burden of the nucleosomal chromatin structure suggest that chromatin-associated factors could probably dictate the targeting of DNA methyltransferases to specific DNA sequences. For example Dnmt1 and Dnmt3a are known to interact with HDAC1 and HDAC2, but the functional consequence of this interaction remains unclear (Fuks *et al.*, 2001; Ling *et al.*, 2004; Robertson *et al.*, 2000; Rountree *et al.*, 2000). Furthermore, the conformation of nucleosomal DNA around the histone is variable, which could have an influence on CpG "base flipping". For numerous DNA repair machines (such as DNA glycosylases) it was reported that these enzymes gain access to their mutated target site via by this "nucleotide flipping" mechanism (Cheng and Roberts, 2001).

To further investigate the role of chromatin remodeling complexes in the process of DNA methylation, it would be necessary to study the DNA methylation efficiency on different DNA sequences in nucleosomal arrays. My experiments were performed in a sequence-unspecific environment, but it has been shown that Dnmt1 exhibits a sequence-dependent activity in chromatin (Okuwaki and Verreault, 2004). My studies have been performed on mononucleosomes that harbor the "601" nucleosome positioning sequence. Therefore it would be interesting to analyze the methylation activity of Dnmt1 on a 601 oligonucleosome (nucleosomal array) substrate. One could insert a 601 dimer (or oligomer) sequence into a vector lacking CpG sites in the backbone and analyze the methylation efficiency of Dnmt1 on the assembled chromatin substrate. Apart from this, it would be interesting to monitor the sequence-dependence of the methylation activity in chromatin arrays. Therefore DNA sequences of genes that are regulated by methylation, like Igf2 / H19 could be tested. Further the influence of chromatin remodeling factors on the methylation activity could be tested for these *in vivo* target sequences.

5. Do Remodelers influence the Dnmt1 nucleosome binding affinity?

My results show that already at the first level of DNA compaction, the nucleosome core particle represents an obstacle for *maintenance* methylation by Dnmt1. Most of the CpG sites within the nucleosomal core region are refractory to DNA methylation. Although Dnmt1, which associates with PCNA during DNA replication in S phase is capable to rapidly methylate a large number of CpGs sites behind the replication fork, a major fraction also shows delayed DNA methylation later on in cell cycle progression (Liang *et al.*, 2002; Woodcock *et al.*, 1986). It was shown that Dnmt1 acts in a biphasic mechanism regarding the timing of methylation, with 10 to 20 % of the methylation delayed, extending beyond 1h post-replication. The additional compaction of chromatin in the cell may further restrict access to certain CpG sites *in vivo*, which would be consistent with our results on a nucleosomal array. Therefore and with regard to the observed inhibition within NCPs, an efficient methylation of nucleosomal CpG sites may require the involvement of ATP-dependent nucleosome remodeling factors. It is conceivable that chromatin remodeling factors modify the binding of Dnmt1 to its substrate, thereby strengthening the interaction. To examine the functional effects of Snf2H interaction with Dnmt1, I performed electrophoretic mobility shift assays using the 77-WID-77 nucleosome (Fig. 40). However, I did not observe an effect of Snf2H on the

binding affinity of Dnmt1 towards nucleosomal DNA. This has to be further investigated by a Dnmt1 titration with lower increments. Additionally, one could detect a potentially formed complex by addition of a Dnmt1 antibody, what would result in a supershift. Further a co-immunoprecipitation would also be conceivable for complex detection. Finally, the ATP-dependency could be further analyzed with the non-hydrolysable ATP analog ATPγS. In contrast to my results, the group of Keith Robertson observed that the addition of human Snf2H enhanced the binding affinity of Dnmt1 by a factor of three in an ATP-independent manner. This effect could be due to an alteration or stabilization of the protein conformation. However, the authors observed that this increased binding affinity had no effect on the enzymatic activity of Dnmt1 with respect to mononucleosomal substrates. These discrepancies regarding our results could be attributed to many factors: First, a different nucleosomal substrate (208 bp rDNA) was used, which could influence the DNA conformation and therefore the binding affinity of Dnmt1. Second, they used histidine-tagged Snf2H, whereas our Snf2H is FLAG-tagged. This could possibly result in different inter- or intramolecular affinities.

Furthermore, it would be interesting to generate NCPs that harbor overhanging DNA without CpG sites and test the methylation efficiency of Dnmt1 in the nucleosomal core, both in the presence and absence of nucleosome remodeling factors.

Indirect evidence suggests that efficient DNA methylation requires ATP-dependent chromatin remodeling. SWI/SNF-type chromatin remodeling factors alter the translational position of nucleosomes effectively exposing naked DNA with its CpG sites to DNA methyltransferase activity. Mutations of genes encoding chromatin remodeling factors, such as *DDM1* in Arabidopsis*, ATRX* in human or *Lsh* in mouse induce hypomethylation at certain genomic regions (Dennis *et al.*, 2001; Fan *et al.*, 2005b; Gibbons *et al.*, 2000; Jeddeloh *et al.*, 1999). Robertson *et al.* observed a direct association of Dnmt1 and hSnf2H by co-immunoprecipitation. Furthermore, immunofluorescent microscopy supports the observed interaction with a significant fraction of both proteins co-localizing in heterochromatic regions in HeLa cells (Robertson *et al.*, 2004). I could also detect an interaction between Dnmt1 and human Snf2H by co-immunoprecipitation assays in human HEK293 cell extracts (Anna Schrader, diploma thesis). Geiman *et al.* could demonstrate a co-localization of Dnmt3b and Snf2H and other chromatin modifying proteins in heterochromatic regions in the nucleus (Geiman *et al.*, 2004b). Furthermore, Dnmt3a interacts physically and

functionally with components of the nucleosome remodeling machinery. Dnmt3a was also shown to associate with constituents of the Brg1 complex in mouse lymphosarcoma cells (Datta *et al.*, 2005). Interestingly, the activity of Dnmt3a was dispensable for repression, whereas Brg1 activity was crucial for silencing (Datta *et al.*, 2005). The nucleolar remodeling factor, NoRC, plays a role in promoting the methylation and silencing at the rDNA gene region. NoRC interacts with the methyltransferases Dnmt1 and Dnmt3a *in vivo* (Santoro *et al.*, 2002) and DNA methylation has a direct effect on transcriptional repression on rDNA (Santoro and Grummt, 2001). Different studies provide evidence that Lsh is primarily involved in *de novo* methylation but is dispensable for *maintenance* methylation (Yan *et al.*, 2003; Zhu *et al.*, 2006). Lsh cooperates with Dnmt1 and Dnmt3b as well as with HDAC1 and HDAC2 to silence transcription. Repression by LSH and its interactions with HDACs are lost in Dnmt1/3b knockout cells. This data suggest that LSH might serve as a "recruiting factor" for Dnmts and HDACs to establish a transcriptionally repressive chromatin. Interestingly, transcriptional repression and recruitment of DNA methyltransferases did not immediately result in DNA methylation (Myant and Stancheva, 2008). Further investigations have to be done to clarify the sequential order of transcriptional repression. It would be interesting to reconstitute LSH *in vitro* to analyze its influences on the methylation and binding properties of Dnmt1 to nucleosomal DNA.

Together these results suggest a tight interaction between the processes of chromatin remodeling and DNA methylation *in vitro*. Numerous lines of evidences suggest, that chromatin remodeling also plays an important role for the preservation of DNA methylation patterns *in vivo*. To further elucidate this, it would be of certain interest to transiently deplete the chromatin remodeling factor Snf2H by RNA interference and subsequently determine the DNA methylation status at a methylation-regulated DNA locus, such as the rDNA promoter. At the mouse rDNA promoter locus a single CpG site (-143) reflects the transcription status, what would be a potential site for methylation analysis following Snf2H knockdown.

The existence of different DNA methylation pathways and potential DNA methylation complexes, being responsible for the methylation of distinct genomic regions has been suggested (see introduction, section B.II.4.3). Numerous studies have elucidated the highly complex crosstalk between DNA methylation and other epigenetic pathways in order to regulate transcriptional activity. These interactions are well summarized in a

recent review (Rottach *et al.*, 2009). Different hypothetical models try to give an understanding of the cooperation between DNA methylation, histone modification (methylation and acetylation) and chromatin remodeling by SNF2 family proteins (Geiman and Robertson, 2002; Robertson, 2001; Robertson, 2002). One scenario could be the following: Deacetylation of histone tails could be the first step in this process. Chromatin remodeling complexes could read specific DNA features in the underlying DNA and translate them into a specific nucleosome positioning. This in combination with histone methylation by HMTases could facilitate the access of DNA methyltransferases to DNA sequences that were previously packaged into an inaccessible conformation. (Martienssen and Henikoff, 1999) Subsequently associated HDACs would again deacetylate newly assembled histones, to ensure the heterochromatic state after the passage of the replication machinery (Baylin *et al.*, 2001; Rountree *et al.*, 2000) (see Fig. 41). It has to be mentioned that the above-described model is rather simplified and the sequential order of events remains uncertain. The participation of proteins that recognize the methylated cytosine such as HP1 and MeCP2 and bind the altered chromatin structue, thereby reinforcing transcriptional silencing, as well as HDACs acting at several steps of this process are conceivable. It has been shown that the relationship between chromatin and DNA methylation is bilateral (D'Alessio and Szyf, 2006).

The main objective of my study was to elucidate the role of ATP-dependent chromatin remodeling enzymes in DNA maintenance methylation by Dnmt1. Characterizing the biochemical properties of Dnmt1 in the context of chromatin, I observed that both the binding as well as the methylation activity of the enzyme is heavily reduced on DNA sequences occupied by the nucleosome core. My data further suggest that Dnmt1 crucially requires to contact flanking DNA for efficiently nucleosome binding. The fact that the addition of chromatin remodeling enzymes abolishes the inhibitory effect of the histone octamer suggests an important role for remodelers in DNA methylation. Although other studies demonstrated an association between chromatin remodeling enzymes and DNA methyltransferases (Geiman *et al.*, 2004b; Robertson *et al.*, 2004; Santoro *et al.*, 2002), my *in vitro* experiments provide for the first time evidence for a direct influence of chromatin remodeling complexes on the enzymatic activity of Dnmt1 in chromatin. Future studies are needed to further elucidate the nature of these interactions and to verify whether these effects also exist *in vivo*.

A
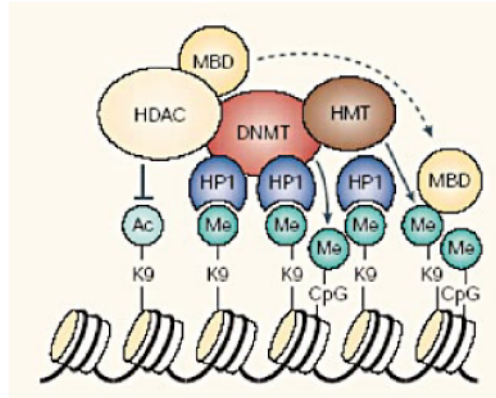
B
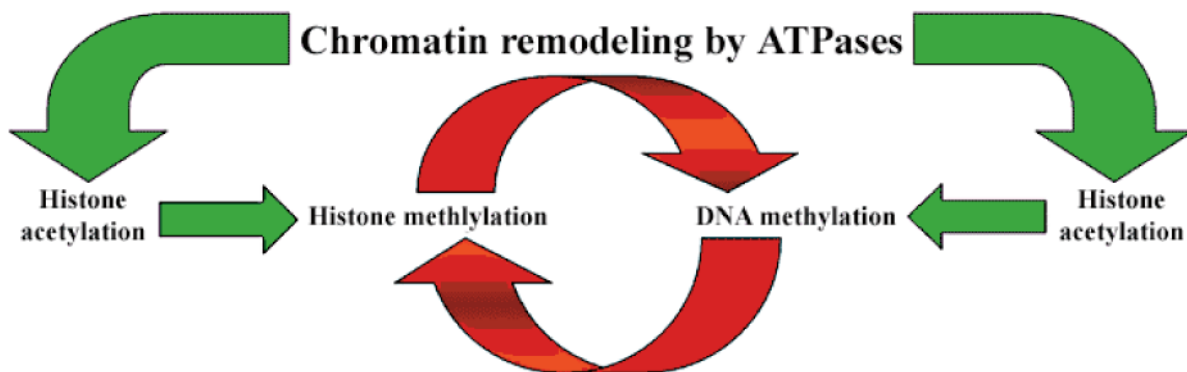
Figure 41. Interactions between DNA methyltransferases and chromatin-associated proteins
A) Hypothetical interaction model how HDACs, histone methyltransferases and other chromatin associated proteins (HP1, MBDs) could cooperate with DNA methyltransferases to set up the specific methylation patterns. ATP-dependent chromatin remodeling enzymes may be required for accessibility of DNA methyltransferases. Chromatin-associated proteins probably dictate the targeting of DNA methyltransferases to specific DNA sequences, what is most likely mediated by protein-protein interactions. Numerous interactions between DNA methyltransferases and components of the chromatin modification machinery were identified. B) Many indirect connections have been established between chromatin modifications and DNA methylation, but the exact mechanistic crosstalk, i.e. which epigenetic modification comes first and the target mechanisms, remain largely unknown.

G. References

Aalfs, J.D., G.J. Narlikar, and R.E. Kingston. 2001. Functional differences between the human ATP-dependent nucleosome remodeling proteins Brg1 and SNF2H. *J Biol Chem.* 276:34270-8.

Aapola, U., K. Kawasaki, H.S. Scott, J. Ollila, M. Vihinen, M. Heino, A. Shintani, S. Minoshima, K. Krohn, S.E. Antonarakis, N. Shimizu, J. Kudoh, and P. Peterson. 2000. Isolation and initial characterization of a novel zinc finger gene, DNMT3L, on 21q22.3, related to the cytosine-5-methyltransferase 3 gene family. *Genomics.* 65:293-298.

Aapola, U., I. Liiv, and P. Peterson. 2002. Imprinting regulator DNMT3L is a transcriptional repressor associated with histone deacetylase activity. *Nucleic Acids Res.* 30:3602-8.

Achour, M., X. Jacq, P. Ronde, M. Alhosin, C. Charlot, T. Chataigneau, M. Jeanblanc, M. Macaluso, A. Giordano, A.D. Hughes, V.B. Schini-Kerth, and C. Bronner. 2008. The interaction of the SRA domain of ICBP90 with a novel domain of DNMT1 is involved in the regulation of VEGF gene expression. *Oncogene.* 27:2187-97.

Aguirre-Arteta, A.M., I. Grunewald, M.C. Cardoso, and H. Leonhardt. 2000. Expression of an alternative Dnmt1 isoform during muscle differentiation. *Cell Growth Differ.* 11:551-559.

Ahmad, K., and S. Henikoff. 2002. The histone variant H3.3 marks active chromatin by replication-independent nucleosome assembly. *Mol Cell.* 9:1191-200.

Akey, C.W., and K. Luger. 2003. Histone chaperones and nucleosome assembly. *Curr Opin Struct Biol.* 13:6-14.

Albert, I., T.N. Mavrich, L.P. Tomsho, J. Qi, S.J. Zanton, S.C. Schuster, and B.F. Pugh. 2007. Translational and rotational settings of H2A.Z nucleosomes across the Saccharomyces cerevisiae genome. *Nature.* 446:572-6.

Alexiadis, V., P.D. Varga-Weisz, E. Bonte, P.B. Becker, and C. Gruss. 1998. In vitro chromatin remodelling by chromatin accessibility complex (CHRAC) at the SV40 origin of DNA replication. *EMBO J.* 17:3428-3438.

Allan, J., P.G. Hartman, C. Crane-Robinson, and F.X. Aviles. 1980a. The structure of histone H1 and its location in chromatin. *Nature.* 288:675-9.

Allan, J., D.Z. Staynov, and H. Gould. 1980b. Reversible dissociation of linker histone from chromatin with preservation of internucleosomal repeat. *Proc Natl Acad Sci U S A.* 77:885-9.

Allfrey, V.G., R. Faulkner, and A.E. Mirsky. 1964. Acetylation and Methylation of Histones and Their Possible Role in the Regulation of Rna Synthesis. *Proc Natl Acad Sci U S A.* 51:786-94.

Allis, C.D., S.L. Berger, J. Cote, S. Dent, T. Jenuwien, T. Kouzarides, L. Pillus, D. Reinberg, Y. Shi, R. Shiekhattar, A. Shilatifard, J. Workman, and Y. Zhang. 2007. New nomenclature for chromatin-modifying enzymes. *Cell.* 131:633-6.

- REFERENCES -

Amir, R.E., d.V.I. Van, M. Wan, C.Q. Tran, U. Francke, and H.Y. Zoghbi. 1999. Rett syndrome is caused by mutations in X-linked MECP2, encoding methyl-CpG-binding protein 2. *Nat.Genet.* 23:185-188.

Anderson, J.D., A. Thastrom, and J. Widom. 2002. Spontaneous access of proteins to buried nucleosomal DNA target sites occurs via a mechanism that is distinct from nucleosome translocation. *Mol.Cell Biol.* 22:7147-7157.

Anderson, J.D., and J. Widom. 2001. Poly(dA-dT) promoter elements increase the equilibrium accessibility of nucleosomal DNA target sites. *Mol Cell Biol.* 21:3830-9.

Anselmi, C., G. Bocchinfuso, P. De Santis, M. Savino, and A. Scipioni. 1999. Dual role of DNA intrinsic curvature and flexibility in determining nucleosome stability. *J Mol Biol.* 286:1293-301.

Antequera, F., J. Boyes, and A. Bird. 1990. High levels of de novo methylation and altered chromatin structure at CpG islands in cell lines. *Cell.* 62:503-14.

Aoki, A., I. Suetake, J. Miyagawa, T. Fujio, T. Chijiwa, H. Sasaki, and S. Tajima. 2001. Enzymatic properties of de novo-type mouse DNA (cytosine-5) methyltransferases. *Nucleic Acids Res.* 29:3506-12.

Aoyagi, S., and J.J. Hayes. 2002. hSWI/SNF-catalyzed nucleosome sliding does not occur solely via a twist-diffusion mechanism. *Mol Cell Biol.* 22:7484-90.

Aoyagi, S., G. Narlikar, C. Zheng, S. Sif, R.E. Kingston, and J.J. Hayes. 2002. Nucleosome remodeling by the human SWI/SNF complex requires transient global disruption of histone-DNA interactions. *Mol Cell Biol.* 22:3653-62.

Araujo, F.D., S. Croteau, A.D. Slack, S. Milutinovic, P. Bigey, G.B. Price, M. Zannis-Hadjopoulos, and M. Szyf. 2001. The DNMT1 target recognition domain resides in the N terminus. *J Biol Chem.* 276:6930-6.

Arita, K., M. Ariyoshi, H. Tochio, Y. Nakamura, and M. Shirakawa. 2008. Recognition of hemi-methylated DNA by the SRA protein UHRF1 by a base-flipping mechanism. *Nature.* 455:818-21.

Ausio, J. 2006. Histone variants--the structure behind the function. *Brief Funct Genomic Proteomic.* 5:228-43.

Ausubel, F.M. 1999. Short protocols in molecular biology : a compendium of methods from Current protocols in molecular biology. Wiley, Wiley, New York.

Ausubel, F.M., and et al. 1994. Current protocols in molecular biology. John Wiley and sons, New York.

Avvakumov, G.V., J.R. Walker, S. Xue, Y. Li, S. Duan, C. Bronner, C.H. Arrowsmith, and S. Dhe-Paganon. 2008. Structural basis for recognition of hemi-methylated DNA by the SRA domain of human UHRF1. *Nature.* 455:822-5.

Bachman, K.E., M.R. Rountree, and S.B. Baylin. 2001. Dnmt3a and Dnmt3b are transcriptional repressors that exhibit unique localization properties to heterochromatin. *J Biol Chem.* 276:32282-7.

Bacolla, A., S. Pradhan, J.E. Larson, R.J. Roberts, and R.D. Wells. 2001. Recombinant human DNA (cytosine-5) methyltransferase. III. Allosteric control, reaction order, and influence of plasmid topology and triplet repeat length on methylation of the fragile X CGG.CCG sequence. *J Biol Chem.* 276:18605-13.

Bacolla, A., S. Pradhan, R.J. Roberts, and R.D. Wells. 1999. Recombinant human DNA (cytosine-5) methyltransferase. II. Steady-state kinetics reveal allosteric activation by methylated dna. *J.Biol.Chem.* 274:33011-33019.

Badis, G., E.T. Chan, H. van Bakel, L. Pena-Castillo, D. Tillo, K. Tsui, C.D. Carlson, A.J. Gossett, M.J. Hasinoff, C.L. Warren, M. Gebbia, S. Talukder, A. Yang, S. Mnaimneh, D. Terterov, D. Coburn, A. Li Yeo, Z.X. Yeo, N.D. Clarke, J.D. Lieb, A.Z. Ansari, C. Nislow, and T.R. Hughes. 2008. A library of yeast transcription factor motifs reveals a widespread function for Rsc3 in targeting nucleosome exclusion at promoters. *Mol Cell.* 32:878-87.

Baker, L.A., C.D. Allis, and G.G. Wang. 2008. PHD fingers in human diseases: disorders arising from misinterpreting epigenetic marks. *Mutat Res.* 647:3-12.

Balganesh, T.S., L. Reiners, R. Lauster, M. Noyer-Weidner, K. Wilke, and T.A. Trautner. 1987. Construction and use of chimeric SPR/phi 3T DNA methyltransferases in the definition of sequence recognizing enzyme regions. *Embo J.* 6:3543-9.

Banine, F., C. Bartlett, R. Gunawardena, C. Muchardt, M. Yaniv, E.S. Knudsen, B.E. Weissman, and L.S. Sherman. 2005. SWI/SNF chromatin-remodeling factors induce changes in DNA methylation to promote transcriptional activation. *Cancer Res.* 65:3542-7.

Bannister, A.J., P. Zegerman, J.F. Partridge, E.A. Miska, J.O. Thomas, R.C. Allshire, and T. Kouzarides. 2001. Selective recognition of methylated lysine 9 on histone H3 by the HP1 chromo domain. *Nature.* 410:120-4.

Banyay, M., and A. Graslund. 2002. Structural effects of cytosine methylation on DNA sugar pucker studied by FTIR. *J Mol Biol.* 324:667-76.

Bao, Y., and X. Shen. 2007. SnapShot: chromatin remodeling complexes. *Cell.* 129:632.

Barra, J.L., L. Rhounim, J.L. Rossignol, and G. Faugeron. 2000. Histone H1 is dispensable for methylation-associated gene silencing in Ascobolus immersus and essential for long life span. *Mol Cell Biol.* 20:61-9.

Baxter, J., M. Merkenschlager, and A.G. Fisher. 2002. Nuclear organisation and gene expression. *Curr.Opin.Cell Biol.* 14:372-376.

Baylin, S.B., M. Esteller, M.R. Rountree, K.E. Bachman, K. Schuebel, and J.G. Herman. 2001. Aberrant patterns of DNA methylation, chromatin formation and gene expression in cancer. *Hum Mol Genet.* 10:687-92.

Baylin, S.B., and J.G. Herman. 2000. DNA hypermethylation in tumorigenesis: epigenetics joins genetics. *Trends Genet.* 16:168-174.

Baylin, S.B., J.G. Herman, J.R. Graff, P.M. Vertino, and J.P. Issa. 1998. Alterations in DNA methylation: a fundamental aspect of neoplasia. *Adv Cancer Res.* 72:141-96.

- References -

Beard, W.A., D.D. Shock, X.P. Yang, S.F. DeLauder, and S.H. Wilson. 2002. Loss of DNA polymerase beta stacking interactions with templating purines, but not pyrimidines, alters catalytic efficiency and fidelity. *J Biol Chem.* 277:8235-42.

Becker, P.B., and W. Hîrz. 2002. ATP-dependent nucleosome remodeling. *Annu.Rev.Biochem.* 71:247-273.

Becker, P.B., and C. Wu. 1992. Cell-free system for assembly of transcriptionally repressed chromatin from *Drosophila* embryos. *Mol.Cell Biol.* 12:2241-2249.

Bednar, J., R.A. Horowitz, S.A. Grigoryev, L.M. Carruthers, J.C. Hansen, A.J. Koster, and C.L. Woodcock. 1998. Nucleosomes, linker DNA, and linker histone form a unique structural motif that directs the higher-order folding and compaction of chromatin. *Proc.Natl.Acad.Sci.U.S.A.* 95:14173-14178.

Bernstein, B.E., C.L. Liu, E.L. Humphrey, E.O. Perlstein, and S.L. Schreiber. 2004. Global nucleosome occupancy in yeast. *Genome Biol.* 5:R62.

Bernstein, E., and S.B. Hake. 2006. The nucleosome: a little variation goes a long way. *Biochem Cell Biol.* 84:505-17.

Berube, N.G., C.A. Smeenk, and D.J. Picketts. 2000. Cell cycle-dependent phosphorylation of the ATRX protein correlates with changes in nuclear matrix and chromatin association. *Hum Mol Genet.* 9:539-47.

Bestor, T.H. 1988. Cloning of a mammalian DNA methyltransferase. *Gene.* 74:9-12.

Bestor, T.H. 2000. The DNA methyltransferases of mammals. *Hum.Mol.Genet.* 9:2395-2402.

Bestor, T.H., G. Gundersen, A.B. Kolsto, and H. Prydz. 1992. CpG islands in mammalian gene promoters are inherently resistant to de novo methylation. *Genet Anal Tech Appl.* 9:48-53.

Bestor, T.H., and V.M. Ingram. 1983. Two DNA methyltransferases from murine erythroleukemia cells: purification, sequence specificity, and mode of interaction with DNA. *Proc.Natl.Acad.Sci.U.S.A.* 80:5559-5563.

Bestor, T.H., and G.L. Verdine. 1994. DNA methyltransferases. *Curr Opin Cell Biol.* 6:380-9.

Bienvenu, T., V. des Portes, N. McDonell, A. Carrie, R. Zemni, P. Couvert, H.H. Ropers, C. Moraine, H. van Bokhoven, J.P. Fryns, K. Allen, C.A. Walsh, J. Boue, A. Kahn, J. Chelly, and C. Beldjord. 2000. Missense mutation in PAK3, R67C, causes X-linked nonspecific mental retardation. *Am J Med Genet.* 93:294-8.

Bird, A. 2002. DNA methylation patterns and epigenetic memory. *Genes Dev.* 16:6-21.

Bird, A., M. Taggart, M. Frommer, O.J. Miller, and D. Macleod. 1985. A fraction of the mouse genome that is derived from islands of nonmethylated, CpG-rich DNA. *Cell.* 40:91-99.

Bird, A.P. 1978. The occurrence and transmission of a pattern of DNA methylation in Xenopus laevis ribosomal DNA. *Philos Trans R Soc Lond B Biol Sci.* 283:325-7.

Bird, A.P. 1996. The relationship of DNA methylation to cancer. *Cancer Surv.* 28:87-101.

Bird, A.P., and E.M. Southern. 1978. Use of restriction enzymes to study eukaryotic DNA methylation: I. The methylation pattern in ribosomal DNA from Xenopus laevis. *J Mol Biol.* 118:27-47.

Bird, A.P., and M.H. Taggart. 1980. Variable patterns of total DNA and rDNA methylation in animals. *Nucleic Acids Res.* 8:1485-97.

Bloom, K.S., and J. Carbon. 1982. Yeast centromere DNA is in a unique and highly ordered structure in chromosomes and small circular minichromosomes. *Cell.* 29:305-17.

Bochar, D.A., J. Savard, W. Wang, D.W. Lafleur, P. Moore, J. Cote, and R. Shiekhattar. 2000. A family of chromatin remodeling factors related to Williams syndrome transcription factor. *Proc.Natl.Acad.Sci.U.S.A.* 97:1038-1043.

Bock, C., S. Reither, T. Mikeska, M. Paulsen, J. Walter, and T. Lengauer. 2005. BiQ Analyzer: visualization and quality control for DNA methylation data from bisulfite sequencing. *Bioinformatics.* 21:4067-8.

Bode, J., S. Goetze, H. Heng, S.A. Krawetz, and C. Benham. 2003. From DNA structure to gene expression: mediators of nuclear compartmentalization and dynamics. *Chromosome Res.* 11:435-45.

Bolshoy, A., P. McNamara, R.E. Harrington, and E.N. Trifonov. 1991. Curved DNA without A-A: experimental estimation of all 16 DNA wedge angles. *Proc Natl Acad Sci U S A.* 88:2312-6.

Bonfils, C., N. Beaulieu, E. Chan, J. Cotton-Montpetit, and A.R. MacLeod. 2000. Characterization of the human DNA methyltransferase splice variant Dnmt1b. *J.Biol.Chem.* 275:10754-10760.

Bonisch, C., S.M. Nieratschker, N.K. Orfanos, and S.B. Hake. 2008. Chromatin proteomics and epigenetic regulatory circuits. *Expert Rev Proteomics.* 5:105-19.

Bostick, M., J.K. Kim, P.O. Esteve, A. Clark, S. Pradhan, and S.E. Jacobsen. 2007. UHRF1 plays a role in maintaining DNA methylation in mammalian cells. *Science.* 317:1760-4.

Bouazoune, K., and A. Brehm. 2005. dMi-2 chromatin binding and remodeling activities are regulated by dCK2 phosphorylation. *J Biol Chem.* 280:41912-20.

Bouazoune, K., A. Mitterweger, G. Langst, A. Imhof, A. Akhtar, P.B. Becker, and A. Brehm. 2002. The dMi-2 chromodomains are DNA binding modules important for ATP-dependent nucleosome mobilization. *Embo J.* 21:2430-40.

Bourchis, D., and T.H. Bestor. 2004. Meiotic catastrophe and retrotransposon reactivation in male germ cells lacking Dnmt3L. *Nature.* 431:96-9.

Bourchis, D., G.L. Xu, C.S. Lin, B. Bollman, and T.H. Bestor. 2001. Dnmt3L and the establishment of maternal genomic imprints. *Science.* 294:2536-9.

Bouvet, P., S. Dimitrov, and A.P. Wolffe. 1994. Specific regulation of Xenopus chromosomal 5S rRNA gene transcription in vivo by histone H1. *Genes Dev.* 8:1147-59.

Bowen, N.J., M.B. Palmer, and P.A. Wade. 2004. Chromosomal regulation by MeCP2: structural and enzymatic considerations. *Cell Mol Life Sci.* 61:2163-7.

- REFERENCES -

Brehm, A., G. Langst, J. Kehle, C.R. Clapier, A. Imhof, A. Eberharter, J. Muller, and P.B. Becker. 2000. dMi-2 and ISWI chromatin remodelling factors have distinct nucleosome binding and mobilization properties. *Embo J.* 19:4332-41.

Brehm, A., K.R. Tufteland, R. Aasland, and P.B. Becker. 2004. The many colours of chromodomains. *Bioessays.* 26:133-40.

Brown, R., and G. Strathdee. 2002. Epigenomics and epigenetic therapy of cancer. *Trends Mol Med.* 8:S43-8.

Brown, S.W. 1966. Heterochromatin. *Science.* 151:417-25.

Bryan, P.N., H. Hofstetter, and M.L. Birnstiel. 1981. Nucleosome arrangement on tRNA genes of Xenopus laevis. *Cell.* 27:459-66.

Butler, J.S., J.H. Lee, and D.G. Skalnik. 2008. CFP1 interacts with DNMT1 independently of association with the Setd1 Histone H3K4 methyltransferase complexes. *DNA Cell Biol.* 27:533-43.

Cairns, B.R. 2007. Chromatin remodeling: insights and intrigue from single-molecule studies. *Nat Struct Mol Biol.* 14:989-96.

Cairns, B.R., Y. Lorch, Y. Li, M. Zhang, L. Lacomis, H. Erdjument-Bromage, P. Tempst, J. Du, B. Laurent, and R.D. Kornberg. 1996. RSC, an essential, abundant chromatin-remodeling complex. *Cell.* 87:1249-60.

Cameron, E.E., K.E. Bachman, S. Myohanen, J.G. Herman, and S.B. Baylin. 1999. Synergy of demethylation and histone deacetylase inhibition in the re-expression of genes silenced in cancer. *Nat.Genet.* 21:103-107.

Cardoso, M.C., and H. Leonhardt. 1999. DNA methyltransferase is actively retained in the cytoplasm during early development. *J.Cell Biol.* 147:25-32.

Carlson, L.L., A.W. Page, and T.H. Bestor. 1992. Properties and localization of DNA methyltransferase in preimplantation mouse embryos: implications for genomic imprinting. *Genes Dev.* 6:2536-2541.

Carlson, M., and B.C. Laurent. 1994. The SNF/SWI family of global transcriptional activators. *Curr Opin Cell Biol.* 6:396-402.

Chang, B., Y. Chen, Y. Zhao, and R.K. Bruick. 2007. JMJD6 is a histone arginine demethylase. *Science.* 318:444-7.

Chao, M.V., J. Gralla, and H.G. Martinson. 1979. DNA sequence directs placement of histone cores on restriction fragments during nucleosome formation. *Biochemistry.* 18:1068-74.

Chen, B., P. Dias, J.J. Jenkins, 3rd, V.H. Savell, and D.M. Parham. 1998. Methylation alterations of the MyoD1 upstream region are predictive of subclassification of human rhabdomyosarcomas. *Am J Pathol.* 152:1071-9.

Chen, L., A.M. MacMillan, W. Chang, K. Ezaz-Nikpay, W.S. Lane, and G.L. Verdine. 1991. Direct identification of the active-site nucleophile in a DNA (cytosine-5)-methyltransferase. *Biochemistry.* 30:11018-25.

Chen, T., S. Hevi, F. Gay, N. Tsujimoto, T. He, B. Zhang, Y. Ueda, and E. Li. 2007. Complete inactivation of DNMT1 leads to mitotic catastrophe in human cancer cells. *Nat Genet.* 39:391-6.

Chen, T., and E. Li. 2004. Structure and function of eukaryotic DNA methyltransferases. *Curr.Top.Dev.Biol.* 60:55-89.

Chen, T., and E. Li. 2006. Establishment and maintenance of DNA methylation patterns in mammals. *Curr Top Microbiol Immunol.* 301:179-201.

Chen, T., N. Tsujimoto, and E. Li. 2004. The PWWP domain of Dnmt3a and Dnmt3b is required for directing DNA methylation to the major satellite repeats at pericentric heterochromatin. *Mol.Cell Biol.* 24:9048-9058.

Cheng, X., and R.J. Roberts. 2001. AdoMet-dependent methylation, DNA methyltransferases and base flipping. *Nucleic Acids Res.* 29:3784-3795.

Chuang, L.S., H.I. Ian, T.W. Koh, H.H. Ng, G. Xu, and B.F. Li. 1997. Human DNA-(cytosine-5) methyltransferase-PCNA complex as a target for p21WAF1. *Science.* 277:1996-2000.

Chuang, L.S., H.H. Ng, J.N. Chia, and B.F. Li. 1996. Characterisation of independent DNA and multiple Zn-binding domains at the N terminus of human DNA-(cytosine-5) methyltransferase: modulating the property of a DNA-binding domain by contiguous Zn-binding motifs. *J.Mol.Biol.* 257:935-948.

Chubb, J.R., and W.A. Bickmore. 2003. Considering nuclear compartmentalization in the light of nuclear dynamics. *Cell.* 112:403-6.

Clapier, C.R., and B.R. Cairns. 2009. The biology of chromatin remodeling complexes. *Annu Rev Biochem.* 78:273-304.

Clapier, C.R., G. Langst, D.F. Corona, P.B. Becker, and K.P. Nightingale. 2001. Critical role for the histone H4 N terminus in nucleosome remodeling by ISWI. *Mol.Cell Biol.* 21:875-883.

Clapier, C.R., K.P. Nightingale, and P.B. Becker. 2002. A critical epitope for substrate recognition by the nucleosome remodeling ATPase ISWI. *Nucleic Acids Res.* 30:649-655.

Clark, D.J., and T. Kimura. 1990. Electrostatic mechanism of chromatin folding. *J Mol Biol.* 211:883-96.

Colot, V., and J.L. Rossignol. 1999. Eukaryotic DNA methylation as an evolutionary device. *Bioessays.* 21:402-411.

Cooper, D.N., and M. Krawczak. 1989. Cytosine methylation and the fate of CpG dinucleotides in vertebrate genomes. *Hum.Genet.* 83:181-188.

Cooper, J.P., S.Y. Roth, and R.T. Simpson. 1994. The global transcriptional regulators, SSN6 and TUP1, play distinct roles in the establishment of a repressive chromatin structure. *Genes Dev.* 8:1400-10.

Corona, D.F., G. Langst, C.R. Clapier, E.J. Bonte, S. Ferrari, J.W. Tamkun, and P.B. Becker. 1999. ISWI is an ATP-dependent nucleosome remodeling factor. *Mol Cell.* 3:239-45.

Cosgrove, M.S., J.D. Boeke, and C. Wolberger. 2004. Regulated nucleosome mobility and the histone code. *Nat Struct Mol Biol.* 11:1037-43.

Costanzi, C., and J.R. Pehrson. 1998. Histone macroH2A1 is concentrated in the inactive X chromosome of female mammals. *Nature.* 393:599-601.

Coulondre, C., and J.H. Miller. 1978. Analysis of base substitutions induced by ultraviolet radiation in Escherichia coli. *Natl Cancer Inst Monogr*:115-9.

Coulondre, C., J.H. Miller, P.J. Farabaugh, and W. Gilbert. 1978. Molecular basis of base substitution hotspots in Escherichia coli. *Nature.* 274:775-80.

- REFERENCES -

Cremer, M., J. von Hase, T. Volm, A. Brero, G. Kreth, J. Walter, C. Fischer, I. Solovei, C. Cremer, and T. Cremer. 2001. Non-random radial higher-order chromatin arrangements in nuclei of diploid human cells. *Chromosome Res.* 9:541-67.

Cremer, T., and C. Cremer. 2001. Chromosome territories, nuclear architecture and gene regulation in mammalian cells. *Nat Rev Genet.* 2:292-301.

Cuatrecasas, P., M. Wilchek, and C.B. Anfinsen. 1968. Selective enzyme purification by affinity chromatography. *Proc Natl Acad Sci U S A.* 61:636-43.

D'Alessio, A.C., and M. Szyf. 2006. Epigenetic tete-a-tete: the bilateral relationship between chromatin modifications and DNA methylation. *Biochem Cell Biol.* 84:463-76.

Dalal, Y., T. Furuyama, D. Vermaak, and S. Henikoff. 2007a. Structure, dynamics, and evolution of centromeric nucleosomes. *Proc Natl Acad Sci U S A.* 104:15974-81.

Dalal, Y., H. Wang, S. Lindsay, and S. Henikoff. 2007b. Tetrameric structure of centromeric nucleosomes in interphase *Drosophila* cells. *PLoS Biol.* 5:e218.

Damelin, M., I. Simon, T.I. Moy, B. Wilson, S. Komili, P. Tempst, F.P. Roth, R.A. Young, B.R. Cairns, and P.A. Silver. 2002. The genome-wide localization of Rsc9, a component of the RSC chromatin-remodeling complex, changes in response to stress. *Mol Cell.* 9:563-73.

Dang, W., M.N. Kagalwala, and B. Bartholomew. 2006. Regulation of ISW2 by concerted action of histone H4 tail and extranucleosomal DNA. *Mol Cell Biol.* 26:7388-96.

Datta, J., K. Ghoshal, S.M. Sharma, S. Tajima, and S.T. Jacob. 2003. Biochemical fractionation reveals association of DNA methyltransferase (Dnmt) 3b with Dnmt1 and that of Dnmt 3a with a histone H3 methyltransferase and Hdac1. *J Cell Biochem.* 88:855-64.

Datta, J., S. Majumder, S. Bai, K. Ghoshal, H. Kutay, D.S. Smith, J.W. Crabb, and S.T. Jacob. 2005. Physical and functional interaction of DNA methyltransferase 3A with Mbd3 and Brg1 in mouse lymphosarcoma cells. *Cancer Res.* 65:10891-900.

Davey, C., and J. Allan. 2003. Nucleosome positioning signals and potential H-DNA within the DNA sequence of the imprinting control region of the mouse Igf2r gene. *Biochim Biophys Acta.* 1630:103-16.

Davey, C., R. Fraser, M. Smolle, M.W. Simmen, and J. Allan. 2003. Nucleosome positioning signals in the DNA sequence of the human and mouse H19 imprinting control regions. *J Mol Biol.* 325:873-87.

Davey, C., S. Pennings, and J. Allan. 1997. CpG methylation remodels chromatin structure in vitro. *J Mol Biol.* 267:276-88.

Davey, C.A., D.F. Sargent, K. Luger, A.W. Maeder, and T.J. Richmond. 2002. Solvent mediated interactions in the structure of the nucleosome core particle at 1.9 a resolution. *J.Mol.Biol.* 319:1097-1113.

Davuluri, R.V., I. Grosse, and M.Q. Zhang. 2001. Computational identification of promoters and first exons in the human genome. *Nat Genet.* 29:412-7.

Delaval, K., and R. Feil. 2004. Epigenetic regulation of mammalian genomic imprinting. *Curr Opin Genet Dev.* 14:188-95.

Delmas, V., D.G. Stokes, and R.P. Perry. 1993. A mammalian DNA-binding protein that contains a chromodomain and an SNF2/SWI2-like helicase domain. *Proc Natl Acad Sci U S A.* 90:2414-8.

Dennis, K., T. Fan, T. Geiman, Q. Yan, and K. Muegge. 2001. Lsh, a member of the SNF2 family, is required for genome-wide methylation. *Genes Dev.* 15:2940-2944.

Deplus, R., C. Brenner, W.A. Burgers, P. Putmans, T. Kouzarides, Y. de Launoit, and F. Fuks. 2002. Dnmt3L is a transcriptional repressor that recruits histone deacetylase. *Nucleic Acids Res.* 30:3831-8.

Derreumaux, S., M. Chaoui, G. Tevanian, and S. Fermandjian. 2001. Impact of CpG methylation on structure, dynamics and solvation of cAMP DNA responsive element. *Nucleic Acids Res.* 29:2314-26.

Dhillon, N., and R.T. Kamakaka. 2002. Breaking through to the other side: silencers and barriers. *Curr Opin Genet Dev.* 12:188-92.

Di Croce, L., V.A. Raker, M. Corsaro, F. Fazi, M. Fanelli, M. Faretta, F. Fuks, F. Lo Coco, T. Kouzarides, C. Nervi, S. Minucci, and P.G. Pelicci. 2002. Methyltransferase recruitment and DNA hypermethylation of target promoters by an oncogenic transcription factor. *Science.* 295:1079-82.

Doherty, A.S., M.S. Bartolomei, and R.M. Schultz. 2002. Regulation of stage-specific nuclear translocation of Dnmt1o during preimplantation mouse development. *Dev.Biol.* 242:255-266.

Dong, A., J.A. Yoder, X. Zhang, L. Zhou, T.H. Bestor, and X. Cheng. 2001. Structure of human DNMT2, an enigmatic DNA methyltransferase homolog that displays denaturant-resistant binding to DNA. *Nucleic Acids Res.* 29:439-48.

Dorigo, B., T. Schalch, K. Bystricky, and T.J. Richmond. 2003. Chromatin fiber folding: requirement for the histone H4 N-terminal tail. *J.Mol.Biol.* 327:85-96.

Dorigo, B., T. Schalch, A. Kulangara, S. Duda, R.R. Schroeder, and T.J. Richmond. 2004. Nucleosome arrays reveal the two-start organization of the chromatin fiber. *Science.* 306:1571-1573.

Drew, H.R., and A.A. Travers. 1985. DNA bending and its relation to nucleosome positioning. *J Mol Biol.* 186:773-90.

Easwaran, H.P., L. Schermelleh, H. Leonhardt, and M.C. Cardoso. 2004. Replication-independent chromatin loading of Dnmt1 during G2 and M phases. *EMBO Rep.* 5:1181-1186.

Ebbert, R., A. Birkmann, and H.J. Schuller. 1999. The product of the SNF2/SWI2 paralogue Ino80 of Saccharomyces cerevisiae required for efficient expression of various yeast structural genes is part of a high-molecular-weight protein complex. *Mol Microbiol.* 32:741-51.

Eberharter, A., and P.B. Becker. 2004. ATP-dependent nucleosome remodelling: factors and functions. *J Cell Sci.* 117:3707-11.

Eberharter, A., S. Ferrari, G. Langst, T. Straub, A. Imhof, P. Varga-Weisz, M. Wilm, and P.B. Becker. 2001. Acf1, the largest subunit of CHRAC, regulates ISWI-induced nucleosome remodelling. *EMBO J.* 20:3781-3788.

Eberharter, A., G. Langst, and P.B. Becker. 2004. A nucleosome sliding assay for chromatin remodeling factors. *Methods Enzymol.* 377:344-53.

Egger, G., S. Jeong, S.G. Escobar, C.C. Cortez, T.W. Li, Y. Saito, C.B. Yoo, P.A. Jones, and G. Liang. 2006. Identification of DNMT1 (DNA methyltransferase 1) hypomorphs in somatic knockouts suggests an essential role for DNMT1 in cell survival. *Proc Natl Acad Sci U S A.* 103:14080-5.

Eisen, J.A., K.S. Sweder, and P.C. Hanawalt. 1995. Evolution of the SNF2 family of proteins: subfamilies with distinct sequences and functions. *Nucleic Acids Res.* 23:2715-2723.

Epsztejn-Litman, S., N. Feldman, M. Abu-Remaileh, Y. Shufaro, A. Gerson, J. Ueda, R. Deplus, F. Fuks, Y. Shinkai, H. Cedar, and Y. Bergman. 2008. De novo DNA methylation promoted by G9a prevents reprogramming of embryonically silenced genes. *Nat Struct Mol Biol.* 15:1176-83.

Esteve, P.O., H.G. Chin, A. Smallwood, G.R. Feehery, O. Gangisetty, A.R. Karpf, M.F. Carey, and S. Pradhan. 2006. Direct interaction between DNMT1 and G9a coordinates DNA and histone methylation during replication. *Genes Dev.* 20:3089-103.

Falls, J.G., D.J. Pulford, A.A. Wylie, and R.L. Jirtle. 1999. Genomic imprinting: implications for human disease. *Am J Pathol.* 154:635-47.

Fan, H.Y., X. He, R.E. Kingston, and G.J. Narlikar. 2003. Distinct strategies to make nucleosomal DNA accessible. *Mol Cell.* 11:1311-22.

Fan, H.Y., K.W. Trotter, T.K. Archer, and R.E. Kingston. 2005a. Swapping function of two chromatin remodeling complexes. *Mol Cell.* 17:805-15.

Fan, T., J.P. Hagan, S.V. Kozlov, C.L. Stewart, and K. Muegge. 2005b. Lsh controls silencing of the imprinted Cdkn1c gene. *Development.* 132:635-44.

Fan, Y., T. Nikitina, J. Zhao, T.J. Fleury, R. Bhattacharyya, E.E. Bouhassira, A. Stein, C.L. Woodcock, and A.I. Skoultchi. 2005c. Histone H1 depletion in mammals alters global chromatin structure but causes specific changes in gene regulation. *Cell.* 123:1199-212.

Fatemi, M., A. Hermann, H. Gowher, and A. Jeltsch. 2002. Dnmt3a and Dnmt1 functionally cooperate during de novo methylation of DNA. *Eur.J.Biochem.* 269:4981-4984.

Fatemi, M., A. Hermann, S. Pradhan, and A. Jeltsch. 2001. The activity of the murine DNA methyltransferase Dnmt1 is controlled by interaction of the catalytic domain with the N-terminal part of the enzyme leading to an allosteric activation of the enzyme after binding to methylated DNA. *J.Mol.Biol.* 309:1189-1199.

Fazzio, T.G., M.E. Gelbart, and T. Tsukiyama. 2005. Two distinct mechanisms of chromatin interaction by the Isw2 chromatin remodeling complex in vivo. *Mol Cell Biol.* 25:9165-74.

Fazzio, T.G., and T. Tsukiyama. 2003. Chromatin remodeling in vivo: evidence for a nucleosome sliding mechanism. *Mol Cell.* 12:1333-40.

Fedor, M.J., N.F. Lue, and R.D. Kornberg. 1988. Statistical positioning of nucleosomes by specific protein-binding to an upstream activating sequence in yeast. *J Mol Biol.* 204:109-27.

Fellinger, K., U. Rothbauer, M. Felle, G. Langst, and H. Leonhardt. 2009. Dimerization of DNA methyltransferase 1 is mediated by its regulatory domain. *J Cell Biochem.* 106:521-8.

Felsenfeld, G. 1996. Chromatin unfolds. *Cell.* 86:13-9.

Felsenfeld, G., and M. Groudine. 2003. Controlling the double helix. *Nature.* 421:448-453.

Felsenfeld, G., and J.D. McGhee. 1986. Structure of the 30 nm chromatin fiber. *Cell.* 44:375-7.

Feltus, F.A., E.K. Lee, J.F. Costello, C. Plass, and P.M. Vertino. 2003. Predicting aberrant CpG island methylation. *Proc Natl Acad Sci U S A.* 100:12253-8.

Ferreira, H., A. Flaus, and T. Owen-Hughes. 2007a. Histone modifications influence the action of Snf2 family remodelling enzymes by different mechanisms. *J Mol Biol.* 374:563-79.

Ferreira, R., A. Eberharter, T. Bonaldi, M. Chioda, A. Imhof, and P.B. Becker. 2007b. Site-specific acetylation of ISWI by GCN5. *BMC Mol Biol.* 8:73.

Field, Y., N. Kaplan, Y. Fondufe-Mittendorf, I.K. Moore, E. Sharon, Y. Lubling, J. Widom, and E. Segal. 2008. Distinct modes of regulation by chromatin encoded through nucleosome positioning signals. *PLoS Comput Biol.* 4:e1000216.

Finch, J.T., and A. Klug. 1976. Solenoidal model for superstructure in chromatin. *Proc.Natl.Acad.Sci.U.S.A.* 73:1897-1901.

Fischle, W. 2008. Talk is cheap--cross-talk in establishment, maintenance, and readout of chromatin modifications. *Genes Dev.* 22:3375-82.

Fischle, W., Y. Wang, and C.D. Allis. 2003a. Binary switches and modification cassettes in histone biology and beyond. *Nature.* 425:475-9.

Fischle, W., Y. Wang, S.A. Jacobs, Y. Kim, C.D. Allis, and S. Khorasanizadeh. 2003b. Molecular basis for the discrimination of repressive methyl-lysine marks in histone H3 by Polycomb and HP1 chromodomains. *Genes Dev.* 17:1870-81.

Fisher, A.G., and M. Merkenschlager. 2002. Gene silencing, cell fate and nuclear organisation. *Curr.Opin.Genet.Dev.* 12:193-197.

Fitzgerald, D.J., and J.N. Anderson. 1998. Unique translational positioning of nucleosomes on synthetic DNAs. *Nucleic Acids Res.* 26:2526-35.

Flaus, A., K. Luger, S. Tan, and T.J. Richmond. 1996. Mapping nucleosome position at single base-pair resolution by using site-directed hydroxyl radicals. *Proc Natl Acad Sci U S A.* 93:1370-5.

Flaus, A., D.M. Martin, G.J. Barton, and T. Owen-Hughes. 2006. Identification of multiple distinct Snf2 subfamilies with conserved structural motifs. *Nucleic Acids Res.* 34:2887-905.

Flaus, A., and T. Owen-Hughes. 2003a. Dynamic properties of nucleosomes during thermal and ATP-driven mobilization. *Mol Cell Biol.* 23:7767-79.

Flaus, A., and T. Owen-Hughes. 2003b. Mechanisms for nucleosome mobilization. *Biopolymers.* 68:563-78.

Fleming, A.B., and S. Pennings. 2001. Antagonistic remodelling by Swi-Snf and Tup1-Ssn6 of an extensive chromatin region forms the background for FLO1 gene regulation. *Embo J.* 20:5219-31.

Flemming, W. 1982. Zellsubstanz, Kern, Zellteilung. *VCW Vogel, Leipzig.*

Flynn, J., J.Y. Fang, J.A. Mikovits, and N.O. Reich. 2003. A potent cell-active allosteric inhibitor of murine DNA cytosine C5 methyltransferase. *J Biol Chem.* 278:8238-43.

Flynn, J., J.F. Glickman, and N.O. Reich. 1996. Murine DNA cytosine-C5 methyltransferase: pre-steady- and steady-state kinetic analysis with regulatory DNA sequences. *Biochemistry.* 35:7308-7315.

Flynn, J., and N. Reich. 1998. Murine DNA (cytosine-5-)-methyltransferase: steady-state and substrate trapping analyses of the kinetic mechanism. *Biochemistry.* 37:15162-15169.

Frommer, M., L.E. McDonald, D.S. Millar, C.M. Collis, F. Watt, G.W. Grigg, P.L. Molloy, and C.L. Paul. 1992. A genomic sequencing protocol that yields a positive display of 5-methylcytosine residues in individual DNA strands. *Proc Natl Acad Sci U S A.* 89:1827-31.

Fuks, F., W.A. Burgers, A. Brehm, L. Hughes-Davies, and T. Kouzarides. 2000. DNA methyltransferase Dnmt1 associates with histone deacetylase activity. *Nat.Genet.* 24:88-91.

Fuks, F., W.A. Burgers, N. Godin, M. Kasai, and T. Kouzarides. 2001. Dnmt3a binds deacetylases and is recruited by a sequence-specific repressor to silence transcription. *EMBO J.* 20:2536-2544.

Fuks, F., P.J. Hurd, R. Deplus, and T. Kouzarides. 2003. The DNA methyltransferases associate with HP1 and the SUV39H1 histone methyltransferase. *Nucleic Acids Res.* 31:2305-2312.

Fyodorov, D.V., and J.T. Kadonaga. 2002. Dynamics of ATP-dependent chromatin assembly by ACF. *Nature.* 418:897-900.

Gangaraju, V.K., and B. Bartholomew. 2007a. Dependency of ISW1a chromatin remodeling on extranucleosomal DNA. *Mol Cell Biol.* 27:3217-25.

Gangaraju, V.K., and B. Bartholomew. 2007b. Mechanisms of ATP dependent chromatin remodeling. *Mutat Res.* 618:3-17.

Ge, Y.Z., M.T. Pu, H. Gowher, H.P. Wu, J.P. Ding, A. Jeltsch, and G.L. Xu. 2004. Chromatin targeting of de novo DNA methyltransferases by the PWWP domain. *J.Biol.Chem.* 279:25447-25454.

Geiman, T.M., and K.D. Robertson. 2002. Chromatin remodeling, histone modifications, and DNA methylation-how does it all fit together? *J.Cell Biochem.* 87:117-125.

Geiman, T.M., U.T. Sankpal, A.K. Robertson, Y. Chen, M. Mazumdar, J.T. Heale, J.A. Schmiesing, W. Kim, K. Yokomori, Y. Zhao, and K.D. Robertson. 2004a. Isolation and characterization of a novel DNA methyltransferase complex linking DNMT3B with components of the mitotic chromosome condensation machinery. *Nucleic Acids Res.* 32:2716-2729.

Geiman, T.M., U.T. Sankpal, A.K. Robertson, Y. Zhao, and K.D. Robertson. 2004b. DNMT3B interacts with hSNF2H chromatin remodeling enzyme, HDACs 1 and 2, and components of the histone methylation system. *Biochem.Biophys.Res.Commun.* 318:544-555.

Gibbons, R.J., S. Bachoo, D.J. Picketts, S. Aftimos, B. Asenbauer, J. Bergoffen, S.A. Berry, N. Dahl, A. Fryer, K. Keppler, K. Kurosawa, M.L. Levin, M. Masuno, G. Neri, M.E. Pierpont, S.F. Slaney, and D.R.

Higgs. 1997. Mutations in transcriptional regulator ATRX establish the functional significance of a PHD-like domain. *Nat Genet.* 17:146-8.

Gibbons, R.J., T.L. McDowell, S. Raman, D.M. O'Rourke, D. Garrick, H. Ayyub, and D.R. Higgs. 2000. Mutations in ATRX, encoding a SWI/SNF-like protein, cause diverse changes in the pattern of DNA methylation. *Nat.Genet.* 24:368-371.

Gilmour, D.S., and J.T. Lis. 1986. RNA polymerase II interacts with the promoter region of the noninduced hsp70 gene in *Drosophila* melanogaster cells. *Mol Cell Biol.* 6:3984-9.

Gold, M., and J. Hurwitz. 1964. The Enzymatic Methylation of Ribonucleic Acid and Deoxyribonucleic Acid. V. Purification and Properties of the Deoxyribonucleic Acid-Methylating Activity of Escherichia Coli. *J Biol Chem.* 239:3858-65.

Goll, M.G., F. Kirpekar, K.A. Maggert, J.A. Yoder, C.L. Hsieh, X. Zhang, K.G. Golic, S.E. Jacobsen, and T.H. Bestor. 2006. Methylation of tRNAAsp by the DNA methyltransferase homolog Dnmt2. *Science.* 311:395-8.

Gonzalez-Zulueta, M., C.M. Bender, A.S. Yang, T. Nguyen, R.W. Beart, J.M. Van Tornout, and P.A. Jones. 1995. Methylation of the 5' CpG island of the p16/CDKN2 tumor suppressor gene in normal and transformed human tissues correlates with gene silencing. *Cancer Res.* 55:4531-5.

Gowher, H., and A. Jeltsch. 2001. Enzymatic properties of recombinant Dnmt3a DNA methyltransferase from mouse: the enzyme modifies DNA in a non-processive manner and also methylates non-CpG [correction of non-CpA] sites. *J.Mol.Biol.* 309:1201-1208.

Gowher, H., and A. Jeltsch. 2002. Molecular enzymology of the catalytic domains of the Dnmt3a and Dnmt3b DNA methyltransferases. *J.Biol.Chem.* 277:20409-20414.

Gowher, H., O. Leismann, and A. Jeltsch. 2000. DNA of *Drosophila* melanogaster contains 5-methylcytosine. *Embo J.* 19:6918-23.

Gowher, H., K. Liebert, A. Hermann, G. Xu, and A. Jeltsch. 2005a. Mechanism of stimulation of catalytic activity of Dnmt3A and Dnmt3B DNA-(cytosine-C5)-methyltransferases by Dnmt3L. *J Biol Chem.* 280:13341-8.

Gowher, H., C.J. Stockdale, R. Goyal, H. Ferreira, T. Owen-Hughes, and A. Jeltsch. 2005b. De novo methylation of nucleosomal DNA by the mammalian Dnmt1 and Dnmt3A DNA methyltransferases. *Biochemistry.* 44:9899-904.

Goyal, R., R. Reinhardt, and A. Jeltsch. 2006. Accuracy of DNA methylation pattern preservation by the Dnmt1 methyltransferase. *Nucleic Acids Res.* 34:1182-8.

Graff, J.R., J.G. Herman, S. Myohanen, S.B. Baylin, and P.M. Vertino. 1997. Mapping patterns of CpG island methylation in normal and neoplastic cells implicates both upstream and downstream regions in de novo methylation. *J Biol Chem.* 272:22322-9.

Grandjean, V., R. Yaman, F. Cuzin, and M. Rassoulzadegan. 2007. Inheritance of an epigenetic mark: the CpG DNA methyltransferase 1 is required for de novo establishment of a complex pattern of non-CpG methylation. *PLoS One.* 2:e1136.

Graziano, V., S.E. Gerchman, D.K. Schneider, and V. Ramakrishnan. 1996. Neutron scattering studies on chromatin higher-order structure. *Basic Life Sci.* 64:127-36.

Greive, S.J., and P.H. von Hippel. 2005. Thinking quantitatively about transcriptional regulation. *Nat Rev Mol Cell Biol.* 6:221-32.

Grewal, S.I., and S.C. Elgin. 2002. Heterochromatin: new possibilities for the inheritance of structure. *Curr Opin Genet Dev.* 12:178-87.

Grewal, S.I., and D. Moazed. 2003. Heterochromatin and epigenetic control of gene expression. *Science.* 301:798-802.

Gruenbaum, Y., H. Cedar, and A. Razin. 1982. Substrate and sequence specificity of a eukaryotic DNA methylase. *Nature.* 295:620-2.

Grummt, I., and C.S. Pikaard. 2003. Epigenetic silencing of RNA polymerase I transcription. *Nat Rev Mol Cell Biol.* 4:641-9.

Grune, T., J. Brzeski, A. Eberharter, C.R. Clapier, D.F. Corona, P.B. Becker, and C.W. Muller. 2003. Crystal structure and functional analysis of a nucleosome recognition module of the remodeling factor ISWI. *Mol Cell.* 12:449-60.

Grunstein, M. 1990. Nucleosomes: regulators of transcription. *Trends Genet.* 6:395-400.

Gupta, S., J. Dennis, R.E. Thurman, R. Kingston, J.A. Stamatoyannopoulos, and W.S. Noble. 2008. Predicting human nucleosome occupancy from primary sequence. *PLoS Comput Biol.* 4:e1000134.

Guschin, D., T.M. Geiman, N. Kikyo, D.J. Tremethick, A.P. Wolffe, and P.A. Wade. 2000. Multiple ISWI ATPase complexes from xenopus laevis. Functional conservation of an ACF/CHRAC homolog. *J Biol Chem.* 275:35248-55.

Gutierrez, J., R. Paredes, F. Cruzat, D.A. Hill, A.J. van Wijnen, J.B. Lian, G.S. Stein, J.L. Stein, A.N. Imbalzano, and M. Montecino. 2007a. Chromatin remodeling by SWI/SNF results in nucleosome mobilization to preferential positions in the rat osteocalcin gene promoter. *J Biol Chem.* 282:9445-57.

Gutierrez, J.L., M. Chandy, M.J. Carrozza, and J.L. Workman. 2007b. Activation domains drive nucleosome eviction by SWI/SNF. *Embo J.* 26:730-40.

Guyon, J.R., G.J. Narlikar, E.K. Sullivan, and R.E. Kingston. 2001. Stability of a human SWI-SNF remodeled nucleosomal array. *Mol Cell Biol.* 21:1132-44.

Hake, S.B., and C.D. Allis. 2006. Histone H3 variants and their potential role in indexing mammalian genomes: the "H3 barcode hypothesis". *Proc Natl Acad Sci U S A.* 103:6428-35.

Hamiche, A., R. Sandaltzopoulos, D.A. Gdula, and C. Wu. 1999. ATP-dependent histone octamer sliding mediated by the chromatin remodeling complex NURF. *Cell.* 97:833-42.

Hancock, R. 2000. A new look at the nuclear matrix. *Chromosoma.* 109:219-25.

Handa, V., and A. Jeltsch. 2005. Profound flanking sequence preference of Dnmt3a and Dnmt3b mammalian DNA methyltransferases shape the human epigenome. *J Mol Biol.* 348:1103-12.

- References -

Hansen, R.S., C. Wijmenga, P. Luo, A.M. Stanek, T.K. Canfield, C.M. Weemaes, and S.M. Gartler. 1999. The DNMT3B DNA methyltransferase gene is mutated in the ICF immunodeficiency syndrome. *Proc Natl Acad Sci U S A.* 96:14412-7.

Hartlepp, K.F., C. Fernandez-Tornero, A. Eberharter, T. Grune, C.W. Muller, and P.B. Becker. 2005. The histone fold subunits of *Drosophila* CHRAC facilitate nucleosome sliding through dynamic DNA interactions. *Mol Cell Biol.* 25:9886-96.

Hashimoto, H., J.R. Horton, X. Zhang, and X. Cheng. 2009. UHRF1, a modular multi-domain protein, regulates replication-coupled crosstalk between DNA methylation and histone modifications. *Epigenetics.* 4:8-14.

Hata, K., M. Okano, H. Lei, and E. Li. 2002. Dnmt3L cooperates with the Dnmt3 family of de novo DNA methyltransferases to establish maternal imprints in mice. *Development.* 129:1983-1993.

Haushalter, K.A., and J.T. Kadonaga. 2003. Chromatin assembly by DNA-translocating motors. *Nat Rev Mol Cell Biol.* 4:613-20.

He, X., H.Y. Fan, G.J. Narlikar, and R.E. Kingston. 2006. Human ACF1 alters the remodeling strategy of SNF2h. *J Biol Chem.* 281:28636-47.

Heard, E., and C.M. Disteche. 2006. Dosage compensation in mammals: fine-tuning the expression of the X chromosome. *Genes Dev.* 20:1848-67.

Heitz, E. 1928. Das Heterochromatin der Moose. *I. Jahrb f wissensch Bot.* 69:762-818.

Henikoff, S., E. McKittrick, and K. Ahmad. 2004. Epigenetics, histone H3 variants, and the inheritance of chromatin states. *Cold Spring Harb Symp Quant Biol.* 69:235-43.

Herman, J.G. 2004. Circulating methylated DNA. *Ann N Y Acad Sci.* 1022:33-9.

Hermann, A., H. Gowher, and A. Jeltsch. 2004a. Biochemistry and biology of mammalian DNA methyltransferases. *Cell Mol.Life Sci.* 61:2571-2587.

Hermann, A., R. Goyal, and A. Jeltsch. 2004b. The Dnmt1 DNA-(cytosine-C5)-methyltransferase methylates DNA processively with high preference for hemimethylated target sites. *J.Biol.Chem.* 279:48350-48359.

Hill, L., and M. Flack. 1910. The influence of oxygen inhalations on muscular work. *J Physiol.* 40:347-72.

Hitt, M.M., T.L. Wu, G. Cohen, and S. Linn. 1988. De novo and maintenance DNA methylation by a mouse plasmacytoma cell DNA methyltransferase. *J.Biol.Chem.* 263:4392-4399.

Hoffmann-Rohrer, U.a.L.P. 2000. Lab FAQS, Find a Quick Solution. Roche Bolecular Biochemicals.

Holliday, R. 2006. Epigenetics: a historical overview. *Epigenetics.* 1:76-80.

Holstege, F.C., U. Fiedler, and H.T. Timmers. 1997. Three transitions in the RNA polymerase II transcription complex during initiation. *Embo J.* 16:7468-80.

Horn, P.J., and C.L. Peterson. 2002. Molecular biology. Chromatin higher order folding--wrapping up transcription. *Science.* 297:1824-1827.

Hotchkiss, R.D. 1948. The quantitative separation of purine, pyrimidine and nucleoside by paper chromatography. *J.Biol.Chem.* 168:315-332.

Hsieh, C.L. 1999. In vivo activity of murine de novo methyltransferases, Dnmt3a and Dnmt3b. *Mol.Cell Biol.* 19:8211-8218.

Hsu, J.M., J. Huang, P.B. Meluh, and B.C. Laurent. 2003. The yeast RSC chromatin-remodeling complex is required for kinetochore function in chromosome segregation. *Mol Cell Biol.* 23:3202-15.

Huang, J., J.M. Hsu, and B.C. Laurent. 2004. The RSC nucleosome-remodeling complex is required for Cohesin's association with chromosome arms. *Mol Cell.* 13:739-50.

Hung, M.S., N. Karthikeyan, B. Huang, H.C. Koo, J. Kiger, and C.J. Shen. 1999. *Drosophila* proteins related to vertebrate DNA (5-cytosine) methyltransferases. *Proc Natl Acad Sci U S A.* 96:11940-5.

Iida, T., I. Suetake, S. Tajima, H. Morioka, S. Ohta, C. Obuse, and T. Tsurimoto. 2002. PCNA clamp facilitates action of DNA cytosine methyltransferase 1 on hemimethylated DNA. *Genes Cells.* 7:997-1007.

Iizuka, M., and M.M. Smith. 2003. Functional consequences of histone modifications. *Curr Opin Genet Dev.* 13:154-60.

Ioshikhes, I., A. Bolshoy, K. Derenshteyn, M. Borodovsky, and E.N. Trifonov. 1996. Nucleosome DNA sequence pattern revealed by multiple alignment of experimentally mapped sequences. *J Mol Biol.* 262:129-39.

Ioshikhes, I.P., I. Albert, S.J. Zanton, and B.F. Pugh. 2006. Nucleosome positions predicted through comparative genomics. *Nat Genet.* 38:1210-5.

Issa, J.P. 2000. CpG-island methylation in aging and cancer. *Curr Top Microbiol Immunol.* 249:101-18.

Ito, T., M. Bulger, M.J. Pazin, R. Kobayashi, and J.T. Kadonaga. 1997a. ACF, an ISWI-containing and ATP-utilizing chromatin assembly and remodeling factor. *Cell.* 90:145-155.

Ito, T., J.K. Tyler, and J.T. Kadonaga. 1997b. Chromatin assembly factors: a dual function in nucleosome formation and mobilization? *Genes Cells.* 2:593-600.

Iyer, V., and K. Struhl. 1995. Poly(dA:dT), a ubiquitous promoter element that stimulates transcription via its intrinsic DNA structure. *Embo J.* 14:2570-9.

Jackson, V. 1990. In vivo studies on the dynamics of histone-DNA interaction: evidence for nucleosome dissolution during replication and transcription and a low level of dissolution independent of both. *Biochemistry.* 29:719-31.

Jacobs, S.A., and S. Khorasanizadeh. 2002. Structure of HP1 chromodomain bound to a lysine 9-methylated histone H3 tail. *Science.* 295:2080-3.

Jacobson, R.H., A.G. Ladurner, D.S. King, and R. Tjian. 2000. Structure and function of a human TAFII250 double bromodomain module. *Science.* 288:1422-5.

Jaenisch, R. 1997. DNA methylation and imprinting: why bother? *Trends Genet.* 13:323-9.

Jair, K.W., K.E. Bachman, H. Suzuki, A.H. Ting, I. Rhee, R.W. Yen, S.B. Baylin, and K.E. Schuebel. 2006. De novo CpG island methylation in human cancer cells. *Cancer Res.* 66:682-92.

Januchowski, R., J. Prokop, and P.P. Jagodzinski. 2004. Role of epigenetic DNA alterations in the pathogenesis of systemic lupus erythematosus. *J Appl Genet.* 45:237-48.

Jarvis, C.D., T. Geiman, M.P. Vila-Storm, O. Osipovich, U. Akella, S. Candeias, I. Nathan, S.K. Durum, and K. Muegge. 1996. A novel putative helicase produced in early murine lymphocytes. *Gene.* 169:203-7.

Jaskelioff, M., I.M. Gavin, C.L. Peterson, and C. Logie. 2000. SWI-SNF-mediated nucleosome remodeling: role of histone octamer mobility in the persistence of the remodeled state. *Mol Cell Biol.* 20:3058-68.

Jeddeloh, J.A., T.L. Stokes, and E.J. Richards. 1999. Maintenance of genomic methylation requires a SWI2/SNF2-like protein. *Nat.Genet.* 22:94-97.

Jeltsch, A. 2002. Beyond Watson and Crick: DNA methylation and molecular enzymology of DNA methyltransferases. *Chembiochem.* 3:274-293.

Jeltsch, A. 2006. Molecular enzymology of mammalian DNA methyltransferases. *Curr Top Microbiol Immunol.* 301:203-25.

Jenuwein, T., and C.D. Allis. 2001. Translating the histone code. *Science.* 293:1074-1080.

Jia, D., R.Z. Jurkowska, X. Zhang, A. Jeltsch, and X. Cheng. 2007. Structure of Dnmt3a bound to Dnmt3L suggests a model for de novo DNA methylation. *Nature.* 449:248-51.

Jiang, C., and B.F. Pugh. 2009. Nucleosome positioning and gene regulation: advances through genomics. *Nat Rev Genet.* 10:161-72.

Jin, J., Y. Cai, T. Yao, A.J. Gottschalk, L. Florens, S.K. Swanson, J.L. Gutierrez, M.K. Coleman, J.L. Workman, A. Mushegian, M.P. Washburn, R.C. Conaway, and J.W. Conaway. 2005. A mammalian chromatin remodeling complex with similarities to the yeast Ino80 complex. *J Biol Chem.* 280:41207-12.

Jones, P.A. 1999. The DNA methylation paradox. *Trends Genet.* 15:34-7.

Jurkowska, R.Z., N. Anspach, C. Urbanke, D. Jia, R. Reinhardt, W. Nellen, X. Cheng, and A. Jeltsch. 2008. Formation of nucleoprotein filaments by mammalian DNA methyltransferase Dnmt3a in complex with regulator Dnmt3L. *Nucleic Acids Res.* 36:6656-63.

Jurkowski, T.P., M. Meusburger, S. Phalke, M. Helm, W. Nellen, G. Reuter, and A. Jeltsch. 2008. Human DNMT2 methylates tRNA(Asp) molecules using a DNA methyltransferase-like catalytic mechanism. *Rna.* 14:1663-70.

Kadam, S., and B.M. Emerson. 2002. Mechanisms of chromatin assembly and transcription. *Curr Opin Cell Biol.* 14:262-8.

Kadam, S., and B.M. Emerson. 2003. Transcriptional specificity of human SWI/SNF Brg1 and BRM chromatin remodeling complexes. *Mol Cell.* 11:377-89.

Kagalwala, M.N., B.J. Glaus, W. Dang, M. Zofall, and B. Bartholomew. 2004. Topography of the ISW2-nucleosome complex: insights into nucleosome spacing and chromatin remodeling. *Embo J.* 23:2092-104.

Kaneda, M., M. Okano, K. Hata, T. Sado, N. Tsujimoto, E. Li, and H. Sasaki. 2004. Essential role for de novo DNA methyltransferase Dnmt3a in paternal and maternal imprinting. *Nature.* 429:900-903.

Kang, E.S., C.W. Park, and J.H. Chung. 2001. Dnmt3b, de novo DNA methyltransferase, interacts with SUMO-1 and Ubc9 through its N-terminal region and is subject to modification by SUMO-1. *Biochem Biophys Res Commun.* 289:862-8.

Kang, J.G., A. Hamiche, and C. Wu. 2002. GAL4 directs nucleosome sliding induced by NURF. *Embo J.* 21:1406-13.

Kaplan, N., I.K. Moore, Y. Fondufe-Mittendorf, A.J. Gossett, D. Tillo, Y. Field, E.M. LeProust, T.R. Hughes, J.D. Lieb, J. Widom, and E. Segal. 2009. The DNA-encoded nucleosome organization of a eukaryotic genome. *Nature.* 458:362-6.

Kaplan, T., C.L. Liu, J.A. Erkmann, J. Holik, M. Grunstein, P.D. Kaufman, N. Friedman, and O.J. Rando. 2008. Cell cycle- and chaperone-mediated regulation of H3K56ac incorporation in yeast. *PLoS Genet.* 4:e1000270.

Kassabov, S.R., N.M. Henry, M. Zofall, T. Tsukiyama, and B. Bartholomew. 2002a. High-resolution mapping of changes in histone-DNA contacts of nucleosomes remodeled by ISW2. *Mol.Cell Biol.* 22:7524-7534.

Kassabov, S.R., N.M. Henry, M. Zofall, T. Tsukiyama, and B. Bartholomew. 2002b. High-resolution mapping of changes in histone-DNA contacts of nucleosomes remodeled by ISW2. *Mol Cell Biol.* 22:7524-34.

Kassabov, S.R., B. Zhang, J. Persinger, and B. Bartholomew. 2003. SWI/SNF unwraps, slides, and rewraps the nucleosome. *Mol Cell.* 11:391-403.

Kastaniotis, A.J., T.A. Mennella, C. Konrad, A.M. Torres, and R.S. Zitomer. 2000. Roles of transcription factor Mot3 and chromatin in repression of the hypoxic gene ANB1 in yeast. *Mol Cell Biol.* 20:7088-98.

Kelley, D.E., D.G. Stokes, and R.P. Perry. 1999. Chd1 interacts with SSRP1 and depends on both its chromodomain and its ATPase/helicase-like domain for proper association with chromatin. *Chromosoma.* 108:10-25.

Khorasanizadeh, S. 2004. The nucleosome: from genomic organization to genomic regulation. *Cell.* 116:259-272.

Kim, G.D., J. Ni, N. Kelesoglu, R.J. Roberts, and S. Pradhan. 2002. Co-operation and communication between the human maintenance and de novo DNA (cytosine-5) methyltransferases. *Embo J.* 21:4183-95.

Kimura, H., T. Nakamura, T. Ogawa, S. Tanaka, and K. Shiota. 2003. Transcription of mouse DNA methyltransferase 1 (Dnmt1) is regulated by both E2F-Rb-HDAC-dependent and -independent pathways. *Nucleic Acids Res.* 31:3101-13.

Kimura, H., and K. Shiota. 2003. Methyl-CpG-binding protein, MeCP2, is a target molecule for maintenance DNA methyltransferase, Dnmt1. *J Biol Chem.* 278:4806-12.

Kiskinis, E., M. Hallberg, M. Christian, M. Olofsson, S.M. Dilworth, R. White, and M.G. Parker. 2007. RIP140 directs histone and DNA methylation to silence Ucp1 expression in white adipocytes. *Embo J.* 26:4831-40.

Klimasauskas, S., S. Kumar, R.J. Roberts, and X. Cheng. 1994. HhaI methyltransferase flips its target base out of the DNA helix. *Cell*. 76:357-369.

Klose, R.J., E.M. Kallin, and Y. Zhang. 2006a. JmjC-domain-containing proteins and histone demethylation. *Nat Rev Genet*. 7:715-27.

Klose, R.J., K. Yamane, Y. Bae, D. Zhang, H. Erdjument-Bromage, P. Tempst, J. Wong, and Y. Zhang. 2006b. The transcriptional repressor JHDM3A demethylates trimethyl histone H3 lysine 9 and lysine 36. *Nature*. 442:312-6.

Klug, M., and M. Rehli. 2006. Functional analysis of promoter CpG methylation using a CpG-free luciferase reporter vector. *Epigenetics*. 1:127-30.

Kondo, T., M.P. Bobek, R. Kuick, B. Lamb, X. Zhu, A. Narayan, D. Bourc'his, E. Viegas-Pequignot, M. Ehrlich, and S.M. Hanash. 2000. Whole-genome methylation scan in ICF syndrome: hypomethylation of non-satellite DNA repeats D4Z4 and NBL2. *Hum Mol Genet*. 9:597-604.

Konev, A.Y., M. Tribus, S.Y. Park, V. Podhraski, C.Y. Lim, A.V. Emelyanov, E. Vershilova, V. Pirrotta, J.T. Kadonaga, A. Lusser, and D.V. Fyodorov. 2007. Chd1 motor protein is required for deposition of histone variant H3.3 into chromatin in vivo. *Science*. 317:1087-90.

Korber, P., and W. Horz. 2004. SWRred not shaken; mixing the histones. *Cell*. 117:5-7.

Korber, P., T. Luckenbach, D. Blaschke, and W. Horz. 2004. Evidence for histone eviction in trans upon induction of the yeast PHO5 promoter. *Mol Cell Biol*. 24:10965-74.

Kornberg, R.D. 1974. Chromatin structure: a repeating unit of histones and DNA. *Science*. 184:868-871.

Kornberg, R.D., and L. Stryer. 1988. Statistical distributions of nucleosomes: nonrandom locations by a stochastic mechanism. *Nucleic Acids Res*. 16:6677-90.

Kouzarides, T. 2007. Chromatin modifications and their function. *Cell*. 128:693-705.

Krumm, A., T. Meulia, M. Brunvand, and M. Groudine. 1992. The block to transcriptional elongation within the human c-myc gene is determined in the promoter-proximal region. *Genes Dev*. 6:2201-13.

Kumar, S., X. Cheng, S. Klimasauskas, S. Mi, J. Posfai, R.J. Roberts, and G.G. Wilson. 1994. The DNA (cytosine-5) methyltransferases. *Nucleic Acids Res*. 22:1-10.

Kunert, N., E. Wagner, M. Murawska, H. Klinker, E. Kremmer, and A. Brehm. 2009. dMec: a novel Mi-2 chromatin remodelling complex involved in transcriptional repression. *Embo J*. 28:533-44.

Kunkel, G.R., and H.G. Martinson. 1981. Nucleosomes will not form on double-stranded RNa or over poly(dA).poly(dT) tracts in recombinant DNA. *Nucleic Acids Res*. 9:6869-88.

Landick, R. 2006. The regulatory roles and mechanism of transcriptional pausing. *Biochem Soc Trans*. 34:1062-6.

Längst, G., and P.B. Becker. 2001a. ISWI induces nucleosome sliding on nicked DNA. *Mol.Cell*. 8:1085-1092.

Längst, G., and P.B. Becker. 2001b. Nucleosome mobilization and positioning by ISWI-containing chromatin-remodeling factors. *J.Cell Sci.* 114:2561-2568.

Längst, G., and P.B. Becker. 2004. Nucleosome remodeling: one mechanism, many phenomena? *Biochim.Biophys.Acta.* 1677:58-63.

Langst, G., E.J. Bonte, D.F. Corona, and P.B. Becker. 1999. Nucleosome movement by CHRAC and ISWI without disruption or trans-displacement of the histone octamer. *Cell.* 97:843-52.

Längst, G., E.J. Bonte, D.F. Corona, and P.B. Becker. 1999. Nucleosome movement by CHRAC and ISWI without disruption or trans-displacement of the histone octamer. *Cell.* 97:843-852.

Langst, G., T. Schatz, J. Langowski, and I. Grummt. 1997. Structural analysis of mouse rDNA: coincidence between nuclease hypersensitive sites, DNA curvature and regulatory elements in the intergenic spacer. *Nucleic Acids Res.* 25:511-7.

Larsen, F., G. Gundersen, R. Lopez, and H. Prydz. 1992. CpG islands as gene markers in the human genome. *Genomics.* 13:1095-107.

Laurent, B.C., I. Treich, and M. Carlson. 1993. The yeast SNF2/SWI2 protein has DNA-stimulated ATPase activity required for transcriptional activation. *Genes Dev.* 7:583-91.

Lehnertz, B., Y. Ueda, A.A. Derijck, U. Braunschweig, L. Perez-Burgos, S. Kubicek, T. Chen, E. Li, T. Jenuwein, and A.H. Peters. 2003. Suv39h-mediated histone H3 lysine 9 methylation directs DNA methylation to major satellite repeats at pericentric heterochromatin. *Curr.Biol.* 13:1192-1200.

Leonhardt, H., and M.C. Cardoso. 2000. DNA methylation, nuclear structure, gene expression and cancer. *J.Cell Biochem.Suppl.* Suppl 35:78-83.

Leonhardt, H., A.W. Page, H.U. Weier, and T.H. Bestor. 1992. A targeting sequence directs DNA methyltransferase to sites of DNA replication in mammalian nuclei. *Cell.* 71:865-873.

LeRoy, G., A. Loyola, W.S. Lane, and D. Reinberg. 2000. Purification and characterization of a human factor that assembles and remodels chromatin. *J Biol Chem.* 275:14787-90.

Li, B., M. Carey, and J.L. Workman. 2007. The role of chromatin during transcription. *Cell.* 128:707-19.

Li, B., S.G. Pattenden, D. Lee, J. Gutierrez, J. Chen, C. Seidel, J. Gerton, and J.L. Workman. 2005. Preferential occupancy of histone variant H2AZ at inactive promoters influences local histone modifications and chromatin remodeling. *Proc Natl Acad Sci U S A.* 102:18385-90.

Li, B., and J.C. Reese. 2001. Ssn6-Tup1 regulates RNR3 by positioning nucleosomes and affecting the chromatin structure at the upstream repression sequence. *J Biol Chem.* 276:33788-97.

Li, E. 2002. Chromatin modification and epigenetic reprogramming in mammalian development. *Nat Rev Genet.* 3:662-73.

Li, E., T.H. Bestor, and R. Jaenisch. 1992. Targeted mutation of the DNA methyltransferase gene results in embryonic lethality. *Cell.* 69:915-926.

Li, J., G. Langst, and I. Grummt. 2006. NoRC-dependent nucleosome positioning silences rRNA genes. *Embo J.* 25:5735-41.

Li, Q., O. Wrange, and P. Eriksson. 1997. The role of chromatin in transcriptional regulation. *Int J Biochem Cell Biol.* 29:731-42.

Liang, G., M.F. Chan, Y. Tomigahara, Y.C. Tsai, F.A. Gonzales, E. Li, P.W. Laird, and P.A. Jones. 2002. Cooperativity between DNA methyltransferases in the maintenance methylation of repetitive elements. *Mol.Cell Biol.* 22:480-491.

Liang, G., C.E. Salem, M.C. Yu, H.D. Nguyen, F.A. Gonzales, T.T. Nguyen, P.W. Nichols, and P.A. Jones. 1998. DNA methylation differences associated with tumor tissues identified by genome scanning analysis. *Genomics.* 53:260-8.

Ling, Y., U.T. Sankpal, A.K. Robertson, J.G. McNally, T. Karpova, and K.D. Robertson. 2004. Modification of de novo DNA methyltransferase 3a (Dnmt3a) by SUMO-1 modulates its interaction with histone deacetylases (HDACs) and its capacity to repress transcription. *Nucleic Acids Res.* 32:598-610.

Liu, K., Y.F. Wang, C. Cantemir, and M.T. Muller. 2003. Endogenous assays of DNA methyltransferases: Evidence for differential activities of DNMT1, DNMT2, and DNMT3 in mammalian cells in vivo. *Mol.Cell Biol.* 23:2709-2719.

Liu, Y., E.J. Oakeley, L. Sun, and J.P. Jost. 1998. Multiple domains are involved in the targeting of the mouse DNA methyltransferase to the DNA replication foci. *Nucleic Acids Res.* 26:1038-1045.

Lorch, Y., J.W. LaPointe, and R.D. Kornberg. 1987. Nucleosomes inhibit the initiation of transcription but allow chain elongation with the displacement of histones. *Cell.* 49:203-10.

Lorch, Y., M. Zhang, and R.D. Kornberg. 2001. RSC unravels the nucleosome. *Mol Cell.* 7:89-95.

Lowary, P.T., and J. Widom. 1998. New DNA sequence rules for high affinity binding to histone octamer and sequence-directed nucleosome positioning. *J.Mol.Biol.* 276:19-42.

Luger, K. 2002. The tail does not always wag the dog. *Nat Genet.* 32:221-2.

Luger, K. 2006. Dynamic nucleosomes. *Chromosome Res.* 14:5-16.

Luger, K., A.W. Mader, R.K. Richmond, D.F. Sargent, and T.J. Richmond. 1997. Crystal structure of the nucleosome core particle at 2.8 A resolution. *Nature.* 389:251-60.

Luger, K., and T.J. Richmond. 1998. The histone tails of the nucleosome. *Curr Opin Genet Dev.* 8:140-6.

Lusser, A., and J.T. Kadonaga. 2003. Chromatin remodeling by ATP-dependent molecular machines. *Bioessays.* 25:1192-1200.

Lusser, A., and J.T. Kadonaga. 2004. Strategies for the reconstitution of chromatin. *Nat Methods.* 1:19-26.

Lusser, A., D.L. Urwin, and J.T. Kadonaga. 2005. Distinct activities of Chd1 and ACF in ATP-dependent chromatin assembly. *Nat Struct Mol Biol.* 12:160-6.

Lyko, F., B.H. Ramsahoye, and R. Jaenisch. 2000. DNA methylation in *Drosophila* melanogaster. *Nature.* 408:538-40.

Lyko, F., B.H. Ramsahoye, H. Kashevsky, M. Tudor, M.A. Mastrangelo, T.L. Orr-Weaver, and R. Jaenisch. 1999. Mammalian (cytosine-5) methyltransferases cause genomic DNA methylation and lethality in *Drosophila. Nat.Genet.* 23:363-366.

Maier, V.K., M. Chioda, D. Rhodes, and P.B. Becker. 2008. ACF catalyses chromatosome movements in chromatin fibres. *Embo J.* 27:817-26.

Maison, C., D. Bailly, A.H. Peters, J.P. Quivy, D. Roche, A. Taddei, M. Lachner, T. Jenuwein, and G. Almouzni. 2002. Higher-order structure in pericentric heterochromatin involves a distinct pattern of histone modification and an RNA component. *Nat Genet.* 30:329-34.

Margot, J.B., A.M. Aguirre-Arteta, B.V. Di Giacco, S. Pradhan, R.J. Roberts, M.C. Cardoso, and H. Leonhardt. 2000. Structure and function of the mouse DNA methyltransferase gene: Dnmt1 shows a tripartite structure. *J.Mol.Biol.* 297:293-300.

Margot, J.B., A.E. Ehrenhofer-Murray, and H. Leonhardt. 2003. Interactions within the mammalian DNA methyltransferase family. *BMC.Mol.Biol.* 4:7.

Marilley, M., and P. Pasero. 1996. Common DNA structural features exhibited by eukaryotic ribosomal gene promoters. *Nucleic Acids Res.* 24:2204-11.

Marmorstein, R., and S.L. Berger. 2001. Structure and function of bromodomains in chromatin-regulating complexes. *Gene.* 272:1-9.

Martens, J.A., and F. Winston. 2003. Recent advances in understanding chromatin remodeling by Swi/Snf complexes. *Curr Opin Genet Dev.* 13:136-42.

Martienssen, R., and S. Henikoff. 1999. The House & Garden guide to chromatin remodelling. *Nat.Genet.* 22:6-7.

Mavrich, T.N., I.P. Ioshikhes, B.J. Venters, C. Jiang, L.P. Tomsho, J. Qi, S.C. Schuster, I. Albert, and B.F. Pugh. 2008a. A barrier nucleosome model for statistical positioning of nucleosomes throughout the yeast genome. *Genome Res.* 18:1073-83.

Mavrich, T.N., C. Jiang, I.P. Ioshikhes, X. Li, B.J. Venters, S.J. Zanton, L.P. Tomsho, J. Qi, R.L. Glaser, S.C. Schuster, D.S. Gilmour, I. Albert, and B.F. Pugh. 2008b. Nucleosome organization in the *Drosophila* genome. *Nature.* 453:358-62.

Mays-Hoopes, L., W. Chao, H.C. Butcher, and R.C. Huang. 1986. Decreased methylation of the major mouse long interspersed repeated DNA during aging and in myeloma cells. *Dev Genet.* 7:65-73.

Meints, G.A., and G.P. Drobny. 2001. Dynamic impact of methylation at the M. Hhai target site: a solid-state deuterium NMR study. *Biochemistry.* 40:12436-43.

Mello, J.A., H.H. Sillje, D.M. Roche, D.B. Kirschner, E.A. Nigg, and G. Almouzni. 2002. Human Asf1 and CAF-1 interact and synergize in a repair-coupled nucleosome assembly pathway. *EMBO Rep.* 3:329-34.

Mellor, J., and A. Morillon. 2004. ISWI complexes in Saccharomyces cerevisiae. *Biochim Biophys Acta.* 1677:100-12.

Mertineit, C., J.A. Yoder, T. Taketo, D.W. Laird, J.M. Trasler, and T.H. Bestor. 1998. Sex-specific exons control DNA methyltransferase in mammalian germ cells. *Development.* 125:889-897.

Miura, A., S. Yonebayashi, K. Watanabe, T. Toyama, H. Shimada, and T. Kakutani. 2001. Mobilization of transposons by a mutation abolishing full DNA methylation in Arabidopsis. *Nature*. 411:212-4.

Mizuguchi, G., X. Shen, J. Landry, W.H. Wu, S. Sen, and C. Wu. 2004. ATP-driven exchange of histone H2AZ variant catalyzed by SWR1 chromatin remodeling complex. *Science*. 303:343-8.

Mizuguchi, G., T. Tsukiyama, J. Wisniewski, and C. Wu. 1997. Role of nucleosome remodeling factor NURF in transcriptional activation of chromatin. *Mol.Cell*. 1:141-150.

Mohrmann, L., and C.P. Verrijzer. 2005. Composition and functional specificity of SWI2/SNF2 class chromatin remodeling complexes. *Biochim Biophys Acta*. 1681:59-73.

Momparler, R.L., and V. Bovenzi. 2000. DNA methylation and cancer. *J Cell Physiol*. 183:145-54.

Morrison, A.J., J. Highland, N.J. Krogan, A. Arbel-Eden, J.F. Greenblatt, J.E. Haber, and X. Shen. 2004. Ino80 and gamma-H2AX interaction links ATP-dependent chromatin remodeling to DNA damage repair. *Cell*. 119:767-75.

Mortusewicz, O., L. Schermelleh, J. Walter, M.C. Cardoso, and H. Leonhardt. 2005. Recruitment of DNA methyltransferase I to DNA repair sites. *Proc Natl Acad Sci U S A*. 102:8905-9.

Mosammaparast, N., C.S. Ewart, and L.F. Pemberton. 2002. A role for nucleosome assembly protein 1 in the nuclear transport of histones H2A and H2B. *Embo J*. 21:6527-38.

Murawska, M., N. Kunert, J. van Vugt, G. Langst, E. Kremmer, C. Logie, and A. Brehm. 2008. dCHD3, a novel ATP-dependent chromatin remodeler associated with sites of active transcription. *Mol Cell Biol*. 28:2745-57.

Murray, K. 1964. The Occurrence of Epsilon-N-Methyl Lysine in Histones. *Biochemistry*. 3:10-5.

Myant, K., and I. Stancheva. 2008. LSH cooperates with DNA methyltransferases to repress transcription. *Mol Cell Biol*. 28:215-26.

Nakao, M. 2001. Epigenetics: interaction of DNA methylation and chromatin. *Gene*. 278:25-31.

Narlikar, L., R. Gordan, and A.J. Hartemink. 2007. A nucleosome-guided map of transcription factor binding sites in yeast. *PLoS Comput Biol*. 3:e215.

Nathan, D., and D.M. Crothers. 2002. Bending and flexibility of methylated and unmethylated EcoRI DNA. *J Mol Biol*. 316:7-17.

Nelson, H.C., J.T. Finch, B.F. Luisi, and A. Klug. 1987. The structure of an oligo(dA).oligo(dT) tract and its biological implications. *Nature*. 330:221-6.

Ng, H.H., F. Robert, R.A. Young, and K. Struhl. 2002. Genome-wide location and regulated recruitment of the RSC nucleosome-remodeling complex. *Genes Dev*. 16:806-19.

Nicholls, R.D., S. Saitoh, and B. Horsthemke. 1998. Imprinting in Prader-Willi and Angelman syndromes. *Trends Genet*. 14:194-200.

Nilsen, H., T. Lindahl, and A. Verreault. 2002. DNA base excision repair of uracil residues in reconstituted nucleosome core particles. *Embo J*. 21:5943-52.

Nirenberg, M.W. 1963. The genetic code. II. *Sci Am.* 208:80-94.

Nirenberg, M.W., J.H. Matthaei, O.W. Jones, R.G. Martin, and S.H. Barondes. 1963. Approximation of genetic code via cell-free protein synthesis directed by template RNA. *Fed Proc.* 22:55-61.

Ohsawa, K., Y. Imai, D. Ito, and S. Kohsaka. 1996. Molecular cloning and characterization of annexin V-binding proteins with highly hydrophilic peptide structure. *J.Neurochem.* 67:89-97.

Okano, M., D.W. Bell, D.A. Haber, and E. Li. 1999a. DNA methyltransferases Dnmt3a and Dnmt3b are essential for de novo methylation and mammalian development. *Cell.* 99:247-257.

Okano, M., S. Takebayashi, K. Okumura, and E. Li. 1999b. Assignment of cytosine-5 DNA methyltransferases Dnmt3a and Dnmt3b to mouse chromosome bands 12A2-A3 and 2H1 by in situ hybridization. *Cytogenet.Cell Genet.* 86:333-334.

Okano, M., S. Xie, and E. Li. 1998a. Cloning and characterization of a family of novel mammalian DNA (cytosine-5) methyltransferases. *Nat.Genet.* 19:219-220.

Okano, M., S. Xie, and E. Li. 1998b. Dnmt2 is not required for de novo and maintenance methylation of viral DNA in embryonic stem cells. *Nucleic Acids Res.* 26:2536-2540.

Okuwaki, M., and A. Verreault. 2004. Maintenance DNA methylation of nucleosome core particles. *J.Biol.Chem.* 279:2904-2912.

Olins, A.L., and D.E. Olins. 1974. Spheroid chromatin units (v bodies). *Science.* 183:330-332.

Olins, D.E., and A.L. Olins. 2003. Chromatin history: our view from the bridge. *Nat.Rev.Mol.Cell Biol.* 4:809-814.

Ooi, S.K., C. Qiu, E. Bernstein, K. Li, D. Jia, Z. Yang, H. Erdjument-Bromage, P. Tempst, S.P. Lin, C.D. Allis, X. Cheng, and T.H. Bestor. 2007. DNMT3L connects unmethylated lysine 4 of histone H3 to de novo methylation of DNA. *Nature.* 448:714-7.

Oudet, P., M. Gross-Bellard, and P. Chambon. 1975. Electron microscopic and biochemical evidence that chromatin structure is a repeating unit. *Cell.* 4:281-300.

Ozsolak, F., J.S. Song, X.S. Liu, and D.E. Fisher. 2007. High-throughput mapping of the chromatin structure of human promoters. *Nat Biotechnol.* 25:244-8.

Palen, T.E., and T.R. Cech. 1984. Chromatin structure at the replication origins and transcription-initiation regions of the ribosomal RNA genes of Tetrahymena. *Cell.* 36:933-42.

Palmer, D.K., K. O'Day, H.L. Trong, H. Charbonneau, and R.L. Margolis. 1991. Purification of the centromere-specific protein CENP-A and demonstration that it is a distinctive histone. *Proc Natl Acad Sci U S A.* 88:3734-8.

Papamichos-Chronakis, M., J.E. Krebs, and C.L. Peterson. 2006. Interplay between Ino80 and Swr1 chromatin remodeling enzymes regulates cell cycle checkpoint adaptation in response to DNA damage. *Genes Dev.* 20:2437-49.

Parnell, T.J., J.T. Huff, and B.R. Cairns. 2008. RSC regulates nucleosome positioning at Pol II genes and density at Pol III genes. *Embo J.* 27:100-10.

Paro, R., and D.S. Hogness. 1991. The Polycomb protein shares a homologous domain with a heterochromatin-associated protein of *Drosophila*. *Proc Natl Acad Sci U S A.* 88:263-7.

Passarge, E. 1979. Emil Heitz and the concept of heterochromatin: longitudinal chromosome differentiation was recognized fifty years ago. *Am J Hum Genet.* 31:106-15.

Pazin, M.J., P. Bhargava, E.P. Geiduschek, and J.T. Kadonaga. 1997. Nucleosome mobility and the maintenance of nucleosome positioning. *Science.* 276:809-12.

Pazin, M.J., and J.T. Kadonaga. 1997. SWI2/SNF2 and related proteins: ATP-driven motors that disrupt protein-DNA interactions? *Cell.* 88:737-40.

Peckham, H.E., R.E. Thurman, Y. Fu, J.A. Stamatoyannopoulos, W.S. Noble, K. Struhl, and Z. Weng. 2007. Nucleosome positioning signals in genomic DNA. *Genome Res.* 17:1170-7.

Pederson, T. 2004. The spatial organization of the genome in mammalian cells. *Curr Opin Genet Dev.* 14:203-9.

Pennings, S., J. Allan, and C.S. Davey. 2005. DNA methylation, nucleosome formation and positioning. *Brief Funct Genomic Proteomic.* 3:351-61.

Peterson, C.L., and I. Herskowitz. 1992. Characterization of the yeast SWI1, SWI2, and SWI3 genes, which encode a global activator of transcription. *Cell.* 68:573-83.

Peterson, C.L., and C. Logie. 2000. Recruitment of chromatin remodeling machines. *J Cell Biochem.* 78:179-85.

Polach, K.J., and J. Widom. 1995. Mechanism of protein access to specific DNA sequences in chromatin: a dynamic equilibrium model for gene regulation. *J Mol Biol.* 254:130-49.

Poot, R.A., L. Bozhenok, D.L. van den Berg, S. Steffensen, F. Ferreira, M. Grimaldi, N. Gilbert, J. Ferreira, and P.D. Varga-Weisz. 2004. The Williams syndrome transcription factor interacts with PCNA to target chromatin remodelling by ISWI to replication foci. *Nat Cell Biol.* 6:1236-44.

Poot, R.A., G. Dellaire, B.B. Hulsmann, M.A. Grimaldi, D.F. Corona, P.B. Becker, W.A. Bickmore, and P.D. Varga-Weisz. 2000a. HuCHRAC, a human ISWI chromatin remodelling complex contains hACF1 and two novel histone-fold proteins. *Embo J.* 19:3377-87.

Poot, R.A., G. Dellaire, B.B. Hulsmann, M.A. Grimaldi, D.F. Corona, P.B. Becker, W.A. Bickmore, and P.D. Varga-Weisz. 2000b. HuCHRAC, a human ISWI chromatin remodelling complex contains hACF1 and two novel histone-fold proteins. *EMBO J.* 19:3377-3387.

Posfai, J., A.S. Bhagwat, G. Posfai, and R.J. Roberts. 1989. Predictive motifs derived from cytosine methyltransferases. *Nucleic Acids Res.* 17:2421-35.

Pradhan, M., P.O. Esteve, H.G. Chin, M. Samaranayke, G.D. Kim, and S. Pradhan. 2008. CXXC domain of human DNMT1 is essential for enzymatic activity. *Biochemistry.* 47:10000-9.

Pradhan, S., A. Bacolla, R.D. Wells, and R.J. Roberts. 1999. Recombinant human DNA (cytosine-5) methyltransferase. I. Expression, purification, and comparison of de novo and maintenance methylation. *J.Biol.Chem.* 274:33002-33010.

Pradhan, S., and P.O. Esteve. 2003a. Allosteric activator domain of maintenance human DNA (cytosine-5) methyltransferase and its role in methylation spreading. *Biochemistry.* 42:5321-5332.

Pradhan, S., and P.O. Esteve. 2003b. Mammalian DNA (cytosine-5) methyltransferases and their expression. *Clin.Immunol.* 109:6-16.

Pradhan, S., and G.D. Kim. 2002. The retinoblastoma gene product interacts with maintenance human DNA (cytosine-5) methyltransferase and modulates its activity. *Embo J.* 21:779-88.

Pradhan, S., D. Talbot, M. Sha, J. Benner, L. Hornstra, E. Li, R. Jaenisch, and R.J. Roberts. 1997. Baculovirus-mediated expression and characterization of the full-length murine DNA methyltransferase. *Nucleic Acids Res.* 25:4666-4673.

Prunell, A., and R.D. Kornberg. 1978. Relation of nucleosomes to nucleotide sequences in the rat. *Philos Trans R Soc Lond B Biol Sci.* 283:269-73.

Qiu, C., K. Sawada, X. Zhang, and X. Cheng. 2002. The PWWP domain of mammalian DNA methyltransferase Dnmt3b defines a new family of DNA-binding folds. *Nat.Struct.Biol.* 9:217-224.

Ramachandran, A., M. Omar, P. Cheslock, and G.R. Schnitzler. 2003. Linker histone H1 modulates nucleosome remodeling by human SWI/SNF. *J Biol Chem.* 278:48590-601.

Ramakrishnan, V. 1997. Histone H1 and chromatin higher-order structure. *Crit Rev Eukaryot Gene Expr.* 7:215-30.

Ramirez-Carrozzi, V.R., D. Braas, D.M. Bhatt, C.S. Cheng, C. Hong, K.R. Doty, J.C. Black, A. Hoffmann, M. Carey, and S.T. Smale. 2009. A unifying model for the selective regulation of inducible transcription by CpG islands and nucleosome remodeling. *Cell.* 138:114-28.

Ramirez-Carrozzi, V.R., A.A. Nazarian, C.C. Li, S.L. Gore, R. Sridharan, A.N. Imbalzano, and S.T. Smale. 2006. Selective and antagonistic functions of SWI/SNF and Mi-2beta nucleosome remodeling complexes during an inflammatory response. *Genes Dev.* 20:282-96.

Ramsahoye, B.H., D. Biniszkiewicz, F. Lyko, V. Clark, A.P. Bird, and R. Jaenisch. 2000. Non-CpG methylation is prevalent in embryonic stem cells and may be mediated by DNA methyltransferase 3a. *Proc Natl Acad Sci U S A.* 97:5237-42.

Ramsay, N., G. Felsenfeld, B.M. Rushton, and J.D. McGhee. 1984. A 145-base pair DNA sequence that positions itself precisely and asymmetrically on the nucleosome core. *Embo J.* 3:2605-11.

Randerath, K., W.C. Tseng, J.S. Harris, and L.J. Lu. 1983. Specific effects of 5-fluoropyrimidines and 5-azapyrimidines on modification of the 5 position of pyrimidines, in particular the synthesis of 5-methyluracil and 5-methylcytosine in nucleic acids. *Recent Results Cancer Res.* 84:283-97.

Ray-Gallet, D., J.P. Quivy, C. Scamps, E.M. Martini, M. Lipinski, and G. Almouzni. 2002. HIRA is critical for a nucleosome assembly pathway independent of DNA synthesis. *Mol Cell.* 9:1091-100.

Razin, A. 1998. CpG methylation, chromatin structure and gene silencing-a three-way connection. *Embo J.* 17:4905-8.

Reale, A., G.D. Matteis, G. Galleazzi, M. Zampieri, and P. Caiafa. 2005. Modulation of DNMT1 activity by ADP-ribose polymers. *Oncogene.* 24:13-9.

Redon, C., D. Pilch, E. Rogakou, O. Sedelnikova, K. Newrock, and W. Bonner. 2002. Histone H2A variants H2AX and H2AZ. *Curr Opin Genet Dev.* 12:162-9.

Reik, W., A. Collick, M.L. Norris, S.C. Barton, and M.A. Surani. 1987. Genomic imprinting determines methylation of parental alleles in transgenic mice. *Nature.* 328:248-51.

Reik, W., W. Dean, and J. Walter. 2001. Epigenetic reprogramming in mammalian development. *Science.* 293:1089-1093.

Reik, W., and E.R. Maher. 1997. Imprinting in clusters: lessons from Beckwith-Wiedemann syndrome. *Trends Genet.* 13:330-4.

Reik, W., and A. Murrell. 2000. Genomic imprinting. Silence across the border. *Nature.* 405:408-409.

Reik, W., and J. Walter. 2001a. Evolution of imprinting mechanisms: the battle of the sexes begins in the zygote. *Nat.Genet.* 27:255-256.

Reik, W., and J. Walter. 2001b. Genomic imprinting: parental influence on the genome. *Nat.Rev.Genet.* 2:21-32.

Reuter, G., and P. Spierer. 1992. Position effect variegation and chromatin proteins. *Bioessays.* 14:605-12.

Rhodes, D., and R.A. Laskey. 1989. Assembly of nucleosomes and chromatin in vitro. *Methods Enzymol.* 170:575-585.

Richmond, T.J., and C.A. Davey. 2003. The structure of DNA in the nucleosome core. *Nature.* 423:145-150.

Rippe, K., A. Schrader, P. Riede, R. Strohner, E. Lehmann, and G. Langst. 2007. DNA sequence- and conformation-directed positioning of nucleosomes by chromatin-remodeling complexes. *Proc Natl Acad Sci U S A.* 104:15635-40.

Roberts, C.W., and S.H. Orkin. 2004. The SWI/SNF complex--chromatin and cancer. *Nat Rev Cancer.* 4:133-42.

Robertson, A.K., T.M. Geiman, U.T. Sankpal, G.L. Hager, and K.D. Robertson. 2004. Effects of chromatin structure on the enzymatic and DNA binding functions of DNA methyltransferases DNMT1 and Dnmt3a in vitro. *Biochem.Biophys.Res.Commun.* 322:110-118.

Robertson, K.D. 2001. DNA methylation, methyltransferases, and cancer. *Oncogene.* 20:3139-3155.

Robertson, K.D. 2002. DNA methylation and chromatin - unraveling the tangled web. *Oncogene.* 21:5361-5379.

Robertson, K.D. 2005. DNA methylation and human disease. *Nat Rev Genet.* 6:597-610.

Robertson, K.D., S. Ait-Si-Ali, T. Yokochi, P.A. Wade, P.L. Jones, and A.P. Wolffe. 2000. DNMT1 forms a complex with Rb, E2F1 and HDAC1 and represses transcription from E2F-responsive promoters. *Nat.Genet.* 25:338-342.

Robertson, K.D., E. Uzvolgyi, G. Liang, C. Talmadge, J. Sumegi, F.A. Gonzales, and P.A. Jones. 1999. The human DNA methyltransferases (DNMTs) 1, 3a and 3b: coordinate mRNA expression in normal tissues and overexpression in tumors. *Nucleic Acids Res.* 27:2291-2298.

Robinson, P.J., W. An, A. Routh, F. Martino, L. Chapman, R.G. Roeder, and D. Rhodes. 2008. 30 nm chromatin fibre decompaction requires both H4-K16 acetylation and linker histone eviction. *J Mol Biol.* 381:816-25.

Robinson, P.J., L. Fairall, V.A. Huynh, and D. Rhodes. 2006. EM measurements define the dimensions of the "30-nm" chromatin fiber: evidence for a compact, interdigitated structure. *Proc Natl Acad Sci U S A.* 103:6506-11.

Robinson, P.J., and D. Rhodes. 2006. Structure of the '30 nm' chromatin fibre: a key role for the linker histone. *Curr Opin Struct Biol.* 16:336-43.

Rollins, R.A., F. Haghighi, J.R. Edwards, R. Das, M.Q. Zhang, J. Ju, and T.H. Bestor. 2006. Large-scale structure of genomic methylation patterns. *Genome Res.* 16:157-63.

Roth, S.Y., A. Dean, and R.T. Simpson. 1990. Yeast alpha 2 repressor positions nucleosomes in TRP1/ARS1 chromatin. *Mol Cell Biol.* 10:2247-60.

Rottach, A., H. Leonhardt, and F. Spada. 2009. DNA methylation-mediated epigenetic control. *J Cell Biochem.*

Rountree, M.R., K.E. Bachman, and S.B. Baylin. 2000. DNMT1 binds HDAC2 and a new co-repressor, DMAP1, to form a complex at replication foci. *Nat.Genet.* 25:269-277.

Rountree, M.R., K.E. Bachman, J.G. Herman, and S.B. Baylin. 2001. DNA methylation, chromatin inheritance, and cancer. *Oncogene.* 20:3156-3165.

Routh, A., S. Sandin, and D. Rhodes. 2008. Nucleosome repeat length and linker histone stoichiometry determine chromatin fiber structure. *Proc Natl Acad Sci U S A.* 105:8872-7.

Roy, P.H., and A. Weissbach. 1975. DNA methylase from HeLa cell nuclei. *Nucleic Acids Res.* 2:1669-84.

Sakai, T., J. Toguchida, N. Ohtani, D.W. Yandell, J.M. Rapaport, and T.P. Dryja. 1991. Allele-specific hypermethylation of the retinoblastoma tumor-suppressor gene. *Am J Hum Genet.* 48:880-8.

Samal, B., A. Worcel, C. Louis, and P. Schedl. 1981. Chromatin structure of the histone genes of D. melanogaster. *Cell.* 23:401-9.

Sambrook, J., E.F. Fritsch, and T. Maniatis. 1989. Molecular Cloning, A laboratory manual. Cold spring harbor laboratory.

Sambrook, J., and D. Russell. 2001. Molecular cloning. *CSHL* First, Second and Third edition.

Santi, D.V., C.E. Garrett, and P.J. Barr. 1983. On the mechanism of inhibition of DNA-cytosine methyltransferases by cytosine analogs. *Cell.* 33:9-10.

Santi, D.V., A. Norment, and C.E. Garrett. 1984. Covalent bond formation between a DNA-cytosine methyltransferase and DNA containing 5-azacytosine. *Proc.Natl.Acad.Sci.U.S.A.* 81:6993-6997.

Santisteban, M.S., T. Kalashnikova, and M.M. Smith. 2000. Histone H2A.Z regulats transcription and is partially redundant with nucleosome remodeling complexes. *Cell.* 103:411-22.

Santoro, R., and I. Grummt. 2001. Molecular mechanisms mediating methylation-dependent silencing of ribosomal gene transcription. *Mol Cell.* 8:719-25.

Santoro, R., J. Li, and I. Grummt. 2002. The nucleolar remodeling complex NoRC mediates heterochromatin formation and silencing of ribosomal gene transcription. *Nat.Genet.* 32:393-396.

Sapienza, C., A.C. Peterson, J. Rossant, and R. Balling. 1987. Degree of methylation of transgenes is dependent on gamete of origin. *Nature.* 328:251-4.

Satchwell, S.C., H.R. Drew, and A.A. Travers. 1986. Sequence periodicities in chicken nucleosome core DNA. *J Mol Biol.* 191:659-75.

Schalch, T., S. Duda, D.F. Sargent, and T.J. Richmond. 2005. X-ray structure of a tetranucleosome and its implications for the chromatin fibre. *Nature.* 436:138-41.

Schermelleh, L., A. Haemmer, F. Spada, N. Rosing, D. Meilinger, U. Rothbauer, M.C. Cardoso, and H. Leonhardt. 2007. Dynamics of Dnmt1 interaction with the replication machinery and its role in postreplicative maintenance of DNA methylation. *Nucleic Acids Res.* 35:4301-12.

Schlissel, M.S., and D.D. Brown. 1984. The transcriptional regulation of Xenopus 5s RNA genes in chromatin: the roles of active stable transcription complexes and histone H1. *Cell.* 37:903-13.

Schnitzler, G.R. 2001. Isolation of histones and nucleosome cores from mammalian cells. *Curr Protoc Mol Biol.* Chapter 21:Unit 21 5.

Schnitzler, G.R., C.L. Cheung, J.H. Hafner, A.J. Saurin, R.E. Kingston, and C.M. Lieber. 2001. Direct imaging of human SWI/SNF-remodeled mono- and polynucleosomes by atomic force microscopy employing carbon nanotube tips. *Mol Cell Biol.* 21:8504-11.

Schones, D.E., K. Cui, S. Cuddapah, T.Y. Roh, A. Barski, Z. Wang, G. Wei, and K. Zhao. 2008. Dynamic regulation of nucleosome positioning in the human genome. *Cell.* 132:887-98.

Schotta, G., A. Ebert, R. Dorn, and G. Reuter. 2003. Position-effect variegation and the genetic dissection of chromatin regulation in *Drosophila. Semin Cell Dev Biol.* 14:67-75.

Schwanbeck, R., H. Xiao, and C. Wu. 2004. Spatial contacts and nucleosome step movements induced by the NURF chromatin remodeling complex. *J Biol Chem.* 279:39933-41.

Segal, E., Y. Fondufe-Mittendorf, L. Chen, A. Thastrom, Y. Field, I.K. Moore, J.P. Wang, and J. Widom. 2006. A genomic code for nucleosome positioning. *Nature.* 442:772-8.

Segal, E., and J. Widom. 2009a. From DNA sequence to transcriptional behaviour: a quantitative approach. *Nat Rev Genet.* 10:443-56.

Segal, E., and J. Widom. 2009b. Poly(dA:dT) tracts: major determinants of nucleosome organization. *Curr Opin Struct Biol.* 19:65-71.

Sekinger, E.A., Z. Moqtaderi, and K. Struhl. 2005. Intrinsic histone-DNA interactions and low nucleosome density are important for preferential accessibility of promoter regions in yeast. *Mol Cell.* 18:735-48.

Sha, K. 2008. A mechanistic view of genomic imprinting. *Annu Rev Genomics Hum Genet.* 9:197-216.

Sharif, J., M. Muto, S. Takebayashi, I. Suetake, A. Iwamatsu, T.A. Endo, J. Shinga, Y. Mizutani-Koseki, T. Toyoda, K. Okamura, S. Tajima, K. Mitsuya, M. Okano, and H. Koseki. 2007. The SRA protein Np95 mediates epigenetic inheritance by recruiting Dnmt1 to methylated DNA. *Nature.* 450:908-12.

Shen, X., and M.A. Gorovsky. 1996. Linker histone H1 regulates specific gene expression but not global transcription in vivo. *Cell.* 86:475-83.

Shen, X., G. Mizuguchi, A. Hamiche, and C. Wu. 2000. A chromatin remodelling complex involved in transcription and DNA processing. *Nature.* 406:541-4.

Shi, Y., F. Lan, C. Matson, P. Mulligan, J.R. Whetstine, P.A. Cole, and R.A. Casero. 2004. Histone demethylation mediated by the nuclear amine oxidase homolog LSD1. *Cell.* 119:941-53.

Shikauchi, Y., A. Saiura, T. Kubo, Y. Niwa, J. Yamamoto, Y. Murase, and H. Yoshikawa. 2009. SALL3 interacts with DNMT3A and shows the ability to inhibit CpG island methylation in hepatocellular carcinoma. *Mol Cell Biol.* 29:1944-58.

Shim, E.Y., C. Woodcock, and K.S. Zaret. 1998. Nucleosome positioning by the winged helix transcription factor HNF3. *Genes Dev.* 12:5-10.

Shimizu, M., S.Y. Roth, C. Szent-Gyorgyi, and R.T. Simpson. 1991. Nucleosomes are positioned with base pair precision adjacent to the alpha 2 operator in Saccharomyces cerevisiae. *Embo J.* 10:3033-41.

Shogren-Knaak, M., H. Ishii, J.M. Sun, M.J. Pazin, J.R. Davie, and C.L. Peterson. 2006. Histone H4-K16 acetylation controls chromatin structure and protein interactions. *Science.* 311:844-7.

Sif, S., A.J. Saurin, A.N. Imbalzano, and R.E. Kingston. 2001. Purification and characterization of mSin3A-containing Brg1 and hBrm chromatin remodeling complexes. *Genes Dev.* 15:603-18.

Simpson, R.T. 1990. Nucleosome positioning can affect the function of a cis-acting DNA element in vivo. *Nature.* 343:387-9.

Simpson, R.T. 1991. Nucleosome positioning: occurrence, mechanisms, and functional consequences. *Prog Nucleic Acid Res Mol Biol.* 40:143-84.

Simpson, R.T., and D.W. Stafford. 1983. Structural features of a phased nucleosome core particle. *Proc Natl Acad Sci U S A.* 80:51-5.

Sims, H.I., J.M. Lane, N.P. Ulyanova, and G.R. Schnitzler. 2007. Human SWI/SNF drives sequence-directed repositioning of nucleosomes on C-myc promoter DNA minicircles. *Biochemistry.* 46:11377-88.

Sleutels, F., and D.P. Barlow. 2002. The origins of genomic imprinting in mammals. *Adv Genet.* 46:119-63.

Smit, A.F. 1999. Interspersed repeats and other mementos of transposable elements in mammalian genomes. *Curr.Opin.Genet.Dev.* 9:657-663.

Smith, C.L., R. Horowitz-Scherer, J.F. Flanagan, C.L. Woodcock, and C.L. Peterson. 2003. Structural analysis of the yeast SWI/SNF chromatin remodeling complex. *Nat Struct Biol.* 10:141-5.

Smith, S., and B. Stillman. 1989. Purification and characterization of CAF-I, a human cell factor required for chromatin assembly during DNA replication in vitro. *Cell.* 58:15-25.

Spada, F., A. Haemmer, D. Kuch, U. Rothbauer, L. Schermelleh, E. Kremmer, T. Carell, G. Langst, and H. Leonhardt. 2007. DNMT1 but not its interaction with the replication machinery is required for maintenance of DNA methylation in human cells. *J Cell Biol.* 176:565-71.

Spada, F., U. Rothbauer, K. Zolghadr, L. Schermelleh, and H. Leonhardt. 2006. Regulation of DNA methyltransferase 1. *Adv Enzyme Regul.* 46:224-34.

Springhetti, E.M., N.E. Istomina, J.C. Whisstock, T. Nikitina, C.L. Woodcock, and S.A. Grigoryev. 2003. Role of the M-loop and reactive center loop domains in the folding and bridging of nucleosome arrays by MENT. *J Biol Chem.* 278:43384-93.

Stein, A., J.P. Whitlock, Jr., and M. Bina. 1979. Acidic polypeptides can assemble both histones and chromatin in vitro at physiological ionic strength. *Proc Natl Acad Sci U S A.* 76:5000-4.

Stockdale, C., A. Flaus, H. Ferreira, and T. Owen-Hughes. 2006. Analysis of nucleosome repositioning by yeast ISWI and Chd1 chromatin remodeling complexes. *J Biol Chem.* 281:16279-88.

Straub, T., and P.B. Becker. 2007. Dosage compensation: the beginning and end of generalization. *Nat Rev Genet.* 8:47-57.

Strohner, R., A. Nemeth, P. Jansa, U. Hofmann-Rohrer, R. Santoro, G. Langst, and I. Grummt. 2001. NoRC--a novel member of mammalian ISWI-containing chromatin remodeling machines. *EMBO J.* 20:4892-4900.

Strohner, R., M. Wachsmuth, K. Dachauer, J. Mazurkiewicz, J. Hochstatter, K. Rippe, and G. Langst. 2005. A 'loop recapture' mechanism for ACF-dependent nucleosome remodeling. *Nat Struct Mol Biol.* 12:683-90.

Sudarsanam, P., and F. Winston. 2000. The Swi/Snf family nucleosome-remodeling complexes and transcriptional control. *Trends Genet.* 16:345-51.

Suetake, I., J. Miyazaki, C. Murakami, H. Takeshima, and S. Tajima. 2003. Distinct enzymatic properties of recombinant mouse DNA methyltransferases Dnmt3a and Dnmt3b. *J Biochem.* 133:737-44.

Suetake, I., F. Shinozaki, J. Miyagawa, H. Takeshima, and S. Tajima. 2004. DNMT3L stimulates the DNA methylation activity of Dnmt3a and Dnmt3b through a direct interaction. *J Biol Chem.* 279:27816-23.

Svedruzic, Z.M., and N.O. Reich. 2005a. DNA cytosine C5 methyltransferase Dnmt1: catalysis-dependent release of allosteric inhibition. *Biochemistry.* 44:9472-85.

Svedruzic, Z.M., and N.O. Reich. 2005b. Mechanism of allosteric regulation of Dnmt1's processivity. *Biochemistry.* 44:14977-88.

Swain, J.L., T.A. Stewart, and P. Leder. 1987. Parental legacy determines methylation and expression of an autosomal transgene: a molecular mechanism for parental imprinting. *Cell.* 50:719-27.

Swaminathan, J., E.M. Baxter, and V.G. Corces. 2005. The role of histone H2Av variant replacement and histone H4 acetylation in the establishment of *Drosophila* heterochromatin. *Genes Dev.* 19:65-76.

Tagami, H., D. Ray-Gallet, G. Almouzni, and Y. Nakatani. 2004. Histone H3.1 and H3.3 complexes mediate nucleosome assembly pathways dependent or independent of DNA synthesis. *Cell.* 116:51-61.

Takai, D., and P.A. Jones. 2003. The CpG island searcher: a new WWW resource. *In Silico Biol.* 3:235-40.

Takeshima, H., I. Suetake, H. Shimahara, K. Ura, S. Tate, and S. Tajima. 2006. Distinct DNA methylation activity of Dnmt3a and Dnmt3b towards naked and nucleosomal DNA. *J Biochem.* 139:503-15.

Takeshima, H., I. Suetake, and S. Tajima. 2008. Mouse Dnmt3a preferentially methylates linker DNA and is inhibited by histone H1. *J Mol Biol.* 383:810-21.

Tatematsu, K.I., T. Yamazaki, and F. Ishikawa. 2000. MBD2-MBD3 complex binds to hemi-methylated DNA and forms a complex containing DNMT1 at the replication foci in late S phase. *Genes Cells.* 5:677-688.

Taylor, I.C., J.L. Workman, T.J. Schuetz, and R.E. Kingston. 1991. Facilitated binding of GAL4 and heat shock factor to nucleosomal templates: differential function of DNA-binding domains. *Genes Dev.* 5:1285-98.

Tazi, J., and A. Bird. 1990. Alternative chromatin structure at CpG islands. *Cell.* 60:909-20.

Thastrom, A., P.T. Lowary, H.R. Widlund, H. Cao, M. Kubista, and J. Widom. 1999. Sequence motifs and free energies of selected natural and non-natural nucleosome positioning DNA sequences. *J.Mol.Biol.* 288:213-229.

Thoma, F., T. Koller, and A. Klug. 1979. Involvement of histone H1 in the organization of the nucleosome and of the salt-dependent superstructures of chromatin. *J Cell Biol.* 83:403-27.

Thomas, J.O., and P.J. Butler. 1980. Size-dependence of a stable higher-order structure of chromatin. *J Mol Biol.* 144:89-93.

Tippin, D.B., and M. Sundaralingam. 1997. Nine polymorphic crystal structures of d(CCGGGCCCGG), d(CCGGGCCm5CGG), d(Cm5CGGGCCm5CGG) and d(CCGGGCC(Br)5CGG) in three different conformations: effects of spermine binding and methylation on the bending and condensation of A-DNA. *J Mol Biol.* 267:1171-85.

Tollefsbol, T.O., and C.A. Hutchison, 3rd. 1997. Control of methylation spreading in synthetic DNA sequences by the murine DNA methyltransferase. *J Mol Biol.* 269:494-504.

Tollefsbol, T.O., and C.A. Hutchison, III 1995. Mammalian DNA (cytosine-5-)-methyltransferase expressed in Escherichia coli, purified and characterized. *J.Biol.Chem.* 270:18543-18550.

Tran, H.G., D.J. Steger, V.R. Iyer, and A.D. Johnson. 2000. The chromo domain protein chd1p from budding yeast is an ATP-dependent chromatin-modifying factor. *Embo J.* 19:2323-31.

Trautner, T.A., T. Balganesh, K. Wilke, M. Noyer-Weidner, E. Rauhut, R. Lauster, B. Behrens, and B. Pawlek. 1988. Organization of target-recognizing domains in the multispecific DNA (cytosine-5)methyltransferases of Bacillus subtilis phages SPR and phi 3T. *Gene.* 74:267.

Tremethick, D.J. 2007. Higher-order structures of chromatin: the elusive 30 nm fiber. *Cell.* 128:651-4.

Trifonov, E.N. 1980. Sequence-dependent deformational anisotropy of chromatin DNA. *Nucleic Acids Res.* 8:4041-53.

Trifonov, E.N., and J.L. Sussman. 1980. The pitch of chromatin DNA is reflected in its nucleotide sequence. *Proc Natl Acad Sci U S A.* 77:3816-20.

Tse, C., T. Sera, A.P. Wolffe, and J.C. Hansen. 1998. Disruption of higher-order folding by core histone acetylation dramatically enhances transcription of nucleosomal arrays by RNA polymerase III. *Mol Cell Biol.* 18:4629-38.

Tsukiyama, T. 2002. The in vivo functions of ATP-dependent chromatin-remodelling factors. *Nat.Rev.Mol.Cell Biol.* 3:422-429.

Tsukiyama, T., P.B. Becker, and C. Wu. 1994. ATP-dependent nucleosome disruption at a heat-shock promoter mediated by binding of GAGA transcription factor. *Nature.* 367:525-32.

Tsukiyama, T., C. Daniel, J. Tamkun, and C. Wu. 1995. ISWI, a member of the SWI2/SNF2 ATPase family, encodes the 140 kDa subunit of the nucleosome remodeling factor. *Cell.* 83:1021-1026.

Tsukiyama, T., J. Palmer, C.C. Landel, J. Shiloach, and C. Wu. 1999. Characterization of the imitation switch subfamily of ATP-dependent chromatin-remodeling factors in Saccharomyces cerevisiae. *Genes Dev.* 13:686-97.

Tsukiyama, T., and C. Wu. 1995. Purification and properties of an ATP-dependent nucleosome remodeling factor. *Cell.* 83:1011-1020.

Tsukiyama, T., and C. Wu. 1997. Chromatin remodeling and transcription. *Curr Opin Genet Dev.* 7:182-91.

Tsukuda, T., A.B. Fleming, J.A. Nickoloff, and M.A. Osley. 2005. Chromatin remodelling at a DNA double-strand break site in Saccharomyces cerevisiae. *Nature.* 438:379-83.

Tuck-Muller, C.M., A. Narayan, F. Tsien, D.F. Smeets, J. Sawyer, E.S. Fiala, O.S. Sohn, and M. Ehrlich. 2000. DNA hypomethylation and unusual chromosome instability in cell lines from ICF syndrome patients. *Cytogenet Cell Genet.* 89:121-8.

Turner, B.M. 2002. Cellular memory and the histone code. *Cell.* 111:285-91.

Tweedie, S., H.H. Ng, A.L. Barlow, B.M. Turner, B. Hendrich, and A. Bird. 1999. Vestiges of a DNA methylation system in *Drosophila* melanogaster? *Nat Genet.* 23:389-90.

Tyler, J.K., C.R. Adams, S.R. Chen, R. Kobayashi, R.T. Kamakaka, and J.T. Kadonaga. 1999. The RCAF complex mediates chromatin assembly during DNA replication and repair. *Nature.* 402:555-60.

Ura, K., M. Araki, H. Saeki, C. Masutani, T. Ito, S. Iwai, T. Mizukoshi, Y. Kaneda, and F. Hanaoka. 2001. ATP-dependent chromatin remodeling facilitates nucleotide excision repair of UV-induced DNA lesions in synthetic dinucleosomes. *EMBO J.* 20:2004-2014.

Ura, K., J.J. Hayes, and A.P. Wolffe. 1995. A positive role for nucleosome mobility in the transcriptional activity of chromatin templates: restriction by linker histones. *Embo J.* 14:3752-65.

Valouev, A., J. Ichikawa, T. Tonthat, J. Stuart, S. Ranade, H. Peckham, K. Zeng, J.A. Malek, G. Costa, K. McKernan, A. Sidow, A. Fire, and S.M. Johnson. 2008. A high-resolution, nucleosome position map of C. elegans reveals a lack of universal sequence-dictated positioning. *Genome Res.* 18:1051-63.

van Attikum, H., O. Fritsch, B. Hohn, and S.M. Gasser. 2004. Recruitment of the Ino80 complex by H2A phosphorylation links ATP-dependent chromatin remodeling with DNA double-strand break repair. *Cell.* 119:777-88.

Van Holde, K. 1989. Chromatin. *Springer-Verlag, New York.*

van Holde, K.E. 1996. A random walk amid the macromolecules. *Protein Sci.* 5:792-6.

Vaquero, A., A. Loyola, and D. Reinberg. 2003. The constantly changing face of chromatin. *Sci Aging Knowledge Environ.* 2003:RE4.

Varga-Weisz, P.D., and P.B. Becker. 1995. Transcription factor-mediated chromatin remodelling: mechanisms and models. *FEBS Lett.* 369:118-21.

Varga-Weisz, P.D., and P.B. Becker. 2006. Regulation of higher-order chromatin structures by nucleosome-remodelling factors. *Curr Opin Genet Dev.* 16:151-6.

Varga-Weisz, P.D., M. Wilm, E. Bonte, K. Dumas, M. Mann, and P.B. Becker. 1997. Chromatin-remodelling factor CHRAC contains the ATPases ISWI and topoisomerase II. *Nature.* 388:598-602.

Vermaak, D., K. Ahmad, and S. Henikoff. 2003. Maintenance of chromatin states: an open-and-shut case. *Curr Opin Cell Biol.* 15:266-74.

Verona, R.I., M.R. Mann, and M.S. Bartolomei. 2003. Genomic imprinting: intricacies of epigenetic regulation in clusters. *Annu Rev Cell Dev Biol.* 19:237-59.

Vignali, M., A.H. Hassan, K.E. Neely, and J.L. Workman. 2000. ATP-dependent chromatin-remodeling complexes. *Mol Cell Biol.* 20:1899-910.

Vilkaitis, G., I. Suetake, S. Klimasauskas, and S. Tajima. 2005. Processive methylation of hemimethylated CpG sites by mouse Dnmt1 DNA methyltransferase. *J Biol Chem.* 280:64-72.

Vire, E., C. Brenner, R. Deplus, L. Blanchon, M. Fraga, C. Didelot, L. Morey, A. Van Eynde, D. Bernard, J.M. Vanderwinden, M. Bollen, M. Esteller, L. Di Croce, Y. de Launoit, and F. Fuks. 2006. The Polycomb group protein EZH2 directly controls DNA methylation. *Nature.* 439:871-4.

Virstedt, J., T. Berge, R.M. Henderson, M.J. Waring, and A.A. Travers. 2004. The influence of DNA stiffness upon nucleosome formation. *J Struct Biol.* 148:66-85.

von Hippel, P.H., and T.D. Yager. 1992. The elongation-termination decision in transcription. *Science.* 255:809-12.

Waddington, C. 1942. The epigenotype. *Endeavour 1.*

Wang, G.G., C.D. Allis, and P. Chi. 2007a. Chromatin remodeling and cancer, Part I: Covalent histone modifications. *Trends Mol Med.* 13:363-72.

Wang, G.G., C.D. Allis, and P. Chi. 2007b. Chromatin remodeling and cancer, Part II: ATP-dependent chromatin remodeling. *Trends Mol Med.* 13:373-80.

Wang, J.P., and J. Widom. 2005. Improved alignment of nucleosome DNA sequences using a mixture model. *Nucleic Acids Res.* 33:6743-55.

Wang, R.Y., C.W. Gehrke, and M. Ehrlich. 1980. Comparison of bisulfite modification of 5-methyldeoxycytidine and deoxycytidine residues. *Nucleic Acids Res.* 8:4777-90.

Wang, W. 2003. The SWI/SNF family of ATP-dependent chromatin remodelers: similar mechanisms for diverse functions. *Curr Top Microbiol Immunol.* 274:143-69.

Wang, Y., W. Fischle, W. Cheung, S. Jacobs, S. Khorasanizadeh, and C.D. Allis. 2004. Beyond the double helix: writing and reading the histone code. *Novartis Found Symp.* 259:3-17; discussion 17-21, 163-9.

Wang, Y.A., Y. Kamarova, K.C. Shen, Z. Jiang, M.J. Hahn, Y. Wang, and S.C. Brooks. 2005. DNA methyltransferase-3a interacts with p53 and represses p53-mediated gene expression. *Cancer Biol Ther.* 4:1138-43.

Weiss, K., and R.T. Simpson. 1997. Cell type-specific chromatin organization of the region that governs directionality of yeast mating type switching. *Embo J.* 16:4352-60.

Whitehouse, I., A. Flaus, B.R. Cairns, M.F. White, J.L. Workman, and T. Owen-Hughes. 1999. Nucleosome mobilization catalysed by the yeast SWI/SNF complex. *Nature.* 400:784-7.

Whitehouse, I., O.J. Rando, J. Delrow, and T. Tsukiyama. 2007. Chromatin remodelling at promoters suppresses antisense transcription. *Nature.* 450:1031-5.

Whitehouse, I., C. Stockdale, A. Flaus, M.D. Szczelkun, and T. Owen-Hughes. 2003. Evidence for DNA translocation by the ISWI chromatin-remodeling enzyme. *Mol Cell Biol.* 23:1935-45.

Whitehouse, I., and T. Tsukiyama. 2006. Antagonistic forces that position nucleosomes in vivo. *Nat Struct Mol Biol.* 13:633-40.

Widom, J. 1997. Getting around the nucleosomes. *Science.* 278:1899-901.

Widom, J. 1998. Structure, dynamics, and function of chromatin in vitro. *Annu.Rev.Biophys.Biomol.Struct.* 27:285-327.

Widom, J., and A. Klug. 1985. Structure of the 300A chromatin filament: X-ray diffraction from oriented samples. *Cell.* 43:207-13.

Wierzbicki, A.T., and A. Jerzmanowski. 2005. Suppression of histone H1 genes in Arabidopsis results in heritable developmental defects and stochastic changes in DNA methylation. *Genetics.* 169:997-1008.

Wilson, C., H.J. Bellen, and W.J. Gehring. 1990. Position effects on eukaryotic gene expression. *Annu Rev Cell Biol.* 6:679-714.

Wilson, G.G., and N.E. Murray. 1991. Restriction and modification systems. *Annu Rev Genet.* 25:585-627.

Wittig, B., S. Wittig, and H. Grunz. 1979. Cloning of chicken embryo tRNA genes using single stranded nucleosomal DNA highly enriched for tRNA complementary sequences. *Nucleic Acids Res.* 6:3759-84.

Wolffe, A.P. 1997. Histone H1. *Int J Biochem Cell Biol.* 29:1463-6.

Wolffe, A.P. 1998. Packaging principle: how DNA methylation and histone acetylation control the transcriptional activity of chromatin. *J Exp Zool.* 282:239-44.

Wolffe, A.P., and H. Kurumizaka. 1998. The nucleosome: a powerful regulator of transcription. *Prog Nucleic Acid Res Mol Biol.* 61:379-422.

Woodcock, C.L., and S. Dimitrov. 2001. Higher-order structure of chromatin and chromosomes. *Curr.Opin.Genet.Dev.* 11:130-135.

Woodcock, D.M., D.L. Simmons, P.J. Crowther, I.A. Cooper, K.J. Trainor, and A.A. Morley. 1986. Delayed DNA methylation is an integral feature of DNA replication in mammalian cells. *Exp Cell Res.* 166:103-12.

Worcel, A., S. Han, and M.L. Wong. 1978. Assembly of newly replicated chromatin. *Cell.* 15:969-77.

Wu, C. 1980. The 5' ends of *Drosophila* heat shock genes in chromatin are hypersensitive to DNase I. *Nature.* 286:854-60.

Wysocka, J., T. Swigut, H. Xiao, T.A. Milne, S.Y. Kwon, J. Landry, M. Kauer, A.J. Tackett, B.T. Chait, P. Badenhorst, C. Wu, and C.D. Allis. 2006. A PHD finger of NURF couples histone H3 lysine 4 trimethylation with chromatin remodelling. *Nature.* 442:86-90.

Xie, S., Z. Wang, M. Okano, M. Nogami, Y. Li, W.W. He, K. Okumura, and E. Li. 1999. Cloning, expression and chromosome locations of the human DNMT3 gene family. *Gene.* 236:87-95.

Xu, G.L., T.H. Bestor, D. Bourc'his, C.L. Hsieh, N. Tommerup, M. Bugge, M. Hulten, X. Qu, J.J. Russo, and E. Viegas-Pequignot. 1999. Chromosome instability and immunodeficiency syndrome caused by mutations in a DNA methyltransferase gene. *Nature.* 402:187-191.

Yan, Q., J. Huang, T. Fan, H. Zhu, and K. Muegge. 2003. Lsh, a modulator of CpG methylation, is crucial for normal histone methylation. *EMBO J.* 22:5154-5162.

Yang, J.G., T.S. Madrid, E. Sevastopoulos, and G.J. Narlikar. 2006. The chromatin-remodeling enzyme ACF is an ATP-dependent DNA length sensor that regulates nucleosome spacing. *Nat Struct Mol Biol.* 13:1078-83.

Yarragudi, A., T. Miyake, R. Li, and R.H. Morse. 2004. Comparison of ABF1 and RAP1 in chromatin opening and transactivator potentiation in the budding yeast Saccharomyces cerevisiae. *Mol Cell Biol.* 24:9152-64.

Yenidunya, A., C. Davey, D. Clark, G. Felsenfeld, and J. Allan. 1994. Nucleosome positioning on chicken and human globin gene promoters in vitro. Novel mapping techniques. *J Mol Biol.* 237:401-14.

Yindeeyoungyeon, W., and M.A. Schell. 2000. Footprinting with an automated capillary DNA sequencer. *Biotechniques.* 29:1034-6, 1038, 1040-1.

Yoder, J.A., and T.H. Bestor. 1998. A candidate mammalian DNA methyltransferase related to pmt1p of fission yeast. *Hum.Mol.Genet.* 7:279-284.

Yoder, J.A., C.P. Walsh, and T.H. Bestor. 1997. Cytosine methylation and the ecology of intragenomic parasites. *Trends Genet.* 13:335-340.

Yokochi, T., and K.D. Robertson. 2002. Preferential methylation of unmethylated DNA by Mammalian de novo DNA methyltransferase Dnmt3a. *J.Biol.Chem.* 277:11735-11745.

Yokochi, T., and K.D. Robertson. 2004. Dimethyl sulfoxide stimulates the catalytic activity of de novo DNA methyltransferase 3a (Dnmt3a) in vitro. *Bioorg.Chem.* 32:234-243.

Yuan, G.C., and J.S. Liu. 2008. Genomic sequence is highly predictive of local nucleosome depletion. *PLoS Comput Biol.* 4:e13.

Yuan, G.C., Y.J. Liu, M.F. Dion, M.D. Slack, L.F. Wu, S.J. Altschuler, and O.J. Rando. 2005. Genome-scale identification of nucleosome positions in S. cerevisiae. *Science.* 309:626-30.

Zacharias, H. 1995. Emil Heitz (1892-1965): chloroplasts, heterochromatin, and polytene chromosomes. *Genetics.* 141:7-14.

Zeng, L., and M.M. Zhou. 2002. Bromodomain: an acetyl-lysine binding domain. *FEBS Lett.* 513:124-8.

Zhang, X., and G.L. Verdine. 1996. Mammalian DNA cytosine-5 methyltransferase interacts with p23 protein. *FEBS Lett.* 392:179-183.

Zhou, Q., A.T. Agoston, P. Atadja, W.G. Nelson, and N.E. Davidson. 2008. Inhibition of histone deacetylases promotes ubiquitin-dependent proteasomal degradation of DNA methyltransferase 1 in human breast cancer cells. *Mol Cancer Res.* 6:873-83.

Zhou, Y., and I. Grummt. 2005. The PHD finger/bromodomain of NoRC interacts with acetylated histone H4K16 and is sufficient for rDNA silencing. *Curr Biol.* 15:1434-8.

Zhu, H., T.M. Geiman, S. Xi, Q. Jiang, A. Schmidtmann, T. Chen, E. Li, and K. Muegge. 2006. Lsh is involved in de novo methylation of DNA. *Embo J.* 25:335-45.

Zianni, M., K. Tessanne, M. Merighi, R. Laguna, and F.R. Tabita. 2006. Identification of the DNA bases of a DNase I footprint by the use of dye primer sequencing on an automated capillary DNA analysis instrument. *J Biomol Tech.* 17:103-13.

Zimmermann, C., E. Guhl, and A. Graessmann. 1997. Mouse DNA methyltransferase (MTase) deletion mutants that retain the catalytic domain display neither de novo nor maintenance methylation activity in vivo. *Biol Chem.* 378:393-405.

Zlatanova, J., P. Caiafa, and K. Van Holde. 2000. Linker histone binding and displacement: versatile mechanism for transcriptional regulation. *Faseb J.* 14:1697-704.

Zofall, M., J. Persinger, and B. Bartholomew. 2004. Functional role of extranucleosomal DNA and the entry site of the nucleosome in chromatin remodeling by ISW2. *Mol Cell Biol.* 24:10047-57.

Zwart, R., F. Sleutels, A. Wutz, A.H. Schinkel, and D.P. Barlow. 2001. Bidirectional action of the Igf2r imprint control element on upstream and downstream imprinted genes. *Genes Dev.* 15:2361-6.

H. Manuscript

DNA SEQUENCE- AND CONFORMATION-DIRECTED POSITIONION OF NUCLEOSOMES BY CHROMATIN-REMODELING COMPLEXES

Karsten Rippe*, Anna Schrader*, Philipp Riede, Ralf Strohner, Elisabeth Lehmann and Gernot Längst

* = equally contributing

DNA sequence- and conformation-directed positioning of nucleosomes by chromatin-remodeling complexes

Karsten Rippe*, Anna Schrader†, Philipp Riede†, Ralf Strohner†, Elisabeth Lehmann‡, and Gernot Längst†§

*Division of Genome Organization and Function, Deutsches Krebsforschungszentrum and Bioquant, Im Neuenheimer Feld 280, 69120 Heidelberg, Germany; ‡Gene Center Munich, Department of Chemistry and Biochemistry, Ludwig-Maximilians-Universität München, Feodor-Lynen-Strasse 25, 81377 Munich, Germany; and †Biochemie III, Universität Regensburg, Universitätsstrasse 31, 93053 Regensburg, Germany

Chromatin-remodeling complexes can translocate nucleosomes along the DNA in an ATP-coupled reaction. This process is an important regulator of all DNA-dependent processes because it determines whether certain DNA sequences are found in regions between nucleosomes with increased accessibility for other factors or wrapped around the histone octamer complex. In a comparison of seven different chromatin-remodeling machines (ACF, ISWI, Snf2H, Chd1, Mi-2, Brg1, and NURF), it is demonstrated that these complexes can read out DNA sequence features to establish specific nucleosome-positioning patterns. For one of the remodelers, ACF, we identified a 40-bp DNA sequence element that directs nucleosome positioning. Furthermore, we show that nucleosome positioning by the remodelers ACF and Chd1 is determined by a reduced affinity to the end product of the translocation reaction. The results suggest that the linkage of differential remodeling activities with the intrinsic binding preferences of nucleosomes can result in establishing distinct chromatin structures that depend on the DNA sequence and define the DNA accessibility for other protein factors.

ACF | nucleosome remodeling | nucleosome positioning

DNA packaging into nucleosomes has long been recognized as a mechanism to control the accessibility of protein–DNA interactions involved in processes like transcription, replication repair, and recombination (1). The specific location of nucleosomes on DNA may play both inhibitory and activating roles (2) and depends on the ATP-coupled activity of chromatin-remodeling complexes that reposition nucleosomes or evict them from the DNA (3). For example, nucleosomes can be located at silent yeast promoters to occlude binding of basal transcription factors (4, 5). In contrast, an alternative nucleosome position with transcription factor-binding sites in the flanking linker DNA was shown to stimulate transcription (6–8).

Because the cell harbors hundreds of different remodeling complexes, it appears likely that they possess distinct activities, rather than solely being unspecific nucleosome-moving entities. Indeed, recent results demonstrate that the majority of nucleosomes in yeast are found at well defined positions (9). These sites can be predicted, in part, from the analysis of DNA dinucleotide sequence motifs (10, 11). However, it is currently unclear whether nucleosome positioning in the cell results only from sequence preferences of histone–DNA interactions or is directed by additional factors like the chromatin-remodeling complexes. As depicted in Fig. 1, these complexes comprise several groups of the Snf2-like ATPases and include the Snf2, ISWI, Mi-2, Chd1, Ino80, ERCC6, ALC1, CHD7, Swr1, RAD54, and Lsh subfamilies (12). Each subfamily consists of at least one to six similar ATPases, many of which have been shown to remodel nucleosomes, transfer histone octamers in trans, and generate superhelical torsion in DNA as reviewed previously (3, 13). The number of specific chromatin-remodeling activities in the cell is further increased by the assembly of the ATPases into large multiprotein complexes, where the same ATPase is shared within different remodeling complexes. For example, the human BAF and PBAF complexes differ by the subunits BAF250 and BAF180 present in the one, but not in the other, complex, and at least three different human NURD complexes containing the ATPase Mi-2 were described (14). In addition, the molecular motors of the complexes can be exchanged with other ATPases of the same subfamily. This finding was documented for the human BAF complex that contains either the hBRM or BRG1 ATPase (15) and for several ISWI complexes.

The diversity of the mammalian ISWI-like chromatin-remodeling complexes is described in Fig. 1. The mammalian genome encodes for at least four ISWI-like ATPases, Snf2H, Snf2L1, SNF2L2, and the catalytically inactive splice-variant Snf2L + 13 (16–18). To date, about a dozen specific mammalian complexes containing one of these ATPases were purified. It was shown that at least four of these complexes (hCHRAC, hRSF, hNURF, and hACF) can exist as isoformic complexes (i.e., they contain alternative ISWI-like ATPases) (16, 19, 20). This result suggests that the exchange of ATPases is a common theme and increases the number and complexity of chromatin-remodeling complexes in the cell. In addition, many of the subunits of the remodeling complexes exist as multiple-splice variants, such as CERC2 (19), BPTF (21), Tip5 (22), and Baz2B (22). This feature would further increase the diversity of ISWI-remodeling complexes. In summary, the current data indicate that a human cell is likely to form >40 different ISWI-like complexes. Extrapolating this finding to other Snf2 subfamilies, it is estimated that the nucleus harbors hundreds or even thousands of different chromatin-remodeling complexes. Furthermore, some of these complexes are highly abundant. Quantification studies in yeast suggest that one chromatin-remodeling complex is present for ≈10 nucleosomes (23, 24). This diversity and high total concentration of remodeling complexes appear to be unnecessary for simply maintaining an unspecific fluid and easily accessible conformation of chromatin. Instead it suggests that chromatin-remodeling complexes provide a higher order regulatory level by establishing specific chromatin structures in the cell. This hypothesis was tested here by comparing seven different remodeling machines. It is demonstrated that each of those machines possesses unique nucleosome-positioning characteristics. For the ACF-remodeling reaction, it is shown that nucleosome positioning is sequence-dependent, in that a short DNA element can determine ACF-dependent nucleosome positions. Finally, the mechanism of remodeler-dependent nucleosome positioning was analyzed. It is concluded that, for the ACF- and Chd1-remodeling machines, differences in the affinity of the remodeler toward differently

This article contains supporting information online at www.pnas.org/cgi/content/full/0702430104/DC1.
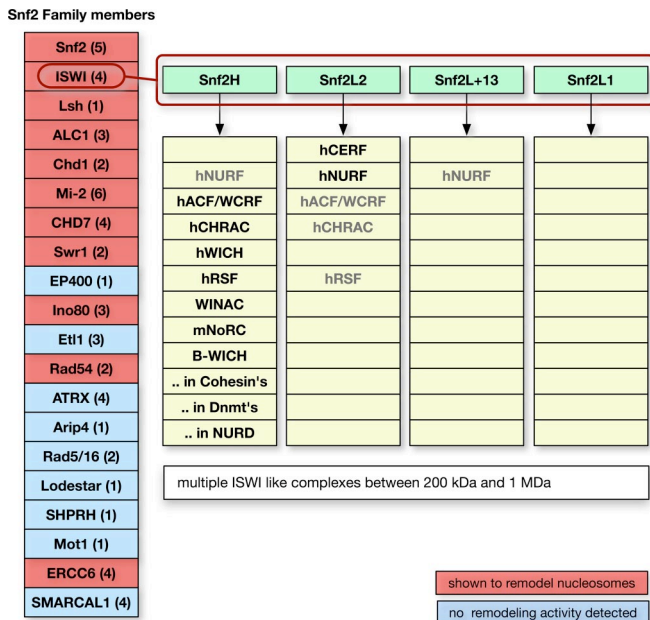
BIOCHEMISTRY

Fig. 1. Mammalian chromatin-remodeling complexes are highly diverse. (*Left*) The Snf2 family members present in humans, with the number of individual proteins within a subfamily in parentheses. The 11 subfamilies marked in red were shown to possess ATP-dependent chromatin-remodeling activities. Each of these subfamilies comprises many different members. (*Right*) The multiple ISWI ATPases complexes known to date. There are four ISWI subgroups (green boxes), and the known chromatin-remodeling complexes containing these ATPases are listed. Complexes in light gray type were shown to exist with the alternative ISWI-type ATPases.

Fig. 2. Chromatin-remodeling complexes position nucleosomes in a DNA sequence-specific manner. The nucleosome substrate was reconstituted by salt dialysis on a radioactively labeled 350-bp fragment carrying the hsp70 promoter. A mixture of a single nucleosome at five different major positions, indicated as N1, N2, N3, N4, and N4′, was obtained (28). This mixed nucleosome population (lane 1) was used as the same substrate for all seven remodelers shown. The endpoint of the nucleosome translocation reaction obtained after incubation for 90 min at 26°C in the presence of ATP is shown for recombinant Brg1 (lane 2), Chd1 (lane 3), ISWI (lane 4), Snf2H (lane 5), Mi-2 (lane 6), ACF (lane 7), and NURF (lane 8).

positioned nucleosomes determine the outcome of the remodeling reactions.

Results

Chromatin-Remodeling ATPases Establish Unique Nucleosome Positions. The DNA sequence-dependent specificity of the chromatin-remodeling reaction was examined in a comparison of seven different chromatin-remodeling machines (ACF, ISWI, Snf2H, Chd1, Mi-2, Brg1, and NURF) (18, 25–29). Two well characterized nucleosome substrates, the *Drosophila hsp70* DNA fragment (28) and the murine rDNA promoter (30, 31), were used [Fig. 2 and supporting information (SI) Figs. 6 and 7A]. Nucleosome assembly on the *hsp70* DNA fragment by salt dialysis gives rise to a distribution of nucleosomes positioned at five dominant positions. The different positions of the nucleosomes are designated as N1, N2, N3, N4, and N4′ and can be visualized by native PAGE because they show differences in their electrophoretic mobility (Fig. 2, lane 1) (28). This mixed nucleosome population was used as a substrate for the seven different chromatin-remodeling complexes listed previously. All remodeling complexes are capable of relocating nucleosomes on the substrate in an ATP-dependent reaction. The endpoint of this reaction obtained with a specific remodeling complex (lanes 2–8) was then compared with the distribution of nucleosomes on the input substrate (lane 1). The results of the remodeling reactions clearly demonstrate that every remodeling enzyme possesses a distinct nucleosome-positioning activity. This striking result cannot be explained by DNA sequence-dependent differences in the histone–DNA interactions. If the remodeling complexes would simply catalyze a transfer of the nucleosomes to their highest affinity histone-binding sites, the same end product should be obtained for the different remodeling complexes. This finding was clearly not the case. For example, NURF-dependent nucleosome remodeling was shown to position the nucleosomes efficiently from
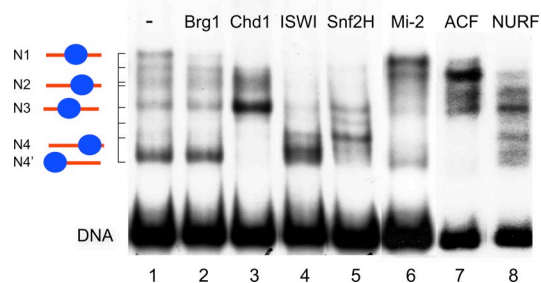
N1, N2, and N4 positions to the N3 position (lane 8) (28). In contrast, ACF, a similar remodeling complex harboring the identical ISWI ATPase, behaves differently and preferentially positions the nucleosomes at position N2 (lane 7). In addition, each isolated molecular motor subunit has a distinct positioning behavior. ISWI, the ATPase of ACF and NURF, positions nucleosomes at N4′ and N4 positions (lane 4). However, Snf2H preferentially places the nucleosomes on three sites between position N3 and a positioning site above N4 (lane 5). BRG1 does not change the nucleosome distribution significantly, but nucleosomes are displaced from the central position N1 (lane 2). Chd1 transfers the nucleosomes almost completely to position N3 (lane 3), whereas Mi-2 positions nucleosomes preferentially at the position N1 (lane 6). A similar complex-specific remodeling activity was observed in the analysis of the rDNA substrate (SI Fig. 7A). At the resolution of these experiments, the remodeling reactions led to a different distribution of nucleosomes at sites N1, N2, N3, N4, and N4′ (Fig. 2) or N1 and N2 (SI Fig. 7A), but no new nucleosome positions (except for the Snf2H reaction) were created (SI Fig. 7B).

It is concluded that remodeling machines do interpret the DNA sequence/structure information in different ways, establishing individual nucleosome-positioning patterns on a given DNA sequence. In particular, the nucleosome positioning depended on both the type of the ATPase motor protein as well as the composition of the multiprotein complex into which it is integrated (see also SI Fig. 7A). The nucleosome movements proceeded predominantly by positions characterized by an intrinsic nucleosome affinity preference (SI Fig. 7B) because the intermediate positions were mostly identical with the initial nucleosome positions generated by salt dialysis assembly. However, the relative occupancy of these sites can be strongly affected by specific chromatin-remodeling activities.

A Small DNA Element Directs ACF-Dependent Nucleosome Positioning. If the DNA sequence encodes information on the positioning of nucleosomes by remodeling complexes, it should be possible to identify specific DNA sequence elements that direct nucleosome positioning independent of the surrounding DNA sequence context. This prediction was tested with ACF in the experiments presented in Fig. 3. On the rDNA sequence, ACF moves the nucleosome from border positions to two rotationally spaced positions occupying nucleotides −190 to −40 and −180 to −30 relative to the rDNA gene transcription start site (30, 31). This finding corresponds to positions 46/56 to 196/206 (N1) on the 248-bp rDNA fragment studied in SI Fig. 7A. Previous studies established that the rDNA promoter of a variety of organisms
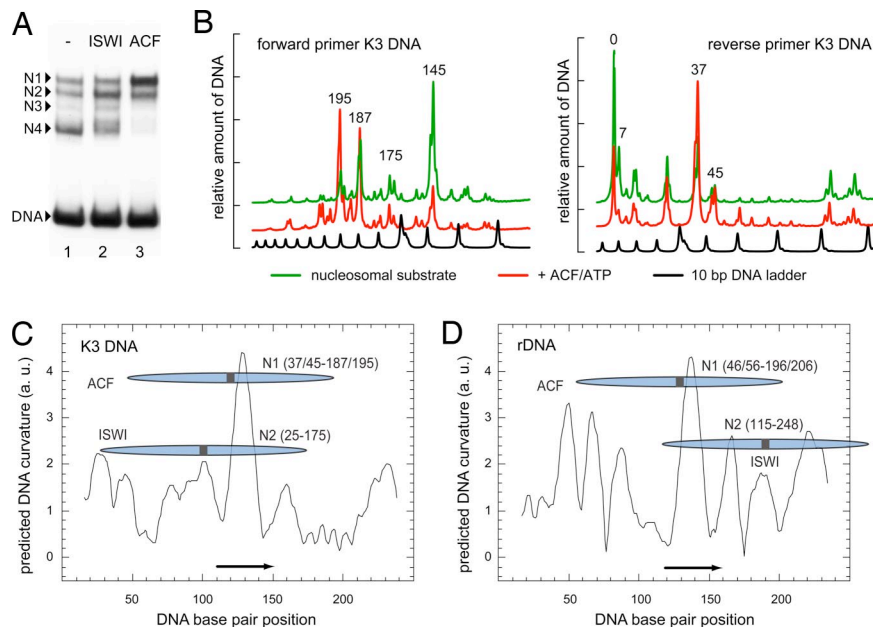
214

Fig. 3. A short DNA element can direct ACF-dependent nucleosome positioning. (*A*) Remodeling reaction with ACF or ISWI with a nucleosome substrate containing a 253-bp-long DNA fragment (K3 DNA) from the pT-K3 plasmid. After nucleosome assembly by salt dialysis on the K3 DNA, a mixed population of a single nucleosome with three main positions (N1, N2, and N4) and one minor position (N3, lane 1) was obtained. This substrate was used in a remodeling reaction with ISWI (lane 2) or ACF (lane 3). (*B*) High-resolution mapping of the remodeler-dependent nucleosome positions on the K3 DNA substrate. MNase protection and subsequent primer extension reactions were conducted. Scans for the primer extension reactions (*Left*, forward primer; *Right*, reverse primer) are shown for the nucleosomal input substrate (green, corresponding to *A*, lane 1) and the remodeling reaction for ACF (red, corresponding to *A*, lane 3). The black curve shows a 10-bp DNA marker. The same analysis was conducted with ISWI (data not shown). The peaks reflect nucleosomes positioned adjacent to this site. Considering that 147 bp of DNA are protected by the nucleosome, the major nucleosome positions were identified as 37/45 to 187/195 for N1, 25 to 175 for N2, and 0/7 to 151/157 for N4. (*C*) The ACF- and ISWI-dependent nucleosome positions determined on the 253-bp K3 DNA fragment were plotted together with the predicted DNA curvature. The black arrow refers to the 40-bp DNA sequence encompassing the region of maximal DNA curvature from the rDNA sequence that was cloned into the K3 DNA. (*D*) Same analysis as in *C*, but for the 248-bp rDNA promoter fragment with the previously determined nucleosome sites (30, 31).

exhibits a conserved sequence-dependent structure (32, 33). An analysis of this sequence for specific features revealed a strong correlation between ACF-dependent nucleosome positioning and the presence of an intrinsically curved DNA region (Fig. 3*D*). The dyad axis of the positioned nucleosome with the rDNA was close to the DNA curvature peak that was verified experimentally (SI Fig. 7*C*). Accordingly, a 40-bp fragment with the center of the curved region (positions 115–155) was then cloned into the DNA vector pT-K3 to examine it in a sequence environment with no apparent sequence similarities to the rDNA fragment. The resulting 253-bp-long DNA was used to assemble nucleosomes by salt dialysis. Nucleosomes were positioned at three major sites (N1, N2, and N4) and one minor site (N3) (Fig. 3*A*, lane 1). This distribution of differently positioned nucleosomes was used as substrate for the remodeling reaction with ISWI or ACF (Fig. 3*A*, lanes 2 and 3). In contrast to the 248-bp rDNA template (SI Fig. 7*A*), the ISWI-dependent nucleosome positioning did not place the nucleosomes to the extremes of the DNA, but preferentially to position N2 on the expense of nucleosomes positioned at the DNA border (N4). This result demonstrates that ISWI is not an unspecific, asymmetric molecular motor that moves any nucleosome to the ends of the DNA fragment, but can recognize certain DNA features (34). ACF, in contrast, translocated the nucleosomes predominantly to the central N1 site. The nucleosome positions involved in the remodeling reaction with the K3 DNA fragment were mapped at a high resolution (Fig. 3*B*). The major nucleosome positions were assigned to N1 being an unresolved mixture of two rotationally positioned nucleosomes at 37/45 to 195/187, N2 covering positions 25 to 175, and the nucleosomes positioned at the DNA ends (N4) consisting mainly of positions 0/7 to 151/157. The preferred sites found with the K3 DNA were superimposed with the DNA curvature prediction plot (Fig. 3*C*). From comparison with Fig. 3*D*, it is apparent

that the 40-base pair sequence element from the rDNA promoter was sufficient to direct ACF-dependent nucleosome positioning also in the K3 fragment, with the dyad axis again being placed close to the region of highest DNA curvature. Due to the possibility that ACF simply moves the nucleosome to the center of the DNA because of its preference for sufficiently long (≈30-bp) DNA flanking the nucleosomes, two additional nucleosome substrates were examined (SI Fig. 8). The results clearly demonstrate that the 40-bp DNA element identified here is able to direct nucleosome positioning by ACF to a position closer to the border of the DNA.

Two Models Can Explain Remodeler-Dependent Nucleosome Positioning. The comparison presented above revealed that the end product of the chromatin-remodeling reaction depends on both the type of chromatin remodeler and the DNA sequence (Figs. 2 and 3 and SI Figs. 7 and 8). To explain how a remodeling machine is able to direct the nucleosome to a specific position, the kinetic model presented in Fig. 4*A* was used. The approach considers the translocation of nucleosomes as an enzymatic reaction that follows a Michaelis–Menten-like model. This finding implies that "good" substrates for the enzyme (in this case, the chromatin-remodeling complex) are characterized by a high affinity of enzyme and its nucleosome substrate (low value of Michaelis–Menten constant K_M) and a high catalytic conversion rate k_{cat} of the enzyme–substrate complex to the product, which is the repositioned nucleosome. In this case, the k_{cat}/K_M ratio is high as expected for an efficient catalytic process. The opposite would be true for "bad" nucleosome-remodeling substrates (i.e., the k_{cat}/K_M ratio is low). This view leads to the proposal that the nucleosome-translocation reaction proceeds by moving nucleosomes from sites where they are good substrates to sites where they are bad substrates. Differences in the remodeling activity are due to DNA sequence-dependent differences for nu-
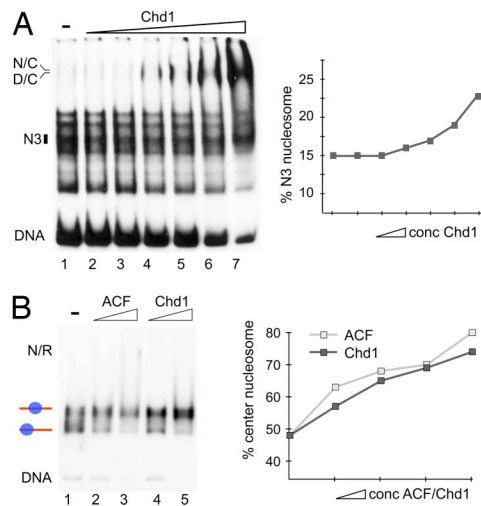
Fig. 4. Mechanisms of nucleosome positioning by chromatin-remodeling complexes. (*A*) Scheme for the remodeling reaction. Three positions on the DNA ($i − 1$, i, and $i + 1$) are considered. The remodeler R can bind to a nucleosome N at each of these three positions with a dissociation constant K_d. Translocation to or from these positions occurs with rate constants k as described in the text. (*B*) Two models for nucleosome positioning are depicted. (*Right*) Corresponding time course of the concentrations of nucleosomes. The reaction starts with all nucleosomes at position i at an initial concentration of $2.5 \times 10^{−9}$ M. If all binding constants and translocation rate constants are identical (uniform K_d and k), a homogenous distribution is obtained in equilibrium, where one-third of the nucleosomes is at positions $i − 1$, i, and $i + 1$, as expected. (*Left*) In the release model, the binding affinity to the nucleosome at position $i + 1$ is reduced by a 10-fold higher value of $K_{d,i+1}$, compared with positions i and $i − 1$. This result leads to a distribution in which ≈80% of the nucleosomes are at this site when an equilibrium is reached. For the arrest model, the rate constant $k_{−1}$ that translocates the nucleosome from position $i + 1$ back to position i is 10 times reduced compared with the other translocation rates. Again ≈80% of the nucleosomes will be positioned at site $i + 1$ as the reaction reaches a steady state. The kinetic simulations were conducted with concentrations similar to those used in the *in vitro* reaction of ≈1 remodeler per 50 nucleosomes.

cleosome locations that make them good and bad substrates for a given complex.

The reaction is described as follows. The nucleosome N can be at position i, $i + 1$, or $i − 1$, and the remodeler R can bind to nucleosomes at these positions. At the beginning of the reaction, all nucleosomes are at position i. The RN_i complex can now translocate the nucleosome by a remodeler-specific number of base pairs (SWI/SNF ≈50 bp, ISW2 ≈10 bp) (35) to the other positions with the rate constants k_{i+1} and $k_{i−1}$ or the RN_i complex can dissociate with the equilibrium dissociation constant $K_{d,i}$ into nucleosome N_i and free remodeler R with $K_{d,i} = [R] \times [N_i]/[RN_i]$. The same reaction can occur at positions $i + 1$ and $i − 1$. To position the

nucleosome at a specific site on the DNA, we propose that certain DNA sequences make nucleosomes bad remodeling substrates with a low escape rate from these sites so that they constitute the preferred end points of the remodeling reaction. This finding is illustrated in Fig. 4*B* for a remodeling reaction that positions the nucleosome preferentially at position $i + 1$.

The escape rate $k_{esc,i+1}$ from position $i + 1$ is given by the translocation rate constant $k_{−i}$ times the concentration of the RN_{i+1} complex, which in turn is determined by the corresponding equilibrium dissociation constant $K_{d,i+1}$. Accordingly, we can conclude that $k_{esc,i+1}$ is proportional to $k_{−i}/K_{d,i+1}$. To position the nucleosome at $i + 1$, either the translocation rate $k_{−i}$ away from this position or the binding affinity of the remodeler to the nucleosome at position $i + 1$ has to be reduced. The latter would be equivalent to increasing the value of $K_{d,i+1}$. This result is referred to here as a "release" mechanism. Its mode of operation is similar to transcription termination by specific DNA terminator sequences that form a hairpin structure in the RNA, which then disrupt the binding of RNA polymerase to the template so that the elongation reaction stops at this site (36, 37). For the second mechanism that involves a low translocation rate $k_{−i}$ away from the corresponding nucleosome position, the term "arrest" mechanism is used. It can again be described by analogy to the transcription reaction, where pausing/arrest of RNA polymerase can occur at certain DNA sequences because of a rearrangement of the enzyme's active site without the dissociation of the enzyme from the template (38). Accordingly, we can envision an arrest mechanism for the chromatin-remodeling reaction, in which a specific intermediate form interferes with the continuation of the translocation reaction. In contrast to the release model, the binding affinity of the remodeler is not reduced. It is noted that any increase of the binding affinity for the nucleosome at a given position will increase the likelihood of moving the nucleosome away from this position if the translocation rate remains unaffected. A particularly tight nucleosome remodeler reaction that induces a block of the translocation reaction (i.e., low rate $k_{−i}$ rate) could potentially position a nucleosome to a certain site. However, this anchoring mechanism would only work effectively under stoichiometric concentrations of remodeler and nucleosome, and its kinetics are not compatible with that of the *in vitro* remodeling reaction under enzymatic conditions studied here of ≈1 remodeling complex per 50 nucleosomes.

Nucleosome Positioning by Chd1 and ACF Follows the Release Model. The release model predicts that the affinity of the remodeler to the nucleosome is reduced at the endpoint of the remodeling reaction. According to the arrest model, binding affinity at the terminal position is not lowered, but the translocation reaction is inhibited. These predictions were tested with Chd1 and ACF. The relative binding affinities of the remodelers to the initial mixture of nucleosome positions were analyzed in EMSAs in the absence of ATP so that only the remodeler nucleosome-binding event is examined. The addition of increasing amounts of Chd1 results in DNA and nucleosome binding and the appearance of DNA–Chd1 and nucleosome–Chd1 complexes (Fig. 5*A*). From a comparison of the relative intensities, it can be seen that nucleosomes at positions N1, N2, and N4 were preferential substrates to form Chd1–nucleosome complexes, whereas the signal for nucleosomes positioned at site N3 decreased to a much lower extent. As shown in Fig. 2, Chd1 positions nucleosomes at N3, the site with the lowest binding affinity for Chd1. This finding suggests that Chd1 translocates nucleosomes according to the release model. Similar results were obtained by ACF with this nucleosomal DNA (data not shown). The same behavior of the two remodelers was also observed for the rDNA nucleosome substrate. Purified nucleosomes positioned at either the center or border of the rDNA fragment were mixed in stoichiometric amounts and used for binding assays (Fig. 5*B*). At increasing concentrations, Chd1 and ACF bound preferentially to nucleosomes positioned at the border of the DNA fragment (lanes

Fig. 5. ACF and Chd1 position nucleosomes according to the release model. Nucleosome position-dependent differences in the affinity of the remodeling complexes to the nucleosomal substrate were analyzed by EMSAs. (*A*) (*Left*) A mixed nucleosomal species reconstituted on the *hsp70* DNA (lane 1) was incubated with increasing concentrations of Chd1 (lanes 2–7) in the absence of ATP. The position of the appearing DNA–Chd1 (D/C) and the nucleosome–Chd1 (N/C) complexes are indicated. The position of the N3 nucleosome is shown by a black box. This position also is the preferred endpoint of the remodeling reaction (see Fig. 2). (*Right*) Percentage of nucleosomes at position N3 (radioactivity in the N3 band divided through the sum of the radioactivity of all nucleosome bands) is plotted versus the Chd1 concentration. An increase of the N3 fraction is apparent, suggesting that this site is the lowest affinity binding site for Chd1 with this substrate. (*B*) Chd1 and ACF binding to nucleosomes reconstituted at the rDNA promoter fragment. A purified mixture of nucleosomes positioned at the center and the border of the rDNA fragment (lane 1) was incubated with increasing concentrations of ACF (lanes 2 and 3) or Chd1 (lanes 4 and 5). The position of remodeler–nucleosome complexes (N/R) is indicated. The graph represents the fraction of nucleosomes at the center position with increasing concentrations of Chd1 or ACF. This lower affinity binding site also is the preferred endpoint of the reaction as shown in SI Fig. 7*B*.

2 to 5; the graph shows the fraction of the central nucleosome obtained with increasing ACF/Chd1 concentrations). Both remodelers displayed weaker binding affinities to the central nucleosome, which is the position to which they translocate the nucleosome in the remodeling reaction (SI Fig. 7*A*). Thus, for the two remodelers and two nucleosome substrates examined here, nucleosome positioning occurs by the release mechanism.

Discussion

The present study demonstrates that the chromatin remodeler can establish specific local chromatin structures by reading out DNA features and targeting nucleosomes to specific positions. To exploit this differential activity of remodeling complexes *in vivo*, it appears necessary to spatially and temporally confine a given complex to certain chromatin regions. Indeed, an increasing number of reports describes such a targeting of chromatin remodelers to specific genomic loci that are characterized by their pattern of epigenetic markers as reviewed recently for *Drosophila* (39). Thus, targeting of chromatin-remodeling complexes in conjunction with their DNA sequence-directed activity would provide a mechanism for the gene-specific regulation of DNA-dependent processes by modulation of the DNA accessibility. For ACF and Chd1, this process follows a release mechanism, according to which the endpoint of the translocation reaction is determined by a reduced affinity of the remodeler to the nucleosome at this site.

The physiological relevance of specifically positioned nucleosomes for the organization of regulatory regions of eukaryotic genes has been demonstrated in numerous systems (40–44). How-

ever, although the ability of certain DNA sequences to position nucleosomes *in vitro* is well established, many of these sequences fail to precisely position nucleosomes *in vivo* (44). This result indicates that, in addition to DNA structure and flexibility, other mechanisms define nucleosome positioning in the cell. For example, it has been shown that DNA-binding factors like the α2–MCM1 complex actively position nucleosomes at repressed genes in yeast α-cells. This process requires the intact histone H4 tail (45, 46), a target of the ISWI-containing remodeling machines (47). Similarly, the Ssn6–Tup1 complex is a global corepressor responsible for nucleosome positioning at a number of genes and the recombination enhancer of the silent mating-type loci in budding yeast (48–52). For the *RNR3* gene, the precise nucleosome positioning required the ISW2 chromatin-remodeling complex in addition to Ssn6–Tup1 (53). Furthermore, recent work demonstrates that the SNF2H-containing remodeling complex NoRC is involved in the repression of the rRNA genes that are characterized by two specific nucleosome positions discriminating between the active and inactive genes (54, 55). In this system, the recruitment of NoRC reorganizes the chromatin structure by moving the promoter-bound nucleosome ≈25 bp downstream to the position found at inactive genes (56).
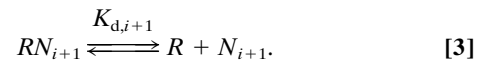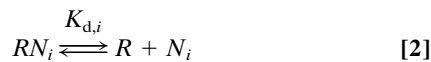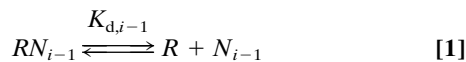
In light of these findings and the results reported here, the high abundance and diversity of remodeling complexes suggests that chromatin-remodeling machines are specific chromatin organizers and not simply nucleosome mobilizers. Their activity seems to be directed by two additional information layers encoded in the DNA sequence. One would represent binding preferences of the histone octamer to certain DNA sequence elements. It has been shown for yeast that about half of the *in vivo* nucleosome positions can be predicted solely from the underlying DNA sequence (10, 11). These sites are likely to provide thermodynamically favorable histone–DNA interactions, and the data reported here suggest that they also are selected as preferred locations in the remodeling reaction (Fig. 3 and SI Fig. 7*B*). However, the relative occupancy of these sites can be strongly affected by the chromatin-remodeling complexes. The coupling of their specific activity with intrinsic nucleosome preferences for certain DNA sequences could contribute significantly to determining nucleosome locations in living cells. Accordingly, the targeting of a significant fraction of nucleosomes to their DNA sites in the cell cannot be predicted without including the characteristic activities of chromatin-remodeling complexes present at the respective genomic loci. This view is consistent with a recent analysis of nucleosome locations in yeast that points to the involvement of additional factors in the determination of nucleosome positions (57). As demonstrated here, one important parameter to be considered is the binding affinity of the remodeler and the nucleosome. Either because of a sequence-specificity of remodeler–DNA interactions or more indirectly by an altered nucleosome structure, a reduced remodeler–nucleosome interaction leads to the release of nucleosomes to these sites. Thus, the positioning of nucleosomes in the cell could involve a chromatin-remodeling code. Features encoded by the DNA sequence are recognized by chromatin-remodeling complexes to establish specific nucleosome-positioning patterns that define the accessibility of DNA and with it on or off states for DNA-dependent processes.
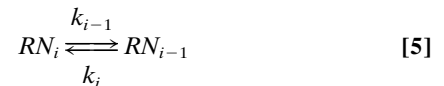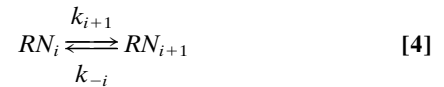
Materials and Methods

Nucleosome-Remodeling Experiments. Recombinant ISWI, ACF, Brg1, Chd1, Snf2H, and Mi-2 were expressed in Sf9 cells and prepared as described previously (27, 34). The hsp70 DNA fragment was generated by PCR with [α-^{32}P]dCTP for labeling (28). The 40-bp fragment encompassing the major DNA bending peak (CTGGGGAGGT GGCCCCAAAA ATGACCCCAT AACGAAAAGA) of this DNA was cloned into the pT7 blue3 Vector. From this vector, the 253-bp-long pT-K3 fragment with the insert was generated by PCR. Nucleosome-reconstitution and nucleosome-remodeling reactions were performed according to the protocol of Längst *et al.* (30). Briefly, nucleosomes and DNA were incubated at ratio of ≈1 remodeler complex per 50 nucleosomes for 90 min at 26°C in the presence of 1 mM ATP, and nucleosome positions were analyzed by native PAGE. EMSAs with reconsti-

tuted nucleosomes and remodeling ATPases were performed as previously described (27, 34). For mapping the nucleosome positions, 1.5 units MNase (Sigma–Aldrich, St. Louis, MO) were added for 40 sec to remodeling reactions. The protected nucleosomal core DNA was isolated and analyzed by a single round of PCR (denaturation, 5 min at 95°C; annealing, 2 min at 56°C; extension, 1 min at 72°C) by using at least three different ^{32}P-labeled oligonucleotides hybridizing to different positions on the DNA fragment. Primer extension fragments were resolved on 8% sequencing gels and quantified with a phosphorimager by using the Aida software (Fuji, Tokyo, Japan). For further details, see *SI Materials and Methods*.

Theoretical Analysis of Nucleosome-Remodeling Reaction. The DNA curvature from the beginning of the enhancer to the end of the promoter was analyzed with the NA-Bench program (M. Busch, R. Kochinke, K.R., and G. Wedemann, unpublished data). The program uses different algorithms for curvature prediction that are reviewed in ref. 58. For the analysis shown here, the parameter set from Bolshoy *et al.* (59) was used. Kinetic simulations were conducted with the COPASI software package, version 4.0 (60) by using the model depicted in Fig. 4, which describes the translocation reaction according to Eqs. **1–5**. The remodeler R can bind to nucleosomes N at positions i, $i-1$, and $i+1$. Under the conditions of the *in vitro* experiments, the binding reaction is fast, compared with the nucleosome-translocation reaction, so that it can be described by an preequilibrium with the equilibrium constant K_d for the dissociation of the RN complex:

$$RN_{i-1} \underset{}{\overset{K_{d,i-1}}{\rightleftharpoons}} R + N_{i-1} \qquad [1]$$

$$RN_i \underset{}{\overset{K_{d,i}}{\rightleftharpoons}} R + N_i \qquad [2]$$

$$RN_{i+1} \underset{}{\overset{K_{d,i+1}}{\rightleftharpoons}} R + N_{i+1}. \qquad [3]$$

Initial conditions for the simulations were a concentration of 2.5×10^{-9} M nucleosomes at position i and a concentration of 5×10^{-11} M remodeler. Translocations of the nucleosomes were described by the Eqs. **4** and **5** with the indicated rate constants.

$$RN_i \underset{k_{-i}}{\overset{k_{i+1}}{\rightleftharpoons}} RN_{i+1} \qquad [4]$$

$$RN_i \underset{k_i}{\overset{k_{i-1}}{\rightleftharpoons}} RN_{i-1} \qquad [5]$$

Default values for the dissociation constants were $K_{d,i} = K_{d,i+1} = K_{d,i-1} = 10^{-9}$ M and for the rate constants $k_{i+1} = k_{i-1} = k_{-i} = k_i = 1$ sec^{-1} (Fig. 4B). For the simulations of the release model, $K_{d,i+1}$ was changed to 10^{-8} M, and the arrest mechanism simulation corresponded to $k_{-i} = 0.1$ sec^{-1}.

1. Muchardt C, Yaniv M (1999) *J Mol Biol* 293:187–198.
2. Wyrick JJ, Holstege FC, Jennings EG, Causton HC, Shore D, Grunstein M, Lander ES, Young RA (1999) *Nature* 402:418–421.
3. Becker PB, Hörz W (2002) *Annu Rev Biochem* 71:247–273.
4. Han M, Kim UJ, Kayne P, Grunstein M (1988) *EMBO J* 7:2221–2228.
5. Roth SY, Shimizu M, Johnson L, Grunstein M, Simpson RT (1992) *Genes Dev* 6:411–425.
6. Lu Q, Wallrath LL, Elgin SC (1995) *EMBO J* 14:4738–4746.
7. Schild C, Claret FX, Wahli W, Wolffe AP (1993) *EMBO J* 12:423–433.
8. Jackson JR, Benyajati C (1993) *Nucleic Acids Res* 21:957–967.
9. Yuan GC, Liu YJ, Dion MF, Slack MD, Wu LF, Altschuler SJ, Rando OJ (2005) *Science* 309:626–630.
10. Segal E, Fondufe-Mittendorf Y, Chen L, Thastrom A, Field Y, Moore IK, Wang JP, Widom J (2006) *Nature* 442:772–778.
11. Ioshikhes IP, Albert I, Zanton SJ, Pugh BF (2006) *Nat Genet* 38:1210–1215.
12. Flaus A, Martin DM, Barton GJ, Owen-Hughes T (2006) *Nucleic Acids Res* 34:2887–2905.
13. Flaus A, Owen-Hughes T (2004) *Curr Opin Genet Dev* 14:165–173.
14. Bowen NJ, Fujita N, Kajita M, Wade PA (2004) *Biochim Biophys Acta* 1677:52–57.
15. Mohrmann L, Verrijzer CP (2005) *Biochim Biophys Acta* 1681:59–73.
16. Barak O, Lazzaro MA, Cooch NS, Picketts DJ, Shiekhattar R (2004) *J Biol Chem* 279:45130–45138.
17. Okabe I, Bailey LC, Attree O, Srinivasan S, Perkel JM, Laurent BC, Carlson M, Nelson DL, Nussbaum RL (1992) *Nucleic Acids Res* 20:4649–4655.
18. Aihara T, Miyoshi Y, Koyama K, Suzuki M, Takahashi E, Monden M, Nakamura Y (1998) *Cytogenet Cell Genet* 81:191–193.
19. Banting GS, Barak O, Ames TM, Burnham AC, Kardel MD, Cooch NS, Davidson CE, Godbout R, McDermid HE, Shiekhattar R (2005) *Hum Mol Genet* 14:513–524.
20. Poot RA, Dellaire G, Hulsmann BB, Grimaldi MA, Corona DF, Becker PB, Bickmore WA, Varga-Weisz PD (2000) *EMBO J* 19:3377–3387.
21. Barak O, Lazzaro MA, Lane WS, Speicher DW, Picketts DJ, Shiekhattar R (2003) *EMBO J* 22:6089–6100.
22. Jones MH, Hamana N, Nezu J, Shimane M (2000) *Genomics* 63:40–45.
23. Ghaemmaghami S, Huh WK, Bower K, Howson RW, Belle A, Dephoure N, O'Shea EK, Weissman JS (2003) *Nature* 425:737–741.
24. Huh WK, Falvo JV, Gerke LC, Carroll AS, Howson RW, Weissman JS, O'Shea EK (2003) *Nature* 425:686–691.
25. Ito T, Bulger M, Pazin MJ, Kobayashi R, Kadonaga JT (1997) *Cell* 90:145–155.
26. Lusser A, Urwin DL, Kadonaga JT (2005) *Nat Struct Mol Biol* 12:160–166.
27. Brehm A, Längst G, Kehle J, Clapier CR, Imhof A, Eberharter A, Muller J, Becker PB (2000) *EMBO J* 19:4332–4341.
28. Hamiche A, Sandaltzopoulos R, Gdula DA, Wu C (1999) *Cell* 97:833–842.
29. Phelan ML, Schnitzler GR, Kingston RE (2000) *Mol Cell Biol* 20:6380–6389.
30. Längst G, Bonte EJ, Corona DF, Becker PB (1999) *Cell* 97:843–852.
31. Strohner R, Wachsmuth M, Dachauer K, Mazurkiewicz J, Hochstatter J, Rippe K, Längst G (2005) *Nat Struct Mol Biol* 12:683–690.
32. Längst G, Schatz T, Langowski J, Grummt I (1997) *Nucleic Acids Res* 25:511–517.
33. Marilley M, Pasero P (1996) *Nucleic Acids Res* 24:2204–2211.
34. Längst G, Becker PB (2001) *Mol Cell* 8:1085–1092.
35. Zofall M, Persinger J, Kassabov SR, Bartholomew B (2006) *Nat Struct Mol Biol* 13:339–346.
36. von Hippel PH, Yager TD (1992) *Science* 255:809–812.
37. Greive SJ, von Hippel PH (2005) *Nat Rev Mol Cell Biol* 6:221–232.
38. Landick R (2006) *Biochem Soc Trans* 34:1062–1066.
39. Bouazoune K, Brehm A (2006) *Chromosome Res* 14:433–449.
40. Simpson RT (1990) *Nature* 343:387–389.
41. Grunstein M (1990) *Annu Rev Cell Biol* 6:643–678.
42. Simpson RT (1991) *Prog Nucleic Acid Res Mol Biol* 40:143–184.
43. Bernstein BE, Liu CL, Humphrey EL, Perlstein EO, Schreiber SL (2004) *Genome Biol* 5:R62.
44. Li Q, Wrange O, Eriksson P (1997) *Int J Biochem Cell Biol* 29:731–742.
45. Shimizu M, Roth SY, Szent-Gyorgyi C, Simpson RT (1991) *EMBO J* 10:3033–3041.
46. Roth SY, Dean A, Simpson RT (1990) *Mol Cell Biol* 10:2247–2260.
47. Clapier CR, Längst G, Corona DF, Becker PB, Nightingale KP (2001) *Mol Cell Biol* 21:875–883.
48. Cooper JP, Roth SY, Simpson RT (1994) *Genes Dev* 8:1400–1410.
49. Weiss K, Simpson RT (1997) *EMBO J* 16:4352–4360.
50. Kastaniotis AJ, Mennella TA, Konrad C, Torres AM, Zitomer RS (2000) *Mol Cell Biol* 20:7088–7098.
51. Fleming AB, Pennings S (2001) *EMBO J* 20:5219–5231.
52. Li B, Reese JC (2001) *J Biol Chem* 276:33788–33797.
53. Zhang Z, Reese JC (2004) *J Biol Chem* 279:39240–39250.
54. Strohner R, Nemeth A, Jansa P, Hofmann-Rohrer U, Santoro R, Längst G, Grummt I (2001) *EMBO J* 20:4892–4900.
55. Santoro R, Li J, Grummt I (2002) *Nat Genet* 32:393–396.
56. Li J, Längst G, Grummt I (2006) *EMBO J* 25:5735–5741.
57. Peckham HE, Thurman RE, Fu Y, Stamatoyannopoulos JA, Noble WS, Struhl K, Weng Z (2007) *Genome Res* 17:1170–1177.
58. Goodsell DS, Dickerson RE (1994) *Nucleic Acids Res* 22:5497–5503.
59. Bolshoy A, McNamara P, Harrington RE, Trifonov EN (1991) *Proc Natl Acad Sci USA* 88:2312–2316.
60. Hoops S, Sahle S, Gauges R, Lee C, Pahle J, Simus N, Singhal M, Xu L, Mendes P, Kummer U (2006) *Bioinformatics* 22:3067–3074.

Rippe *et al*. 10.1073/pnas.0702430104.

Supporting Information

Files in this Data Supplement:

SI Figure 6
SI Figure 7
SI Figure 8
SI Material and Methods

This Article

▶ **Abstract**

Services

▶ **Email this article to a colleague**
▶ **Alert me to new issues of the journal**
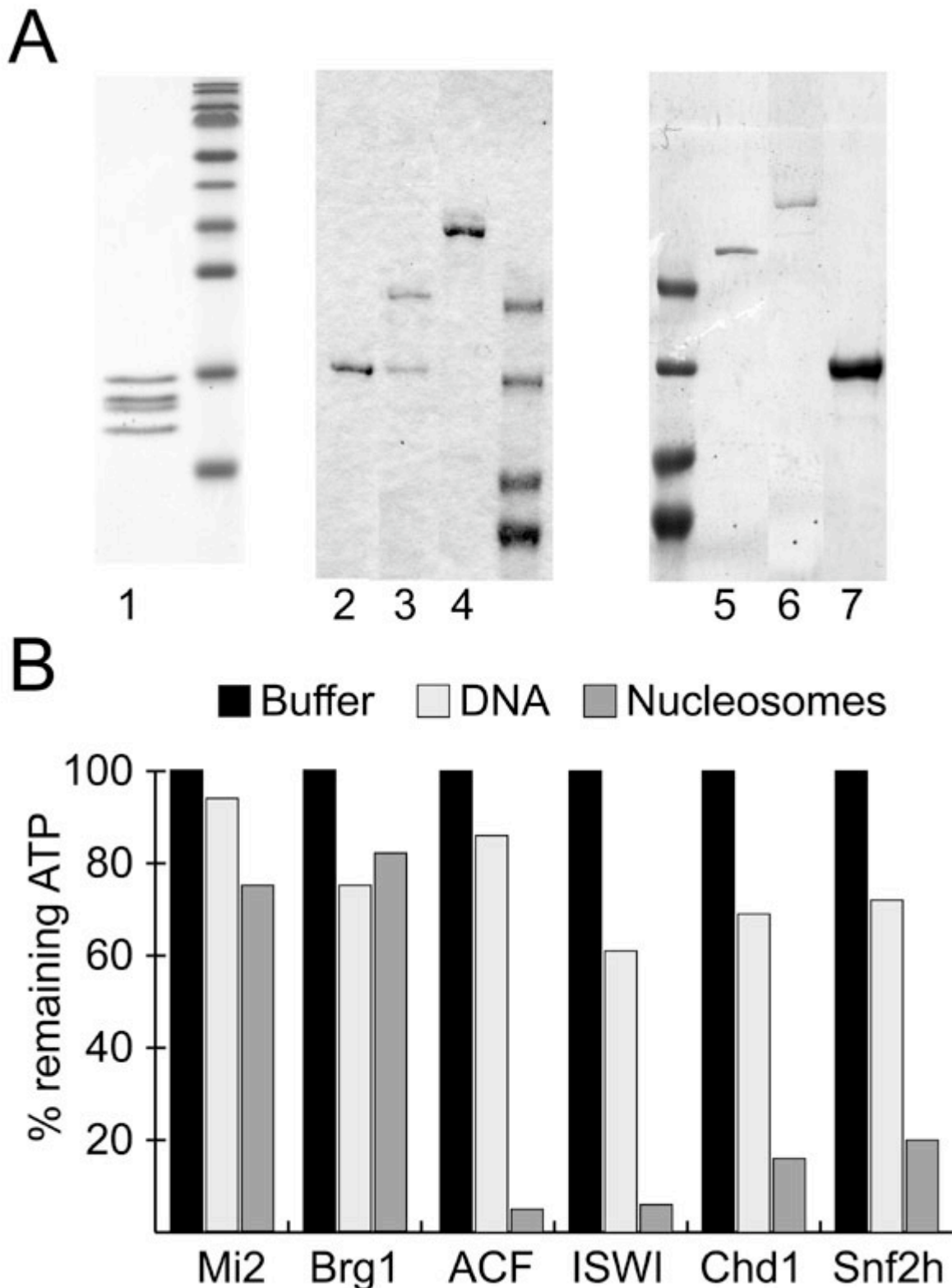▶ **Request Copyright Permission**

Fig. 6. Characterization of histone proteins and chromatin-remodeling complexes. (*A*) Core histone were purified from Drosophila embryos (lane 1), whereas recombinant-remodeling complexes were prepared from Sf9 cells as described previously (1, 2). The purified proteins were analyzed by SDS/PAGE and visualized by Coomassie blue staining. Histones (lane 1), ISWI (lane 2), ACF (lane 3), Chd1 (lane 4), Brg1 (lane 5), Mi-2 (lane 6), and Snf2H (lane 7) are shown. (*B*) ATPase activity of purified recombinant-remodeling complexes. Proteins were incubated in the absence or presence of DNA (150 ng) or chromatin (150 ng) and ATP (13 μM) for 30 min at 26°C. ATP concentrations at the end of the reaction were quantified in a luciferase assay and displayed relative to the initial ATP concentrations. It can be seen that all complexes are active because they show a chromatin-stimulated ATPase activity.

1. Brehm A, Längst G, Kehle J, Clapier CR, Imhof A, Eberharter A, Müller J, Becker PB (2000) *Embo J* 19:4332-4341.

2. Längst G, Becker PB (2001) *Mol Cell* 8:1085-1092.
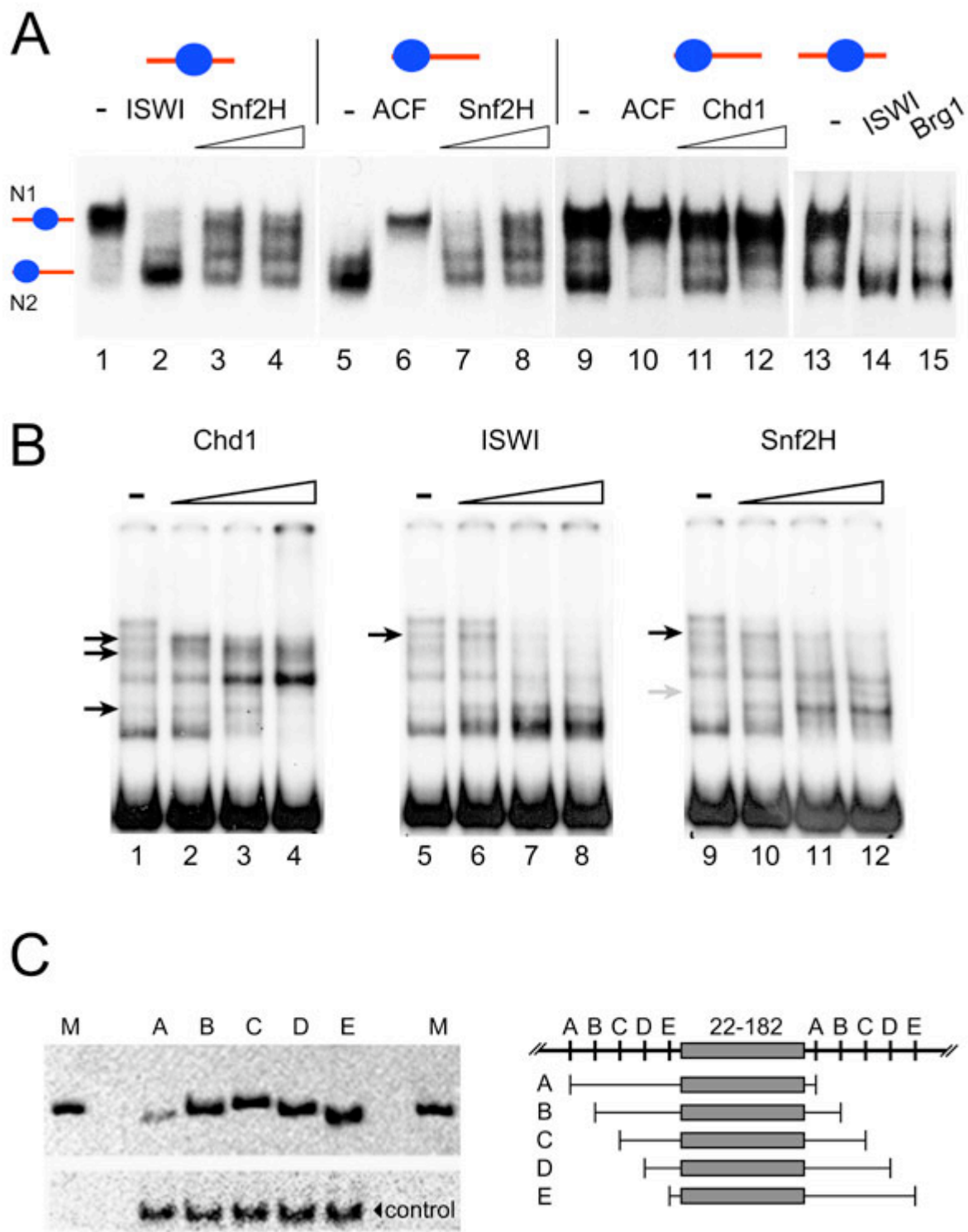
Fig. 7. Nucleosome translocations occur in discrete steps by the preferred nucleosome-assembly positions. (*A*) Analysis of remodeler-dependent nucleosome positions on the 248-bp-long rDNA promoter fragment (1). A purified nucleosome positioned at the center of the rDNA fragment (N1, lane

1), at the border of the DNA fragment (N2, lane 5), or a mixed population of these two nucleosome substrates (lanes 9 and 13) were used for the remodeling reaction with ISWI (lanes 2 and 14), Snf2H (lanes 3, 4, 7, and 8), ACF (lanes 6 and 10), Chd1 (lanes 11 and 12), and Brg1 (lane 15). Nucleosome positions (N1 and N2) are indicated by the blue ovals with the DNA marked in red. The murine rDNA promoter fragment (from position -232 to + 16 relative to the transcription start site) contains two well characterized nucleosome positions, a dominant-central position (N1) and the N2 position at the borders (1, 2). The nucleosome-remodeling reactions showed marked differences, for example, in the comparison of the three isolated ATPases (ISWI and its human counterpart Snf2H, lanes 2-4; Brg1, lane 15) or the isolated motor (ISWI), compared with ISWI and the associated Acf1 subunit in the ACF complex (lanes 2 and 6). The latter also is evident from the remodeling reaction with the hsp70 DNA (Fig. 2). Thus, Acf1, the large subunit of ACF, determines the directionality of the nucleosome-positioning reaction. This finding confirms previous results obtained for the ACF complex in Drosophila (3) and more recently for human ACF (4). The Brg1 protein catalyzes only a minor change of the nucleosome position distribution on the hsp70 DNA fragment with an elimination of the hsp70 N1 position (Fig. 2). However, it efficiently repositions the N1 nucleosomes on the rDNA fragment to the N2 site as shown in this figure. (*B*) Nucleosomes reconstituted on the hsp70 DNA were incubated with increasing amounts of the indicated remodeling complexes to monitor the progression of nucleosome movements in EMSAs. As expected, increasing concentrations of remodeling enzymes were found to increase the kinetics of the nucleosome-remodeling reaction (5, 6). In preparatory experiments with varying remodeler concentrations (shown here) or the incubation time (data not shown), the endpoints of the remodeling reaction were identified. In these types of experiments, intermediate nucleosome positions can be observed (marked by arrows). This finding also addresses a general question in remodeler-dependent nucleosome repositioning: Are the nucleosomes moved in a single step to the final destination or do new, intermediate nucleosome positions appear in the course of the remodeling reaction? The analysis for Chd1, ISWI, and Snf2H suggests that nucleosome remodeling does not occur in one step because the amount of nucleosomes at other sites (black arrows) increases before the final nucleosome positions are reached. Interestingly, the intermediate positions are predominantly those with a higher intrinsic histone-DNA affinity, which are obtained in the initial salt dialysis reconstitution (black arrows). In the case of Snf2H-dependent nucleosome positioning, a nucleosome position was formed (gray arrow). Thus, the nucleosome remodeling does not occur with a discrete step length, but the enzymes translocate the nucleosomes from one stable position to the next. (*C*) Experimental verification of predicted DNA curvature in the sequence element from the rDNA. The region 22-182 from the rDNA fragment was analyzed in a gel permutation assay by PAGE. Fragments were isolated by restriction digestion at sites A-E, the position of which are indicated in the adjacent scheme. The centrally located insert obtained by digestion at site C showed the lowest electrophoretic mobility as characteristic for the presence of intrinsic DNA curvature. By studying the electrophoretic mobility of this region in a circular permutation assay, it was confirmed experimentally that the rDNA fragment indeed contains an intrinsically curved DNA region (SI Fig. 7*B*). The region 22-182 from the rDNA fragment was cloned into the vector XUMEI for the curvature analysis. The DNA was cleaved with the restriction enzymes MluI, XhoI, BglI, Acc65I, and BamHI that release the DNA fragments A-E, as indicated in SI Fig. 7*B*. The centrally located insert obtained by digestion with BglI at the C site showed the lowest electrophoretic mobility, which is indicative of intrinsic DNA curvature in the rDNA insert.

1. Längst G, Bonte EJ, Corona DF, Becker PB (1999) *Cell* 97:843-852.

2. Strohner R, Wachsmuth M, Dachauer K, Mazurkiewicz J, Hochstatter J, Rippe K, Längst G (2005) *Nat Struct Mol Biol* 12:683-690.

3. Eberharter A, Ferrari S, Längst G, Straub T, Imhof A, Varga-Weisz P, Wilm M, Becker PB (2001) *Embo J* 20:3781-3788.

4. He X, Fan HY, Narlikar GJ, Kingston RE (2006) *J Biol Chem* 281:28636-28647.

5. Bonaldi T, Längst G, Strohner R, Becker PB, Bianchi ME (2002) *Embo J* 21:6865-6873.

6. Eberharter A, Vetter I, Ferreira R, Becker PB (2004) *EMBO J* 23:4029-4039.
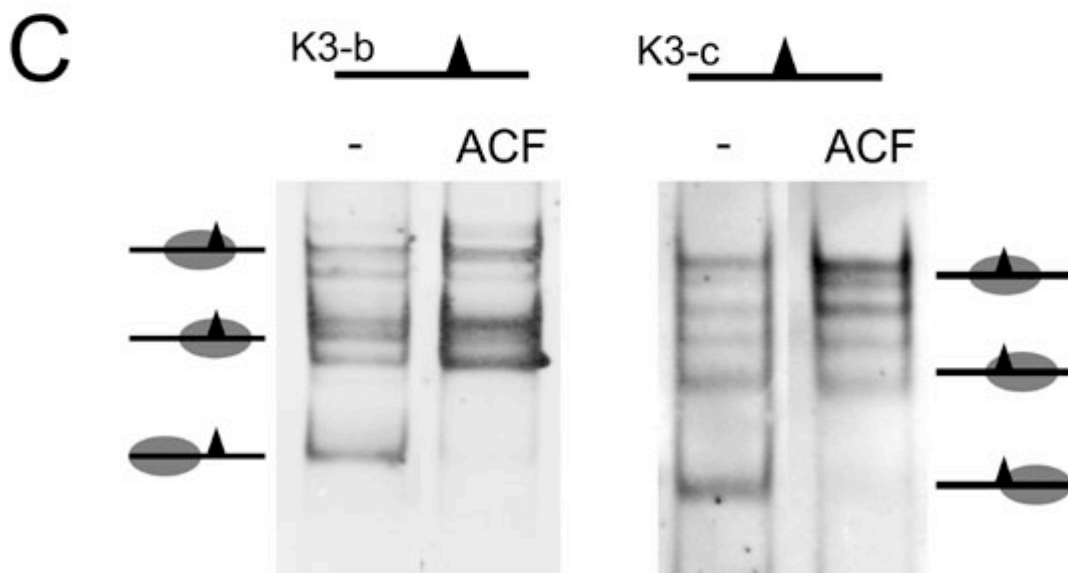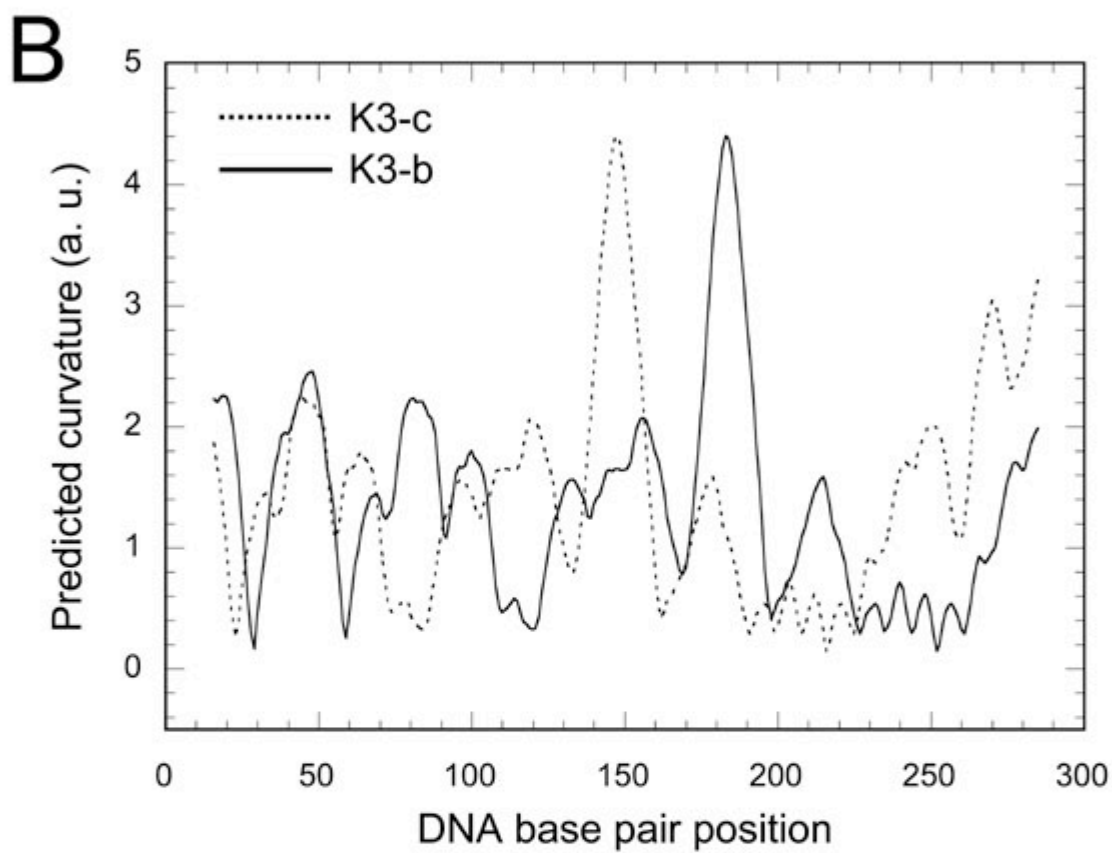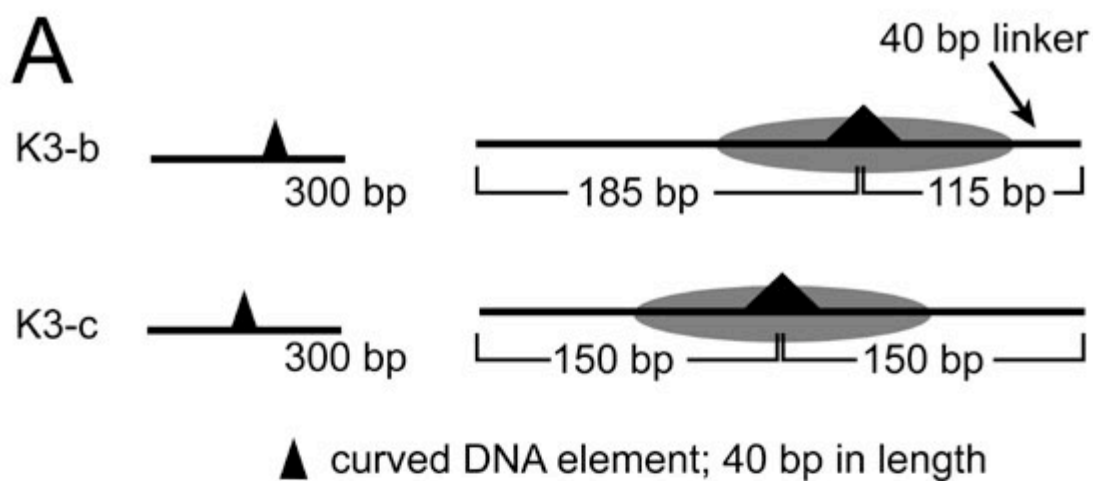
A

K3-b   300 bp

185 bp   115 bp

40 bp linker

K3-c   300 bp

150 bp   150 bp

▲ curved DNA element; 40 bp in length

B

K3-c
K3-b

Predicted curvature (a. u.)

DNA base pair position

C

K3-b ▲   K3-c ▲

-          ACF   -   ACF

223

Fig. 8. A curved 40-bp DNA element guides ACF-dependent nucleosome positioning. Previous studies indicated that ACF moves nucleosomes to central DNA positions because the complex has higher affinities to longer DNA (1-3). It also was shown that ACF binds symmetrically to the nucleosome protecting about 30 bp of linker DNA on both sites (2). Thus, on short nucleosome substrates (below 210 bp), the ACF remodeling reaction is guided, at least to some extent, by the length of the flanking DNA. To separate this effect from the positioning ability of the 40-bp DNA element identified in Fig. 3, two additional nucleosome substrates were studied: nucleosomes reconstituted on the 300-bp K3-b DNA that had the curved DNA element located closer to one end and the 300-bp K3-c DNA with a centrally located insert. As shown in the figure, ACF-dependent remodeling places the nucleosome on the center of the DNA fragment if the curved DNA is located at the center and places the nucleosome close to the DNA border if the DNA element is placed more laterally. These experiments confirm the conclusion made from the experiment depicted in Fig. 3 that the 40-bp DNA element is able to direct ACF-dependent nucleosome positioning. (*A*) Schematic depiction of nucleosome remodeling substrates that should place nucleosomes more centrally (K3-c) or close to the border (K3-b) according to the location of the 40-bp DNA element. Both DNAs are 300 bp in length with the K3-c DNA carrying the curved DNA element at the center, whereas in K3-b it is located 115 bp from one DNA end. This design ensures that nucleosomes positioned at these sites contain sufficient flanking DNA so that binding of the remodeling complex is not affected. (*B*) Predicted DNA curvature of the K3-c and K3-b DNA fragments according to the parameter set of Bolshoy *et al.* (4). The existence of a region of high intrinsic curvature of DNA fragment inserted into pT-K3 to yield the K3-b and K3-c DNA fragments also was shown experimentally as described in SI Fig. 7*C*. (*C*) ACF-dependent nucleosome remodeling on the K3-b and K3-c DNA substrate. Nucleosomes were reconstituted on these DNA fragments and incubated with ACF and ATP as indicated. The endpoints of the reaction were analyzed by ethidium bromide staining of the native polyacrylamide gels. The nucleosome positions are indicated by the gray ovals. The triangle demarcates the position of the curved DNA element. The majority of nucleosomes are placed at central positions on the K3-c nucleosomal DNA, whereas nucleosomes were preferentially positioned at the border of the K3-b DNA. This finding demonstrates the ability of the 40-bp DNA element to direct the nucleosome translocation reaction by ACF.

1. Längst G, Bonte EJ, Corona DF, Becker PB (1999) *Cell* 97:843-852.

2. Strohner R, Wachsmuth M, Dachauer K, Mazurkiewicz J, Hochstatter J, Rippe K, Längst G (2005) *Nat Struct Mol Biol* 12:683-690.

3. Yang JG, Madrid TS, Sevastopoulos E, Narlikar GJ (2006) *Nat Struct Mol Biol* 13:1078-1083.

4. Bolshoy A, McNamara P, Harrington RE, Trifonov EN (1991) *Proc Natl Acad Sci USA* 88:2312-2316.

SI Material and Methods

Nucleosome-Remodeling Assay. DNA fragments K3-c and K3-b were prepared by PCR using the pTblue7-K3 DNA. PCR fragments were purified and reconstituted into chromatin as described (1). Nucleosome-remodeling reactions were stopped by the addition of 1 μg of plasmid DNA, further incubated for 5 min, and then loaded on 5% polyacrylamide gels in 0.5x TBE. Gels were stained with ethidium bromide.

DNA Curvature Analysis. The rDNA sequences from positions 22-182 containing the predicted curved DNA was cloned into the plasmid XUMEI kindly provided by Michael Meisterernst (GSF, Munich, Germany). The insert is flanked on both sites by an identical sequence harboring the restriction enzyme sites for MluI, *Xho*I, *Bgl*I, Acc65I, and *Bam*HI spaced by 36, 27, 19, and 19 bp. The 302-bp DNA fragment was released by restriction enzyme digestion and analyzed on 10% polyacrylamide gels in TB-buffer (89 mM Tris/89 mM boric acid).

ATPase Assay. Nucleosome-remodeling reactions were performed in Ex40 buffer [40 mM KCl/20

mM Tris×HCl (pH 7.6)/1.5 mM $MgCl_2$/0.5 mM EGTA/10% glycerol] containing 13 μM ATP. Reactions were supplemented with 10 ng/μl of DNA or chromatin reconstituted by salt dialysis and 20-200 ng of the remodeling enzyme. After the indicated time points, the reactions were diluted 1:1,000 in water, and the ATP levels were quantified in a luciferase assay with the Enliten kit (Promega, Madison, WI) according to the manufacturer's protocol.

1. Längst G, Bonte EJ, Corona DF, Becker PB (1999) *Cell* 97:843-852.

I. Acknowledgements / Danksagung

Besonderen Dank möchte ich all denjenigen aussprechen, die meine Arbeit kritisch und geduldig gelesen haben. Für das sorgfältige Korrekturlesen und die Verbesserungsvorschläge bedanke ich mich insbesondere bei Axel Berger, Josef Exler, Joachim Griesenbeck, Claudia Huber, Attila Nemeth, Philipp Riede und ganz besonders auch bei Ana Villar.

Am Lehrstuhl möchte ich mich speziell bei Andi, Attila, Claudia, Hannah, Josef, Juliane, Kathrin und Tom für die schöne Zeit danken.

Ganz besonders und von Herzen möchte ich Axel für sein großes Verständnis während dieser Arbeit danken. Du hast mich in dieser schwierigen Zeit konstant und liebevoll unterstützt, mich ermutigt und glücklich gemacht, was diese Arbeit ernorm gefördert hat. Ich bin froh, dass unsere Wege durch diese Arbeit zusammengeführt wurden.

Mein größter Dank gilt meinen Eltern, die mich mein ganzes Leben lang unterstützt und immer wieder motiviert haben. Ich danke Ihnen für ihre Liebe, ihr Verständnis, ihre Geduld und dafür, dass sie immer an mich geglaubt haben.

Meinen Freunden möchte ich abschließend ein Dank für ihre intensive Unterstützung und Geduld während der letzten Jahre aussprechen.

Eidesstattliche Erklärung

Hiermit erkläre ich, Anna-Kristin Schrader an Eides statt, dass ich die vorliegende Doktorarbeit selbstständig und ausschliesslich mit den angegebenen Hilfsmitteln und Quellen angefertigt habe.

Regensburg,   …………………………………

                                              (Anna-Kristin Schrader)

Curriculum Vitae

ANNA-KRISTIN SCHRADER

Personal information:

Date of birth	17.06.1979
Place of birth	Hamburg
Nationality	German
Work address	Universität Regensburg
	Department of Biochemistry III
	Universitätsstrasse 31, 93049 Regensburg

Education:

2006 – present	PhD student at the Institute of Biochemistry III; University of Regensburg
	Topic: "Molecular mechanisms of nucleosome positioning and DNA methylation in chromatin"
2001- 2005	Main Studies of biology: Diplom
	Topic: "Funktionelle Charakterisierung der DNA Methylierung in Chromatin" at the Adolf-Butenandt-Institut, Lehrstuhl Peter Becker, Ludwig Maximilians University München
1998 – 2001	Basic Studies of Biology: Vordiplom University of Regensburg
1989-1998	Secondary Education: Abitur; Helene-Lange Gymnasium, Hamburg

Publication:

Rippe, K*. and **Schrader**, A*.; Riede, P.; Strohner, R.; Lehmann, E. and Längst, G. (2007). DNA sequence-and conformation-directed positioning of nucleosomes by chromatin-remodeling complexes. **PNAS** 104 (40) 15635-15640.

* = equally contributing